

The Regulation of Peptide Mimotope/Epitope Recognition
by Monoclonal Antibodies

by Richard Gary Smith B.Sc. (Hons)

Thesis submitted to the University of Nottingham for the degree of Doctor of

Philosophy,

March 2002.

TABLE OF CONTENTS

Abstract.....	8
Acknowledgements.....	9
Glossary of terms.....	10
Chapter 1 Antibody Purification.....	11
1.1 Introduction	11
1.1.1 Antibodies	11
1.1.2 Monoclonal and engineered Antibodies.....	12
1.2 Examples of a therapeutic and a commercially applied monoclonal antibody	17
1.2.1 C595 monoclonal antibody (NCRC48).....	17
1.2.2 mAb 4155.....	18
1.3 Approaches to antibody purification	20
1.3.1 Column chromatography.....	20
1.3.2 Fluidized bed and expanded bed adsorption	20
1.3.3 High performance Tangential Flow Filtration (HPTFF).....	21
1.3.4 Magnetic beads.....	21
1.4 Physical separation techniques.....	22
1.4.1 Ion exchange	22
1.4.2 Gel filtration.....	23
1.4.3 Hydrophobic Interaction Chromatography (HIC).....	23
1.5 Affinity Purification Techniques.....	23
1.5.1 Fc Binding Proteins	24
1.5.2 Recombinant Protein Tags	24
1.5.3 Paratope specific binding ligands.....	25
1.5.4 Non-proteinaceous, paratope specific affinity ligands	30
1.6 Summary	32
Chapter 2 Regulation of peptide antibody interactions.....	33
2.1 Introduction	33
2.1.1 Library Technologies	35
2.1.2 The distinction between screening and selection in library technologies	36
2.2 Synthetic Peptide Libraries	40
2.2.1 Pepscan – The application of synthetic peptides in Epitope mapping.	40
2.2.2 Replacement Net (RNET) analysis	40

2.2.3	Combinatorial peptide libraries.....	41
2.3	Biological libraries	42
2.3.1	<i>In vivo</i> libraries.....	42
2.3.2	<i>In vitro</i> libraries	47
2.4	Other non-peptide ligands	51
2.4.1	Synthetic Libraries	51
2.4.2	Biological Libraries.....	51
2.5	Mutagenesis.....	52
2.6	Aims and Objectives of the research.....	55
Chapter 3	Materials and Methods.....	57
3.1	Reagents	57
3.2	Enzymes	59
3.3	Buffers and Solutions.....	60
3.4	Methods.....	65
3.4.1	Monoclonal Antibody Production.....	65
3.4.2	Biopanning of phage library.....	65
3.4.3	PCR analysis of individual phage clones	66
3.4.4	Direct sequencing of PCR products	67
3.4.5	Phage Capture ELISA	68
3.4.6	Sepharose Bead Assay	69
3.4.7	Peptide Affinity Chromatography.....	69
3.4.8	Sodium dodecyl sulphate polyacrylamide gel electrophoresis	70
3.4.9	Circular Dichroism.....	71
3.4.10	Fluorescence Quenching Immunoassay.....	72
3.4.11	Conjugation of peptides to BSA using glutaraldehyde.....	73
3.4.12	Production of a BSA-Estrone Conjugate	73
3.4.13	Enzyme linked immunosorbent assay (ELISA).....	73
3.4.14	Surface Plasmon Resonance (SPR) analysis of the C595 – mucin core peptide APDTRPAPG interaction.....	76
3.4.15	SPR analysis of the interaction between peptide conjugate BSA-(D)DYFLG, and the anti E3G monoclonal antibody 4155.....	79
3.4.16	Production of pCANTAB-5E [C595scFvGFP]. A Phagemid expression vector containing a C595 ScFv – Green Fluorescent Protein Gene fusion.....	81

3.4.17 Protein expression	88
3.4.18 Western blot analysis	90
3.4.19 ELISA of Supernatant, Periplasmic Extract, Whole Cell Extract and fractions from affinity purification of supernatant.....	90
3.4.20 Random mutagenesis of the C595-ScFv gene – analysis of a selection of mutants.....	91
3.4.21 Evaluation of pSKGFP expression system.....	92
Chapter 4 - Results. Phage Display of Peptides.....	93
4.1 Introduction	93
4.2 The T7Select415 phage display library.....	94
4.3 Determination of initial phage library titer and stability of the library	97
4.4 Analysis of passive adsorption of proteins on the surface of NUNC immunotubes by ELISA method.....	98
4.5 Removal of non-specifically binding phage.....	99
4.6 Biopanning - Screening of library against 4155 mAb.....	100
4.6.1 Determination of the extent of enrichment that can be observed.....	100
4.7 Screening of library against C595 mAb.....	101
4.7.1 Determination of the extent of enrichment that can be observed.....	101
4.7.2 Capture ELISA of phage populations from biopanning rounds.....	102
4.7.3 Capture ELISA of phage clones from rounds one and four of screening.	104
4.8 SPR analysis of selected phage clones.....	106
4.9 PCR analysis of phage clones from round four of initial screen.....	109
4.10 Sequencing of phage clones	110
4.10.1 Sequencing of clones from the fourth round of biopanning.....	110
4.10.2 Sequence analysis of all four biopanning rounds.....	114
4.11 Summary	121
Chapter 5 - Results. Analysis of peptides derived from phage display.....	123
5.1 Introduction	123
5.2 ELISA of BSA – peptide conjugates.....	124
5.3 Sepharose bead assay	125
5.4 Peptide Affinity Purification of antibody from solution	127
5.4.1 Peptide Affinity Purification using the phage derived peptide and the mucin core peptide.	127

5.4.2	Purification of C595 antibody from hybridoma supernatant.	128
5.5	Fluorescence Quenching (FQ) analysis of peptides.....	134
5.6	Circular Dichroism (CD) analysis of peptides.	136
5.7	Kinetic analysis of the interaction between C595 antibody and the mucin core peptide APDTRPAPG using surface plasmon resonance.	139
5.7.1	Optimisation of peptide APDTRPAPG immobilisation on the surface of a Pioneer CMD sensor chip.	139
5.7.2	Kinetic analysis of the interaction between immobilised mucin core peptide APDTRPAPG (ligand) and C595 mAb (ligate).....	142
5.8	Summary and Discussion.....	145
Chapter 6 - Results. Mimotope peptides cross- reactive with an anti-steroid hormone antibody.....		149
6.1	Introduction.....	149
6.2	Optimisation of peptide mimotope ligands from lead sequences obtained from a phage display library.....	151
6.2.1	Lead sequence identification.....	151
6.2.2	Identification of the minimum binding unit.....	154
6.2.3	Affinity maturation of the minimum binding unit.....	155
6.2.4	Establishing the correct presentation in the desired application.....	163
6.3	Rationalisation of the process involved in the optimisation of peptide mimotope ligands from lead sequences obtained from a phage display library	166
6.3.1	An ELISA to estimate relative values of the equilibrium association constant (K_A).....	166
6.3.2	Inhibition ELISA's.....	170
6.3.3	Determination of rate constants in the interaction of the affinity-matured, phage derived peptide (d) DYLFQ and mAb 4155.....	176
6.4	Summary and Discussion.....	181
Chapter 7 - Results. Towards the production of a scFv-GFP fusion protein...		184
7.1	Introduction.....	184
7.1.1	Affinity maturation of antibodies.....	184
7.1.2	Selection of high affinity antibodies <i>in vitro</i>	186
7.1.3	Anti-MUC1 scFv construction.....	187
7.1.4	Green fluorescent protein (GFP).....	187
7.1.5	Published examples of scFv-GFP fusion proteins.....	188

7.1.6	Fluorescence activated cell sorting and affinity maturation.....	190
7.2	Strategy for the production of a scFv-GFP gene fusion.....	192
7.3	Mutagenic Primer design	195
7.4	Amplification of C595 scFv and GFP genes with concurrent introduction of unique restriction sites.....	198
7.4.1	Initial plasmid preparation	198
7.4.2	Polymerase Chain reaction to amplify C595 scFv and GFP.....	198
7.4.3	TOPO-TA cloning of PCR products	199
7.5	Production of scFv-GFP gene fusion	200
7.5.1	Restriction digests of pCR 2.1 vectors containing the C595 scFv and GFP mutated PCR products.....	201
7.5.2	Ligation of C595 scFv fragment to GFP fragment	202
7.5.3	TOPO TA cloning of the PCR product of the ligation reaction.....	203
7.6	Ligation of scFv-GFP gene fusion into pCANTAB-5E.....	204
7.6.1	The pCANTAB 5E vector.....	204
7.6.2	Preparation of pCANTAB 5E vector for ligation	205
7.6.3	Preparation of scFv-GFP gene fusion for ligation	206
7.6.4	Ligation of scFv-GFP gene fusion into pCANTAB-5E.....	207
7.7	Expression of scFv-GFP fusion protein using pCANTAB-5E	209
7.7.1	Small scale expression experiment	209
7.7.2	Affinity purification of protein from the supernatant of a small-scale expression experiment.....	211
7.8	Production of a library of mutated C595 scFv genes	213
7.8.1	Mutagenesis of C595 scFv	213
7.8.2	Sequence analysis of C595 scFv mutants	216
7.9	Summary and Discussion	218
	Chapter 8 - General Discussion and Future Work.....	221
	Chapter 9 - Bibliography.....	233
	Appendices.....	251
10.1	Appendix 1 - Sequence Data.....	251
10.2	Appendix 2 - Publications	252

ABSTRACT

Protein-based therapeutics play an increasingly important role in medicine, and the exquisite bio-recognition properties exhibited by antibodies has also led their use in a number of other fields apart from medicine. The increasing use of these molecules requires more efficient methods of purification. A review of the current purification strategies was conducted. Of all the purification methods studied, peptide epitope/mimotope affinity chromatography proved to be the method of choice – resulting in antibodies exhibiting high specific immunoreactivity. The need to tailor unique affinity ligands for each antibody to be purified by peptide epitope/ mimotope affinity chromatography was identified as the major problem with this technique. A review of the technologies available to regulate the antibody-antigen interaction was conducted. Little was published on the use of phage display for the discovery of peptide ligands for use in peptide mimotope affinity chromatography.

Experiments were conducted using a polyvalent phage display library to identify novel peptide ligands for the purification of the therapeutic monoclonal antibody C595. A novel peptide was isolated which demonstrated improved chromatographic performance compared to the standard epitope peptide used to purify mAb C595 from biological supernatants. Circular dichroism showed that the novel peptide had a more highly ordered structure at 4°C and room temperature than the epitope peptide, and fluorescence quenching revealed a higher equilibrium association constant.

A method for the optimisation of peptide mimotopes derived from phage display, cross-reactive with an anti-steroid antibody was investigated. Improvements relating to the selection of lead peptide sequences are described, and the use of mimotopes in an assay to determine concentrations of steroid in solution has been demonstrated. The optimised mimotope was used as an effective paratope-specific affinity ligand.

A novel method for selecting high affinity antibody fragments *in vivo* is described. The C595 scFv gene was fused to a gene encoding green fluorescent protein and incorporated into the phagemid vector pCANTAB 5E. The fusion protein could not be expressed at high levels and could only be detected using epitope affinity chromatography in combination with ELISA.

ACKNOWLEDGEMENTS

I would like to thank all my colleagues at the Cancer Research Laboratories at the University of Nottingham for their help and support.

I thank my supervisor Dr Charlie Laughton and Dr Kevin Brady for their helpful advice during my research. Thank you to my late supervisor Professor Mike Price, for his encouragement and motivation. I also thank Dr Andrea Murray for her guidance in the initial stages of my research.

I thank Dr Sotiris Missailidis for providing help with some of the biophysical techniques used in this thesis. Thanks also go to Mr Ian Davies for his help with the biopanning experiments and good humour.

I also thank the BBSRC for kindly providing funding for my study, and Dr Steve Howell and Dr Andy Badley of Unilever research, for the use of their BIAcore. Thank you to Dr Neil Thomas of the Chemistry department at the University of Nottingham for the use of their facilities.

Finally I would like to thank my parents for their support.

GLOSSARY OF TERMS

bp – Base pairs
BSAU – Biopolymer synthesis and analysis unit
BSA – Bovine Serum albumin
CD – Circular dichroism
CDR – Complementarity determining region
cDNA – Complementary DNA
DNA – Deoxyribonucleic acid
E-3-G – Estrone-3-glucuronide
E. coli – Escherichia coli
EDC – 1-[3-(Dimethylamino)propyl]-3-ethylcarbodiimide
ELISA – Enzyme linked immunosorbent assay
Fab – Antigen binding fragment
FACS – Fluorescence activated cell sorting
Fc – Constant fragment
FDA – Federal Drug Administration (USA)
Fv – Variable fragment
FQ – Fluorescence quenching
GFP – Green Fluorescent Protein
HIC – Hydrophobic interaction chromatography
HIV – Human immunodeficiency virus
HPTFF – High performance tangential flow filtration
IgG – One class of Immunoglobulin
IPTG – Isopropyl- β -D-thiogalactopyranoside
 K_A – Equilibrium association constant
 K_D – Equilibrium dissociation constant
 k_{on} – Association rate constant
 k_{off} – Dissociation rate constant
LB – Luria broth
mAb – Monoclonal antibody
MRNA – Messenger ribonucleic acid
NHS – N-Hydroxysuccinimide
OD – Optical density

PBS – Phosphate buffered saline
PBSA – PBS containing the preservative sodium azide
PCR – Polymerase chain reaction
PECS – Periplasmic expression with cytometric screening
pfu – Plaque forming units
rpm – Revolutions per minute
RNET – Replacement Net
RU – Resonance units
SB – Super broth
scFv – Single chain variable fragment
SELEX – Systematic evolution of ligands by exponential enrichment
SPCL – Synthetic peptide combinatorial library
SPR – Surface plasmon resonance
Taq polymerase – *Thermus aquaticus* DNA polymerase
TBE – Tris-borate-EDTA buffer
UV – Ultra violet
VH – Heavy variable chain
VL – Variable light chain

Chapter 1 Antibody Purification.

1.1 Introduction

1.1.1 Antibodies

Antibodies are members of a family of proteins known as Immunoglobulins. Immunoglobulins are the most critical components of an organism's immune system. The exquisite specificity of recognition demonstrated by Immunoglobulins enables the initiation of a defensive response to foreign substances introduced into an organism. B-lymphocytes carrying specific receptors recognise and bind to the antigenic determinants of the foreign antigen which then stimulates a process of division and differentiation – transforming the B-lymphocytes into plasma cells which synthesise antibody.

Immunoglobulins are divided into five major classes according to their heavy chain components: IgG (γ), IgA (α), IgM (μ), IgD (δ) and IgE (ϵ). The IgG class of antibody is the most useful tool of the immunochemist as a result of their overall stability, this is the class of antibody described here and later in this thesis. IgG exists in four subclasses in humans as a result of minor amino acid differences in each class. The IgG antibody has a molecular weight of approximately 150 kDa. Its structure consists of four polypeptide chains (figure 1.1), two heavy (H) chains (approximately 50 kDa each) linked to two light (L) chains (approximately 25 kDa each) by means of interdomain disulphide bonds. The two variable regions (Fv) contain the antigen recognition elements. These regions contain amino acid sequences that are hyper-variable between different antibodies, these regions which interact with the target antigen are termed complementarity determining regions (CDRs). Each Fv region contains six of these CDRs.

Antibodies can be expressed in *E.coli*. in the form of a Fv fragment. Heavy- and light-chain variable domains (VH and VL) (see figure 1.1) are separately expressed into the periplasmic space where they associate to form a Fv which retains the binding specificity of the parent antibody. However there is a tendency for the Fv fragment to dissociate in some clones (Kay, 1996). This problem has been overcome by joining the genes encoding the heavy- and light-chain variable domains with DNA encoding a flexible linker peptide. This results in the expression of a single protein with covalently linked heavy- and light-chain variable regions and is termed a single-chain Fv (scFv) molecule. The other molecules described above (diabodies, triabodies and tetrabodies) are formed by varying the length of the linker peptide (Hudson, 1999). Fab fragments in which the heavy chain variable region, along with its first constant domain, associates with a whole light chain, have also been constructed (Pluckthun and Skerra, 1989). The association between the constant domains means that this heterodimer is also more stable than the Fv fragment.

1.1.2.1 Applications of monoclonal and engineered antibodies

The use of monoclonal antibodies as therapeutic reagents is well documented (Hudson 1999; Murray *et al.* 2000) and as more molecules receive FDA approval and new targets are discovered, their use is likely to increase (Hudson 1999). The exquisite biorecognition properties displayed by antibodies and antibody fragments can also be put to good use in many consumer goods and industrial reagents. Some of the potential uses of antibody fragments in non-pharmaceutical sectors are outlined in table 1 (Harris 1999). Current examples of the use of antibodies in consumer goods include home pregnancy testing kits, home ovulation tests (Unipath, Bedford, UK), and personal contraceptive systems. Many other examples of the use of antibodies and antibody fragments exist particularly in biosensors.

The use of whole antibodies in consumer goods and industrial reagents does have limitations, because antibodies are large and contain redundant material that is not required in their biological recognition function. Genetically engineered antibody fragments are much more preferable. The use of genetically engineered antibody fragments has many other advantages over whole antibodies: the recognition properties of a particular fragment have the potential to be fine-tuned for a particular

application using the technologies outlined in chapter two. Fusion proteins can also be developed (Kerschbaumer *et al.* 1996; Kerschbaumer *et al.* 1997; Chamow and Ashkenazi 1999; Griep *et al.* 1999), including bispecific recognition elements as described in the biosensor application below. Different expression systems can be utilised (including transgenic milk (Pollock *et al.* 1999), bacteria, insect cells, plants and mammalian cells) for the expression of the reagents at high concentrations.

(Badley *et al.* 1999) describe a biosensor utilising an engineered bispecific antibody (Figure 1.2), whereby the bispecific antibody can be reversibly displaced from its immobilised anchor (a lower affinity analogue of the analyte) by the analyte. The second binding site on the displaced complex is then captured by a second, different immobilised capture molecule. This capture process can then be monitored either electrochemically or by surface plasmon resonance (SPR). The patent also describes a different format for this biosensor. The bispecific antibody is replaced by an antibody-mimotope fusion (see section **1.7.3.3** for description of a mimotope), whereby the initial anchor consists of an antibody immobilised onto the surface, which binds to the mimotope in the mimotope-antibody fusion. The mimotope-antibody fusion is displaced by the analyte (for which the peptide is a mimotope) and the antibody binding to a different site is measured. The regulation of the mimotope recognition reaction by monoclonal antibodies is crucial to the design of this type of sensor.

Antibody fragments as specific binding agents	Application
Food industry	Inhibition of enzymes that cause food spoilage. Protection of sensitive motifs during processing. Molecular mimics to enhance or mask flavours and odours. Antimicrobial preservatives.
Cosmetics and toiletries	Antibacterials and antifungals for toothpastes and mouthwashes. Inhibition of enzymes that cause body odours. Specific antibacterials against dandruff.
Detergents	Stain removal.
Environmental protection	Removal of microorganisms and viruses from water. Removal of organic pollutants from water (e.g. pharmaceuticals). Bioremediation of land. Detection of contaminants.
Manufacturing industry	Separation of products from their intermediates. Clean up of process waters.
Military	Detection of chemical and biological weapons of mass destruction. Detection of explosives.

Table 1: Potential uses for antibody fragments in non-pharmaceutical sectors. Adapted from Trends in Biotechnology July 1999 (Vol 19), B. Harris – Exploiting antibody-based technologies to manage environmental pollution.

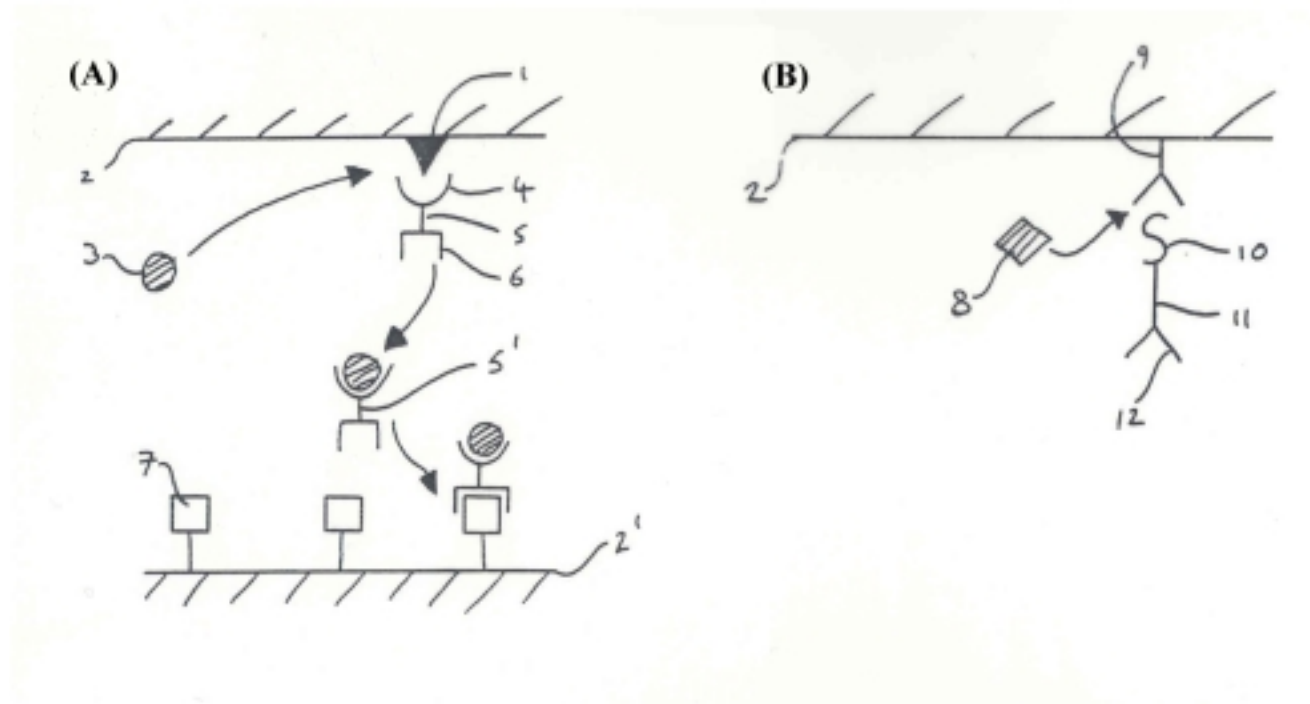


Figure 1.2: Reproduced from (Badley, *et al.* 1999). (A) First surface (2), second surface (2'), analyte of interest (3), structural analogue of analyte (1), bispecific antibody (5), analyte binding site of bispecific antibody (4), capture moiety (7), binding site of bispecific antibody which has binding specificity for the capture moiety (6); (B) First surface (2), Immunoglobulin with affinity for capture moiety on second surface (not shown) (11), binding site which binds to capture moiety on second surface (12), analyte of interest (8), mimotope of analyte of interest (10), immobilised antibody with lower affinity to mimotope than to analyte of interest (9).

1.2 Examples of a therapeutic and a commercially applied monoclonal antibody

The majority of work presented in this thesis involves the murine monoclonal antibodies C595 and 4155. These are described below.

1.2.1 C595 monoclonal antibody (NCRC48)

C595 mAb is a murine IgG3, κ -light chain monoclonal antibody raised against human MUC1 mucin (Price, *et al.* 1990). PCR and cloning technology have been used to determine the primary amino acid sequences of the heavy chain variable region (V_H) and the light chain variable region (V_L) of C595 mAb, enabling modelling of the variable region of C595 mAb to be conducted (Denton, *et al.* 1995). This development facilitated the production of engineered antibodies and fragments, namely a recombinant single-chain fragment (scFv) (Denton, *et al.* 1997), a recombinant diabody (Denton, *et al.* 1999), a human chimera and a humanized antibody all reactive with MUC1 antigen, synthetic peptides and tumour cells (Personal communication Dr. B. Lo, University of Nottingham).

1.2.1.1 MUC1 mucin

MUC1 mucin is a large molecular weight glycoprotein that is composed of over 50% carbohydrate, having a protein core rich in serine, threonine, glycine and alanine (Shimizu and Yamauchi 1982). The protein core contains a large domain of a variable number of highly conserved 20 amino acid repeat sequences (**PDTRPAPGSTAPPAHGV TSA**) (Gendler, *et al.* 1988). Variation in the number of tandem repeats leads to extensive polymorphism (Swallow, *et al.* 1987). The unmasking of epitopes in the protein core; the appearance of novel carbohydrate epitopes, resulting from aberrant glycosylation and expression at elevated levels in malignant cells, mean that MUC1 has been comprehensively studied as an effective tumour marker. A large number of monoclonal antibodies have been developed which are reactive with various epitopes contained within MUC1 (Rye and Price 1996). Monoclonal antibody C595 is one such antibody.

1.2.1.2 Clinical uses of C595 mAb

The use of antibodies in the diagnosis and treatment of disease has previously been reviewed (Murray, *et al.* 2000). The C595 mAb has been used for *in vivo* diagnostic tests to enable the identification of malignant ovarian tumours using immunoscintigraphy (Perkins 1993) and also to measure circulating mucin in breast cancer patients *in vitro* using immunoassay (Dixon, *et al.* 1993). Intra-vesicle administration of radiolabelled ($^{111}\text{Indium}$) C595 mAb followed by gamma camera imaging has been used to detect bladder tumours (Hughes, *et al.* 2001). This work has been followed by the use of Technetium-99m labelled C595 mAb, improving the quality of imaging (Murray, *et al.* 1999; Simms, *et al.* 2001). ^{188}Re – C595 antibody conjugates are currently being used for radioimmunotherapy of transitional cell bladder cancer (Murray, *et al.* 2001). Figures 1.3 and 1.4 provide an excellent example of the benefits of immunoscintigraphy compared to more conventional techniques. Figure 1.3 shows the tumour as a poorly visible opaque region, but figure 1.4 clearly defines a red “hot-spot” where the radiolabelled antibody has accumulated. The image in figure 1.4 is clearly a much greater aid to diagnosis than the grainy image displayed in figure 1.3.

1.2.2 mAb 4155

Monoclonal antibody 4155 is a commercially developed murine IgG1 anti-steroid antibody (Unilever Research, UK), raised against estrone-3-glucuronide (E-3-G) (Badley, *et al.* 1999). E-3-G is a urinary metabolite of estradiol. A rise in the levels of E-3-G in female urine can be used to determine the start of the most fertile period in the human menstrual cycle. A surge in the urinary concentration of luteinizing hormone (LH) can also be used to mark the end of this fertile period. MAb 4155 and an anti-LH mAb have been incorporated in a commercial test-kit (PersonaTM, Unipath, Bedford, UK) to enable the determination of the most fertile period in the human menstrual cycle (May 1994).

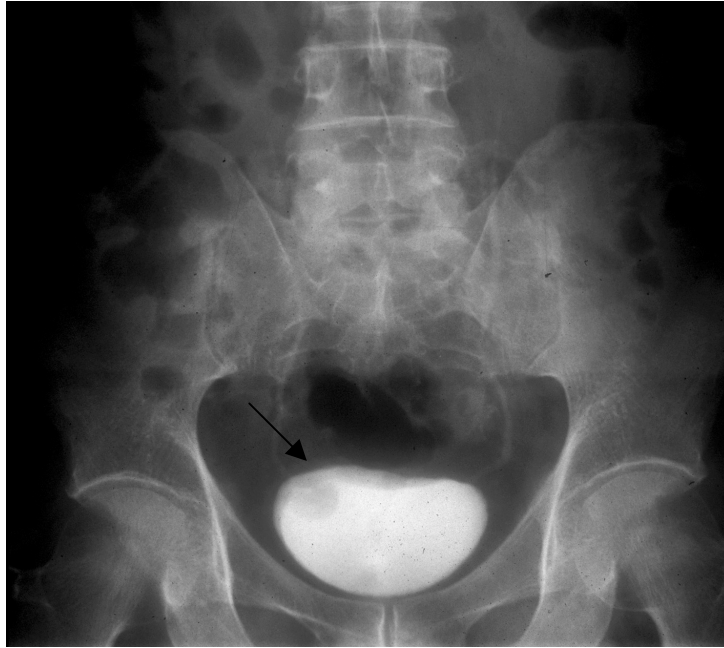


Figure 1.3: Intravesical urogram. Bladder is filled with a contrasting agent. There is a suspicion of the presence of a tumour which takes the form of a filling defect (arrow).

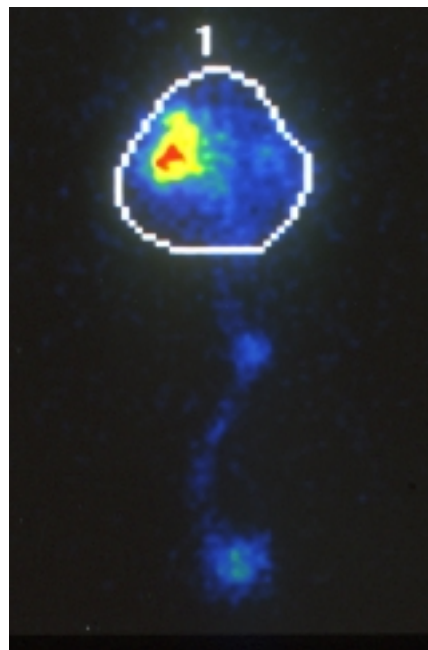


Figure 1.4: Radioimmunosintigraphy reveals the tumour and corresponds to the region of the filling defect. Tissue at this site later identified as being cancerous by histopathology. (Pictures courtesy of Dr A. Murray, University of Nottingham).

1.3 Approaches to antibody purification

The increasing use of antibodies and engineered antibody fragments in medicine, consumer goods and as industrial reagents necessitates the application of methodologies for the efficient purification and concentration of these reagents from biological media. Protein purification techniques require the selective adsorption of either the biomolecule of interest or contaminating molecules to produce a pure homogeneous product. The adsorption medium can be presented to the feed in a number of different ways, each with their own unique advantages.

1.3.1 Column chromatography

Column chromatography is the conventional technique used to house a variety of matrices; including media for ion exchange chromatography, hydrophobic interaction chromatography, affinity chromatography and gel filtration. Conventional column chromatography necessitates clarification of the crude feed before application to the column, to prevent fouling of the column. Clarification of the crude feed requires centrifugation and microfiltration steps to remove particulate matter. Centrifugation is time consuming and with the microfiltration step, fouling of microfiltration membranes can occur. Product may also be lost by degradation in the clarification process. All of these factors add to the operational cost of the process when dealing with industrial scales of biological material (feed).

1.3.2 Fluidized bed and expanded bed adsorption

Fluidized bed and expanded bed adsorption eliminate the need for clarification of the crude feed. The adsorbent is first expanded and equilibrated by applying an upward liquid flow to the column. The balance between particle sedimentation velocity and upward liquid flow velocity creates a stable fluidized bed. Unclarified feed is applied to the expanded bed in the upward liquid flow. The target proteins bind to the adsorbent and contaminants pass through. Non-specifically weak binding contaminants are then washed through. Liquid flow is then stopped and the adsorbent material settles in the column. The column adapter is then lowered onto the surface of the sedimented bed. The direction of buffer flow is reversed and using a suitable buffer the target protein is eluted from the column. The column can then be regenerated ready for use. This technique can be used with an affinity ligand on the

adsorbent and also in ion exchange techniques. An overall yield >90% obtained by an expanded bed ion exchange adsorption procedure, followed by a final affinity chromatography polishing step has been reported (Hansson, *et al.* 1991).

1.3.3 High performance Tangential Flow Filtration (HPTFF)

HPTFF is a separation technique that exploits differences in both the size and the charge characteristics of biomolecules. These differences in size and charge are used in conjunction with membranes with a carefully controlled pore size to elicit effective separations. The technique requires the samples to be in a reasonably pure state already, otherwise membrane fouling can occur. Membrane fouling occurs when the pores of the membrane become blocked with debris present in the sample, perturbing the carefully engineered properties of the membrane. Charged membranes are often used to enhance the selectivity of the separation. Similar to ion exchange chromatography, adjustments in pH and ionic strength enable the maximisation of the differences in charge and size between the product and the impurity. The separation is carried out with a transmembrane pressure gradient to elicit the separation. HPTFF enables the purification of proteins in a single purification step. But as with ion exchange chromatography, when selecting purely using the parameters of size and charge, there is no guarantee of the standardisation of the immunoreactivity of the purified antibody. Since this is a 2D-separation technique – separating by both size and charge, the likelihood that proteins with similar biochemical characteristics will be co-purified is less than in ion exchange chromatography.

1.3.4 Magnetic beads

Magnetic beads are available from a number of manufacturers. These include magnetic beads coated with streptavidin and magnetic agarose beads incorporating Fe₃O₄ (Magnogel (Dean, *et al.* 1985)) in the interior of the gel beads. These reagents have applications in situations where column operation is not favoured, for example with viscous solutions or in the presence of partly soluble cell debris. The cost of such beads in comparison to other media used in expanded bed and fluidized bed techniques generally prohibits their use in large-scale industrial applications.

1.4 Physical separation techniques

Physical separation techniques are based on the differences in biochemical properties (such as overall charge, size of molecules, and hydrophobicity) between the protein of interest and the contaminants to elicit a separation of the two.

1.4.1 Ion exchange

Ion exchange chromatographic separation techniques utilise the overall charge of the protein to effect a separation. Utilising buffers at different pH it is possible to impose a particular charge on the biomolecule. Antibodies for instance have isoelectric points within the range 6-8 (Danielsson, *et al.* 1988). Thus if the pH of the buffer containing the antibody is lower than the pI for the antibody, the antibody will have a net positive charge, since both acidic and basic moieties will be protonated. Conversely increasing the pH of the buffer containing the antibody above the pI for the antibody will give the antibody a net negative charge.

Ion exchange chromatography can be used either as a positive chromatographic step (protein of interest is retained on the matrix and the contaminants pass through); or as a negative chromatographic step (contaminants bind to the matrix and the protein of interest passes through). When used as a positive chromatographic step for the purification of antibodies, $\text{pH} < \text{pI}$ (antibody) the antibody has a net positive charge enabling a cation exchange matrix to be used to bind antibody. When used as a negative chromatographic step, $\text{pH} \sim 7$ and an anion exchange column is used; at this pH immunoglobulins pass through (relatively de-ionised at this pH) and many contaminating proteins including albumin ($\text{pI} \sim 4.7$) bind to the matrix. Isolation of mAb C595 from murine hybridoma cell culture supernatant utilising a cation exchange matrix has been reported (Denton, *et al.* 2001).

The use of ion exchange chromatography to purify monoclonal antibodies has the disadvantage that the activity of the purified antibody is not standardised. That is, all of the antibody purified may not be fully immunoreactive. There is also no guarantee that proteins with similar biochemical parameters to those of the antibody will not be co-purified. Ion exchange chromatography can be used in the conventional column format and in an expanded bed or fluidized bed format.

1.4.2 Gel filtration

The process of gel filtration molecules in solution are separated according to differences in their sizes as they pass through a column packed with a chromatographic medium which is a gel. Gels manufactured for use in gel filtration contain a carefully controlled range of pore sizes. Relatively small molecules are able to diffuse into the gel from the surrounding solution, whereas relatively large molecules are prevented by their size from diffusing into the gel and are confined to the outside solution. The mixture containing the molecules to be separated is applied to the top of the column in solution. The sample zone moves down the bed as eluent is added to the top. Small molecules that are able to diffuse into the gel are retarded in their passage through the column compared to the larger molecules that cannot enter the pores. Larger molecules elute from the column first, followed (in order of size) by smaller molecules. Gel filtration can also be used as an effective desalting step, where the larger biomolecules pass through the column unretarded compared to the salt ions. Gel filtration is superior to dialysis techniques, where considerable levels of product loss can occur. Gel filtration was used to desalt samples eluted under chaotropic conditions in the experiments described in this Thesis. Gel filtration is conducted in a conventional column chromatography format.

1.4.3 Hydrophobic Interaction Chromatography (HIC)

HIC utilises the differences in hydrophobicity between proteins to effect separations. Purification techniques use the reversible interaction between the protein and the hydrophobic surface of the chromatographic medium. Samples are bound to the column in high ionic strength buffer and are eluted by a decreasing salt gradient. Target proteins may also be eluted by adding chaotropic species; adding detergents; changing pH; changing temperature; or reducing eluent polarity (ethylene glycol gradient up to 50%). HIC is useful for removing major serum contaminants such as albumin and transferrin, which are washed straight through the column.

1.5 Affinity Purification Techniques

Affinity purification techniques involve the selective adsorption of a specific binding agent (e.g. a monoclonal antibody) onto a solid phase adsorption matrix from which the specific binding agent can subsequently be eluted. The solid phase material may take one of a number of formats. These include the use of chromatography columns

that hold a conventional packed bed of adsorbent (onto which the target ligand is immobilised); fluidized bed adsorption; expanded bed adsorption and magnetic beads. None of the physical techniques discussed in the previous sections generally produce the degree of purity and concentration achieved with the relative ease of using affinity techniques. Several different steps may need to be incorporated into a purification strategy using physical separation techniques (Amersham Pharmacia Biotech. 2000).

1.5.1 Fc Binding Proteins

Protein A (Forsgren and Sjoquist 1966) and protein G (Olsson *et al.* 1987) are bacterial proteins from *Staphylococcus* and *Streptococcus* respectively, which bind specifically to the Fc region of polyclonal and monoclonal IgG type antibodies. Immobilised on a matrix they can be used to purify monoclonal IgG type antibodies. Synthetic and recombinant mimics of protein A also exist which also elicit effective purification (Fassina, *et al.* 1996; Li, *et al.* 1998). Protein G elution is conducted by changing the pH of the running buffer. Protein A elution can be conducted by changing the pH, using denaturing agents or chaotropic salts. Protein A and Protein G have the disadvantages that both active and inactive antibody is potentially purified, and by the nature of their action (Fc binding) are unable to purify antibody fragments.

1.5.2 Recombinant Protein Tags

A common method employed in the purification of antibody fragments is the use of protein affinity tags. Genetic engineering techniques enable the addition of specifically designed tags to create gene fusions for use in affinity purification. A large number of affinity tails have been developed to facilitate the downstream processing of recombinant proteins (Nygren, *et al.* 1994; Boldicke *et al.* 2000). Kits based on several of these tails have been produced commercially where the expression vector is manufactured with the corresponding affinity resin. A number of affinity tail/binding partner systems exist, they can be divided into three categories:-

(i) EPITOPE TAGS

Commonly used epitope tags include the FlagTM peptide – an 8aa peptide **DYKDDDK** (Gama and Breitwieser 1999) that binds to a specific mAb (IBI Kodak, USA); the E-tag – a 13aa peptide **GAPVPYDPLEPR** (Krammer 1998) that binds to a specific mAb and is incorporated into the pCANTAB vector in the RPAS

expression system (Pharmacia, Sweden). The peptide tag **CLDKSGLPSDRFFA** has also been used to purify a fusion protein by immunoaffinity chromatography (Boldicke *et al.* 2000).

(ii) METAL CHELATORS

These consist of polyhistidine tails enabling the purifying of recombinant protein by immobilised-metal-ion affinity chromatography (IMAC) (Novagen, USA; Invitrogen, USA; Qiagen, USA).

(iii) PROTEIN PROTEIN INTERACTIONS

Commonly used protein tags include fusions with glutathione-S-transferase (GST), GST binds to glutathione (Pharmacia, Sweden); fusions with maltose-binding protein (MBP), MBP binds to amylose (New England Biolabs, USA); staphylococcal protein A and its derivative ZZ, binding to IgG (Pharmacia, Sweden).

Another example which does not fit into these categories is the PinPoint™ system which utilises the *in vivo* biotinylation by *E.coli* of a 13kDa sequence attached to the target protein, combined with affinity purification of the fusion protein on monomeric streptavidin (Promega, USA).

Gene fusion strategies introduce an additional problem into the downstream processing since a site-specific cleavage is required to remove the affinity tag. A large number of chemical and enzymatic methods are available to facilitate this (Nygren, *et al.* 1994). Purification of antibody fragments using this method has the disadvantage that inactive recombinant antibody fragments may be co-purified alongside active antibody fragments.

1.5.3 Paratope specific binding ligands

The paratope of an antibody is the binding cleft in the structure of the antibody that binds specifically to a particular antigen or hapten molecule. Paratope specific binding ligands offer the unique advantage that purified antibodies are of high and standardised immunoreactivity, since only functional molecules bind to the affinity matrix and are later eluted. The key feature of this purification method is the need to

discover and fine tune the ligand used. Some ligands may have too high affinity for the matrix (E3G – 4155 mAb interaction (Badley, *et al.* 1999) and the elution conditions needed may be too harsh; other ligands will have too low affinity and so not effectively concentrate antibody from the feed. Hence the need for the regulation of the affinity of the recognition process of epitopes/mimotopes by monoclonal antibodies.

1.5.3.1 Antigen affinity chromatography

Antigen affinity chromatography enables the purification of a specific antibody from a polyclonal antiserum. It enables the purification of monoclonal antibody samples contaminated with irrelevant or unreactive immunoglobulin protein, or other contaminants. The antigen is coupled to an appropriate matrix. Large amounts of antigen may be required in the preparation of the matrix, and there may be significant loss as well as inactivation during successive rounds of use. It is these problems of antigen availability, high cost, poor chemical and biological stability that prohibit the large-scale use of this technique. For this reason the use of smaller more stable ligands immobilised onto the affinity matrix is much more preferable.

1.5.3.2 Epitope affinity chromatography

The regions of a protein antigen that are recognised by the combining sites of an antibody are known as antigenic determinants or epitopes. Epitopes can be divided into two types: - continuous and discontinuous epitopes.

Continuous epitopes

Sequences obtained by screening peptide libraries are often identical to those of the recognition sequences of the corresponding natural ligands (Katz 1997). There are many examples where the core consensus sequences of phage-displayed epitopes recognised by monoclonal antibodies are similar to the sequences of the proteins against which the antibodies were originally raised (Cwirla, *et al.* 1990; Scott and Smith 1990; Felici 1991; Stephen and Lane 1992; Katz 1997; Tighe, *et al.* 1999). C595 monoclonal antibody has been demonstrated to bind to the **RPAP** motif found in phage libraries (Laing, *et al.* 1995; Smith 2000); and synthetic peptide libraries (Murray, *et al.* 2000). The **RPAP** motif is present in the primary sequence of the

antigen to which the antibody was originally raised (Price, *et al.* 1990). The **RPAP** motif is termed a continuous epitope.

Discontinuous epitopes

Examples of discontinuous epitopes exist where the sequences of the proteins against which the antibodies were originally raised bears no relation to sequences derived from phage display or other peptide libraries (Felici, *et al.* 1993; Luzzago, *et al.* 1993). Such epitopes are made up of residues that are not contiguous in the sequence but are brought together by the folding of the peptide chain (Regenmortel 1995). These discontinuous epitopes may also be termed as structural epitopes since the binding properties of the residues in the antigen are directly as a result of the structure of the antigen and not the primary sequence.

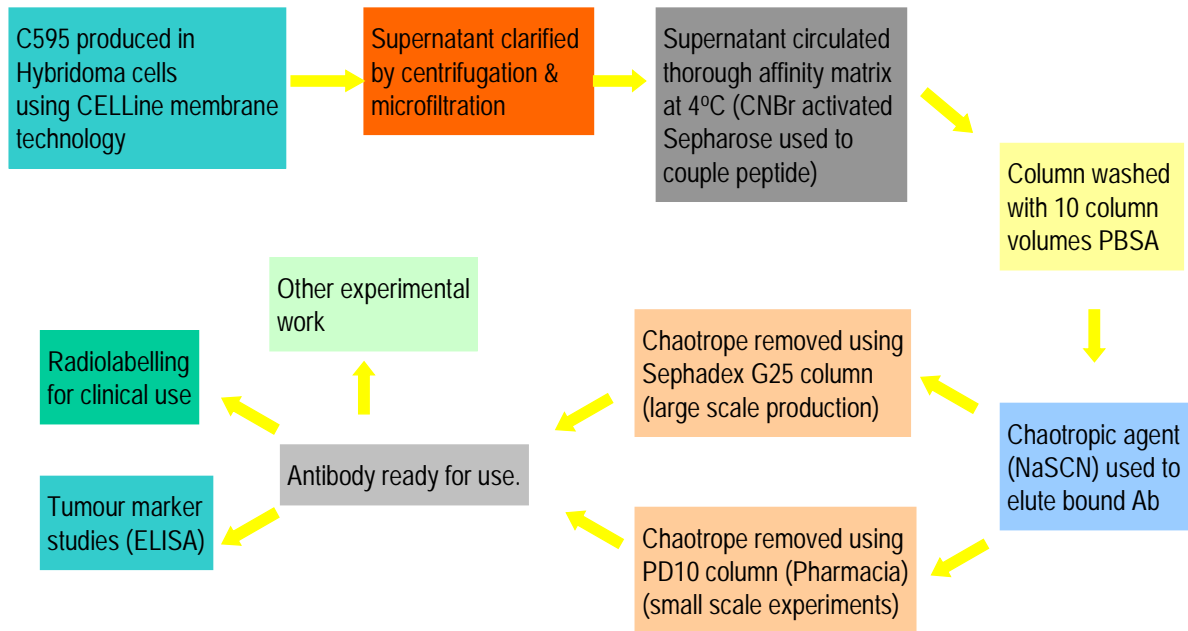


Figure 1.5: Strategy for the purification of mAb C595 from hybridoma supernatant.

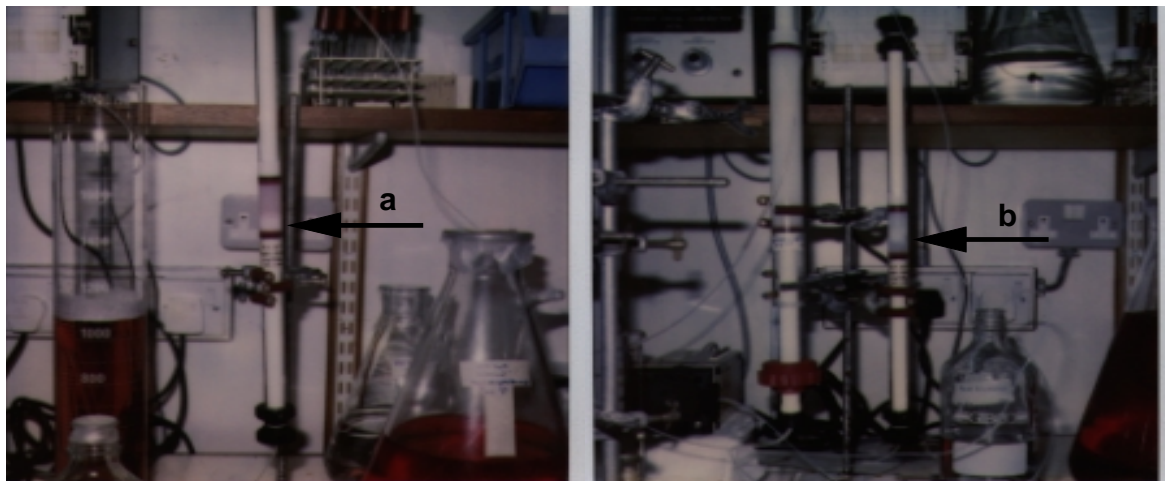


Figure 1.6: Peptide affinity purification of monoclonal antibody C595 from tissue culture supernatant. Arrow (a) illustrates colour change of column upon antibody binding (column flow bottom – top); arrow (b) illustrates band movement through the column upon elution using 3M sodium thiocyanate. The second picture also shows the G25 column used to de-salt the eluted fractions. The G25 column was used in line with the peptide affinity column, and fractions were collected from the eluent of the G25 column.

The critical binding region represented by the epitope is typically synthesized using conventional solid phase techniques, and then covalently linked to a chromatographic matrix. A variety of chemical coupling methods are available to ensure optimal presentation of the ligand to the target molecule (Wilchek and Miron 1999). The smaller peptide (compared to the whole antigen) is likely to be much more stable with less risk of inactivation during successive rounds of use. However since the peptide is synthesized from naturally occurring (L) amino acids, the peptides may be susceptible to proteolysis (Guichard, *et al.* 1994). Overall synthetic peptide ligands have many advantages over using whole antigens; notably they are generally resistant to both chemical and biochemical degradation, are sterilizable in situ and can be produced at an affordable price.

Epitope affinity chromatography is the technique that is currently used to concentrate and purify C595 mAb from hybridoma supernatant for clinical and laboratory use (Murray, *et al.* 1997; Murray 1998; Denton, Murray *et al.* 1999). Figure 1.5 outlines the overall purification strategy.

1.5.3.3 Mimotope affinity chromatography

A mimotope is a molecular sequence which mimics the epitopic region of a particular antigen, but which does not contain the specific amino acid sequence that comprise the epitope. A mimotope is structurally distinct from the primary structure of an epitope (for proteinaceous ligands), but functionally very similar and capable of binding in a similar fashion to the binding cleft of the antibody (Paratope) directed to the antigen containing the particular epitope (Katz 1997).

Peptide sequences have also been discovered that are mimics of antigens that are non-proteinaceous. These include biotin peptide mimotopes that bind to streptavidin (Giebel, *et al.* 1995), peptide mimotopes of carbohydrate antigens (Agadjanyan, *et al.* 1997; Kieber-Emmons 1998), peptide mimotopes of DNA (Sibille, *et al.* 1997) and peptide mimotopes of a steroid hormone (Murray, *et al.* 2001). A review of the discovery and applications of mimotopes is given by (Meloan, *et al.* 2000).

Mimotope affinity chromatography is identical to epitope affinity chromatography, except that a mimotope peptide is immobilised onto the affinity matrix instead of an

epitope peptide. Mimotope peptides can have higher as well as lower affinities for a particular monoclonal antibody, and so elution conditions for a particular antibody may well differ between epitope and mimotope matrices. Peptide analogues can be synthesized replacing the L-amino acid residues with D-amino acid residues (Murray, *et al.* 2000), reducing their susceptibility to proteolysis. Other examples of peptide analogues include the replacement of L-amino acid residues by unnatural residues (e.g., sarcosine and β -alanine) and the modification of peptide bonds (Guichard, *et al.* 1994; Farlie, *et al.* 1998).

Mimotope affinity chromatography using mimotopes derived from phage display has been demonstrated to effectively purify and concentrate C595 mAb from hybridoma supernatant (Smith, *et al.* 2002). Mimotope affinity chromatography using an affinity-matured mimotope (N/C terminal reduction, replacement net analysis), derived from a phage display library has been demonstrated to effectively purify and concentrate 4155 mAb from hybridoma supernatant (Murray, *et al.* 2001).

As with epitope affinity chromatography, the same problems of natural target availability, high cost, poor chemical and biological stability that prohibit the large-scale use of the natural target as an affinity ligand are overcome by mimotope affinity chromatography. Small short peptide sequences stable to sanitization, less susceptible to proteolysis (synthesized using (D) amino acids), cheap and easy to synthesize are much preferable to using the immobilised natural target molecule.

Non-proteinaceous, paratope specific affinity ligands

The anti-steroid antibody mAb 4155, raised against estrone-3-glucuronide (E-3-G) (as described in section 1.2.2) is purified using lower affinity analogues of the target ligand (Badley, *et al.* 1999). Mab 4155 cross-reacts with several analogues of E-3-G, the structures of which are shown in figure 1.7. The hapten to which the antibody was raised (E-3-G) has the highest affinity for the antibody, followed by 17 beta-Estradiol 3-(beta-D-glucuronide), Estriol 3-(beta-D-glucuronide) and finally estrone with the lowest affinity. For the purification of mAb 4155 estrone is linked to beaded agarose through the hydroxyl group of estrone (Pharmacia epoxy 6B Sepharose). Hybridoma feedstock clarified by centrifugation is then applied to a column containing the chromatography media. The interaction of mAb 4155 with the estrone immobilised

on the column is a high affinity interaction that is not perturbed by non-denaturing buffers, allowing contaminating proteins to be washed off the column. The higher affinity analogue estradiol 3-(beta-D-glucuronide) is then applied to the column to desorb the bound antibody, which is then passed down a gel filtration column to remove unbound estradiol 3-(beta-D-glucuronide).

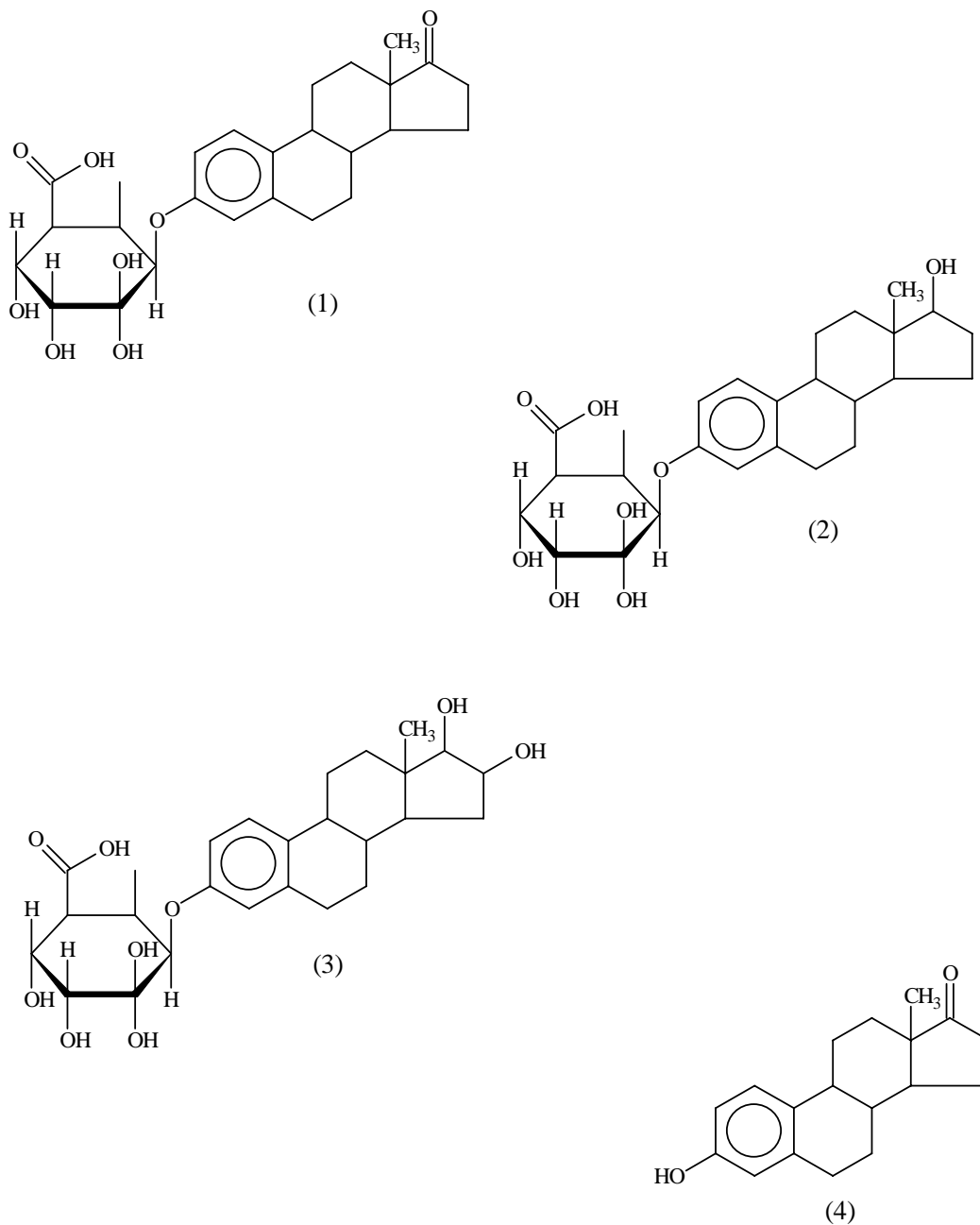


Figure 1.7: (1) Estrone beta-D-glucuronide (“Estrone-3-glucuronide”), (2) 17beta-Estradiol 3-(beta-D-glucuronide), (3) Estriol 3-(beta-D-glucuronide) and (4) Estrone.

The affinity-purified antibody has estradiol 3-(beta-D-glucuronide) bound, allowing subsequent use in a competition assay format. This resultant antibody-hapten complex (the antibody is bound to blue latex particles) is used in the Persona™ (Unilever, UK) test kits, where the bound estradiol 3-(beta-D-glucuronide) is competed from the antibody by E-3-G present either in the urine sample, or E-3-G on the test-strip. The intensity of the blue latex beads on the test strip gives a direct indication of E-3-G levels in the urine sample (May 1994).

Another example of a non-proteinaceous paratope-specific binding ligand, is the use of DNA-aptamers as specific affinity ligands. Purification of a human L-selectin-Ig fusion using an immobilised DNA-aptamer has been described (Romig, *et al.* 1999).

1.6 Summary

Epitope / mimotope affinity chromatography is the method of choice for the purification and concentration of monoclonal antibodies and engineered antibody fragments. These methods produce a product of standardized and high immunoreactivity from biological feedstocks. Epitope / mimotope affinity chromatography enables the single-step purification and concentration of monoclonal antibodies and engineered antibody fragments raised against proteinaceous and non proteinaceous species utilising matrices linked to non-costly, easily synthesized robust ligands, which can be sanitised in situ.

The discovery of epitopes / mimotopes is crucial to the design of ligands for application in epitope / mimotope affinity chromatography; and for the application of mimotopes in biosensors used to detect proteinaceous or non-proteinaceous analytes utilising monoclonal antibodies and engineered antibody fragments.

The fine-tuning of the recognition properties of engineered antibody fragments and fusion proteins is also crucial to their application alongside mimotopes in biosensors.

The next chapter outlines the methodologies which can be used to manipulate the recognition of peptide epitopes / peptide mimotopes by monoclonal antibodies and antibody fragments.

2 Chapter 2 Regulation of peptide antibody interactions.

2.1 Introduction

As outlined in the previous chapter, the fine specificity of the interaction between antibodies and their derivatives, and the species they bind to, has led to these molecules being used in a wide range of applications. The work contained within this thesis has sought to look at the two components of this interaction.

In regulating the interaction between antibodies and peptide epitopes / mimotopes two different approaches can be taken:

1. The antibody (or antibody fragment) can be considered as constant and methods employed to vary the structure of the binding moiety such that the affinity of the antibody for the specific binding moiety is up regulated or down regulated.
2. The binding ligand can be considered as constant and methods employed to vary the structure/residues contained within the Paratope of the antibody or antibody fragment, or the residues outside the Paratope can be changed in order to influence the binding characteristics of the antibody.

The question may be asked why one may need to down regulate the affinity of interaction in such binding events. The need to be able to regulate the affinity of the interaction is important in a number of areas.

(i) The affinity purification of proteins.

It is of little use discovering a novel binding peptide to purify a particular protein (e.g. antibodies) from biological media, if the conditions required to break the interaction and release the protein are too harsh and result in the permanent destruction of the recovered protein (an example of this was given in chapter one (section **1.5.3.4**)). It is also of little use if the interaction between the peptide and the protein is too weak to elicit an effective separation of the protein of interest from the biological milieu. Hence the need to regulate the affinity of the interaction such that the protein-ligand

interaction can easily be perturbed, allowing the recovery of active product; and also to regulate the affinity of an interaction so that an efficient separation can be achieved. Chapters 4 and 5 of this thesis describe work that has been conducted to investigate the regulation of peptide recognition by a monoclonal antibody, in this case the affinity of the monoclonal antibody for the ligand was increased relative to the native epitope sequence.

(ii) Competition ELISA.

The dynamic range of a competition ELISA is intrinsically linked to the affinity of the antibody for the immobilised ligand. High affinity ligands (small K_D) will be useful for measuring small concentrations of competing analyte in solution within the normal timescale of an assay. The kinetics of the interaction mean that high concentrations of analyte will not be easily measured with high affinity ligands, since the time taken for the assay to reach equilibrium conditions may well be outside the timescale in which the assay is performed. Hence high affinity ligands will be limited to low analyte concentrations, and lower affinity ligands will be limited to higher analyte concentrations. For a useful assay (one occurring on a practical timescale) which is measuring a particular analyte that could be present over a range of concentrations it is desirable to have a combination of low affinity and high affinity ligands. This work is described in chapter 5.

(iii) Therapeutic applications.

The use of antibodies and their derivatives as “magic bullets” delivering therapeutic reagents to specific sites within the body, and for diagnosis is well documented. Higher affinity antibodies could reduce the amount of antibody required for use as a diagnostic reagent for tumour markers displayed on the cell surface. However high affinity antibodies may reduce tumour penetration as a result of strong binding to cells immediately outside capillaries, reducing the overall uptake of the reagent by the tumour. There is a continuing debate as to whether MUC1 antigen displayed on the cell surface is internalised, internalisation of antigen bound to the therapeutic antibody would favour the use of higher affinity antibodies. Chapter 6 describes work carried out to construct a library of scFv mutants displayed on the surface of bacteriophage, which could be interrogated by selecting for binding and isolated by fluorescence

activated cell sorting (FACS). The eventual aim being the isolation of scFv molecules with increased affinity for the target molecule.

Determining the key components involved in the regulation of antibody affinity for peptide epitopes / peptide mimotopes will enhance our understanding of the antibody recognition process. The aim of this chapter is to outline the different library technologies that are currently available and provide a rationale for the choice of library technologies that were used to conduct the work described in this thesis.

2.1.1 Library Technologies

Libraries can be divided into two distinct types: non-biological libraries containing synthetic, low molecular weight compounds; and biological libraries consisting of nucleic acids, peptides and proteins. Figure 2.1 illustrates this. When a library is constructed, the information detailing the composition of the compound must be readily recoverable. Examples used for both biological and non-biological libraries include the use of array technology to allow a particular compound to be linked to a spatial address in a matrix, and various labelling systems including nucleotide tags for example (see section 2.2.3).

Biological libraries can be further classified into two different types: **Displaying systems**, (where a protein or peptide is physically linked to the genetic information encoding it, thus enabling the recovery of sequence information for a particular peptide or protein) see table 2.1; and **“Display-less”** systems (where the link between a protein or peptide and the genetic information encoding it is purely a spatial association with no direct physical link) see table 2.2.

The displaying and “display-less” systems can be further divided into two more categories: *in vivo* and *in vitro* systems. *In vivo* systems all rely on the use of cells and/or virus particles. These methods are subject to biological constraints associated with protein export and presentation that may compromise the viability of the cell or virus.

The size of these libraries is also limited by the particular transformation efficiency of the cells used. These constraints impose an upper limit of diversity obtained using *in vivo* systems of $\sim 10^9$ recombinants, although exceptional libraries of $>10^{10}$ members have been described (Fitzgerald, 2000). *In vitro* systems are not subject to the biological constraints associated with cell and virus viability, and since whole cells are not used, the transformation efficiency is not a relevant factor. *In vitro* libraries are thus capable of exhibiting a much larger diversity since they are limited only by the quantity of DNA that can be physically added to cell-free protein synthesis systems (potentially up to 10^{14} – 10^{15} molecules (Fitzgerald, 2000).

2.1.2 The distinction between screening and selection in library technologies

It is important to note the distinction between the interrogation of libraries by either *screening* or *selection*. Selection strategies are much more powerful than screening strategies. In a screen, variants are analysed on an individual basis for a given property (e.g. the ability to bind to a particular ligand) to obtain the variant with the “best” properties. Selection involves a pool of all the variants. The whole pool is subjected to a selection step that directly yields molecules that exhibit the “best” properties. The enriched pool can then be propagated and re-selected. The key consequence of the selection and propagation steps is the enrichment process which enables the rapid isolation of mutated proteins from the library. The rapid isolation of binding proteins from the library enables the surveying of a greater portion of sequence space. For example, the mutation of multiple residues in the protein enables the study of complex “non-additive” combinatorial effects that could not have been predicted *a priori*. This has led to the use of libraries as sources of proteins exhibiting *de novo* binding activities. One example is the use of filamentous bacteriophage displaying antibody repertoires to mimic immune selection (Hoogenboom and Winter, 1992). This work demonstrated that human antibody fragments with specific binding affinities could be made entirely *in vitro*.

The use of “second generation” libraries, enables the sequence landscape around a clone isolated from an initial selection process (“first generation” library) to be examined to find local optima. The second-generation library consists of variants of the sequence of a particular clone isolated from the first generation library. The

second-generation library of variants is typically constructed using the mutagenesis techniques as described in section **2.5**.

			Library size	Encoded entity	Valency of encoded entity	Linker	Code
Displaying system	<i>In vivo</i>	Viral display	10^9 - 10^{10}	Protein / Peptide	Monovalent or polyvalent	Viral capsid	DNA
		Peptide on plasmid	10^6	Peptide	Monovalent	DNA binding	DNA
		Peptide Barcode	10^6	Protein	Monovalent	Protease cleavage site	Peptide sequence
		Cell-based display	10^6	Protein / Peptide	Polyvalent	Prokaryotic or Eukaryotic cells	DNA
	<i>In vitro</i>	Ribosome display	10^{14} - 10^{15}	Protein / Peptide	Monovalent	DNA binding	DNA / RNA
		Covalent Display Technology	$>10^{12}$	Protein/ Peptide	Monovalent	Physical Attachment	DNA
		RNA-peptide fusions	10^{14} - 10^{15}	Peptide	Monovalent	Physical Attachment	DNA
		Non-biological Display	10^6	Protein / Peptide / other components	Monovalent or polyvalent	Physical attachment	DNA / spatial address/ chromatographic property

Table 2.1: Displaying selection systems, showing larger library sizes are achieved using *in vitro* systems compared to *in vivo* systems, where the limiting factor is the transformation efficiency of the cells used. Also shown is the link between genotype (code) and phenotype (encoded entity). Note the valency of the displayed entity.

			Library size (transformants)	Encoded Entity	Valency of encoded entity	Linker	Code
Display-less system	<i>In vivo</i>	Protein expression	10^6	Protein	Monovalent	Spatial address	DNA
		Periplasmic expression with cytometric screening (PECS)	10^6	Protein	Monovalent	Periplasmic space inside the cell	DNA
	<i>In vitro</i>	Man-made cell compartments	$>10^7$	Protein (catalyst)	Monovalent	Aqueous cells in oil/water emulsion	DNA

Table 2.2: Display-less selection systems. Note that for display-less systems the link between the encoded protein/peptide and the DNA is a spatial association.

Screening of synthetic peptide libraries still has an important role to play in analysing the interaction between antibodies and the antigens they bind.

2.2 Synthetic Peptide Libraries

The foundations of synthetic peptide libraries lie with the work of Mario Geysen (Geysen, *et al.* 1984) who developed mimotope libraries and Lam, *et al.* 1991 and Furka *et al.* 1991, who described methods for synthesizing peptides on individual beads. The work of Geysen allowed the concurrent synthesis of large peptide libraries on derivatized polyethylene or polypropylene pins arranged in a microtitre plate format allowing ELISA to be conducted to measure antibody binding (Murray, *et al.* 2000). These synthetic peptide libraries enable the study of epitopes defined by antibodies reactive with antigens of known primary structure. Critical information concerning the role of individual residues in a particular antigen can be determined using the methods described below.

2.2.1 Pepscan – The application of synthetic peptides in epitope mapping.

A set of overlapping peptides are synthesized that span the length of the antigenic sequence of interest. As such this method is limited to the discovery of continuous epitopes where knowledge of the primary antigenic sequence already exists. This set of peptides spanning the antigenic sequence is linked to derivatized polyethylene or polypropylene pins, allowing them to be placed in the wells of microtitre plates so that ELISA can be used to measure antibody binding. (Murray, *et al.* 2000). This enables the linear epitope to be defined for a particular antibody. The application of this technology to been used to characterise the epitopes of a number of MUC1 mucin antibodies (Blockzijl, 1998). This information can then be used to synthesize a second library to probe the influence of individual residues on antibody binding (see section 2.2.2).

2.2.2 Replacement Net (RNET) analysis

RNET analysis allows the contribution of the individual residues in an epitope to the binding interaction between a peptide and an antibody to be determined. It is usually found that several of the residues in a continuous epitope can be replaced by many or

even all of the 19 amino acids without affecting the binding (Getzoff, *et al.* 1988; Briggs, *et al.* 1993; Pinilla, *et al.* 1993). The peptides are synthesized on derivatized polyethylene or polypropylene pins as described in 2.2.1 allowing ELISA to be used to measure antibody binding. A library of peptides is synthesized on the pins, where each of the residues in the epitope is substituted by each of the other 19 naturally occurring amino acids. RNET analysis has been used to investigate the fine specificity of epitope recognition by C595 mAb (Briggs, *et al.* 1993; Murray, *et al.* 1998). It was demonstrated that in the **RPAP** epitope, the arginine at position one and a proline residue at position four are essential to bind to the antibody.

2.2.3 Combinatorial peptide libraries

Random peptide libraries can be produced from organic synthesis using amino acids polymerised on inert solid support such as beads. A split and mix strategy is used for generating such combinatorial libraries (Lam, *et al.* 1991). The solid support is aliquoted into 20 portions and a different amino acid is coupled separately to each portion. The portions are pooled, resplit and the process repeated. The resulting bead mixture can then be directly used to select for binding peptides, which could be detected colourmetrically and the beads physically removed from the mixture for microsequencing.

An alternative approach is the synthetic peptide combinatorial library approach (SPCL) (Houghton, *et al.* 1991). Here the mixture generated from the split and mix methodology is split into 20 portions prior to the coupling of the final amino acid, so only the final amino acid residue of a particular sequence is known. Each of the 20 pools is assayed for binding to the target protein. The pool containing the best binding amino acid is resynthesized, but the last residue is kept constant (identified previously according to pool), the mixture being split into 20 portions prior to the addition of the penultimate amino acid. The penultimate amino acid is added (according to which pool the mixture is in). The amino acid residue selected in the previous round is then coupled to each of the 20 portions. The process is repeated, selected the best-binding pool, working back along the peptide chain until the best binding peptides are selected.

Microanalysis is a limiting factor in the identification of compounds from these libraries. Several methods of tagging each of the individual components of the library during the synthesis process, so linking the phenotype to an easily interpreted “genotype”, have been used. Strategies include the tagging of beads with nucleotide sequences synthesized in parallel to the peptide sequence (Needels, *et al* 1993). The individual beads are thus readily identifiable by PCR.

2.3 Biological libraries

As outlined in the introduction, biological libraries can be divided into two classes: *in vivo* and *in vitro* libraries. *In vivo* libraries are subject to selection pressure pertaining to the particular host. For example the phage display of particular peptides and proteins in a library is dependent upon efficient phage coat assembly. Displayed proteins may be toxic to filamentous phage assembly or incompatible with bacterial secretion pathways. *In vivo* libraries are free of these selection pressures and have the capacity for subsequent chemical or biochemical modifications of the peptides.

2.3.1 *In vivo* libraries

Phage Display Libraries

Phage display libraries have been used to display short peptide libraries and a variety of small proteins (Clackson and Wells 1994; Smith and Petrenko 1997). The most ubiquitous of these small proteins are antibody-related species such as the single-chain Fv (scFv) and Fab fragments. Random peptide libraries are akin to the work of Geysen who used solid phase peptide synthesis techniques to probe the structure of epitopes (Geysen, *et al.* 1987). Phage display has a number of advantages over the synthetic strategies: (i) Much larger library size achievable; (ii) Choice of monovalent or polyvalent display; (iii) Phage display enables selection instead of screening.

The relatively small number of nucleotides used to code for a short peptide mean that it is practical to chemically synthesize a single-stranded degenerate oligonucleotide insert, from which a clonable double-stranded DNA insert can be assembled. A number of different methods have been utilised to produce clonable library inserts from chemically synthesized single-stranded DNA (Cwirla, *et al.* 1990; Devlin, *et al.* 1990; Scott and Smith 1990; Christian, *et al.* 1992; Kay, *et al.* 1993; Sparks, *et al.*

1996). Digestion of the restriction enzyme recognition sequences within the constant regions of the degenerate insert enable the cloning of the random DNA library into the display vector.

Encoding a degenerate library using NNN (where N is an equimolar representation of all four bases) produces all 64 possible codons – including 3 stop codons. The presence of the 3 stop codons reduces the effective size of the library. This is circumvented by synthesizing a degenerate insert using a NN(G/T) or NN(G/C) scheme. 32 codons are used to encode all 20 amino acids, but only one stop codon – the frequency with which this stop codon appears in the library is only a problem when very large peptides (>50 amino acids) are encoded for (see figure 4.2 – chapter 4). Degenerate inserts can also be synthesized from mixtures of trinucleotide codons representing all 20 amino acids, and containing no stop codons. But the construction of this library requires more complex manipulation of the nucleotides than the NN(G/T), NN(G/C) strategy.

Genomic libraries have been constructed using total chromosomal DNA, potentially all of an organism's genetic complement is represented among the displayed peptides. In cDNA libraries the inserts are DNA copies of messenger RNAs (mRNAs) extracted from some tissue or cell population. All or parts of specific protein domains can be displayed, positions in the domain can be randomised in some way to create a library of sequence variants to enable the selection of rare clones with enhanced function.

Several different viral systems have been used to display peptides, each with their own display advantages: -

Lysogenic filamentous phage (Smith and Petrenko 1997) remains the most commonly used phage display system, with commonly used phage strains including M13, fd, and f1 vectors. Synthetic oligonucleotide libraries can be cloned as fusions to genes III or VIII of M13 bacteriophage (Rodi and Makowski 1999). Random peptide libraries fused to pIII or pVIII have been used to identify immunodominant peptide sequences of antigens, to generate peptide competitors of antigen-antibody interactions, to map accessible and/or functional sites of numerous antigens, and to identify peptide ligands for a variety of receptors (Kay, 1996).

T7 bacteriophage is a lytic phage display system. T7 is a double-stranded DNA phage. Phage assembly takes place inside the host *E.coli* cell and mature phage are released by cell lysis. Unlike the filamentous systems, peptides or proteins displayed on the surface of T7 do not need to be capable of secretion through the cell membrane, a necessary step in filamentous phage assembly. Small peptides (up to ~50 amino acids) can be polyvalently displayed (415 copies) on the T7 capsid 10B protein. Larger proteins can be displayed at a lower copy number (0.1-1 per phage) on the capsid, including *E. coli* β -galactosidase (1015 aa) (Rosenberg, *et al.* 1996).

Lytic lambda phage has been used to express the entire β -galactosidase at the C terminus of protein V with full enzymatic activity (Maruyama, *et al.* 1994).

T4 bacteriophage has also been used as a surface display vector (Efimov, *et al.* 1995).

Phage display libraries are typically limited by transfection efficiency to less than 10^9 independent members (Roberts and Szostak 1997). The upper limit on library size (around 10^9) is set by the transformation efficiency of *E.coli* and by the volume of cells that can be handled. Libraries of 10^7 – 10^8 are typical (Clackson and Wells 1994).

2.3.1.1 Cell based display

Cell based display can be divided into two sections – intracellular selection systems and extracellular display systems.

2.3.1.1.1 Extracellular display

Antibody and peptide libraries have been displayed on the surface of a number of cell types including yeast and *E. coli*. These cell display technologies allow the display of thousands of each polypeptide clone on the surface of each cell. (Compare this with pIII fusions in phage that display one to five copies, and the 10B fusions in T7 phage (Rosenberg, *et al.* 1996) that can display a maximum of 415 peptide clones). Screening of antibodies and peptides displayed on the cell surface by flow cytometry allows finer affinity discrimination compared with the panning of phage on

immobilised antigen (Boder and Wittrup 1997) Examples of extracellular display include the display of random peptide libraries on the pili (Rondot, *et al.* 1998) and flagellin (Lu, *et al.* 1995) of *E. coli*, by fusing random nucleotide libraries to the respective genes (F-pilin and flagellin). The display of peptides on the flagellin of *E. coli* was used to successfully map three different epitopes (Lu, *et al.* 1995).

As with phage display, affinity maturation of antibodies by *E. coli* display is limited by potential library bias due to expression of members in a prokaryotic host poorly adapted for post-translational processing of mammalian proteins. A C-terminal fusion of a randomly mutated scFv library, to the Aga2p mating adhesion receptor of the yeast *Saccharomyces cerevisiae* has been used for the selection of scFv antibody fragments with threefold antigen dissociation rate (Boder and Wittrup 1997).

2.3.1.1.2 Intracellular display – The yeast two-hybrid system

Intracellular display systems express both the combinatorial library and protein target inside living cells. The advantage of these systems is that the proteins are expressed and selected in an intracellular environment, ensuring the function of the selected protein is retained when expressed in that particular cell type.

Fields and Song (Fields and Song 1989) utilised the modular structure of eukaryotic transcription factors to show that transcription of a yeast reporter gene could be used to detect the interaction between two proteins. One protein was fused to a DNA-binding domain, the other to an activation domain. They proposed that libraries (Prey) fused to an activation domain (encoded by a vector producing activation domain-Prey fusions) could be screened for members that interact with a given protein (Bait) fused to a DNA-binding domain. When the activation domain and DNA-binding domain are in the same vicinity of one another the transcription factor becomes active, and a reporter gene (e.g. *E. coli lacZ*) downstream of the DNA binding site (recognised by the DNA-binding moiety of the bait) is activated. The Prey-plasmid insert is isolated from cells that exhibit an interaction phenotype, enabling sequencing and identification of the interacting protein. More advanced techniques based on this technology have been reviewed (Colas and Brent 1998).

2.3.1.2 Peptide-on-Plasmid

The link between peptide and genetic material is achieved through the use of DNA binding proteins. One such example is the use of the LacI DNA binding protein. Peptides are fused to the C-terminus of the *lac* repressor LacI by cloning degenerate oligonucleotides at the 3' end of the repressor gene (*lacI*) present on a plasmid. The DNA binding activity of the repressor protein physically links the peptides to the plasmid encoding them by binding to the *lac* repressor binding sites on the plasmid. These peptide-Lac-I-plasmid complexes are screened in a manner analogous to the phage systems, allowing the enrichment of specific peptide ligands from a random population. After lysis of cells containing the random library, those plasmid-repressor-peptide complexes that specifically bind to an immobilised receptor are enriched by affinity purification. Transformation of *E coli* with recovered plasmids allows additional rounds of panning or sequencing of isolated clones. Using this technique, a monoclonal antibody was screened and peptides displaying consensus sequences similar to a segment in the antigen (to which the antibodies were raised) were identified (Cull, *et al.* 1992).

2.3.1.3 Barcode systems

A number of systems are described in the literature which involve the use of unique “barcode” tags to label the members of a library. These include a commercially available system (BIODISPLAY™, Biovation, England) (Fox, 2000) which utilises an expression vector incorporating a 20mer 3' peptide barcode. A library of Fab genes are cloned into the vector and expressed as a soluble peptide-Fab fusion. The 20mer peptide barcode is unique to each particular Fab clone in the library. Fab fragments are selected for their ability to bind to antigen. Non-binders are then washed away. The peptide barcode is then released by protease digestion of a protease cleavage site linking the Fab fragment to the 20mer barcode peptide. The barcode is then sequenced by tandem mass spectroscopy enabling the design of primers which can be used to directly isolate the Fab genes. Other systems include multicolour optical coding based on wavelength and intensity multiplexing (Quantum-dots) (Han, *et al.* 2000); and a method based on the tuneable optical properties of porous silicon nanoparticles to dramatically increase the number of colour codes available compared to quantum-dots (Cunin, *et al.* 2002).

2.3.1.4 Periplasmic expression with cytometric screening (PECS)

This technique utilises the bacterial cell envelope to selectively retain receptor-fluorescent probe complexes but not free ligand. *E. coli* cells expressing a library of receptors secreted into the periplasmic space are incubated with a fluorescent conjugate to the target ligand. Flow cytometry is then used to isolate cells exhibiting increased fluorescence. The cell envelope is effectively being used as a dialysis bag to retain the protein-ligand complexes. PECS has been used to isolate high affinity scFv molecules to digoxigenin (Chen, *et al.* 2001). PECS can be used to screen existing libraries constructed for display on bacteriophage without the need for subcloning.

2.3.2 *In vitro* libraries

As outlined in the introduction *in vitro* libraries are immune from the major biological constraints found in *in vivo* libraries. This results in the opportunity to interrogate much larger areas of sequence space, potentially enabling the isolation of much higher affinity ligands (a proposed direct correlation exists between library size and binding affinities of isolated ligands for a particular target (Pearlson and Oster 1979)). The lack of transformation or infection steps when using *in vitro* selection systems enables automation of the procedures, allowing ligand discovery to be conducted on the genomics scale.

2.3.2.1 Ribosome display

The construction of large libraries in the previously described biological systems is limited by the initial transformation following the assembly and ligation of the library into the host vector. In ribosome display a mRNA-ribosome-protein complex creates a link between the genotype and phenotype *in vitro*, completely circumventing the problems of transformation efficiency associated with *in vivo* methodologies. All steps of ribosome display are carried out completely *in vitro*, allowing the reaction conditions of individual steps to be tailored to the requirements of the protein species investigated (but under conditions that preserve the integrity of the ribosome-mRNA-peptide ternary complex). A comprehensive review of ribosome display as a method for totally *in vitro* protein selection has been conducted (Roberts 1999). Examples of the use of ribosome display for the selection and evolution of antibodies *in vitro* have been published (Hanes, *et al.* 1998; Makeyev, *et al.* 1999; Schaffitzel, *et al.* 1999)

2.3.2.2 RNA-peptide fusions

The next development from ribosome display is the use of RNA-peptide fusions. These systems have the advantage of being more robust than the ribosomal display systems. The peptide becomes directly attached to the mRNA that encodes it by a stable covalent linkage. The peptide-mRNA fusion can then be enriched from a complex mixture of peptide-mRNA fusions. *In vitro* translation of synthetic mRNAs that carry puromycin (a peptidyl receptor) at their 3' end creates a covalent fusion between a mRNA and the peptide or protein that it encodes. This system has been used to enrich a *myc* epitope peptide from a pool of random sequence mRNA-peptide fusions (Roberts and Szostak 1997).

2.3.2.3 Covalent Display Technology (CDT)

CDT is a proprietary *in vitro* library platform (Actinova Ltd., Cambridge UK; David Andrews and Yun Li, McMaster University, Hamilton, Canada) which exploits the properties of a replication initiator protein (P2A) from the *E. coli* bacteriophage P2. P2a is a DNA-binding protein that attaches covalently to its own coding sequence (Fitzgerald 2000). Concurrent *in vitro* transcription and translation of gene fusions comprising the coding sequence for P2A and the coding sequences for potential target-binding proteins (containing "random" sequences) results in the formation of covalently linked DNA-protein complexes. This library can then be interrogated and those members of the library which bind to a particular ligand by affinity selection. Specifically binding complexes can then be propagated by amplification using the polymerase chain reaction (PCR) for subsequent rounds of selection or cloning into a bacterial host for example.

2.3.2.4 Man-made cell-like compartments for molecular evolution

A different approach to linking genotype to phenotype has been demonstrated using aqueous compartments of water-in-oil emulsions (Tawfik and Griffiths 1998). Here a substrate was attached to a random library of genes, and dispersed into the water-in-oil emulsion such that only single genes occupied each aqueous compartment. Genes that encode for catalysts converted the substrate attached to the gene that encoded it to product, all other compartments that did not contain catalysts remain unmodified. Those compartments containing functioning catalysts can then be isolated (using Fluorescence Activated Cell Sorting (FACS) for example). The coding information

contained in the cell can then be isolated by PCR and used in subsequent rounds of selection or expression of functional enzyme.

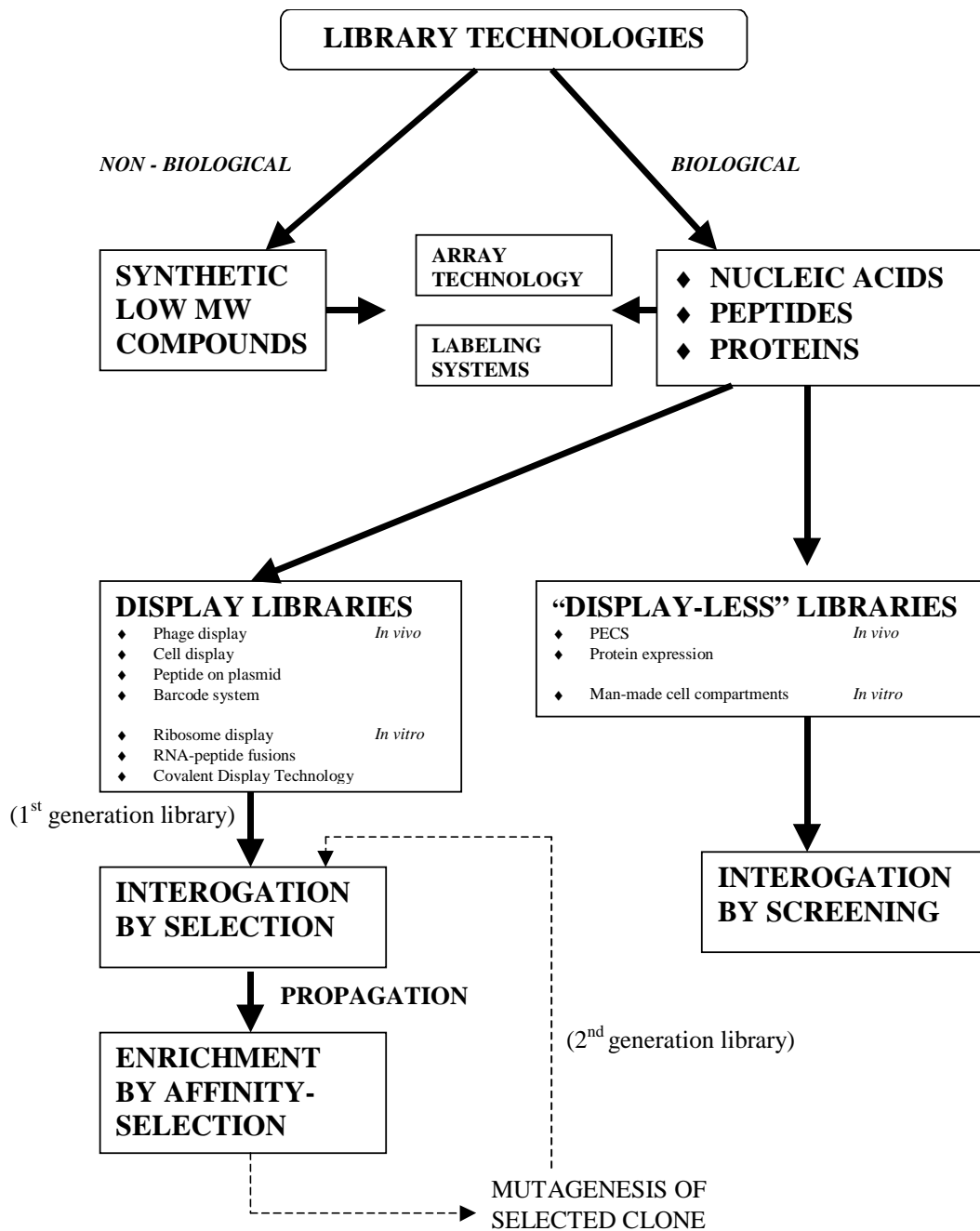


Fig. 2.1: Library technologies, illustrating the division between totally synthetic compounds (generated using combinatorial chemistry techniques), and those based on biological compounds. Differences between display-less and display systems are shown.

2.4 Other non-peptide ligands

2.4.1 Synthetic Libraries

2.4.1.1 Non-peptide chemical libraries

The principal advantage of solid phase techniques over the other biologically based combinatorial approaches, is the opportunity to greatly vary the chemistry involved within the library. Biological systems are restricted to the 20 naturally occurring amino acids, or 4 nucleotide bases (see section 2.5.2.1), however with chemical libraries other elements can be introduced that increase the structural diversity of the library. These include peptoids (Simon and al 1992) vinylogous polypeptides (Hagihara, *et al.* 1992) unnatural D-amino acids and other templates to induce secondary structural motifs (Farlie, *et al.* 1998). Cyclic peptide libraries not limited to disulphide constraints can also be synthesized (Zuckerman 1993).

2.4.2 Biological Libraries

2.4.2.1 Nucleotide Libraries

The ability of different nucleic acid sequences to fold into distinct three-dimensional shapes, which are chemically complementary to the surface of a particular target molecule, has lead to the use of nucleotide libraries as sources of receptor binding ligands (Bacher and Ellington 1998). The **SELEX** (the systematic evolution of ligands by exponential enrichment) process allows the rapid isolation of rare oligonucleotide sequences from large random single-stranded sequence libraries.

The initially chemically synthesized library can be amplified using PCR; binding species are selectively eluted from the receptor, these binding species can then be amplified by PCR. The process of selecting for binding sequences is then repeated. An enrichment process takes place similar to that observed in the other biological systems. This technique has been applied to the affinity purification of a human L-selectin-Ig fusion protein from Chinese hamster ovary cell-conditioned medium by using a DNA-aptamer discovered using the SELEX process (Romig, *et al.* 1999).

The initial random sequence pool which is typically generated by chemical DNA synthesis contains a core of randomised nucleotides flanked by constant regions, which are required for enzymatic amplification (these constant regions may include specific restriction sites that aid cloning of selected species as well as promoter sequences to enable in vitro transcription of RNA. Unnatural nucleotides can also be included in the DNA or RNA polymerisation reaction to generate different chemistries.

2.5 Mutagenesis

Why conduct mutagenesis of proteins?

As outlined in the introductory section of this chapter, the application of combinatorial selection approaches enable the simultaneous mutation of multiple residues in a protein to produce “non-additive” changes that could not have been predicted *a priori*. It has been demonstrated that combinatorial approaches can be used to select binding antibodies from naïve immunoglobulin libraries (Gram, *et al.* 1992). Combinatorial approaches can also be applied to existing proteins in order to select for particular attributes, or analyse function.

There are three different approaches for the molecular evolution of a protein involving mutagenesis:

(i) Point mutations

These types of mutations can be divided into two classes: site directed mutations and random mutations. Specific residues within a protein may be selected for directed mutation, based on an analysis of the crystal structure of the protein binding to a ligand. Residues can be selected that are in the binding site. Using site directed mutagenesis, the contribution to binding made by cavities, salt links, van der Waals contacts and hydrogen bonds can be analysed. One example of such an approach was given by (Dougan, *et al.* 1998). Here 14 amino acid residue replacements were made at six contact residues in a scFv fragment by site-directed mutagenesis. From a kinetic analysis of the interactions between the antigen and the mutants, the role of hydrophobic (van der Waals contacts), hydrogen bonds, salt links and the importance of cavity bound water molecules in the binding of the scFv fragment to the antigen were determined.

Another approach to improving antibody affinity is the point mutation of residues throughout the CDR regions of an antibody. One such technique is termed CDR walking mutagenesis. This involves the systematic mutagenesis of individual residues in the CDR regions of antibodies and selection for fitness with monovalent phage display. One example of the application of CDR walking mutagenesis is the optimisation of the affinity of a human antibody to the human envelope glycoprotein gp120 of human immunodeficiency virus type 1 (HIV-1) (Yang, *et al.* 1995). Another example introduced random mutations into specific “hot-spots” within the variable regions of an antibody. These “hot-spots” were identified as being prone to hypermutations, random mutations were introduced into a few of these hot spots to produce libraries. Panning of these libraries yielded mutants with up to a 55-fold increase in affinity compared a 4-fold increase observed from a library constructed in which mutagenesis was done outside the hotspots (Chowdhury and Pastan 1999).

(ii) Random mutagenesis

Random mutagenesis utilising error-prone PCR (Cadwell and Joyce 1994) has been used to select phage antibodies by binding affinity (Hawkins, *et al.* 1992). Error-prone PCR was used to introduce mutations into antibody genes *in vitro*, and affinity selection using biotinylated hapten (4-hydroxy-5-iodo-3-nitrophenacetyl-(NIP)-caproic acid) was used to select for mutants with improved affinity. A mutant was isolated with a four-fold increase in affinity to the hapten ($K_d = 9.4 (\pm 0.3) \text{ nM}$).

A quantitative analysis of the effect of mutation frequency on the affinity maturation of scFv antibodies has been conducted on a high affinity scFv antibody that binds to cardiac glycoside digoxigenin (Daughterty, *et al.* 1999). Error prone PCR was used to generate libraries of mutants displayed on *E. coli*. Three libraries were constructed with; (i) a low error rate (m) of 1.7 base substitutions per gene; (ii) a moderate error rate $m=3.8$; and (iii) a high error rate $m=22.5$. The moderate and high error rate libraries were found to give rise to clones exhibiting the greatest affinity improvement. The majority of scFv mutations leading to higher affinity clones corresponded to residues distant from the binding site. The mutations distant from the binding site could not have been predicted from molecular modelling studies. This highlights the advantages of using such “irrational” techniques over “rational”

techniques based on crystal structures of binding sites and molecular modelling studies alone.

An example of the use of random mutagenesis to select for improved stability was published by (Sieber, *et al.* 1998). A repertoire of variants was displayed between the N2 and CT domains of the gene-3-protein of the fd phage. The infectivity of the phage is lost when the two domains are disconnected by the proteolytic cleavage of unstable protein inserts. Using this method proteins were selected from a library of variants with improved stability.

(iii) DNA Shuffling

A segment of DNA is amplified by PCR and purified free of primers. The amplified segment is then cleaved into small, random fragments with DnaseI and size selected. The fragments are denatured, annealed and extended with DNA polymerase in the absence of any primers. After several cycles the restored fragment is amplified by PCR. The fragment is then digested with restriction enzymes outside the area targeted for mutagenesis, to generate a cassette for cloning. The process of reassembling can be mutagenic in the absence of a proof-reading polymerase. A combination of directed and random mutagenesis (DNA shuffling) has been used to construct libraries of mutants from which scFv's can be selected with improved stability. A library of scFv fragments was generated and phage display selection was carried out under selective pressures for higher thermodynamic stability. Stable mutants were isolated which exhibited increased thermodynamic stability, increased expression levels and a 20-fold better binding constant than the wild-type scFv (Jung, *et al.* 1999).

(iv) Cassette Mutagenesis

Cassette mutagenesis can be used to introduce mutations at particular site(s) within a coding region. A "cassette" of double stranded DNA containing the required mutation(s) is produced and cloned into the region of interest by conducting a restriction digest followed by a ligation reaction. Several methods are available to generate the cassette, utilising either oligonucleotides as the method for introducing mutations, or error-prone PCR (1996).

(v) Random Elongation Mutagenesis

This technique exploits the stabilising capacity in certain proteins, of terminal arms of amino acids that fold across a susceptible part of the structure, stabilising it under unfavourable conditions such as high temperature. A partially randomised oligonucleotide is inserted ahead of the stop codon in an expression vector in order to introduce short chains – 16 amino acids in length – onto the carboxyl terminus of a protein (Scopes 1999).

(vi) Bacterial mutator strains

Another method, which can be employed in the evolution of proteins, is the use of bacterial mutator strains. These bacteria introduce random mutations into a particular plasmid. The disadvantage with such systems is that the library size is reduced by mutations that take place outside the cloning region, in restriction sites, and promoters for example. (Low, *et al.* 1996).

2.6 Aims and Objectives of the research

Epitope / mimotope affinity chromatography was demonstrated to be the method of choice in chapter one for the purification and concentration of monoclonal antibodies and engineered antibody fragments to a standardised and high immunoreactivity in a single step, from biological feed stocks. Use of this procedure necessitates the discovery of Paratope-specific binding ligands. A review of the different combinatorial approaches available has led to the conclusion that a polyvalent, lytic phage display system offers the most efficient way of searching sequence space for ligands that interact with the antibody in a similar orientation to ligands immobilised on a chromatographic matrix. The T7 phage display system was investigated for its ability to discover high affinity peptide ligands which are capable of functioning as paratope-specific peptide-mimotope affinity ligands.

The process of discovery and refinement of paratope specific binding ligands, such as peptide mimotopes, leads to the generation of peptide ligands exhibiting tuneable affinities for antibodies and their derivatives. Whilst the higher affinity mimotopes may well find use as paratope-specific ligands for application in the affinity purification of antibodies, the range of affinities that can be achieved using these

peptide mimotopes may also find application in biosensors. An investigation into the use of solid phase peptide synthesis techniques to further refine lead peptide sequences derived from phage display was conducted. The use of mimotope peptides (derived from this process) for the detection of non-protein analytes was also investigated. The aim was to determine whether such mimotopes could be employed in assays for non-protein analytes.

Manipulation of the ligand offers one method for increasing the affinity of the antigen-antibody interaction. Whilst this is useful for the purification of target antibodies, the use of antibody-related molecules for *in vivo* diagnostic purposes requires the optimisation of the binding properties of the antibody-related molecule. The use of molecular biology techniques enables the construction of novel gene-fusions, which can be expressed as bi-functional proteins. The aim of the final part of research presented in this thesis was to construct a scFv-GFP gene fusion consisting of a library of randomly mutated scFv genes fused to green fluorescent protein. The aim was to screen the library using FACS to obtain scFv clones exhibiting a higher affinity for the target antigen expressed on tumour cell lines.

3 Chapter 3 Materials and Methods.

3.1 Reagents

Clontech Laboratories, Inc., Palo Alto, CA, USA

Anhydrotetracycline

Pierce, Rockford, Illinois, USA.

Succinimide ester of biotin.

Difco Labs. Ltd. , west Molesey, U.K.

Bacto agar

Bacto tryptone

Bacto yeast extract

BDH Biochemical reagents, Poole, U.K.

Glycerol

Hydrochloric acid

Sigma-Aldrich Company Ltd., Gillingham, Dorset, U.K.

Ampicillin

Boric acid

Bovine Serum Albumin

Casein

Citric acid

Deoxynucleotide 5' –triphosphates (dNTPs)

N-ethyl-N'-(3-dimethyl-amino propyl)-carbodiimide hydrochloride (EDC)

Ethanol

Ethanolamine

Ethidium Bromide

Ethylenediaminetetraacetic acid (EDTA)

Extravidin-Peroxidase

Glacial acetic acid

Glutaraldehyde

Glucose
Hydrogen peroxide
Isopropanol
Magnesium Chloride
Mercaptoethanol
Mineral oil, light
N-hydroxysuccinimide (NHS)
Nalidixic acid
Phenol : chloroform : isoamyl alcohol
Polyoxyethylene-sorbitan monolaurate (Tween 20)
Sodium azide
Sodium chloride
Sodium dodecyl sulphate (SDS)
Trichloroacetic acid (TCA)
Tris-(hydroxymethyl)-aminomethane (Trizma base)

BSAU - Queens Medical Centre, Nottingham, U.K

Peptides APDTRPAPG, APDTRPAPGC, APDTREAPG, RNREPARGKICS, KSKAGVC, GLFED, GLFYD, (D) DYFLG were synthesised by the Biopolymer Synthesis and Analysis Unit (BSAU) (Queens Medical Centre, Nottingham, U.K.). The purity of the peptides was established to be >97% by reverse phase high performance liquid chromatography and mass spectroscopy.

Flowgen Instruments Ltd., Sittingbourne, U.K.

Low melt NuSieve agarose
High melt agarose

BIACORE AB, Uppsala, Sweden.

Pioneer Sensor Chip F1
Sensor Chip CM5 (research grade)
HBS-EP buffer
Surfactant P20

Promega Corporation, Madison, WI, USA.

Wizard Plus SV Minipreps DNA Purification System

Invitrogen BV, Groningen, The Netherlands.

TOPO TA cloning kit

Chemically competent *E. coli* TOP10 cells

Amersham Pharmacia Biotech U.K. Ltd., Little Chalfont, Bucks., U.K.

CNBr-activated Sepharose 4B

PD10 column (containing Sephadex G-25 M)

Anti-E Tag Antibody

pCANTAB 5 E phagemid vector

3.2 Enzymes

Advanced Biotechnologies, Epsom, Surrey, U.K.

Taq DNA polymerase (isolated from *Thermus aquaticus*, 5 Units/ μ l).

New England Biolabs (U.K.) Ltd., Hitchin, Herts., U.K.

Bgl II (10,000 U/ml)

Hind III (10,000 U/ml)

Sfi I (20,000 U/ml)

Not I (10,000 U/ml)

T4 DNA ligase (400,000 units/ml)

USB Corp., Cleveland, Ohio, USA.

Shrimp alkaline phosphatase (1.0 U/ μ l). [One unit of enzyme catalyses the hydrolysis of one μ mole of p-nitrophenyl phosphate per minute at pH 10.7 (glycine/NaOH buffer) and 37⁰C.

Sigma biochemicals

Exonuclease I

Extravidin-Horseradish peroxidase

3.3 Buffers and Solutions

All buffers were prepared with de-ionised double distilled water. Buffers used for FPLC, fluorescence quenching, circular dichroism or biosensor analysis were sterile filtered and degassed prior to use.

Phosphate buffered saline (PBS) –pH7.3

PBS was prepared by dissolving 1 PBS tablet (Oxoid, Basingstoke, Hants, U.K.) in 100 ml of water.

Tris Buffered saline (TBS) – pH 7.5

TBS was prepared by dissolving Tris HCl (7.9g, pH 7.5) and sodium chloride (8.8g) in water 1 litre of water.

Tris-Borate-EDTA (TBE) buffer (10x stock)

Was obtained as 10x concentrate from sigma-aldrich. Consisted of 0.89M Tris Borate, pH 8.3 containing 0.02 M EDTA

PBSA – pH 7.3

Sodium azide (NaN_3) was added to PBS buffer to a final concentration of 0.05 % (w/v).

PBS/Tween – pH 7.3

PBS/Tween was prepared by adding Tween 20 to PBS to give a final concentration of 0.1% (v/v).

PBS + 0.1% Casein – pH 7.3

The PBS + 0.1% casein solution was prepared by dissolving 100 mg of casein in 100ml PBS solution.

TBS + 0.1% Casein – pH 7.5

The TBS + 0.1% casein solution was prepared by dissolving 100 mg of casein in 100ml TBS solution.

PBS + 1% Bovine Serum Albumin – pH 7.3

The PBS + 1% bovine serum albumin (BSA) solution was prepared by dissolving 1g BSA in 100ml PBS.

HBS-EP buffer

The buffer was purchased from BIACORE (Uppsala, Sweden).

N- [2-Hydroxyethyl] piperazine-N'-[2-ethanesulfonic acid] (HEPES) (0.1M, pH 7.4), sodium chloride (0.15M), Ethylenediaminetetraacetic acid (EDTA) (3mM) and Surfactant P20 (0.005% v/v).

Disruption Buffer

Sodium dodecyl sulphate (0.1% w/v) was dissolved in sodium dihydrogen orthophosphate buffer (0.1M, pH 7.2). β -mercaptoethanol (5ml) was added immediately before use.

Citrate Phosphate Buffer – pH 4.0

Anhydrous disodium hydrogen phosphate (4.06g) and citric acid (4.53g) were dissolved in 450ml water. The pH of the solution self adjusted to pH 4.0

2-Azino-di- (3-ethyl benzthiazoline-6-sulphonic acid)-diammonium salt (ABTS) Solution.

ABTS solution was prepared at a concentration of 0.05% (w/v) ABTS in citrate phosphate buffer. Shortly before use, hydrogen peroxide (~30% vol) was added to the ABTS solution to produce a final concentration of 140 μ l per 100ml.

LB growth medium pH 7.5

LB growth medium was prepared by dissolving Bacto Tryptone (DIFCO) (10g), Yeast extract (DIFCO) (5g) and sodium chloride (10g) in 1 litre of water. The pH of the solution was adjusted to 7.5 with 1N sodium hydroxide. The LB growth medium was autoclaved for 20 minutes prior to use.

Chapter 3 Materials and Methods.

Sodium dodecyl sulphate solution (SDS) – 1 % w/v

1% w/v SDS solution was prepared by dissolving 1g of sodium dodecyl sulphate in 100ml water.

LB Agar Plates

LB Agar plates were prepared by dissolving 7.5g of agar in 500ml of LB growth medium – pH 7.5. The mixture was then autoclaved for 20 minutes, left to cool to 50°C and poured into 10cm petri dishes. After the plates cooled they were stored at 4°C until used.

LB Top Agarose

LB Top Agarose was prepared by dissolving Bacto Tryptone (1g), Yeast extract (0.5g), sodium chloride (0.5g) and agarose in 100ml of water.

Coupling Buffer – pH 8.3

Coupling buffer was prepared by dissolving NaHCO₃ (8.4g) and NaCl (29.2g) in 1 litre of water, the pH was adjusted to 8.3.

Tris-HCl Buffer pH 8.0

Tris-HCl Buffer pH 8.0 was prepared by dissolving Tris-HCl (15.8g) and sodium chloride (29.2g) in 1 litre of water and adjusting the pH to 8.0.

SOBAG (SB) Medium

Water (~900 ml) was added to Bacto-tryptone (20g), Bacto-yeast extract (5g) and sodium chloride (0.5g) and the mixture autoclaved. After the mixture had cooled to 50~60 °C, MgCl₂ (1 M, 10 ml), sterile glucose (2 M, 55.6 ml) and sterile-filtered ampicillin (20% w/v, 5.0 ml) were added

SOBAG – N Medium

SOBAG medium containing nalidixic acid. SOBAG-N plates were made by adding bacto-agar (15g) before autoclaving.

SOBAG-AG (SB-AG) Medium

SB medium containing 100µg/ml ampicillin and 2% glucose.

SOBAG-AI (SB-AI) Medium

SB medium containing 100µg/ml ampicillin and 1 mM IPTG.

20% Trichloroacetic acid (TCA) solution

First 100% trichloroacetic acid (TCA) was prepared by adding 227 ml of distilled water to TCA (500 g). The TCA was allowed to completely dissolve. TCA (200ml, 100%) was added to 800 ml of distilled water to make 1 litre of 20% TCA.

TES buffer

A solution containing Tris-HCl (0.2 M, pH 8.0), EDTA (0.5 mM) and sucrose (0.5 M) was prepared and filter sterilised using a 0.2 µM filter (Sartori, Gottingen, Germany). The solution was stored at 4°C.

Triethanolamine Buffered Saline

Sodium chloride (7.5g) and triethanolamine (2.8 ml) were added to water (800 ml). The pH was adjusted to 7.5 with concentrated HCl, water was then added to a total volume of 1 litre.

4-chloro-1-naphthol (4-CN) substrate

A stock solution of 4-CN was prepared by dissolving 4-chloro-1-naphthol (30 mg) in methanol (10 ml).

Substrate was prepared for use by adding 4-CN stock solution (4.0 ml) and hydrogen peroxide (30%, 10 µl) to triethanolamine buffered saline and mixing well.

Acetate Buffer pH 4.0

Acetate Buffer was prepared by dissolving sodium acetate (8.2g) and sodium chloride (29.2g) in 1 litre of water and adjusting the pH to 4.0.

Chapter 3 Materials and Methods.

2x Bacteriophage T4 DNA ligase mixture

Tris HCl (pH 7.6, 1 M, 1.0 μ l), MgCl₂ (100 mM, 1.0 μ l), dithiothreitol (200 mM, 1.0 μ l), ATP (10 mM, 1.0 μ l), dH₂O (5.5 μ l) and bacteriophage T4 DNA ligase (1 Weiss unit) were mixed in a tube stored on an ice bath. (Sambrook, Fritsch *et al.* 1989)

10x mutagenic PCR buffer

10x mutagenic PCR buffer was prepared by dissolving magnesium chloride (70 mM) and potassium chloride (500 mM) in Tris buffer (100 mM, pH 8.3). Gelatin was added at 0.1% w/v.

10x mutagenic dNTP mix

The 10x mutagenic dNTP mix was prepared by diluting dGTP (2 mM), dATP (2 mM), dCTP (10 mM) and TTP (10mM) in water.

3.4 Methods

3.4.1 Monoclonal Antibody Production

The murine anti-MUC1 monoclonal antibody C595 (IgG3 subclass) was originally prepared by conventional hybridoma technology using spleen cells from a BALB/c mouse immunised against purified urinary MUC1 mucin (Price, *et al.* 1990). Hybridoma supernatant was clarified by ultracentrifugation (40,000g, 30 min) and ultrafiltration through a 0.2µm filter (Sartorius, Gottingen, Germany). The antibody was stored at 4°C with sodium azide (0.05% w/v) as a preservative.

3.4.2 Biopanning of phage library

The T7Select415-1b vector containing a degenerate oligonucleotide insert was kindly donated by Dr. P. Tighe (Division of molecular and clinical immunology, The University of Nottingham, UK). The oligonucleotide insert was synthesized, containing EcoRI and HindIII restriction sites to enable insertion into the cloning region of the T7Select415-1b vector. Measurements of phage titer were carried out using a plaque assay. *E.coli* strain BL21 were grown to mid-log phase, and aliquots inoculated with phage preparations serially diluted in LB media. These were then mixed with top agar and poured onto LB plates. The plates were then incubated at 37°C for 3h. The number of phage plaques was then counted and the initial phage titer determined.

The phage library was screened against antibody passively adsorbed onto Maxisorb immunotubes (75x12 mm; NUNC). The library was first screened against an “irrelevant” antibody that would not be expected to bind specifically to MUC1 epitopes. Anti-Estrone beta-D-glucuronide antibody (Badley, *et al.* 1999) was used for this purpose. The antibody (2.5ml @ 10µg/ml in TBS buffer (50mM Tris HCl pH 7.5, 150mM NaCl) was passively adsorbed onto Maxisorp immunotubes by incubation at room temperature for 4h. Unbound target protein was removed by washing the tubes three times with TBS buffer. The tubes were then incubated for 1h at room temperature with 2.5ml of blocking solution (1% w/v casein in TBS). The tube was then washed five times with deionised water and once with TBS buffer.

The phage library (2.5ml phage lysate) was incubated in the immunotube (with anti-estrone beta-D-glucuronide antibody adsorbed) for 30 minutes at room temperature. The phage lysate in the tube was then gently agitated and transferred to an immunotube with C595 antibody adsorbed (10µg/ml) and incubated at room temperature for 30 minutes. The phage lysate was then decanted from the immunotube and the tube was washed five times with TBS buffer containing 0.05% Tween20. A one-minute incubation was used for each wash. Excess buffer was removed by blotting on a paper towel. Bound phage were eluted using a 20 minute incubation with sodium dodecyl sulphate (SDS, 1% (w/v), 2.5ml), and transferred to a sterile glass tube. An aliquot of the eluted phage solution (250µl) was then added to 50 ml of *E. coli* BL21 grown to mid-log growth phase (OD₆₀₀ ~ 0.5 AU) and incubated in a 250ml baffled flask with shaking at 37°C until lysis of the culture was observed. The phage lysate was then purified from the cell debris by centrifugation at 8,000g for 10 minutes. The supernatant was transferred to a sterile glass tube. The phage titer of the eluted phage was determined using a plaque assay as described above. The amplified phage were used in the next round of biopanning. The phage titer of the eluted phage (prior to amplification) was monitored after each round of biopanning using the plaque assay.

3.4.3 PCR analysis of individual phage clones

Two primers (R1FOR 5'GCT AAG GAC AAC GTT ATC GGC CTG TTC ATG C^{3'} and R2REV 5'CGT TGA TAC CGG AGG TTC ACC GAT AGA CGC C^{3'}) were designed to allow PCR amplification of the region surrounding the degenerate oligonucleotide insert. A third primer was designed to anneal inside this PCR amplification product (SEQFOR 5'GGT ACT GTT AAG CTG CGT GAC TTG GC^{3'}) to enable direct sequencing of the PCR product (see fig. 4.1 – Chapter 4). A scrape from an individual phage plaque was dispersed in 100µl of 10mM EDTA, pH 8.0. The tube was briefly vortexed and heated at 65°C for ten minutes. The mixture was cooled to room temperature and clarified by centrifugation at 14,000 g for 3 minutes. PCR reactions were performed in 50µl aliquots, each reaction was set up as follows: -

Chapter 3 Materials and Methods.

10 x Buffer	5 μ l
10 mM dNTP's	1 μ l
25 mM MgCl ₂	3 μ l
Primers (25 pmol each)	2 μ l
Phage DNA Template	1 μ l
dH ₂ O	<u>37 μl</u>
	49 μ l

Light mineral was added to the top of the reaction to prevent evaporation of reagents during the cycling reaction. The reaction was conducted on an OmniGene Thermal Cycler Controller (Hybaid, Teddington, UK); and consisted first of a "hot-start" by heating the tube for 5 minutes prior to the introduction of 1 μ l Taq DNA polymerase (ABGene); 35 cycles of 94°C for 50s, 50°C for 60s, 72°C for 60s; and a final extension at 72°C for 6 minutes. Agarose gel electrophoresis was used to analyse the PCR products to ascertain that only a single PCR product of the expected size was present before sequencing. Agarose gels (1%) were prepared by dissolving NuSieve agarose (Flowgen, Sittingbourne, UK) in TBE buffer (0.09 M Tris-borate, 0.02 M EDTA). Ethidium bromide (0.2 μ g ml⁻¹) was incorporated into the gel before pouring. Samples were diluted with DNA loading buffer (sigma biochemicals). After electrophoresis, DNA was visualised using a Spectroline TM-312A Ultra Violet Transilluminator, and photographs were recorded using a Polaroid DS-34 Direct Screen Instant Camera.

Primer notation

Primers denoted FOR in this thesis refer to primers that bind to the 3'-5' antisense strand. Primers denoted REV in this thesis refer to primers that bind to the 3'-5' sense strand.

3.4.4 Direct sequencing of PCR products

Exonuclease I (Exo I) (Sigma Biochemicals) was used to degrade excess single-stranded DNA (Phage DNA and excess primers); and Shrimp Alkaline Phosphatase (SAP) (Sigma Biochemicals) was used to cleave 5' phosphate groups from excess single stranded DNA preventing the incorporation of primers/degraded fragments and phage DNA into the sequencing reaction. Exo I (5U) and SAP (1U) were added to 5 μ l of PCR product, heated at 37°C for 15 minutes and then heated at 80°C for 15 minutes. Sequencing reactions were conducted (ABI PRISM Big-Dye Terminator

Cycle Sequencing reaction) in 10µl aliquots using 0.1µM SEQFOR primer, 5µl of Big Dye sequencing buffer (Tris-HCl (80mM, pH9.0) and MgCl₂ (2mM)), 2.5µl of enzyme treated PCR product and 2µl Big Dye mix; on an OmniGene Thermal Cycler Controller (Hybaid, Teddington, UK). Using a program consisting of 96°C for 90s; 25 cycles of 96°C for 30s, 50°C for 15s, 60°C for 240s; and a finally 28°C for 1 minute. Prior to sequencing an ethanol precipitation step was conducted to remove excess dye terminator in the reaction mix.

Ethanol precipitation.

Water (20 µl) was added to the completed sequencing reaction (10µl). This mixture was then added to a centrifuge tube containing sodium acetate (2µl, 3M, pH 5.0) and 95% ethanol (50µl). The mixture was then vortexed and placed on ice for ten minutes. The tube was then placed in a bench-top centrifuge and spun at full speed for ten minutes. All liquid was then aspirated off, and the pellet washed with 70% ethanol (250 µl). The tube was again centrifuged at full speed for ten minutes. All liquid was aspirated off and the remaining pellet was allowed to dry in open air for a few minutes.

Sequence analysis was performed on an ABI 373A DNA Sequencer (ABI).

3.4.5 Phage Capture ELISA

C595 antibody was adsorbed onto the wells of a microtitre plate (96 well NUNC) by incubation at 37°C for 4 hours. After blocking non-specific binding sites by incubation with PBS + 0.1% casein, phage preparations were titrated by serial dilution with 50µl added per well. After incubation for 2 hours, the plates were washed four times with PBS/Tween. Antibody C595 was biotinylated using the succinimide ester of biotin as outlined in (Sambrook, *et al.* 1989). Biotinylated C595 antibody was added at 50µl per well. After 2 hours incubation, the plates were washed four times with PBS/Tween and HRP-conjugated avidin (ExtrAvidin[®] - Sigma Biochemicals) was added at 50µl per well. Plates were incubated for 1 hour, washed four times with PBS/Tween. ABTS substrate was added to the wells at 50µl per well. Colour development was measured using a Milenia Kinetic Analyser (Diagnostic Products Corporation, Llanberis, UK).

3.4.6 Sepharose Bead Assay

The peptide of interest was conjugated to beaded agarose (cyanogen-bromide activated Sepharose 4B) at a concentration of 1 μ mole peptide per ml gel using conjugation procedures as recommended by the manufacturer. A standard ELISA procedure was conducted using approximately 50 μ l of the peptide coupled swollen beads as follows: -

In an eppendorf tube, the beads were first washed with PBS/Tween wash buffer. The beads were suspended in the wash buffer (1.0 ml) and gently agitated by inverting the tube four times. The tube was then placed in a centrifuge and briefly spun. The liquid was carefully aspirated from above the beads, and replaced with fresh wash buffer. This process was repeated four times. After the final wash the liquid above the beads was replaced with blocking buffer (PBS + 0.1% casein, 1.0 ml) to block non-specific adsorption sites. The tube was gently agitated on a roller for one hour at room temperature. The tube containing the bead suspension was briefly centrifuged. The blocking solution was carefully aspirated from above the beads, and replaced with the antibody solution at the appropriate dilution. The beads were re-suspended in solution by gentle agitation. The tube was gently agitated on a roller for one hour at room temperature. The tube was then briefly centrifuged and washed with PBS/Tween wash solution as described above. The wash solution was aspirated from above the centrifuged beads and replaced with marker antibody (rabbit anti-mouse IgG peroxidase conjugate, 1.0 ml) at 1/1000 dilution in PBS. The beads were incubated with the marker antibody for one hour, with agitation on a roller at room temperature. The beads were then washed again in wash buffer as described above. Finally ABTS solution was used to suspend the beads. After colour development the tube was spun in a centrifuge and the liquid dispensed into the wells of an ELISA plate (NUNC) and the endpoint measured using a Milenia Kinetic Analyser (Diagnostic Products corporations, Llanberis, UK).

3.4.7 Peptide Affinity Chromatography

Data acquisition and analysis was performed using FPLCdirector Software (Pharmacia Biotech).

3.4.7.1 Preparation of Immunoaffinity Matrices

Synthetic peptides were linked to beaded agarose (Sepharose 4B, Pharmacia) via their N-termini using CNBr-activated matrix. Peptides were coupled at a ratio of 1 μ mole peptide per ml gel using conjugation procedures as recommended by the manufacturer.

3.4.7.2 FPLC

Chromatography columns (10mm internal diameter, Amersham Pharmacia Biotech) were packed with 2 ml of each affinity matrix. Chromatography was performed using an automated FPLC system (Amersham Pharmacia Biotech). Columns were first equilibrated with 10 column volumes (20 ml) of PBS at a flow rate of 1.0 ml/min. Loading of antibody solutions in PBS (100ml) was conducted at room temperature (unless stated otherwise) at a flow rate of 1.0 ml/min. Loading of clarified hybridoma supernatant (100ml) was carried out at 4°C, with the supernatant circulating around the column for 48 hour. The columns were then washed with 10 column volumes (20 ml) of PBSA at 1.0 ml/min, or until the trace from the UV monitor returned to zero. All elutions were conducted at room temperature. The gradient elution consisted of a linear gradient of NaSCN (Buffer B), in PBS (Buffer A) from 0 to 3M NaSCN over 20ml. At the end of the gradient Buffer B was held for 5 ml before switching to buffer A for a further 15 ml. Samples containing NaSCN were detected using filter paper previously soaked with copper sulphate solution (1% w/v) and dried. Eluted fractions were desalted using PD10 columns (Amersham Pharmacia Biotech) containing Sephadex G25 matrix, according to the manufacturers instructions. The step gradient consisted of an immediate switch from buffer A to buffer B (33%) and back to buffer A after 20 ml for a further 15 ml. Eluted fractions were desalted using PD10 columns containing Sephadex G25.

3.4.8 Sodium dodecyl sulphate polyacrylamide gel electrophoresis

Affinity-purified C595 antibody was electrophoresed on a PhastSystem separation and control unit (Pharmacia) in conjunction with PhastGel precast gels (homogeneous acrylamide, 12.5 % w/v) using SDS buffer strips (Pharmacia). Silver staining was performed using the PhastGel silver-staining kit on the PhastSystem development unit.

3.4.9 Circular Dichroism

The structural content of the peptides was evaluated using Circular Dichroism (CD). The peptides were used at concentrations of 4 μ M and CD spectra for the peptides were recorded in the far UV region (190-250nm) both at room temperature and at 4°C.

The monoclonal antibody C595 and peptides were used at a concentration of 4 μ M and at a ratio of 1:1 of peptide to antibody binding site in 50 mM phosphate buffer for the room temperature measurements and for the temperature denaturation of the antibody. The thermal denaturation of the antibody was measured in the absence of the peptides as a control and in the presence of individual peptides at a 1:1 ratio to assess the possible stabilisation effect of the peptide binding to the antibody binding-pocket. For this experiment, pre-made mixture of peptide-antibody complex was used to measure the CD spectrum of the antibody at 25, 35, 45, 55, 65, 75 and 85°C. CD spectra were recorded under N₂ using a Jasco J720 Spectrometers (Jasco Inc., Tokyo, Japan). All measurements were taken using a 0.05 cm optical path length quartz cell. The band width was 2 nm and the slit width controlled automatically, the sensitivity was set at 20 mdegrees with a time constant of 4 (arbitrary units), a step resolution of 0.2 nm and scan speed of 10 nm sec⁻¹. One scan was sufficient for accumulating spectra with high signal to low noise ratios.

3.4.9.1 Analysis of CD data versus temperature and pH

The CD signal from the C595 antibody in the presence and absence of antigenic peptides was recorded at 220 nm. The signal was analysed versus temperature to determine the melting temperature (T_m) of the antibody molecule and the possible Δ T_m (were Δ T_m = T_m of bound Ab - T_m of free Ab) obtained as the difference between free and peptide-bound antibody stability. The Van't Hoff equation was used to fit the experimental results (Missailidis, *et al.* 1997) and to determine the T_m of the antibody.

$$d(t) := \left[\frac{Eu1 \cdot \exp\left(-\frac{k1}{t} + \frac{k1}{T1 + 273}\right) + E11}{1 + \exp\left(-\frac{k1}{t} + \frac{k1}{T1 + 273}\right)} \right] + \left[\frac{Eu2 \cdot \exp\left(-\frac{k2}{t} + \frac{k2}{T2 + 273}\right) + E12}{1 + \exp\left(-\frac{k2}{t} + \frac{k2}{T2 + 273}\right)} \right] + (-Eu1)$$

Where E_l is the Lower Temperature CD limit, E_u the Upper Temperature limit, T the Temperature mid-point (T_m), E_x the Experimental CD at Temperature T_x and k is a constant related to entropy and enthalpy and the cooperativity of the melting. For every antibody, two curves were plotted, one ($d(t)$ vs t , solid line in graphs) from the theoretical values calculated from the above equation for $t = 100, 101, \dots, 500$ and another (E_{x_i} vs $273+T_i$, x 's in graphs) from the experimental data. $i = 1 \dots n$ where n is the number of experimental data.

3.4.10 Fluorescence Quenching Immunoassay

The antibody solution (2.5 ml in a 3 ml quartz cuvette, 1 cm path length) in PBS (pH 7.4) and previously filtered through a Minisart NML 0.2 μm pore membrane (Sartorius, Gottingen, Germany), was excited at 290 nm and the emitted light was measured at 345 nm using a Perkin Elmer LS-5 luminescence spectrometer (Perkin Elmer, Beaconsfield, UK). The excitation slit width was set at 5 nm and the emission slit width was set at 10 nm. The test peptides were titrated into the antibody from a concentrated stock solution ($\sim 200 \mu\text{M}$) until maximum fluorescence quenching of the antibody was observed. Dilution effects of titrating a peptide solution into the Ab solution were ascertained by titrating PBS solution into 2.5 ml of antibody solution as a control and were used for correction of the actual peptide titration data. The values of F_0 (observed intensity of fluorescence in the absence of peptides) and F (observed intensity of fluorescence in the presence of varying amounts of peptides) were noted during all the titrations. In order to obtain equilibrium constants from the results for a single mode of binding, the following formula (Missailidis, *et al.* 1997) was used:

$$A_{\text{calc}}(P_0) := \left[\left[\frac{(E_1 - E_2) \cdot \left[(1 + K \cdot D + K \cdot P_0) - \sqrt{(1 + K \cdot D + K \cdot P_0)^2 - 4 \cdot K \cdot K \cdot D \cdot P_0} \right]}{2 \cdot K} \right] + E_2 \cdot D \right] \cdot \frac{1}{D}$$

where E_1 is the minimum value of F_0/F , E_2 is the value of F_0/F corresponding to the fluorescence of the Ab on its own, K is the binding constant and D is the molar concentration of the Ab in solution. Using the observed F_0/F experimental data and the peptide molar concentrations added to the Ab solution, the $A_{\text{calc}}(P_0)$ values were

calculated by a method of computation involving an iterative procedure designed to satisfy the above equation.

3.4.11 Conjugation of peptides to BSA using glutaraldehyde

Sodium hydrogen carbonate buffer (500 μ l, 0.1M, pH 8.4) was added to bovine serum albumin (BSA) (8.0 mg), and mixed by pipetting followed by rolling. Peptide (10 μ mole) was then dissolved in sodium hydrogen carbonate buffer (1.0 ml, 0.1M, pH 8.4). The BSA solution was then added to a clean glass vial, and the following were added in the given order: -

Sodium hydrogen carbonate buffer (2.5 ml, 0.1M, pH 8.4)

Peptide solution (1.0 ml)

Glutaraldehyde (10.0 μ l)

The vial was sealed and agitated on a roller for 4 hours at room temperature. The resulting solution was then dialysed in 30cm of dialysis tube, against sodium chloride solution (0.9% w/v) for 24 hours at 4°C with stirring. The conjugate was stored at – 20°C until ready for use.

3.4.12 Production of a BSA-Estrone Conjugate

Estrone (102.2mg, 378 μ mole) was dissolved in a stirred mixture of dioxane (5.11ml) and sodium hydroxide (2M, 5.11ml). Epichlorohydrin (15.5 μ l, 189 μ mole) was added to the stirred mixture. The mixture was left stirring overnight at room temperature. Bovine serum albumin (2g) was dissolved in PBS (100ml, pH 10.0). The epichlorohydrin-estrone mixture (10.0ml) was then added to the BSA solution (10.0 ml) and stirred overnight at room temperature. The resulting solution was dialysed against five litres of PBS over the period of a weekend (at 4°C with stirring).

3.4.13 Enzyme linked immunosorbent assay (ELISA)

The antigen was dispensed into the wells of a microtitre plate (NUNC) at 50 μ l/well. Antigen was either BSA-synthetic peptide conjugate or BSA-Estrone conjugate. One row of the plate was filled with PBSA (50 μ l/well) only, to serve as an antigen blank. The plate was dried overnight to allow the conjugates to adsorb onto the wells. The plate was then washed four times with PBS/Tween wash buffer. After the final wash, care was taken to ensure that all wash buffer was removed from the wells. To remove all remaining non-specific adsorption sites, the plate was then blocked by dispensing

100µl of 1% BSA/PBS solution into the wells and incubated for one hour at room temperature with agitation. After the blocking step, blocking buffer was removed and antibody dilutions were dispensed at 50µl/well and incubated at room temperature with agitation for one hour (this incubation period was varied for some experiments). After incubation the antibody solutions were removed and the plate washed four times with washing buffer as before. The marker antibody (usually rabbit anti-mouse IgG peroxidase conjugate) was dispensed at 50µl/well at 1/1000 dilution (as recommended by the manufacturer) in PBS, and incubated for one hour at room temperature with agitation. Again the plate was washed four times in washing buffer. Finally ABTS solution was dispensed into each well at 50µl/well and colour development was measured using a Milenia Kinetic Analyser (Diagnostic Products corporation, Llanberis, UK).

3.4.13.1 Investigation of the blocking of 4155 Ab binding to a synthetic peptide library tethered to polyethylene pins by estriol-3-glucuronide.

A Replacement Net (RNET) array of peptides tethered to the heads of polyethylene pins (as described in Chapter 1) was used to probe the specificity of 4155 antibody. The RNET array consisted of peptides based on the general sequence GXFED, GLXED, GLFXD and GLFEX where residue X was replaced with each of the 20 naturally occurring amino acids. Each individual peptide was synthesised on two different pins.

4155 antibody (10µg/ml) was incubated overnight at 4°C with estriol-3-glucuronide at several different concentrations (100, 000 and 10, 000 times the antibody concentration). The estriol-3-glucuronide / antibody mixture was dispensed into the wells of a microtitre plate, such that one pair of the RNET peptide pins would be incubated. The other duplicate peptide was incubated with antibody 4155 only (150µl, 5µg/ml).

To ensure that antibody could be effectively desorbed from the pins after each experiment, the background level of binding was assessed using steps (i), (iv), (v) and (vi) of the protocol listed below. If a significant level of antibody to the pins was detected, step (vi) was repeated and the level of binding reassessed prior to continuing

with the next stage of the assay. The next stage of the assay involved using all of the steps given below to determine the binding of mAb 4155 to the pins.

(i) The pins were immersed into the wells of a microtitre plate containing blocking buffer (200µl/well), for one hour with agitation; to minimize non-specific binding. The pins were then removed from the plate and excess blocking buffer was shaken off the pins, and the pins placed onto a thickness of tissue paper for five minutes to allow the draining of any remaining buffer.

(ii) The primary antibody reaction mixture was diluted to the appropriate concentration in blocking buffer and dispensed into the wells of a microtitre plate (150µl/well). The pins were then immersed in this plate and incubated at 4°C overnight.

(iii) The pins were removed from the microtitre plate and washed. (The washing consisted of four washes, of five minutes duration each. In each wash the pins were immersed in a bath of PBS/Tween and agitated for the duration of the wash.)

(iv) Rabbit-anti-mouse horseradish peroxidase labeled IgG secondary antibody conjugate was diluted in PBS and dispensed into the wells of a microtitre plate (150µl/well). The washed pins were then immersed in the wells of the plate and incubated for one hour with agitation.

(v) The pins were then washed (as in (iv)). ABTS substrate was prepared immediately before use and dispensed into the wells of a microtitre plate (150µl/well). The pins were immersed in the substrate solution for 15 minutes and then removed to stop the reaction. The OD of each well was determined by using a Milenia Kinetic analyzer at a wavelength of 405nm.

(vi) Antibody was removed from the pins by sonication in disruption buffer at 60°C for the appropriate time period (four hours for Ab4155/GLFED RNET and two hours for C595 RPAP RNET). The pins were then rinsed four times with distilled

water at 60°C, and immersed in methanol for ten minutes. The pins were then allowed to dry fully in air.

3.4.13.2 Measurement of Mimotope Peptide Binding to 4155Ab By Competitive Inhibition ELISA

BSA-epichlorohydrin-estrone conjugate was dried overnight onto the wells of a microtitre plate (NUNC) at a concentration of 3µg/ml BSA in PBS. The general ELISA protocol described above was conducted; but the antibody dilutions consisted of mimotope peptides ((d)DYFLG, (d)GLFYD, (l)AAERGLFED) and a negative control peptide ((l)KSKAGVC), which had been incubated overnight at 4°C with the antibody dilutions.

3.4.13.3 Empirical Binding Rate Experiments

Synthetic peptides conjugated to BSA, or Estrone conjugated to BSA were dried down onto the wells of a microtitre plate (NUNC) overnight (10µg/ml BSA diluted in PBS, 50µl/well). A standard ELISA procedure was used as described above to determine the levels of antibody binding at a number of different incubation periods.

3.4.14 Surface Plasmon Resonance (SPR) analysis of the C595 – mucin core peptide APDTRPAPG interaction

Analysis of the results of kinetic experiments was conducted using BIAevaluation software, version 3.0.2 (BIAcore, Uppsala, Sweden).

3.4.14.1 Determination of the binding kinetics between antibody C595 and the MUC1 mucin related peptide APDTRPAPG.

The MUC1 mucin core peptide APDTRPAPG was immobilized onto the surface of a BIAcore Pioneer (Carboxymethyl dextran surface) F1 sensor chip. Experiments were conducted to reduce the surface binding capacity of the resulting sensor chip; and so reduce the effects of mass transport (Schuck and Minton 1996) (Edwards 1999), steric hinderance, crowding, avidity and aggregation (Myszka 1999). The aim was to minimize the amount of peptide immobilised onto the surface of the sensor chip; while still giving a measurable signal for the interacting antibody. Initial optimization experiments were conducted on a BIAcore 2000 instrument. This had the advantage

of automation and the presence of four flow cells on each sensor chip. Kinetic experiments were then repeated on a BIAcore-X instrument.

3.4.14.2 Optimization of ligand immobilization level

Several methods were tested to reduce the amount of peptide ligand APDTRPAPG immobilized onto the surface of the activated sensor chip. These included the use of competing ligands which would be non-specific for C595 antibody and varying the pH of buffer used so as to bring the charge of the peptide and the activated surface into effect. The most efficient way discovered to reduce the amount of peptide immobilized onto the activated surface was to vary the volume of peptide passed over the activated surface. This was achieved using the Pioneer CMD F1 sensor chip, with the shortened dextran matrix, rather than the BIAcore CMD CM5 chip.

To activate the carboxymethyl dextran surface, a 30 μL mixture of EDC/NHS was injected through flowcell one over a pioneer F1 sensor chip surface at a flow rate of 10 $\mu\text{L}/\text{min}$. The peptide (1 mM, 50 μL) was injected into flowcell one in HBS buffer at a flow rate of 5 $\mu\text{L}/\text{min}$. This was followed by 20 μL injection of ethanolamine-HCl (pH 8.5) to cap the remaining activated carboxyl groups. Two pulses of sodium hydroxide (250 mM, 5 μL) at 5 $\mu\text{L}/\text{min}$, followed by a third pulse (250mM, 5 μL) at 30 $\mu\text{L}/\text{min}$ were used to wash out any unbound peptide. Flowcell two was then activated as above. The same procedure was conducted individually for flowcells two, three and four respectively, except that 40 μL , 35 μL and 30 μL of peptide (1mM) were injected into each of the respective activated flowcells.

To ascertain the level of binding that could be observed when antibody bound to the peptide; the flow path was changed to include all four flow cells. Monoclonal antibody C595 (3.0 μM) in HBS buffer was then injected into the flowcells at a flow rate of 30 $\mu\text{L}/\text{min}$, and allowed to associate for 600s, and dissociate for 350s. Regeneration was conducted using two 5s pulses of sodium hydroxide (250mM).

3.4.14.3 Measurement of kinetics of the interaction

A second sensor chip was then set up using the optimized conditions of peptide immobilization derived from the previous experiment. A second flow cell was activated and deactivated without coupling the peptide as a control surface for

refractive index change and nonspecific binding. Monoclonal C595 antibody samples contained 3.0 μM , 2.5 μM , 1.5 μM , 1.0 μM and 0.5 μM protein. To perform kinetic binding studies, the flow path was changed to include both flow cells and the data collection rate was set to high. The sample (100 μL) was injected at a flow rate of 30 $\mu\text{L}/\text{min}$ with a 200 s dissociation phase. After the end of the dissociation time, the flowcells were washed with 250 mM sodium hydroxide to regenerate the sensor surfaces. Each antibody sample was injected in random order. The effect of flow rate was assessed by injecting C595 antibody (1.0 μM) at 5, 15 and 75 $\mu\text{L}/\text{min}$.

3.4.14.4 Data analysis

The raw sensor data were prepared for global analysis by subtracting the average response over 15 s prior to the antibody injection and zeroing the time of injection for each flow cell. The responses obtained from the control surface were subtracted from the peptide surface data – to correct for refractive index changes and nonspecific binding events. The corrected data was then analyzed using BIAevaluation software (BIAcore, version 3.02) by direct curve fitting to a several different models.

These models included:

1:1 (Langmuir) binding model – ($A + B = AB$)

two state reaction (conformation change)

heterogeneous ligand - (parallel reactions)

bivalent analyte

1:1 binding with mass transfer (BIAcore, 1997)

Modelled data sets were generated by numerical integration of the differential equations that describe the reaction. These were fitted to the association and dissociation phase sensor data at all antibody concentrations simultaneously using the algorithms described. The closeness of fit is described by the value χ^2 . This figure represents the average squared residual per data point for sensorgram data. Values below 10 are acceptable, since if the model fits the experimental data precisely, χ^2 represents the mean square of the signal noise (BIAcore, 1997).

3.4.15 SPR analysis of the interaction between peptide conjugate BSA-(D)DYFLG, and the anti E3G monoclonal antibody 4155.

To reduce the effects of the biosensor surface on the interaction between the peptide mimotope (D)DYFLG and the anti-E3G monoclonal antibody 4155, the interaction between the monoclonal antibody and the peptide BSA-conjugate was studied. Studying this interaction had the advantage that the reaction could be studied with either partner immobilised. A comparison was made between the kinetics observed when (i) the antibody was immobilised and (ii) the BSA-peptide conjugate was immobilised.

3.4.15.1 Immobilisation of monoclonal antibody 4155 onto the surface of Pioneer F1 CMD sensor chip.

The monoclonal antibody was immobilised using NHS/EDC coupling chemistry. To activate the carboxymethyl dextran surface, a 35 μL mixture of NHS/EDC was injected over the sensor surface at a flow rate of 5 $\mu\text{L}/\text{min}$. The 4155 mAb (50 $\mu\text{g}/\text{ml}$) was injected in sodium citrate buffer (pH 3.5) in flowcell one until the desired level of immobilisation was achieved – determined by experiment to give a signal of less than 100 RU on binding of the BSA–peptide conjugates. This was followed by 20 μL injection of 1M ethanolamine-HCl (pH 8.5) to cap the remaining activated carboxyl groups. The same procedure was conducted using flowcell two, immobilising an irrelevant monoclonal antibody under the same conditions. The surface was conditioned by passing two short pulses of the regeneration buffer through both flow cells (20 mM HCl, 10 μL pulses).

3.4.15.2 Immobilisation of the peptide (D) DYFLG-BSA conjugate onto the surface of a pioneer F1 CMD sensor chip.

Peptide (D)DYFLG was conjugated to bovine serum albumin at a concentration of 2.5 mg/ml. The surface of a sensor chip was activated by passing a mixture of EDC/NHS through flowcell one of a Pioneer F1 sensor chip. The peptide conjugate was injected into flowcell one in 10mM acetate buffer at a rate of 5 $\mu\text{L}/\text{min}$. This was followed by a 20 μL injection of ethanolamine-HCl (pH 8.5) to cap the remaining activated carboxyl groups. Flowcell two of the sensor chip was also activated identically. An irrelevant BSA-peptide conjugate was immobilised onto this flowcell under the same

conditions as flowcell one. The surface was conditioned with two pulses of the regeneration buffer through both flow cells (20 mM HCl, 10 μ L pulses).

3.4.15.3 Investigating the kinetics of the interaction.

3.4.15.3.1 Immobilised antibody.

BSA – peptide conjugate samples were prepared containing peptide at concentrations of 500, 200, 100 and 50 nM. To perform kinetic studies the flowpath was set to include both flowcells one and two, and the data collection rate was set to high. The sample was injected at a flow rate of 5 μ L/min with a 180s association phase and a 500s dissociation phase. After the end of the dissociation phase, the flowcells were washed with 20mM HCl to regenerate the sensor surfaces. Each peptide sample was injected in random order.

3.4.15.3.2 Immobilised peptide – BSA conjugate.

Antibody samples containing 500, 200, 100 and 50 nM protein were prepared. The flowpath was set to include both flowcells one and two, and data collection was set to high. The sample was injected at a flowrate of 30 μ L/min with a 500s dissociation phase. At the end of the dissociation phase, the flowcells were washed with 20 mM HCl to regenerate the sensor surfaces. Each antibody sample was injected in random order.

3.4.15.3.3 The effect of temperature on the interaction.

The effect of temperature on the kinetic parameters of the interaction between immobilised antibody an BSA-peptide conjugate was investigated. Kinetic parameters were obtained by globally fitting a Langmuir association model (simple 1:1 interaction) to each data set (using conjugate concentrations at 500, 200, 100 and 50 nM) for each temperature studied (10, 15, 20 and 30 °C).

3.4.16 Production of pCANTAB-5E [C595scFvGFP]. A Phagemid expression vector containing a C595 ScFv – Green Fluorescent Protein Gene fusion.

3.4.16.1 Preparation of Electrocompetent Cells

LB growth media (1 litre) was inoculated with 1/10 volume of fresh overnight culture. The cells were grown at 37°C with shaking (200 rpm). When the cells had reached early to mid log phase growth (OD_{600nm} of ~ 0.5), they were harvested as follows.

The flask was chilled on ice for 30 minutes and then the contents were centrifuged in a cold rotor at 4000 x g for 15 minutes. The cell pellets were resuspended in ice cold dH₂O (1 litre), and centrifuged as before. The cell pellets were again resuspended in ice cold dH₂O (0.5 litre), and centrifuged as before. The cell pellets were resuspended in ~20 ml of the cryoprotectant (10% v/v glycerol), and centrifuged as before. Finally the cell pellets were resuspended to a final volume of 3.0 ml in 10% glycerol. The resuspended pellets were stored at -70°C ready for use.

3.4.16.2 Transformation of competent cells - electroporation

Transformations by electroporation were conducted using a commercially available electroporator.

3.4.16.3 Isolation of the plasmid vector pCANTAB-5E containing C595 single-chain Fv (scFv) gene.

E.coli strain HB2151 were transformed with the plasmid vector pCANTAB-5E containing the C595 scFv gene (Denton, *et al.* 1997). The transformed *E.coli* bacteria were spread on LB-agar plates containing ampicillin (50 µg/ml), and incubated at 37 °C overnight. One colony of transformed bacteria was picked and incubated at 37 °C in LB medium (25 ml) containing ampicillin (50 µg/ml), with shaking (300 rpm) overnight. Plasmid DNA was isolated from cells using the protocol described in the Wizard Plus SV miniprep DNA purification system (Promega Corporation, Madison, USA). A restriction digest using restriction enzymes Sfi I and Not I was conducted to confirm the integrity of the Sfi I and Not I restriction sites flanking the ScFv gene (see section 2.4.16.10).

3.4.16.4 Isolation of the plasmid vector pTRACER-cmv containing the Green Fluorescent Protein Gene.

Chemically competent *E.coli* strain TOP10 (Invitrogen BV, Groningen, The Netherlands) were transformed with the pTracer-CMV expression vector containing the GFP gene, according to the manufacturers instructions. The transformed bacteria were spread on LB-agar plates (containing ampicillin (50 µg/ml)) and incubated overnight at 37 °C. An LB-agar plate containing individual colonies was placed on a Spectroline TM-312A Ultra Violet Transilluminator, and a fluorescing colony was picked and grown up in LB (25 ml) containing ampicillin (50 µg/ml). The culture was incubated overnight with shaking (300 rpm) at 37 °C. Plasmid DNA was isolated from cells using the protocol described in the Wizard Plus SV miniprep DNA purification system (Promega Corporation, Madison, USA).

3.4.16.5 Design of primers to amplify the C595 single-chain Fv gene.

Primers were designed to amplify the C595 ScFv gene in the pCANTAB-5E vector. The primers enabled the retention of the unique Sfi I restriction site at the 5' end of the gene; and mutated the unique Not I restriction site at the 3' end of the gene to another unique Bgl II restriction site (in the scFv gene). (See figure 7.3 – chapter 7)

3.4.16.6 Design of primers to amplify Green Fluorescent Protein Gene.

Primers were designed to amplify the GFP gene in the pTracer-CMV vector. The primers enabled the introduction of a unique Bgl II restriction site at the 5' end of the gene; and the introduction of a unique Not I restriction site at the 3' end of the gene. (See figure 7.3 – chapter 7)

3.4.16.7 PCR amplification of ScFv and GFP genes.

PCR reactions were performed on plasmid minipreps (Wizard PlusSV minipreps, Promega, USA), the amount of DNA was visually estimated by gel electrophoresis (~10µg/100µl) , in 50 µl aliquots using 25 pM of each primer and 2.5 mM of each dNTP. Each reaction was set up as follows: -

10 x Buffer	5 μ l
10 mM dNTP's	1 μ l
25 mM MgCl ₂	3 μ l
Primers (25 pmol each)	2 μ l
DNA Template	1 μ l
dH ₂ O	<u>37 μl</u>
	49 μ l

Each reaction was overlaid with 25 μ l of light mineral oil.

A hot start was conducted prior to the addition of Taq polymerase (2.5 units), consisting of heating the reaction mix to 95 °C for 5 minutes. The PCR program initially consisted of 30 cycles of 94 °C for 45s, 60 °C for 45s and 72 °C for 90s (representing denaturation, annealing and elongation temperatures respectively); followed by a single extended elongation step of 72 °C for 30 min. The extended elongation step was present to ensure that all PCR products are full length and 3' adenylated (necessary for an efficient TOPO-TA cloning reaction).

Experimentation showed that the number of PCR cycles could be reduced from 30 to 10, still enabling the PCR band to be visualised on an agarose gel.

3.4.16.8 Low-Melt Agarose purification of PCR products.

Agarose gels (1%) were prepared by dissolving low-melt NuSieve agarose in TAE buffer. Ethidium bromide (0.2 μ g/ml) was incorporated into the gel before pouring. Samples were diluted with DNA loading buffer, and electrophoresis was performed. DNA was visualised using a Spectroline TM-312A Ultra Violet Transilluminator, and photographs were recorded using a Polaroid DS-34 Direct Screen Instant Camera. The band of interest was excised using a sharp scalpel.

3.4.16.9 TOPO-TA cloning of amplified PCR products.

The gel slice was placed in a microcentrifuge tube and incubated at 65 °C until the gel slice melted. The tube was then placed at 37 °C to keep the agarose gel melted. A sample of the melted agarose (4 μ l) containing the PCR product was mixed with the TOPO TA cloning vector (1 μ l) (Invitrogen BV, Groningen, The Netherlands) and incubated at 37 °C for 10 minutes. A sample of the mixture (4 μ l) was transformed directly into TOP10 one shot cells using the method as described by the manufacturer.

A small number of the resulting white colonies were analysed (blue colonies contain no insert and so were not picked) using M13 Forward and M13 Reverse primers as described by the manufacturer. A pick from each colony to be analysed was suspended in 20 µl of LB media and vortexed. 1.0 µl of the suspended sample was used in each PCR reaction.

Positive clones (those containing an insert of the correct size) were then grown by inoculating LB media (10.0 ml) containing ampicillin (50 µg/ml) overnight at 37 °C with shaking (300 rpm). Plasmid DNA was isolated from cells using the protocol described in the Wizard Plus SV miniprep DNA purification system (Promega Corporation, Madison, USA). The positive clones were then analysed using restriction analysis to confirm that the Sfi I, Bgl II and Not I restriction sites were functional. Restriction digestion of the C595 ScFv TOPO clones containing the unique Sfi I and Bgl II restriction sites was conducted by performing individual Sfi I and Bgl II digests; alongside a double digestion of the vector with Sfi I and Bgl II restriction enzymes. Restriction digestion of the GFP TOPO clones containing the unique Bgl II and Not I restriction sites were conducted by performing individual Bgl II and Not I restriction digests; alongside a double digestion of the vector with Bgl II and Not I. See section (3.4.16.10) for details of restriction digests. Positive TOPO clones (PCR and Restriction analysis) were sequenced using M13 forward and M13 reverse drivers.

3.4.16.10 Digestion and ligation of TOPO-cloned genes.

Cleaving a DNA substrate with two restriction endonucleases simultaneously (double digestion) enables more efficient restriction digests to be conducted, providing a reaction buffer can be selected in which both enzymes function effectively. This was the case with the restriction enzymes used in this case. The Sfi I / Bgl II and Bgl II / Not I digests were used to confirm the integrity of the restriction sites resulting from the previous PCR. The restriction digests were set up as follows: -

Restriction analysis of C595 ScFv TOPO clones

The optimum functional temperature for the restriction enzyme Sfi I is 50°C, but the optimum functional temperature for Bgl II I is 37°C. In order to perform the sequential digestion using the Sfi I and Bgl II restriction enzymes in the same reaction

Chapter 3 Materials and Methods.

mixture, the reaction was first incubated at 37°C for three hours followed by an incubation at 50°C for three hours to enable the efficient digestion of both the Bgl II and Sfi I restriction sites respectively.

Sfi I digest		Bgl II digest		Sfi I / Bgl II digest	
10 x NEB 2 buffer	2.5µl	10 x NEB 2 buffer	2.5µl	10 x NEB 2 buffer	2.5µl
Sfi I (20,000 units/ml)	0.25µl	Not I (10,000 units/ml)	0.5µl	Not I (10,000 units/ml)	0.5µl
100 x BSA	0.25µl	100 x BSA	0.25µl	Sfi I (20,000 units/ml)	0.25µl
Plasmid DNA	22.0µl	Plasmid DNA	21.75µl	100 x BSA	0.25µl
				Plasmid DNA	21.5µl

A control reaction was set up consisting of plasmid DNA, 100 x BSA and 10 x NEB 2 buffer to ensure that no contamination of the reagents with restriction enzyme had occurred.

Restriction analysis of GFP TOPO clones

The optimum functional temperatures for the Bgl II and Not I restriction enzymes are identical at 37°C, enabling the sequential digestion using Bgl II and Not I restriction enzymes to be conducted at the same temperature. The restriction digests were conducted at 37°C for three hours.

Bgl II digest		Not I digest		Bgl II / Not I digest	
10 x NEB 3 buffer	2.5µl	10 x NEB 3 buffer	2.5µl	10 x NEB 3 buffer	2.5µl
Bgl II (10,000 units/ml)	0.5µl	Not I (10,000 units/ml)	0.5µl	Bgl II (10,000 units/ml)	0.5µl
100 x BSA	0.25µl	100 x BSA	0.25µl	Not I (10,000 units/ml)	0.5µl
Plasmid DNA	21.75µl	Plasmid DNA	21.75µl	100 x BSA	0.25µl
				Plasmid DNA	21.25µl

A control reaction was set up consisting of plasmid DNA, 100 x BSA and 10 x NEB 3 buffer to ensure that no contamination of the reagents with restriction enzyme had occurred.

Restriction digests of TOPO clones for ligation

A Hind III / Bgl II double digest was used to isolate the scFv and GFP genes prior to the ligation reaction. Hind III was chosen instead of Sfi I or Not I since the pCR 2.1 TOPO cloning vector contains a unique Hind III restriction site close to the cloning region, and this enables the use of the original primers to amplify the ligation product.

Digests incorporating Sfi I and Not I would have resulted in products with shortened termini resulting in a less efficient final PCR reaction. The optimum functional temperatures for the Bgl II and Hind III restriction enzymes are identical at 37°C, enabling the sequential digestion using Bgl II and Hind III restriction enzymes to be conducted at the same temperature. The restriction digests were conducted at 37°C for three hours.

Bgl II / Hind III digest

10 x NEB 2 buffer	2.5µl
Bgl II (10,000 units/ml)	0.5µl
Hind III (10,000 units/ml)	0.5µl
Plasmid DNA	21.5µl

3.4.16.10.1 Low melt agarose purification of products from restriction digests

Agarose gels (1%) were prepared by dissolving low-melt NuSieve agarose (Flowgen, Sittingbourne, UK) in TAE buffer. Ethidium bromide (0.2 µg/ml) was incorporated into the gel before pouring. Samples were diluted with DNA loading buffer, and electrophoresis was performed. DNA was visualised using a Spectroline TM-312A Ultra Violet Transilluminator, and photographs were recorded using a Polaroid DS-34 Direct Screen Instant Camera. The band of interest was excised using a sharp scalpel.

3.4.16.10.2 In-gel ligation of excised scFv and GFP genes

The excised slices of gel containing the scFv and GFP gene fragments were placed in separate, labelled microfuge tubes. The tubes were heated to 70 °C for 15 minutes to melt the agarose. Aliquots (5 µl each) of the melted bands to be ligated were combined in a prewarmed ependorf tube (37 °C). The molar ratio of the two genes was estimated to be roughly equal. The reaction was incubated for 10 minutes at 37°C. Ice cold 2 x bacteriophage T4 DNA ligase mixture (10 µl) was added to the tube, and mixed well with the contents of the tube before the gel hardened. The reaction was incubated at 16 °C for 16 hours. The agarose in the ligation mixture was then remelted by heating to 70 °C for 15 minutes. A 1µl aliquot of the remelted mixture was then used in a PCR with C595 SfiI FOR and GFP NotI REV primers, following the protocol outlined in section 3.4.16.7. A TOPO-TA cloning reaction of the PCR product was then carried out using the protocol outlined in section 3.4.16.9. and the insert sequenced to verify ligation of the two gene fragments. The clone

containing functional Sfi I and Not I restriction sites and containing the correct sequence was named pCR2.1-TOPO[C595scFvGFP].

3.4.16.10.3 In-gel ligation of C595-ScFv – GFP fusion into pCANTAB-5E vector.

Double digestions were carried out on the pCANTAB-5E and pCR2.1-TOPO[C595scFvGFP] vectors to enable isolation of the pCANTAB-5E plasmid and the C595scFvGFP DNA insert. The restriction digests for each vector were set up as follows: -

<u>Sfi I digest</u>		<u>Not I digest</u>		<u>Sfi I / Not I digest</u>	
10 x NEB 2 buffer	2.5µl	10 x NEB 2 buffer	2.5µl	10 x NEB 2 buffer	2.5µl
Sfi I (20,000 units/ml)	0.25µl	Not I (10,000 units/ml)	0.5µl	Not I (10,000 units/ml)	0.5µl
100 x BSA	0.25µl	100 x BSA	0.25µl	Sfi I (20,000 units/ml)	0.25µl
Plasmid DNA	22.0µl	Plasmid DNA	21.75µl	100 x BSA	0.25µl
				Plasmid DNA	21.5µl

A control reaction was set up consisting of plasmid DNA, 100 x BSA and 10 x NEB 2 buffer to ensure that no contamination of the reagents with restriction enzyme had occurred. The restriction digests were heated for 3 hours at 37°C followed by heating for 3 hours at 50°C to enable Not I and Sfi I enzymes respectively to both function.

Agarose gel electrophoresis was used to analyse the digests, and the required gel fragments were excised from the gel. An in-gel ligation was conducted as follows:

The excised slices of gel were placed in separate, labelled microfuge tubes. The tubes were heated to 70 °C for 15 minutes to melt the agarose. Aliquots (5 µl each) of the melted bands to be ligated were combined in a prewarmed ependorf tube (37 °C). The molar ratio of foreign DNA : plasmid vector was estimated to be approximately 2:1 (estimated from the relative fluorescence intensities of the desired bands (Sambrook, et al. 1989)). Two additional ligation reactions were set up in separate tubes as controls; one containing the plasmid vector alone and the other containing only the fragment of foreign DNA. The three tubes were incubated for 10 minutes at 37 °C. To each tube ice cold 2 x bacteriophage T4 DNA ligase mixture (10 µl) was added, and mixed well with the contents of the tube before the gel hardened. The reactions were incubated at 16 °C for 16 hours. The agarose in the ligation mixture was then

remelted by heating to 70 °C for 15 minutes. An aliquot (5 µl) of one of the ligation mixtures was used to transform 100 µl of chemically competent *E.coli* strain TOP10 (Invitrogen BV, Groningen, The Netherlands) according to the manufacturers instructions. Transformed cells were plated out onto LB-agar plates containing ampicillin (50 µg/ml). The plates were incubated at 37 °C overnight.

A small sample of colonies were picked from the plate using a sterile pipette tip and suspended in 20 µl of LB media. Samples were analysed by PCR using the method described in section (3.4.16.7) using primers S1 and S6 (Denton, *et al.* 1997). Samples containing an insert of the desired size were then analysed by restriction enzyme digestion (Sfi I, Bgl II and Not I) using the methods described in section (3.4.16.10). Positive clones were then sequenced. The positive clone containing the correct sequence was named pCANTAB-5E [C595scFvGFP]. A sample of the bacteria containing the engineered plasmid were stored as a glycerol stock (10 % w/v glycerol) at -70°C.

3.4.17 Protein expression

Plasmid pCANTAB-5E [C595scFvGFP] isolated as described in section (3.4.16.10.3) was used to transform the nonsuppressor strain of *E.coli*. (strain HB2151) by electroporation. This strain recognizes the amber stop codon after the C595scFvGFP gene insert, enabling the production of soluble fusion protein. Electrocompetent *E.coli*. (strain HB2151) were prepared as described in section (3.4.16.1). The transformed *E.coli*. were streaked onto a SOBAG-N plate and incubated overnight at 30 °C.

3.4.17.1 Expression in supernatant

An overnight culture of was prepared by transferring a colony from the SOBAG-N plate prepared in section (3.4.17) to 5.0 ml of freshly prepared SB-AG medium and incubated overnight at 30 °C with shaking at 250 rpm. The overnight culture was then added to 50.0 ml of freshly prepared SB-AG medium. The culture was incubated for one hour at 30 °C with shaking at 250rpm. The culture was centrifuged at 1500 x g for 20 minutes at 4 °C. The supernatant was carefully removed from the sedimented cells. The cells were then resuspended in 50.0 ml of freshly prepared SB-AI medium and incubated overnight at 30 °C with shaking at 250 rpm in baffled flasks. The

culture was divided into two centrifuge tubes and centrifuged at 1500 x g for 20 minutes at room temperature. The supernatants were removed from both pellets and transferred to a single clean glass container. The supernatant was filtered through a 0.45 µM filter (Satorius, Gottingen, Germany) and stored at -20 °C. One pellet was retained for preparation of the periplasmic extract and the other pellet for preparation of whole cell extract.

3.4.17.2 Affinity Purification of induced supernatant

The supernatant (~50 ml) was applied to a chromatography column consisting of peptide APDTRPAPG linked to beaded agarose at a concentration of 1µmole peptide per ml gel, as described in section (3.4.7.1). After extensive washing of the column with PBSA (100ml), a gradient elution was conducted using NaSCN (3M), as described in section (3.4.7.2). Fractions (2.5 ml) were collected and desalted using a PD10 column (Amersham, Pharmacia, Biotech) containing Sephadex G25.

3.4.17.3 Trichloroacetic acid (TCA) precipitation of protein

The soluble antibody fractions were too dilute to visualise on western blot. A TCA precipitation step was conducted to establish if concentration of protein could be achieved to enable visualisation on western blot. Trichloroacetic acid (250 µl, 20% w/v) was added to a microcentrifuge tube containing 250 µl of sample and mixed. The mixture was incubated on ice for 15 minutes and centrifuged on a bench top centrifuge for 15 minutes at 12,000 rpm. The supernatant was removed and the pellet resuspended in 20 µl of water. The sample was then used for electrophoresis as described in section (3.4.8)

3.4.17.4 Periplasmic Extract

One of the pellets from (3.4.17.1) was resuspended in ice cold TES buffer (0.5 ml). Ice-cold 1/5 x TES (0.75 ml) was added, and the mixture was vortexed. The mixture was incubated on ice for 30 minutes. The contents were transferred to a microcentrifuge tube (1.5 ml) and centrifuged at full speed for 10 minutes. The supernatant was carefully removed and placed in a clean tube and stored at -20 °C.

3.4.17.5 Whole Cell Extract

The second pellet from (3.4.17.1) was resuspended in PBS (0.5 ml) and boiled for 5 minutes. The cell debris was pelleted as in (3.4.17.2) and the supernatant was carefully transferred into a clean tube, and stored at -20°C until use.

3.4.18 Western blot analysis

Periplasmic extract (20 μl) was mixed with 6X loading buffer (4 μl) (Novagen). A prestained molecular weight marker was run in parallel with the samples. All samples were heated to 99°C for 5 minutes, cooled to room temperature and briefly spun. Each sample was loaded onto an SDS-polyacrylamide gel and electrophoresed until the dye contained in the loading buffer reached the bottom of the gel.

The proteins were transferred from the gel to a nitrocellulose membrane. When the transfer was complete, the membrane was incubated in Blocking Buffer (20.0 ml) for 1 hour at room temperature, in a closed container. The anti-E Tag HRP (2.0 μl) conjugate was diluted in blocking buffer (20.0 ml). The blocking buffer was removed from the blot and replaced with the diluted anti-E Tag HRP conjugate solution. The blot was incubated for one hour at room temperature with gentle agitation in a closed container. The diluted conjugate solution was removed from the blot. The blot was washed six times (2 minutes per wash) with an excess of wash buffer, and once with distilled deionized water. Excess water was drained from the blot, and the blot was placed in freshly prepared 4-chloro-1-naphthol substrate. The blot was gently agitated in a sealed container until a blue colour developed, indicated that a reaction had occurred. The blot was rinsed with deionized water to stop the reaction.

3.4.19 ELISA of Supernatant, Periplasmic Extract, Whole Cell Extract and fractions from affinity purification of supernatant.

A Standard ELISA technique was conducted using the procedure described in section 2.4.12. BSA-APDTRPAPG peptide conjugate was dried down in the wells of a microtitre plate overnight. The various products of the expression were incubated on the plate. The marker antibody in this case was HRP/Anti-E Tag conjugate (Amersham Pharmacia Biotech). ABTS was used as the revealing substrate. Colour development was measured using a Milenia Kinetic Analyser (Diagnostic Products corporation, Llanberis, UK).

3.4.20 Random mutagenesis of the C595-ScFv gene – analysis of a selection of mutants.

The method employed consisted of a modified polymerase chain reaction which was used to produce random point mutations in the C595 ScFv gene. The ScFv gene was amplified using the polymerase chain reaction (PCR) under conditions that reduce the fidelity of DNA synthesis by *Thermus aquaticus* (Taq) DNA polymerase. The pool of amplified DNA fragments containing the point mutations was then inserted into the pCR 2.1-TOPO cloning vector to produce a library of random mutants.

3.4.20.1 Cloning of ScFv gene from pCANTAB-5E into pCR2.1 TOPO

The C595 scFv gene was cloned from the pCANTAB-5E using C595Sfi FOR and C595 Not I REV primers as described in sections (2.4.16.7 – 2.4.16.9).

3.4.20.2 Mutagenic PCR reaction

The method of mutagenic PCR as described by Cadwell *et al* was employed (Cadwell and Joyce 1994). The protocol is derived from standard PCR conditions (Coen 1991), using changes which enhance the mutation rate as follows: -

	Standard PCR	Mutagenic PCR
[MgCl ₂]	1.5 mM	7.0 mM ¹
[MnCl ₂]	-	0.5 mM ²
[dATP]	0.2 mM	0.2 mM
[dCTP]	0.2 mM	1.0 mM ³
[dGTP]	0.2 mM	0.2 mM
[dTTP]	0.2 mM	1.0 mM ³
Taq polymerase	2.5 U	5.0 U ⁴

Note: -

1. Stabilize noncomplementary pairs.
2. Diminish template specificity of the polymerase.
3. Promote misincorporation.
4. Promote chain extension beyond positions of base mismatch.

The mutagenic PCR reaction was set up alongside the normal PCR reaction as follows: -

Mutagenic PCR		Normal PCR	
10 x mutagenic buffer	10 μ l	10 x PCR buffer	10 μ l
10 x mutagenic dNTP mix	10 μ l	10 x dNTP mix	10 μ l
C595 Sfi I FOR primer	2 μ l	C595 Sfi I FOR primer	2 μ l
C595 Not I REV primer	2 μ l	C595 Not I REV primer	2 μ l
Plasmid DNA	2 μ l	Plasmid DNA	2 μ l
DH ₂ O	62 μ l	dH ₂ O	72 μ l
MnCl ₂ *	10 μ l	-	

* MnCl₂ added last to prevent formation of a precipitate that disrupts PCR amplification.

The appropriate amount of Taq polymerase was added to each of the reactions (see above), bringing the final volume to 100 μ l. The mixture was covered with mineral oil. The reactions were incubated for 30 cycles of 94°C for 1 min, 45°C for 1 min, and 72°C for 1 min.

3.4.21 Evaluation of pSKGFP expression system

The vector pSK-GFPmut1 (Griep, vanTwisk *et al.* 1999) was supplied in lyophilised form. The vector was resuspended in TBE buffer and used to transform *E.coli* strain XL1-Blue-MRF' (Invitrogen. Directions were carried out as written by the authors to see if their results could be reproduced.

4 Chapter 4 - Results. Phage Display of Peptides.

4.1 Introduction

Chapter 1 described the various techniques that are available to purify antibodies from crude biological feedstocks. Affinity purification utilising synthetic peptides as paratope-specific binding ligands was observed to be the method of choice. Unlike any of the other methods described, the use of this method to isolate antibodies from crude feedstocks can yield antibodies of high and standardized immunoreactivity in a single purification step (Price, *et al.* 1991; Murray, *et al.* 2000; Smith, *et al.* 2001). Chapter 2 outlined the different library technologies that are currently available to facilitate the discovery of paratope specific binding ligands. This chapter focuses on the use of one of these technologies – phage display. In this chapter, a description and analysis is given of the results obtained when the polyvalent T7 display library was used to isolate a novel binding ligand for the anti-MUC1 murine monoclonal antibody C595.

The process relies on the use of a technique known as “biopanning”. Biopanning (or affinity selection) is a procedure for the enrichment of molecules that bind to a given target protein. The target protein can be linked to a solid support (e.g. biotinylated antigen can be linked to streptavidin coated magnetic beads) or the target protein can be non-specifically absorbed onto a solid support (e.g. ELISA plate, immunotubes ...etc.). The use of biotinylated target proteins offers advantages in terms of tailoring the selection conditions to select for a desirable kinetic in the interaction (e.g. slow off-rate). Elution conditions can be tailored to select for desirable kinetic traits when biopanning using proteins which are non-specifically adsorbed to solid supports. Parameters such as the stringency of the washes can be varied, and so too can the elution buffers. Specific phage bind to the target protein, whilst non-specifically binding phage are washed off. Bound phage removed in the elution step can then be quantified (e.g. plaque assay and sequencing of individual clones) and propagated for repeated rounds of selection and enrichment.

4.2 The T7Select415 phage display library

The T7 phage was described in section 2.3.1.1. Peptides were encoded for by a degenerate oligonucleotide insert, consisting of a randomized library of 9-residue peptides flanked by cysteine residues (to impose a structural constraint on the C-terminus of the displayed peptides (McConnell, *et al.* 1994). The cysteine residues were also flanked with serine residues, such that the N terminus of the peptide was linked to the capsid head through a serine residue (see fig. 4.1). The nine randomized residues were incorporated into the insert using a sequential synthesis strategy for each codon of NNK; where N is an equimolar mixture of the bases A, G, C and T; and K is an equimolar mixture of the bases G and T only. Using this method the number of stop codons that can be coded for falls from three to one at each codon (see fig. 4.2).

The chemically synthesized single-stranded degenerate oligonucleotide insert was converted into a clonable double-stranded DNA insert containing EcoRI and HindIII restriction sites. This was done by annealing a second short oligonucleotide incorporating the HindIII restriction site, and using Taq polymerase to fill in the rest of the strand. Taq polymerase fills in complementary strand of degenerate oligo. The insert was digested using EcoRI and Hind III restriction enzymes and ligated into the T7Select415-1b vector. From the initial ligation reaction 1.4×10^8 independent clones were obtained (Dr P. Tighe, University of Nottingham – personal communication). Propagation of the library resulted in a lysate consisting of 4.36×10^{10} pfu/ml. This is equivalent to 311 copies of each individual clone per ml of lysate ($4.36 \times 10^{10} / 1.4 \times 10^8 = 311$).

Chapter 4 - Results. Phage Display of Peptides.

21271
 AAA GGT GAG GGT AAT GTC AAG GTT **GCT AAG GAC AAC GTT ATC GGC CTG**
 T7 Select 415-1b Vector 5' 21295 R1 FOR Primer →
 CGA TTC CTG TTG CAA TAG CCG GAC

3' 21340
TTC ATG CAC CGC TCT GCG GTA GGT ACT GTT AAG CTG CGT GAC TTG GCT
 AAG TAC GTG GCG AGA GCG CAT CCA TGA CAA TTC GAC GCA CTG AAC CGA
 GGT ACT GTT AAG CTG CGT GAC TTG GC
 5' SEQ FOR Primer → 3'

CTG GAG CGC GCT CGC CGT GCT AAC TTC CAA GCG GAC CAG ATT ATC GCT
 GAC CTC GCG CGA GCG GCA CGA TTG AAG GTT CGC CTG GTC TAA TAG CTA

AAG TAC GCA ATG GGC CAC GGT GGT CTT CGC CCA GAA GCT GCA GGA GCT
 TTC ATG CGT TAC CCG GTG CCA CCA GAA GCG GGT CTT CGA CGT CCT CGA
 Ala Ala Gly Ala

GTC GTA TTC CAG TCA GGT GTG ATG CTC GGG GAT CCG AAT TCC TGC xxx
 CAG CAT AAG GTC AGT CCA CAC TAC GAG CCC CTA GGC TTA AGC ACG xxx
 Val Val Phe Gln Ser Gly Val Met Leu Gly Asp Pro Asn Ser Cys xxx
 1

Degenerate oligonucleotide insert Hind III
 xxx xxx xxx xxx xxx xxx xxx xxx TGC TCT TGA AGC TTG CGG CCG CAC
 xxx xxx xxx xxx xxx xxx xxx xxx **ACG AGA ACT TCG AAC** GCC GGC GTG
 xxx xxx xxx xxx xxx xxx xxx xxx Cys Ser STOP
 2 3 4 5 6 7 8 9

CAC TCG AGT AAC TAG TTA ACC CCT TGG GGC CTC TAA ACG GGT CTT GAG
 GTG AGC TCA TTG ATC AAT TGG GGA ACC CCG GAG ATT TGC CCA GAA CTC

GGG TTT TTT GCT GAA AGG AGG AAC TAT ATG CGC TCA TAC GAT ATG AAC
 CCC AAA AAA CGA CTT TCC TCC TTG ATA TAC GCG AGT ATG CTA TAC TTG

GTT GAG ACT GCC GCT GAG TTA TCA GCT GTG AAC GAC ATT CTG GCG TCT
 CAA CTC TGA CGG CGA CTC AAT AGT CGA CAC TTG CTC TAA **GAC CGC AGA**
 3'

21697
 ATC GGT GAA CCT CCG GTA TCA ACG CGA AGG TGA CGC TAA CGC AGA TGC
TAG CCA CTT GGA GGC CAT AGT TGC
 ← R2 Rev Primer 5'

21748 3'
 AGC GAA CGC TCG GCG TAT TCT CAA CAA

xxx = NNK Where N is an equimolar mixture of A, G, C & T
 K is an equimolar mixture of G and T

Figure 4.1: Cloning region of the T7Select415-1b vector.

	A	C	G	T
A	AAG (K) AAT (N)	ACG (T) ACT (T)	AGG (R) AGT (S)	ATG (M) ATT (I)
C	CAG (Q) CAT (H)	CCG (P) CCT (P)	CGG (R) CGT (R)	CTG (L) CTT (L)
G	GAG (E) GAT (D)	GCG (A) GCT (A)	GGG (G) GGT (G)	GTG (V) GTT (V)
T	TAG Stop TAT (Y)	TCG (S) TCT (C)	TGG (W) TGT (C)	TTT (F) TTG (L)

A	R	N	D	C	Q	E	G	H	I	L	K	M	F	P	S	T	W	Y	V
GCG GCT	AGG CGG CGT	AAT	GAT	TCT TGT	CAG	GAG	GGG GGT	CAT	ATT	CTG CTT TTG	AAG	ATG	TTT	CCG CCT	AGT TCG	ACG ACT	TGG	TAT	GTG GTT

Figure 4.2: Illustration of the NN(K/T) strategy used to reduce the number of stop codons present in the degenerate oligonucleotide insert. The table shows that only the TAG stop codon is present. Also shown is a table illustrating the relative frequencies of codons for each amino acid using this strategy.

4.3 Determination of initial phage library titer and stability of the library

In order to calculate the volume of the phage library that was needed to give a large enough representation of all the clones within the library, it was necessary to determine the concentration of viable (infectious) phage within the sample. Clarified phage lysates are normally stable at 4°C, but a gradual decrease in phage titer is usually observed [Tighe personal communication]. The change in the concentration of infectious phage was monitored by conducting a second plaque assay - after the clarified phage solution was stored at 4°C for two months. The multiplicity (theoretical number of indential, independent phage clones per ml of lysate) of the phage library was then calculated by using the following formula:-

$$\text{Multiplicity (independent clones/ml)} = \frac{\text{Titer of amplified library}}{\text{N}^{\circ} \text{ of independent clones from initial ligation reaction}}$$

The plaque assays were conducted as described in chapter 3.

1/Dilution factor	N ^o Plaques	N ^o Plaques (after 2 months)
10 ⁶	>200	>200
10 ⁷	27	15
10 ⁸	2	0
10 ⁹	0	0
10 ¹⁰	0	0

Titer (pfu/ml)	2.7 x 10 ⁹	1.5 x 10 ⁹
Multiplicity (independent clones/ml)	19	10

Table 4.1: Results of phage plaque assays. 100µl of each phage dilution were added to 250µl of E.coli (strain BL21) cells grown to OD₆₀₀ = 1.0. 3.0 ml of top agarose was added and the mixture poured onto LB agar plates. Plaques were counted after incubation overnight at 37°C.

Note the reduction in the multiplicity of the library after 2 months of storage at 4°C. The multiplicity has approximately halved. To compensate for this the volume of library screened would have to be doubled to ensure that the number of clones screened remained consistent.

4.4 Analysis of passive adsorption of proteins on the surface of NUNC immunotubes by ELISA method

An ELISA was performed to evaluate the adsorption of the two antibodies onto the surface of NUNC immunotubes (using the protocol described in Chapter 3). A 2.5-ml volume of the serially diluted protein was dispensed (in triplicate) into the immunotubes, which were then incubated at 37°C for 3 hours. The two antibodies were probed with Horseradish peroxidase conjugated rabbit-anti-mouse antibody.

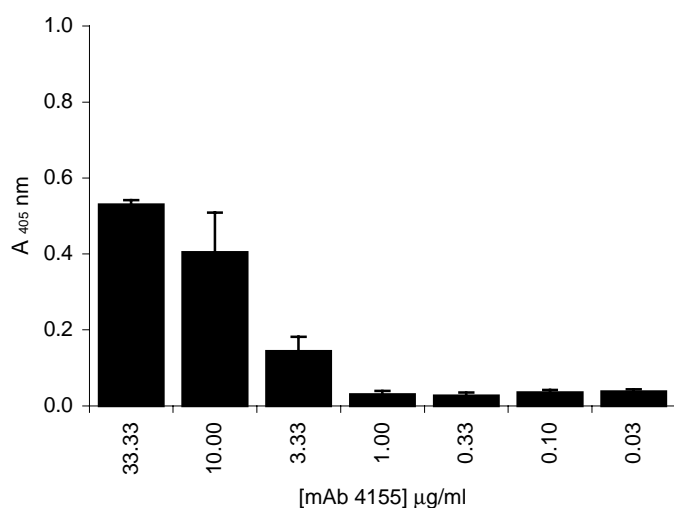


Figure 4.3: Passive adsorption of monoclonal antibody 4155 onto the surface of NUNC immunotubes. The antibody was diluted in PBS. Rabbit anti-mouse horseradish peroxidase conjugated antibody was used at a 1/1000 dilution. ABTS was used as the revealing substrate.

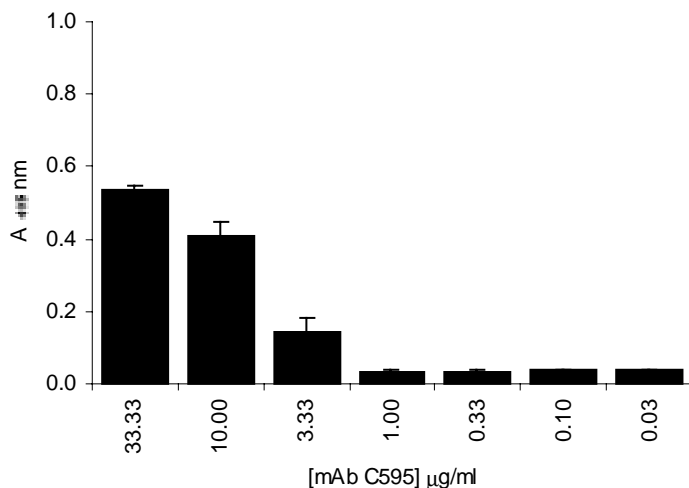


Figure 4.4: Passive adsorption of mAb C595 onto the surface of NUNC immunotubes. The antibody was diluted in PBS. Rabbit anti-mouse horseradish peroxidase conjugated antibody was used at a 1/1000 dilution. ABTS was used as the revealing substrate.

These results demonstrate the C595 and 4155 monoclonal antibodies are both adsorbed at equivalent levels onto the NUNC immunotubes.

4.5 Removal of non-specifically binding phage.

In order to reduce the number of phage displaying peptides that bound non-specifically to the adsorbed protein, an initial screen was conducted in which an “irrelevant protein” was adsorbed to the immunotube. After amplification, the eluted phages were then used in the first round of biopanning against the desired target molecule.

For the screen against mAb 4155, mAb C595 was used as the irrelevant protein; likewise for the screen against mAb C595, mAb 4155 was used as the irrelevant protein.

After each screen of the phage against the respective proteins, the titer of the eluted phage was determined using the plaque assay described in chapter 4.

Titration of phage eluate	
MAb 4155 @ 10µg/ml	mAb C595 @ 10µg/ml
2.1 x 10 ⁵ pfu/ml	7.1 x 10 ⁵ pfu/ml

Table 4.2: Titer of eluted phage from prescreen to remove non-specifically binding phage.

4.6 Biopanning - Screening of library against 4155 mAb

Previous work has been published in which 4155 mAb was screened using a filamentous phage display library displaying a library of random nonapeptides, each peptide flanked with two cysteine residues in order to promote disulphide bond formation resulting in constrained peptides (Murray, *et al.* 2001). Here the same antibody was used to screen the T7 phage displaying a cysteine constrained random nonapeptide library. The T7 phage differs in the presentation of peptides to that observed with the filamentous phage used in the previous study (Murray, *et al.* 2001)

T7 phage lysate with an initial titer of 3.98×10^{10} pfu/ml was used in the screen.

4.6.1 Determination of the extent of enrichment that can be observed

Five rounds of enrichment were conducted, using the protocol described in chapter 3. The titer of the eluted phage was measured by plaque assay, as described in chapter 3. The results are presented in table 4.3.

Biopanning round	[viable phage] in eluate (pfu/ml)
Φ ₁	2.6 x 10 ⁵
Φ ₂	5.8 x 10 ⁵
Φ ₃	2.4 x 10 ⁴
Φ ₄	3.7 x 10 ⁵
Φ ₅	5.0 x 10 ⁵

Table 4.3: Results from the screening of Ab4155 (passively adsorbed to NUNC immunotubes) with the phage library.

These results show that no significant level of enrichment of the phage titer occurred over the five successive rounds of biopanning. The level of phage titer remained constant at around 10^5 pfu/ml. The biopanning (affinity selection) process did not selectively enrich any phage clones displaying peptides which exhibited an increased affinity for the antibody.

4.7 Screening of library against C595 mAb

A library consisting of single random hexapeptides encoded by, and expressed on the surface of filamentous bacteriophage has previously been used to examine the fine specificity of the C595 mAb (Laing, *et al.* 1995). In this library the displayed peptide was expressed as part of the gene III (pIII) protein. The peptide was limited in expression to approximately five molecules per virion. The peptide was also non-constrained.

In these experiments C595 mAb was screened using the T7 library displaying the constrained nonapeptide library. Approximately 415 copies of the peptide are displayed on the virion. First an experiment was conducted to see if any enrichment of the phage library could be observed over five rounds of biopanning.

4.7.1 Determination of the extent of enrichment that can be observed

The results presented in table 4.5 and figure 4.6 show that a significant increase in the titer of the eluted phage has occurred during the first four rounds of biopanning. The titer of the eluted phage declined slightly in the 5th round of biopanning.

Biopanning round	[viable phage] in eluate (pfu/ml)
ϕ_1	4.2×10^4
ϕ_2	6.0×10^5
ϕ_3	1.1×10^6
ϕ_4	2.2×10^7
ϕ_5	1.7×10^7

Table 4.5: Results investigation into enrichment of phage. Initial phage titer = 1.5×10^9 pfu/ml.

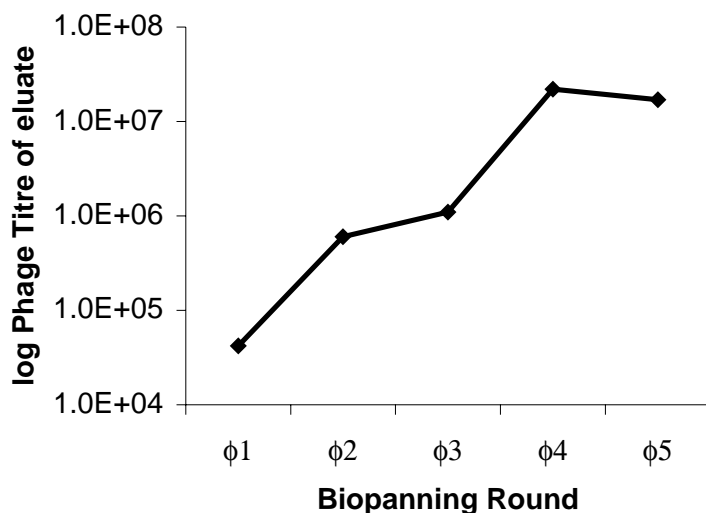


Figure 4.6: Graph illustrating the extent of enrichment observed over the five rounds of biopanning.

Comparing these results to those obtained in section 4.6.1, it is clear that enrichment of the phage library is occurring in the first four rounds of biopanning.

4.7.2 Capture ELISA of phage populations from biopanning rounds

An ELISA was performed to confirm the results of the plaque assay conducted on the amplified eluate from each round of biopanning (i.e that phage were being selectively enriched for their ability to bind to mAb C595). Antibody C595 was passively adsorbed onto the wells of a microtitre plate, and used to capture phage from the amplified phage lysate. After washing captured phage were then probed with biotinylated C595. antibody, utilising an avidin-horseradish peroxidase conjugate to reveal the sandwiched phage particles (as described in chapter 3).

The results are presented in figure 4.4. The amplified phage populations from rounds 1,2,3 and 4 gave positive signals on the ELISA. The amplified phage population lacking the degenerate insert and the naïve (unenriched) library were not able to form a sandwich between the adsorbed antibody and the biotinylated antibody.

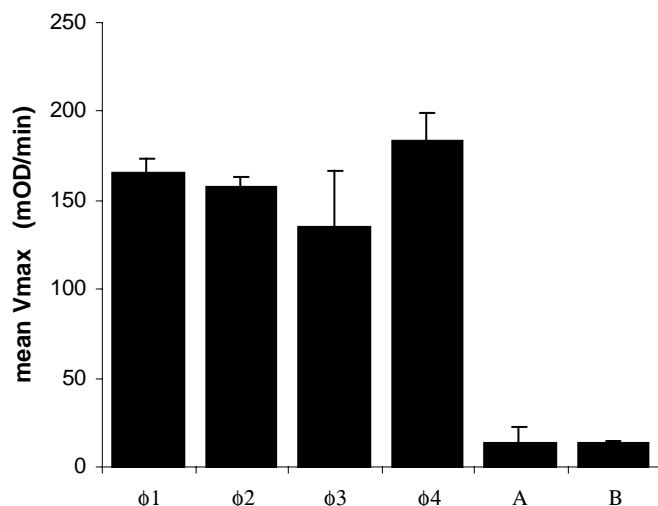


Figure 4.4: Results of capture ELISA read at 405nm. $\phi 1 - \phi 4$ are the amplified phage populations from biopanning rounds 1 – 4 respectively. (A) is the amplified phage population lacking the degenerate oligonucleotide coding for the peptide library; and (B) is the amplified naïve parent library.

This assay ascertained that the ELISA could be used to discriminate between binding and non-binding phage particles. The results of ELISA did not reflect the increase in phage titer after each round of biopanning as seen from the plaque assay. One possible explanation for this is that the levels of phage used in the ELISA were saturating the available binding sites of the adsorbed antibody. The ELISA was repeated with a serial dilution of the amplified phage lysate from each round of biopanning. The results from this experiment are presented in figure 4.5.

These results show that there is a large difference in the signal between the first three rounds of biopanning, but there is an overlap in the signal between the third and fourth rounds. This result was not observed with the plaque assay, where the phage titer was seen to reach a maximum in the fourth round of biopanning. The ELISA measures only the net binding ability of the phage particles from each respective round of biopanning. The plaque assay (by nature of the selection process used) also measures the net binding ability of the phage particles in each round of biopanning; but one must also take into account the selective growth pressures that may occur during each round of phage propagation. In each round of phage binding and

propagation, not only are the best binders being selected for, but also the fittest phage are being selected. Certain peptides displayed on the capsid head of the bacteriophage may confer a specific growth advantage to a particular phage clone. These phage particles will also undergo enrichment at each round of propagation

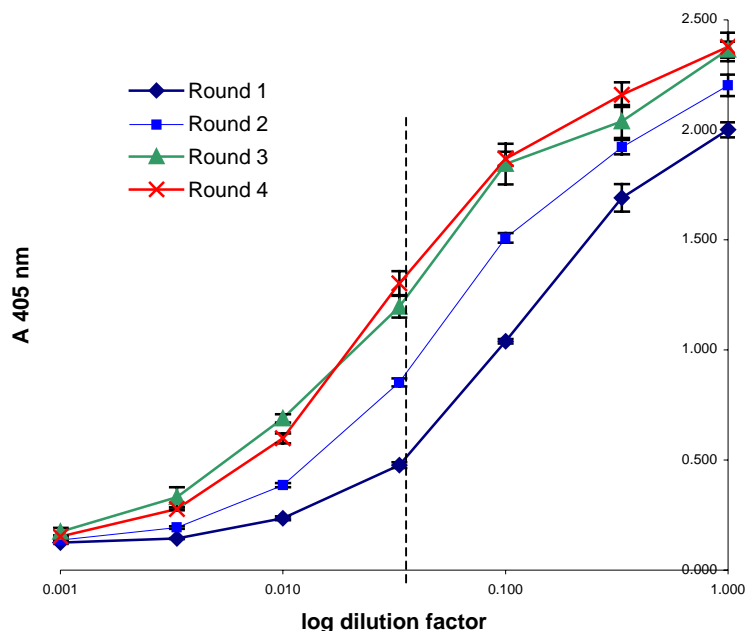


Figure 4.5: Titration of amplified phage from rounds 1 to 4 of biopanning. Dotted vertical line used as a reference point to compare the binding of the phage at a single dilution.

4.7.3 Capture ELISA of phage clones from rounds one and four of screening.

Individual phage clones were isolated from the eluate of rounds one and four of the biopanning. The phage capture ELISA (as described in section 4.7.2.) was used to compare the spectrum of reactivity of the clones sampled in round one with those sampled from round four. The results from rounds one and four are presented in figures 4.6 and 4.7 respectively. Phage clones from round four display a more pronounced activity in the assay (see figure 4.7); compared to a more even distribution of activity (overall majority $V_{max} < 100$ mOD/min) in the clones sampled from round one of biopanning (see figure 4.6).

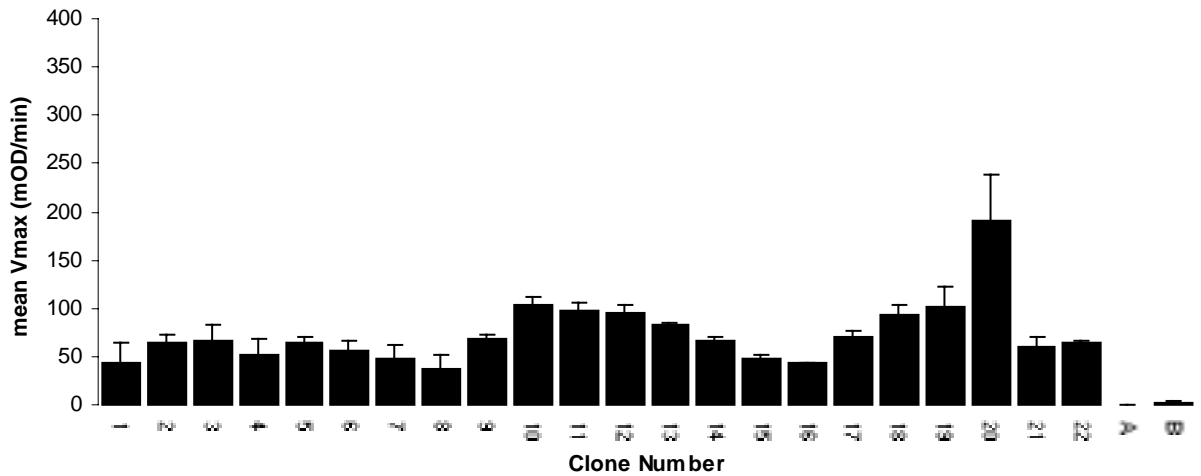


Figure 4.6: Phage-capture ELISA of amplified clones (1) to (22) from the first round of biopanning. (A is phage lacking the degenerate oligonucleotide insert; B is no phage)

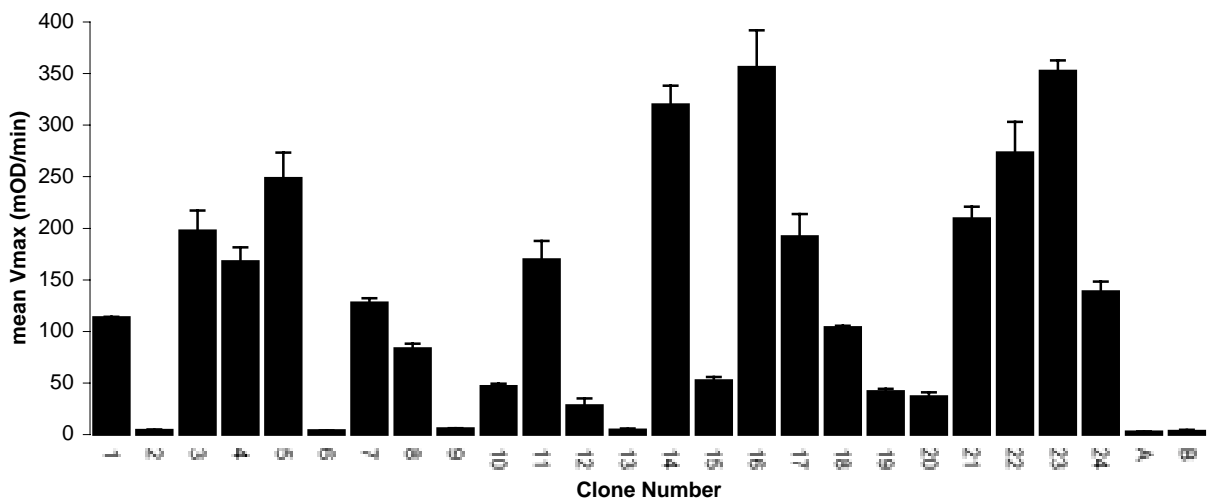


Figure 4.7: Phage-capture ELISA of randomly chosen amplified phage clones from fourth round of biopanning. A is phage lacking the degenerate oligonucleotide insert; B is PBS only.

It was decided that since the phage concentrations had not been normalised for each clone, it would be misleading to try and associate binding ability in the capture assay of individual clones with a particular sequence. The purpose of the figure is to demonstrate that enrichment of specific clones has occurred, compared to the naïve library and the vector containing no degenerate insert. Normalising for protein concentration was attempted by determining protein concentration for each clone, but this proved unsuccessful. Another approach would be to conduct a plaque assay for each clone, and normalise the assay by using the same concentration of phage for all of the samples. This is not a trivial task for a large number of clones, and was not feasible in the time allocated for this work.

4.8 SPR analysis of selected phage clones

To add evidence to the ELISA data which demonstrated that phage clones were capable of binding in a sandwich assay to mAb C595, surface plasmon resonance (SPR) analysis (using a BIAcore 2000 instrument) was conducted. The aim of this experiment was to demonstrate, in real time, a specific binding event occurring between a phage particle displaying a peptide sequence containing an **RXXP** peptide motif, and mAb C595. Ethanolamine, mAb C595, mAb HMFG1, and anti- M13 antibody, were all immobilised using NHS/EDC coupling chemistry on the four flowcells of a BIAcore sensor chip (As described in chapter 3). The ethanolamine was to be used as a measure of the background level for binding to the sensor surface. The anti-M13 mAb was used as a control for non-specific binding of the phage species to antibodies. Figure 4.8 illustrates the immobilisation of the species in the respective flowcells of the BIAcore 2000 instrument.

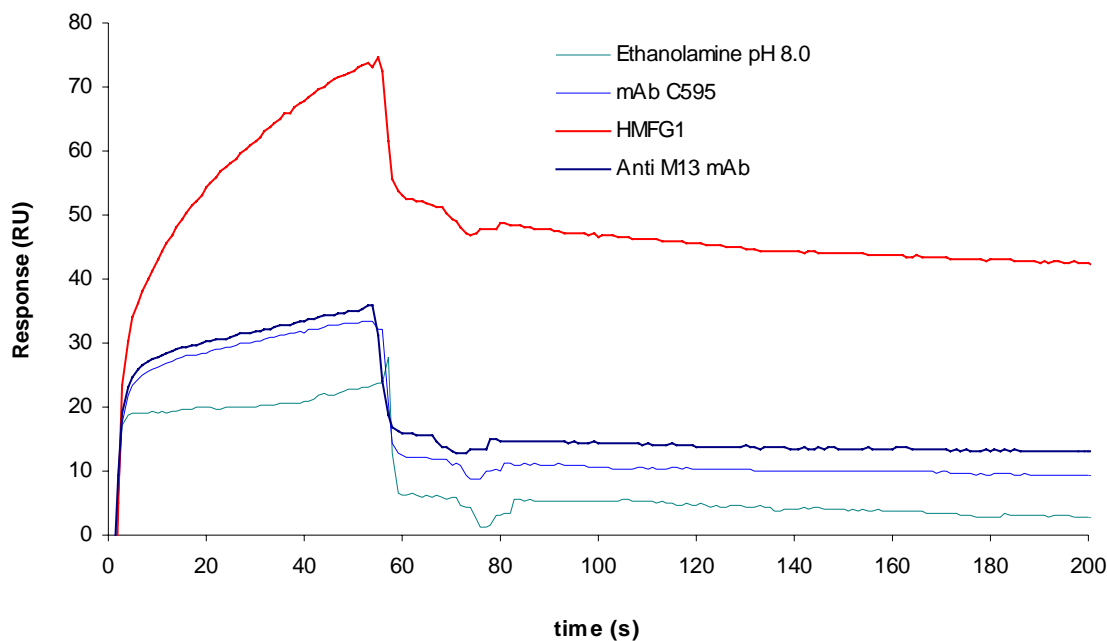


Figure 4.8: Covalent linking of ethanolamine (pH 8.0) and three antibodies to the channels of a carboxymethyl-dextran coated sensor chip using NHS-EDC coupling chemistry.

The peptide **APDTRAAPG** was used to demonstrate the specific binding of the **RXXP** motif to immobilised mAb C595. The peptide is derived from the mucin epitope peptide **APDTRPAPG**, with the 6th residue substituted with alanine. Figure 4.9 illustrates the specific binding of the BSA-peptide conjugate, using peptide **APDTPAAPG**. Note the very low level of non-specific binding observed for the anti-M13 antibody. The background level of binding to the flowcell in which ethanolamine was immobilised, was subtracted from each of the traces. The level of binding to mAb C595 was approximately 10x the level observed for the anti-M13 mAb.

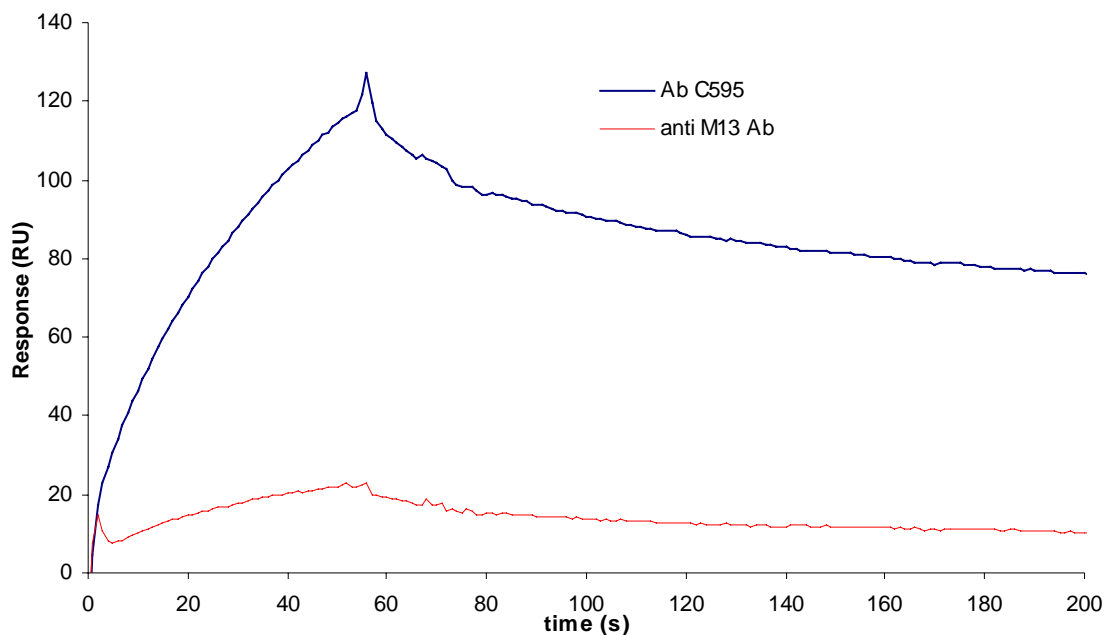


Figure 4.9: Binding of BSA-**APDTRAAPG** to C595 antibody covalently linked to the surface of a biosensor chip (50µg/ml in acetate buffer pH 4.0), using NHS/EDC coupling chemistry. Showing low level of non-specific binding to anti-M13 antibody linked under identical conditions.

Figure 4.10 illustrates the binding of a phage clone isolated from the fourth round in the preliminary biopanning experiment. The clone used was clone 4, displaying the peptide **YRTAPK** from the initial biopanning experiment. This clone was chosen because of its simplicity, containing the **RXXP** motif flanked on either side by single amino acid residues. Here the HMFG1 mAb was used as a control for non-specific binding, since this binds to the **PDTR** region of the mucin epitope peptide **APDTRPAPG**. Note the much slower on-rate and much slower off-rate compared to the binding of the BSA – peptide conjugate presented in figure 4.9.

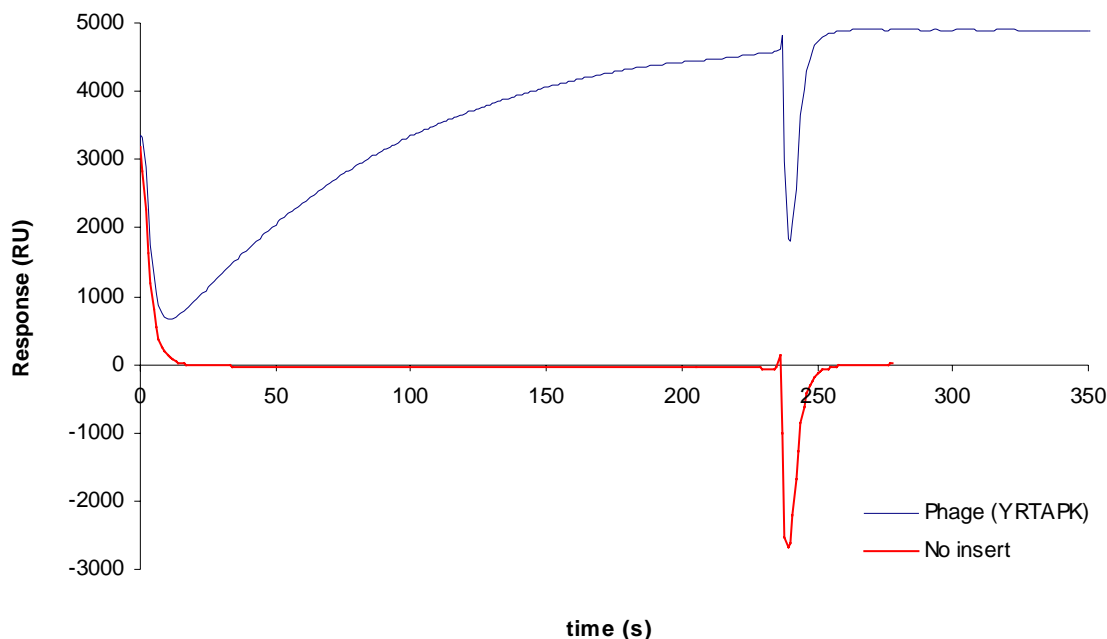


Figure 4.10: Binding of phage clone **YRTAPK** and naïve phage library to C595 antibody covalently linked to the surface of a CMD sensor chip. Antibody HMFG1 was used as a control.

The size of the phage particles compared to the size of the BSA-peptide conjugate is the most likely factor influencing the dramatic decrease in the observed on-rate. The polyvalency of the phage, meaning that rebinding is highly probable is one possible explanation for the much-reduced off-rate.

4.9 PCR analysis of phage clones from round four of initial screen

Two primers (R1FOR $5'$ GCT AAG GAC AAC GTT ATC GGC CTG TTC ATG C $3'$ and R2REV $5'$ CGT TGA TAC CGG AGG TTC ACC GAT AGA CGC C $3'$) were designed to allow PCR amplification of the region surrounding the degenerate oligonucleotide insert. A third primer was designed to anneal inside this PCR amplification product (SEQFOR $5'$ GGT ACT GTT AAG CTG CGT GAC TTG GC $3'$) to enable direct sequencing of the PCR product (see fig. 1). PCR reactions were conducted as described in Chapter 3. Agarose gel electrophoresis was used to analyse the PCR products to ascertain that only a single PCR product of the expected size was present before sequencing. An example of the analysis of the PCR products is presented in figure 4.11.

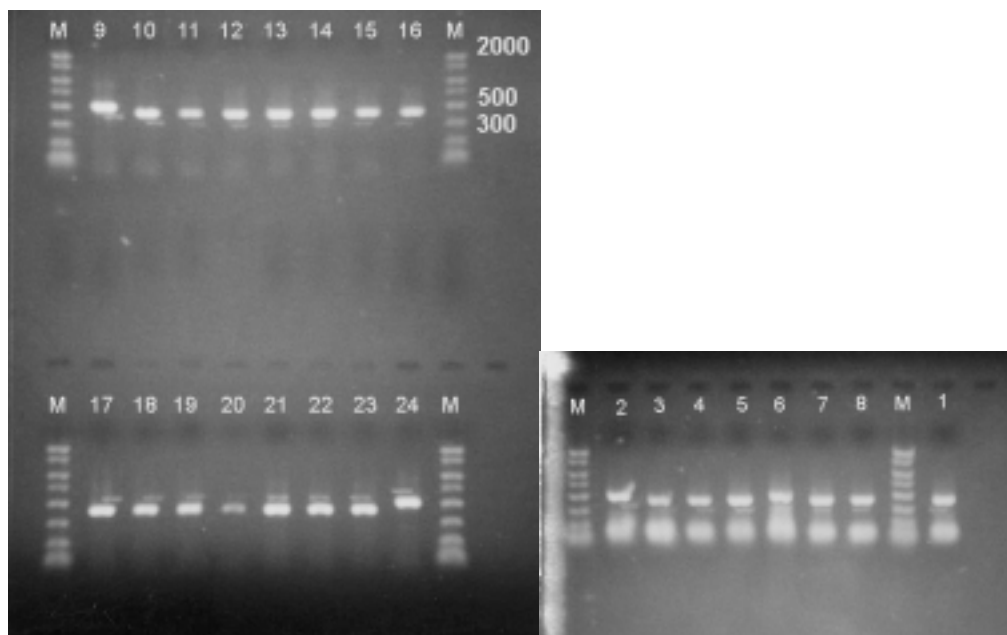


Figure 4.11: Agarose gels showing the results of a PCR conducted on 24 individual phage clones recovered from the fourth round of biopanning, using primers R1 and R2.

A positive band of 480 b.p. in size was expected from the PCR (see figure 4.1). Figure 4.11 shows that all of the phage clones tested contain an insert in the region of 300 - 500 b.p. in size. The last well in the gels contained a -ve control consisting of PCR primers only, with no template present. This indicated that all of the clones sampled contained a degenerate oligonucleotide insert.

4.10 Sequencing of phage clones

Direct sequencing of the PCR products was conducted - as described in Chapter 3. This enabled the elimination of any clones not containing an insert from the sequencing reaction. Two preliminary experiments in which only the fourth round of phage were sequenced were first conducted.

4.10.1 Sequencing of clones from the fourth round of biopanning.

Table 4.7 illustrates the results of the first sequencing reactions conducted on the fourth round of biopanning. It can be seen that two sets of consensus sequences

emerged. The first set of consensus sequences consisted of a set of **RXXP** motifs. This motif was observed in the previous study using filamentous phage displaying non-constrained hexa-peptides (Laing, *et al.* 1995), and has been observed in solid phase peptide studies (Murray, *et al.* 2000). The second set of consensus sequences consisting of a set of **RXP** motifs had not been identified in any previous studies. None of the sequences selected contained the full nine residues, or both of the flanking cysteine residues. Analysis of the sequence of the degenerate oligonucleotide insert shows that the absence of the 5' cysteine residue in seven of the sequences can be accounted for by five T-C transitions, one G-A transition and one G-C transversion. The absence of the 3' cysteine residue in 13/13 of the sequences is the result of the TAG stop codon. As illustrated in figure 4.2, this is the only stop codon present in the NN(K/T) synthesis strategy.

The experiment was repeated, and the results of the sequence analysis are presented in table 4.8. The presence of the **RXXP** and **RXP** sequences is confirmed by the second set of sequence analysis.

Clone	Displayed peptide	5' Nucleotide sequence of degenerate insert 3'
1 2 3 4 5	RHAPRS CLRSSPNPR RGGRPVP SA YRTAPK SRPNPRQ	<u>CGC</u> CAT GCG CCT CGG TCG <i>TAG</i> AGG GGT CTT <u>GCT CTT</u> <i>GAA</i> <u>TGC</u> TTA CGT AGT AGT CCT AAT CCT CGG <i>TAG</i> <u>TGC TCT</u> <i>TGA</i> <u>CGC</u> GGT GGT CGG CCT GTG CCG TCG GCG <i>TAG</i> <u>TGC TCT</u> <i>TGA</i> <u>TAC</u> CGT ACG GCT CCG AAG <i>TAG</i> AGG GAG TTT <u>GCT CTT</u> <i>GAA</i> <u>TCC</u> CGT CCG AAT CCG CGG CAG <i>TAG</i> CTG GAT <u>TGC TCT</u> <i>TGA</i>
6 7 8 9 10 12	CNSSVRKPV CSSRKPASL RGPGR CRSQRSPA RQPAR CNSSVRKPV	<u>TGC</u> AAT AGT TCG GTG CGG AAG CCG GTG <i>TAG</i> <u>TGC TCT</u> <i>TGA</i> <u>TGC</u> AGT AGT CGG AAG CCT GCT AGT CTG <i>TAG</i> <u>TGC TCT</u> <i>TGA</i> <u>CGC</u> GGT CCA GGT CGG <i>TAG</i> CTT TGG GTT ATG <u>TGC TCT</u> <i>TGA</i> <u>TGC</u> CGG TCT CAG CGT TCG CCT GCT <i>TAG</i> GAG <u>TGC TCT</u> <i>TGA</i> <u>CGC</u> CAG CCG GCG CGG <i>TAG</i> AGC TTT TAT AAT <u>TGC TCT</u> <i>TGA</i> <u>TGC</u> AAT AGT TCG GTG CGG AAG CCG GTG <i>TAG</i> <u>TGC TCT</u> <i>TGA</i>
11 18	RYDHRSSK CATRGVAGR	<u>CGC</u> TAT GAT CAT AGG TCT TCG AAG <i>TAG</i> GCG <u>TGC TCT</u> <i>TGA</i> <u>TGC</u> GCT ACG CGT GGT GTT GCG GGG CGT <i>TAG</i> <u>TGC TCT</u> <i>TGA</i>

Table 4.7: Summary of results from round 4 of initial biopanning experiment. Sequence data and displayed peptides for 13 randomly chosen phage clones. The sequencing data is arranged in three groups: the first group consisting of clones displaying sequences containing the **RXXP** motif, the second group consisting of sequences containing the **RXP** motif, and the third group displaying no consensus motif. Underlined nucleotide residues represent constant regions in the degenerate oligonucleotide insert. Individual residues in bold highlight mutations of the nucleotides in the constant regions of the degenerate insert. The stop codons (amber *TAG* stop codon encoded in the degenerate library and opal stop codon *TGA* in the 3' terminal constant region) are highlighted in italics.

Clone	Displayed peptide	5' Nucleotide sequence of degenerate insert 3'
2 8 17 20 5	CRPAPQRLAKCS CARDKP CGRDRKAP CATRAIPTRDCS CDAKRRSPPVCS	<u>TGC CGT CCT GCT CCG CAG CGG TTG GCT AAG TGC TCT TGA</u> <u>TGC GCG AGG GAT AAG CCT TAG CGG AAG TGG TGC TCT TGA</u> <u>TGC GGT CGG GAT CGG AAG GCT CCT TAG GGT TGC TCT TGA</u> <u>TGC GCG ACG CGG GCG ATT CCG ACG CGT GAT TGC TCT TGA</u> <u>TGC GAT GCT AAG CGT AGG TCT CCG CCG GTG TGC TCT TGA</u>
5 6 10 21 22 24	CDAKRRSPPVCS CVTD RHPGDKCS CERGPARRHCS CRVTRL PACVCS STGRLPRM CMRGPESKERCS	<i>See above</i> <u>TGC GTT ACT GAT AGG CAT CCG GGG GAT AAG TGC TCT TGA</u> <u>TGC GAG CGT GGG CCG GCG CGG CGG GAG CAT TGC TCT TGA</u> <u>TGC CGT GTG ACG AGG CTT CCG GCG TCT GTT TGC TCT TGA</u> <u>TCC ACG GGT AGG CTG CCT CGT ATG TAG AAG TGC TCT TGA</u> <u>TGC ATG AGG GGT CCG GAG TCT AAG GAG CGG TGC TCT TGA</u>
11	CLPANGRPAQSS	<u>TGC CTG CCT GCT AAT GGG CGG CCG GCG CAG TCC TCT TGA</u>
12 16 19 3 4 8 9	CR CRR CY C CV CRQGRGGC CVSDRRVRS HCS	<u>TGC AGG TAG CGG GCT CGG ACT GCT CCT CGT GCT CTT GAA</u> <u>TGC CGG CGT TAG ACG AGG ATT ATG AAG TAT TGC TCT TGA</u> <u>TGC TAT TAG CGT CAG AAT AGG CTT ATG AGT TGC TCT TGA</u> <u>TGC TAG AGT GGG CCT GTT TGT GAG AGT ATG TGC TCT TGA</u> <u>TGC GTG TAG TTG TGT GAG GGG TCG CGG AAG TGC TCT GAA</u> <u>TGC AGG CAG GGT CGG GGC GGA TGC TGA CTT TTT GCT CTT GA</u> <u>TGC GTT TCG GAT CGT CGG GTT CGT TCC CAT TGC TCT TGA</u>

Table 4.8: Repeat of biopanning experiment. Sequence and binding data from 18 randomly chosen phage clones from round 4 of biopanning. See Table 4.6 for description of table.

Only one G-C transversion was present at the 5' end of the degenerate insert in the second set of sequencing data, resulting in the mutation of the flanking cysteine residue to a serine residue. One G-C transversion was present at the 3' end of another sequence, resulting in the mutation of the flanking cysteine residue to a serine residue. 8/19 of the sequences analysed consisted of a nonamer peptide flanked with the two terminal cysteines. (G-C transversion). One sequence contained a TGA stop codon, but the sequence upstream of the stop codon was mutated, containing a 2 b.p. insertion. The remainder of the sequences contained TAG stop codons.

4.10.2 Sequence analysis of all four biopanning rounds

To gain more of an insight as to the source of these mutations, a third biopanning experiment was conducted. In this experiment, a random sample of individual phage clones was selected from the eluate of each round of biopanning. The sequences of these clones were examined. The results of the sequencing are presented tables 4.9 - 4.12.

In the first round of biopanning, a sequence containing the **RXP** motif was obtained (clone 1). This sequence contained no mutations at the 5' or 3' ends of the degenerate insert, or any stop codons in the randomised region and so was flanked by terminal cysteine residues. No sequences containing the **RXXP** motif were obtained. 2/5 of the sequences contained T-G and T-C transitions at the 5' terminal cysteine codon. A portion of the degenerate insert in clone 3 appeared to have been deleted at the 5' end. The hyphens present in clone 4 represent residues containing an undeterminable nucleotide (denoted N in the sequence). No T-A or G-C transversions were observed.

In the sequence analysis of the clones obtained from the second round of biopanning, one sequence containing the **RXXP** motif was obtained (Clone 1). This sequence contained the TAG stop codon prior to the 3' terminal cysteine codon, and so only an eight-residue peptide was displayed. All of the other sequences were also free from any mutations. Clones 2, 3 and 4 encoded for nine-residue peptides flanked by terminal cycteine residues, but no consensus motifs could be observed. The

remaining clones (5-9) all contained the TAG stop codon prior to the 3' terminal stop codon. The peptides encoded varied in length from seven residues down to only the 5' terminal cysteine. No consensus sequence was observed in these peptides.

In the sequence data from the clones obtained in the third round of biopanning, a striking consensus sequence consisting of the residues **RNREAPRGKICS** emerged. Of the sequences obtained in this round, 17/25 contained mutations in the codon for the 5' terminal cysteine (compared to only 1/25 containing mutations at the 3' terminal cysteine). The mutation of the first cysteine residue to an arginine residue in the consensus sequence **RNREAPRGKICS** is the result of a T-C transition. 8/25 of the sequences consisted of the **RNREAPRGICS** sequence (clones 1-8). 2/25 sequences (clones 9 and 10) contained the **RXXP** motif. These contained mutations in the codon for the 5' cysteine residue (T-C transition, and what appears to be the deletion of a codon for clone 9; and a G-T transition in clone 10). 2/25 sequences (clones 11 and 12) contained the **RXP** motif. Both of these clones were mutation free, and so the flanking cysteine residues were present. The remaining 13 sequences contained four which were mutation free (clones 18, 20, 22 and 23), four clones appeared to have portions of the degenerate insert deleted (clones 13-16). The remainder consisted of a G-C transversion (clone 17), a T-A transversion and a base deletion (clone 25). Clone 24 contained a number of undeterminable nucleotides.

The frequency at which the **RNREAPRGKICS** peptide was detected dropped from 8/25 clones in the third round of biopanning, to 5/42 in the fourth round. (Clone 5 contained a single undetermined nucleotide in the first amino acid residue; it is highly probable that the undetermined nucleotide is Guanine, resulting in a CGC codon - coding for arginine. This can be asserted since the remaining 11 residues are identical to those in clones 1-4). Of the sequences obtained for the clones sampled in the fourth round of biopanning, 7/42 contained mutations in the codon for the 5' flanking cysteine residue; and 1/42 contained a mutation in the codon for the 3' flanking cysteine residue. The **RXXP** motif was present in 3/42 of the clones (clones 6-8) sequenced in the fourth round of biopanning. The **RXXP** motif in all three of these clones took the form **RXAP**. Clone 6 contained the **RPAP** motif - the simple linear peptide motif which is present in the mucin core variable number of tandem repeat sequence (VNTR) **PDTRPAPGSTAPPAHGV TSA** (Gendler, *et al.* 1988), to which

mAb C595 has been shown to bind (Price, *et al.* 1990). Clone 7 contained a single G-C transversion in the 5' terminal cysteine residue. The **RXP** motif was present in 4/42 of the clones (clones 9-12). Clones 10 and 11 were mutation free, but clones 9 and 12 contained T-C transitions in the codon for the 5' flanking cysteine residue. Clone 13 consisted of a 9-mer peptide containing an **RP** motif. Such a motif was also observed in the second biopanning experiment (see table 4.8 - clone 11). This sequence was free of mutations and so was flanked by terminal cysteine residues. Clones 14-17 and 20-22 all contained 9-mer peptides which were mutation free. No consensus sequence could be identified in these clones. Clone 23 was also mutation free at the terminal cysteine residues, but contained a number of undeterminable nucleotides. Clone 18 contained a G-A transversion in the codon for the 5' terminal cysteine. The majority of the remaining peptides were mutation free, with the exceptions of clones 26 and 29 which contained mutations (T-C transitions) in the 5' and 3' terminal cysteine residues respectively. Notably the 5' terminal cysteine residue in clone 42 contained a C-A transition and so encoded for the TGA stop codon.

A summary of the frequency and location of the mutations observed in each of the four rounds of biopanning is presented in table 4.13. Note that the vast majority of the mutations that occur in the constant flanking cysteine residues, do so at the 5' cysteine residue. This cysteine is the one closest to the phage capsid proteins. This may have a bearing on the increased frequency of mutations seen at this residue. Peptide residues closest to the capsid proteins are likely to have the greatest influence on the capsid protein rather than the 3' terminal residues. It is also interesting to note that the frequency of these mutations in the codon of the 5' cysteine residue peaks in the third round and reduces in the fourth round. This is coincidental with the emergence of the **RNREAPRGKICS** peptide in the third round followed by a decline in frequency at which this peptide was observed the fourth biopanning round. This is also coincidental with the peak of the phage capture ELISA signal after the third round of biopanning (see figure 4.5). It is important to note that this peptide does not account for all of these mutations (8/25 different clones displayed the **RNREAPRGKICS** peptide in round three of the biopanning, and 5/42 different clones in round four). Compare this to 17/25 and 8/42 clones respectively containing mutations at the 5' terminal cysteine residue. These figures suggest that residues close to the capsid head proteins are most vulnerable to mutation.

Clone	Displayed peptide	5' Nucleotide sequence of degenerate insert 3'
1	CERGPGRSRS	<u>TGC</u> GAG AGG GGT CCT GGG AAG TCG AGG TCT <u>TGC TCT TGA</u>
2	CGNRVSKAPK-S	<u>TGC</u> GGG AAT CGT GTG AGT AAG GCA CCT AAG <u>NGC TCT TGA</u>
3	GRKVKCS	GGG CGG AAG GTG AAG <u>TGC TCT TGA</u>
4	R-AA-MEKP-S	<u>CGC</u> CNT GCG GCG GNT CNG ATG GAG AAA CCG <u>NGC TCT TGA</u>
5	RRAAVRMEKPCS	<u>CGC</u> CGT GCG GCG GTT CGG ATG GAG AAG CCG <u>TGC TCT TGA</u>

Table 4.9: Round one biopanning sequence results.

Clone	Displayed peptide	5' Nucleotide sequence of degenerate insert 3'
1	CSRVAPNRK	<u>TGC</u> TCG AGG GTG GCT CCG AAT AGG AAG <u>TAG TGC TCT -GA</u>
2	CVKRTASGSGCS	<u>TGC</u> GTT AAG CGT ACG GCT AGT GGT TCT GGT <u>TGC TCT TGA</u>
3	CSMRASGGPKCS	<u>TGC</u> TCG ATG CGT GCG TCT GGG GGG CCG AAG <u>TGC TCT TGA</u>
4	CTVPVVRPQQKCS	<u>TGC</u> ACT GTT CCG GTG AGG CCG CAG CAG AAG <u>TGC TCT TGA</u>
5	CPATTHLG	<u>TGC</u> CCT GCT ACT ACG CAT TTG GGG <u>TAG ATG TGC TCT TGA</u>
6	CHLAGT	<u>TGC</u> CAT CTT GCG GGT ACT <u>TAG TGG GTT CAG TGC TCT TGA</u>
7	CEE	<u>TGC</u> GAG GAG <u>TAG CAT CTG CTG CCG GAT TCG TGC TCT TGA</u>
8	C	<u>TGC</u> <u>TAG CAG TTT AAT TCT ACG TCT ACT AAG TGC TCT TGA</u>
9	C	<u>TGC</u> <u>TAG TAT TGT TAG CTT AAT GCG CTT TTT TGC TCT TGA</u>

Table 4.10: Round two biopanning sequence results.

Clone	Displayed peptide	5' Nucleotide sequence of degenerate insert 3'
1	RNREAPRGKICS	<u>CGC</u> AAT CGG GAA GCG CCT AGG GGG AAG ATT <u>TGC TCT TGA</u>
2	RNREAPRGKICS	<u>CGC</u> AAT CGG GAA GCG CCT AGG GGG AAG ATT <u>TGC TCT TGA</u>
3	RNREAPRGKICS	<u>CGC</u> AAT CGG GAA GCG CCT AGG GGG AAG ATT <u>TGC TCT TGA</u>
4	RNREAPRGKICS	<u>CGC</u> AAT CGG GAA GCG CCT AGG GGG AAG ATT <u>TGC TCT TGA</u>
5	RNREAPRGKICS	<u>CGC</u> AAT CGG GAA GCG CCT AGG GGG AAG ATT <u>TGC TCT TGA</u>
6	RNREAPRGKICS	<u>CGC</u> AAT CGG GAA GCG CCT AGG GGG AAG ATT <u>TGC TCT TGA</u>
7	RNREAPRGKICS	<u>CGC</u> AAT CGG GAA GCG CCT AGG GGG AAG ATT <u>TGC TCT TGA</u>
8	RNREAPRGKIC-	<u>CGC</u> AAT CGG GAA GCG CCT AGG GGG AAG ATT <u>TGC TCT TGA</u>
9	RRPPMTTASCS	<u>CGC</u> CGG CCG CCT ATG ACG ACT GCG TCG <u>TGC TCT TGA</u>
10	FERIAPKGGNCS	<u>TTC</u> GAG CGG ATT GCT CCG AAG GGT GGG AAT <u>TGC TCT TGA</u>
11	CSRGPAGRTVCS	<u>TGC</u> TCT CGT GGG CCG GCT GGG CGG ACG GTG <u>TGC TCT TGA</u>
12	CRAPAGSKKMCS	<u>TGC</u> AGG GCG CCG GCG GGG TCG AAG AAG ATG <u>TGC TCT TGA</u>
13	GKRMGVTRCS	GGT AAG CGG ATG GGT GTG ACG CGT <u>TGC TCT TGA</u>
14	GKRMGVTRCS	GGT AAG CGG ATG GGT GTG ACG CGT <u>TGC TCT TGA</u>
15	GRKVKCS	GGG CGG AAG GTG AAG <u>TGC TCT TGA</u>
16	GRKVKCS	GGG CGG AAG GTG AAG <u>TGC TCT TGA</u>
17	SLMQRASGRTCS	<u>TCC</u> CTG ATG CAG AGG GCG AGC GGG CGT ACG <u>TGC TCT TGA</u>
18	CSKKGKNSLSKCS	<u>TGC</u> TCT AAG AAG GGG AAT AGT TTG AGT AAG <u>TGC TCT TGA</u>
19	SAR-ERSKGKCS	<u>TCC</u> GCG CGG CAN GAG AGG AGT AAG GGG AAG <u>TGC TCT TGA</u>
20	CM-S-TANGKCS	<u>TGC</u> ATG ANT AGT ANG ACT GCG AAT GGT AAG <u>TGC TCT TGA</u>
21	SSVDKLAAALE	<u>AGC</u> TCC GTC GAC AAG CTT GCG GCC GCA CTC GAG TAA
22	CLP-LLHF	<u>TGC</u> TTG CCG CCN AAG AAA CAT TTT TAG AAT <u>TGC TCT TGA</u>
23	CVRTKKV	<u>TGC</u> GTG CGG ACG AAG AAG GTC TAG ATG CGG <u>TGC TCT TGA</u>
24	C---P---RT-CS	<u>TGC</u> TNT CGN GNG CCG NNT NGG CGG ACG GNN <u>TGC TCT TGA</u>
25	CD	<u>TGC</u> GAT TAG CGG GCG TTC TTT AGG TGT CTT <u>GCT CTT GAA</u>

Table 4.11: Round three biopanning sequence results.

Clone	Displayed peptide	5' Nucleotide sequence of degenerate insert 3'
1 2 3 4 5	RNREAPRGKICS RNREAPRGKICS RNREAPRGKICS RNREAPRGKICS - NREAPRGKICS	<u>CGC</u> AAT CGG GAA GCG CCT AGG GGG AAG ATT <u>TGC TCT TGA</u> <u>CGC</u> AAT CGG GAA GCG CCT AGG GGG AAG ATT <u>TGC TCT TGA</u> <u>CGC</u> AAT CGG GAA GCG CCT AGG GGG AAG ATT <u>TGC TCT TGA</u> <u>CGC</u> AAT CGG GAA GCG CCT AGG GGG AAG ATT <u>TGC TCT TGA</u> <u>CNC</u> AAT CGG GAA GCG CCT AGG GGG AAG ATT <u>TGC TCT TGA</u>
6 7 8	CRPAPSAKVACS FERIAPKGGNCS CDSERTAPKSCS	<u>TGC</u> AGG CCT GCG CCT TCT GCT AAG GTG GCT <u>TGC TCT TGA</u> <u>TCC</u> GAG CGG ATT GCT CCG AAG GGT GGG AAT <u>TGC TCT TGA</u> <u>TGC</u> GAT AGT GAG AGG ACG GCT CCT AAG TCG <u>TGC TCT TGA</u>
9 10 11 12	RQAGRKPVNNCS CSRGPAVRTVCS CSDRMPCEPSCS RRPSR	<u>CGC</u> CAG GCG GGA CGG AAG CCG GTG AAT AAT <u>TGC TCT TGA</u> <u>TGC</u> TCT CGT GGG CCG GCT GGG CGG ACG GTG <u>TGC TCT TGA</u> <u>TGC</u> AGT GAT CGT ATG CCT TGT GAG CCG AGT <u>TGC TCT TGA</u> <u>CGC</u> CGG CCTC AGT CGT <u>TAG</u> ATT GCG AGG CTG <u>TGC TCT TGA</u>
13	CGNSLKSRPDCS	<u>TGC</u> GGT AAT TCT CTT AAG TCG CGT CCG GAT <u>TGC TCT TGA</u>

Table 4.12: Results from round four of biopanning. This table shows the four groups of consensus sequences isolated.

Clone	Displayed peptide	5' Nucleotide sequence of degenerate insert 3'
14	CGNGRGERDTCS	<u>TGC</u> GGG AAT GGG AGG GGT GAG CGG GAT ACG <u>TGC TCT TGA</u>
15	CGAEIKTGARCS	<u>TGC</u> GGT GCG GAG ATT AAG ACT GGT GCC CGG <u>TGC TCT TGA</u>
16	CSNKYTTKSQCS	<u>TGC</u> TCT AAT AAG TAT ACT ACG AAG TCT CAG <u>TGC TCT TGA</u>
17	CGNRVSKAPKCS	<u>TGC</u> GGG AAT CGT GTG AGT AAG GCA CCT AAG <u>TGC TCT TGA</u>
18	YGRMSKATGSCS	<u>TAC</u> GGG AGG ATG TCG AAG GCG ACG GGG TCG <u>TGC TCT TGA</u>
19	AGVKQLKRACS	<u>GCC</u> GGC GTG AAG CAG CTT AAG CGG GCG <u>TGC TCT TGA</u>
20	CYEANKASKACS	<u>TGC</u> TAT GAG GCG AAT AAG GCG TCT AAG GCG <u>TGC TCT TGA</u>
21	CVSSGAKRQCS	<u>TGC</u> GTT TCT TCG GGG GCG AAG GCG AGG CAG <u>TGC TCT TGA</u>
22	CPSNRSSQEDCS	<u>TGC</u> CCT TCT AAT CGG AGT TCT CAG GAG GAT <u>TGC TCT TGA</u>
23	CAKRGM-R-ICS	<u>TGC</u> GCG AAG CGT GGT ATG TAN CGT NCT ATT <u>TGC TCT TGA</u>
24	CGLACG	<u>TGC</u> GGT CTG GCG TGT GGG <u>TAG</u> ACT GCG CTT <u>TGC TCT TGA</u>
25	CGRT-EP	<u>TGC</u> GGG AGG ACG TAN GAG CCT <u>TAG</u> CAT ATT <u>TGC TCT TGA</u>
26	RN-GSA	<u>CGC</u> AAT CNG GGA AGC GCC <u>TAG</u> GGG GAA GAT TTG CTC TTG...
27	CVEA	<u>TGC</u> GTG GAG GCT <u>TAG</u> TAG TAT ATG ATT TAG <u>TGC TCT TGA</u>
28	CVEA	<u>TGC</u> GTG GAG GCT <u>TAG</u> TAG TAT ATG ATT TAG <u>TGC TCT TGA</u>
29	CVE-	<u>TGC</u> GTG GAG GCN <u>TAG</u> TAG CAT ATG ATT TAC <u>CGC NCT TGA</u>
30	CVRS	<u>TGC</u> GTG CGG TCT <u>TAG</u> CTT GTT CTG TCT ATG <u>TGC TCT AGA</u>
31	CRTR	<u>TGC</u> CGT ACT CGG <u>TAG</u> GCG GAG CGG AGG CCG <u>TGC TCT TGA</u>
32	CISPA	<u>TGC</u> ATT TCG CCT GCT <u>TAG</u> GGG TGG CAG TTT <u>TGC TCT TGA</u>
33	CRD	<u>TGC</u> CGG GAT <u>TAG</u> CAT TCT GCG TAT AAT TTG <u>TGC TCT TGA</u>
34	CRS	<u>TGC</u> CGG AGT <u>TAG</u> GCT ACG TAG CGT AGT CAT <u>TGC TCT NGA</u>
35	CEE	<u>TGC</u> GAG GAG <u>TAG</u> CAT CTG CTG CCG GAT <u>TGC TCT TGA</u>
36	CA	<u>TGC</u> GCG <u>TAG</u> CAG CGT TCT TTG AAT CTT CAG <u>TGC TCT TGA</u>
37	CS	<u>TGC</u> TCT <u>TAA</u> ATT CGG CTG TAG AAG CGT GCT <u>TGC TCT TGA</u>
38	CS	<u>TGC</u> AGT <u>TAG</u> CAG AGT CCG CTG ACG GGT GCT <u>TGC TCT TGA</u>
39	CV	<u>TGC</u> GTT <u>TAG</u> TGG GAT ATG AGG CCG TCT TGT <u>GCT CTT</u>
40	CV	<u>TGC</u> GTT <u>TAG</u> TGG GAT ATG AGG CCG TCT TGT <u>GCT CTT GA</u>
41	C	<u>TGC</u> <u>TAG</u> GCT GAC GTA GTG GAC TGA TCG TTG <u>CTC TTG AA</u>
42	No peptide displayed	<u>TGA</u> CGG CAG GTT ATT ATT TGT AGG CAG TCT <u>TGC TCT TGA</u>

Table 4.12 continued: Results from round four of biopanning showing sequences from this round of biopanning that did not fall into any of these consensus sequences.

Biopanning round	5' Cysteine mutations	3' Cysteine mutations
Round 1	2/5	0/5
Round 2	0/5	0/5
Round 3	17/25	1/25
Round 4	8/42	1/42

Table 4.13: Summary of the mutation frequency observed at the 5' and 3' flanking cysteine residues through all four rounds of biopanning.

4.11 Summary

Phage display was used to discover novel peptide sequences that bind to the therapeutic monoclonal antibody C595. A number of biopanning experiments were conducted using the anti-MUC1 mAb C595 and the anti-steroid hormone mAb 4155 as the target receptor. No enrichment of titer of eluted phage was observed when mAb 4155 was used as the target receptor. A 500-fold level of enrichment was observed when mAb C595 was used as the target receptor.

Analysis of phage populations from each of the four rounds of biopanning revealed that affinity-based enrichment was occurring, with eluted phage recovered from each round producing a much larger signal in a phage capture ELISA compared with naïve library and bacteriophage with no degenerate oligonucleotide insert. Using Surface Plasmon Resonance (SPR), the real-time binding of a phage clone displaying the **RXXP** motif, to immobilised mAb C595 was demonstrated.

Sequence analysis of phage clones revealed the emergence of two novel consensus motifs: **RXXP** and **RXP**. A possible third consensus motif of **RP** also emerged, but the two clones displaying peptides containing this motif were from separate experiments. A predominant peptide sequence of **RNREAPRGKICS** emerged in one experiment, with highest frequency in the third round of biopanning, reducing in the fourth round of biopanning. Sequence analysis of the phage clones from all rounds of biopanning, also revealed the extent of mutation occurring in the constant regions flanking the degenerate oligonucleotide insert. The majority of mutations were found to have occurred in the third round of biopanning, at the 5' flanking

cysteine residue. This residue is closest to the capsid head of the phage particle. Only two mutations were detected at the 3' terminal cysteine residue.

The peak of mutation frequency at the 5' terminal cysteine residue was coincidental with the emergence of the **RNREAPRGKICS** peptide sequence displayed on the selected phage in round 3. The phage capture ELISA also demonstrated a peak at the third round of biopanning.

From these experiments, it could not be determined whether the **RNREAPRGKICS** peptide was purely the result of affinity selection. As the first cysteine residue was mutated to arginine the clone could be the result of selection for growth advantage, rather than binding ability.

5 Chapter 5 - Results. Analysis of peptides derived from phage display.

5.1 Introduction

The presence of the peptide **RNREAPRGKICS** which emerged as the predominant sequence at the peak of phage enrichment in the last chapter merited further study. The fully conserved nature of all the residues in this peptide (compared to the residues flanking the **RXXP** and **RXP** consensus sequences) was striking. From the experiments conducted in chapter 4, it could not be determined whether the **RNREAPRGKICS** peptide was selected for affinity, or whether the mutation of the 5' terminal cysteine had conferred a growth advantage to this particular phage clone. This chapter describes the experiments that were conducted to try and answer this question.

In this chapter a comparison of affinity constants and structural content is made between the phage derived peptide **RNREAPRGKICS** and the MUC1 derived mucin core peptide **APDTRPAPG** (containing the native epitope **RPAP**). Two control peptides were also used: **APDTRPEAPG** (used as a control peptide for a possible **REAP** mimotope) and **APDTRPAPGC** (used as a control for potential peptide dimerisation).

Standard ELISA techniques were first used to establish the relative antigenicity of the phage-derived peptide, compared to the mucin core peptide.

A sepharose bead assay was then conducted to determine if the phage derived peptide would function as an affinity ligand, and to establish the relative antigenicity compared to the mucin core peptide in this different environment. Peptide affinity chromatography was then used to examine the point at which any retained antibody eluted along a gradient elution profile. It has been postulated that gradient elution using a chaotropic agent can be used as a means of confirming relative affinities from fluorescence quenching (Murray, *et al.* 1998).

Fluorescence quenching immunoassay was then used to test the above hypothesis with regard to the phage derived peptide and mucin core peptide.

Conformational analysis was then conducted on the peptides **APDTRPAPG**, **APDTREAPG** and **RNREAPRGKICS** using circular dichroism techniques. Previous studies have demonstrated that the synthetic peptide representing the natural antigen of C595 (**APDTRPAPG**) exists in a PII helical conformation, and that this conformation is stabilised in cryogenic studies and with increased glycosylation (Murray, *et al.* 1998),(Spencer, *et al.* 1999).

Surface Plasmon Resonance (SPR) was then used to conduct an in-depth analysis of the kinetic parameters involved in the interaction between mAb C595 and the mucin core peptide **APDTRPAPG** immobilised onto the surface of a biosensor chip. The use of SPR enables a more complex analysis of the interaction, since unlike FQ, on and off rates can be examined, enabling the fitting of more complex models to the data set. A comparison will be made between the data obtained in the FQ experiments with the data obtained in the SPR experiments.

5.2 ELISA of BSA – peptide conjugates

There are a number of examples where peptides derived from phage-display libraries lose their ability bind to the target antibody when synthesised and are no longer part of the phage. Examples include the phage-derived low affinity mimic of a discontinuous epitope of glucoseoxidase (gluox) (Meloan *et al.* 2000), which only bound anti-gluox antibody when part of the phage; and the phage-derived mimic of a steroid hormone (Murray, *et al.* 2000), which only weakly bound to the anti-steroid antibody.

In order to ascertain whether the phage derived peptide **RNREAPRGKICS** could bind mAb C595 in the absence of phage, the phage-derived peptides, and mucin core peptide were conjugated to BSA using the method described in chapter 3. The BSA-peptide conjugates were then serially diluted, and the ability of mAb C595 to bind to the conjugates was determined using a standard ELISA as described in chapter 3. Figure 5.1 shows the results of this ELISA. The phage-derived peptide

(**RNREAPRGKICS**) formed an insoluble pink precipitate when conjugated to BSA. The precipitate is probably the result of conjugation through N-terminus amine and the amine side-chain of lysine. From the data presented in figure 5.1, it appears that the precipitation observed in the conjugation reaction has resulted in less of the peptide **RNREAPRGKICS** (in the form of the BSA conjugate) binding to the microtitre plate – compared to the BSA conjugate containing the mucin epitope peptide (**APDTRPAPG**).

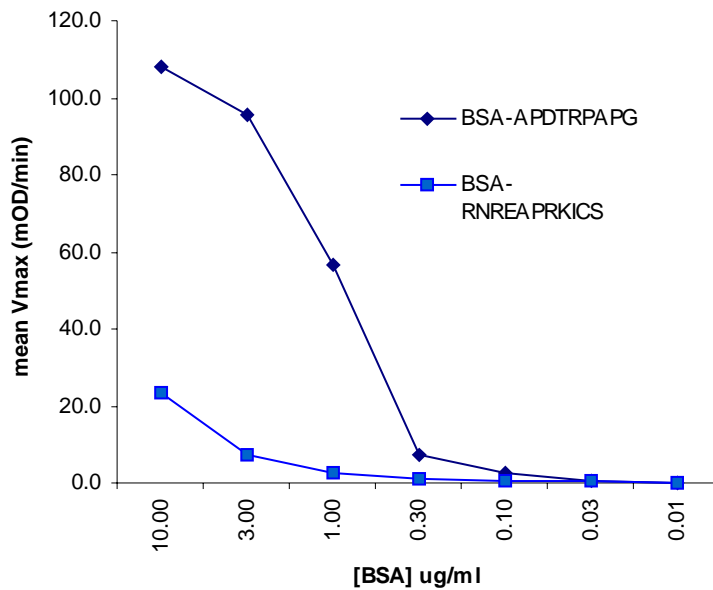


Figure 5.1: ELISA of BSA – peptide conjugates dried down onto the wells of a microtitre plate at various concentrations.

As a result of the precipitation observed during the synthesis of the BSA – **RNREAPRGKICS** peptide conjugate, it is not possible to make a direct comparison between the two peptides using this method.

5.3 Sepharose bead assay

The phage-derived peptide **RNREAPRGKICS** and the mucin core peptide **APDTRPAPG** were coupled to cyanogen bromide activated Sepharose 4B as described in chapter 3. A sepharose bead assay was conducted as described in chapter 3. A control assay was run in parallel, to establish the level of binding of the marker antibody to the peptides linked to the beads. In the control assay, only marker

antibody (rabbit anti-mouse IgG peroxidase conjugate) was added to the beads. The results are presents in figure 5.2.

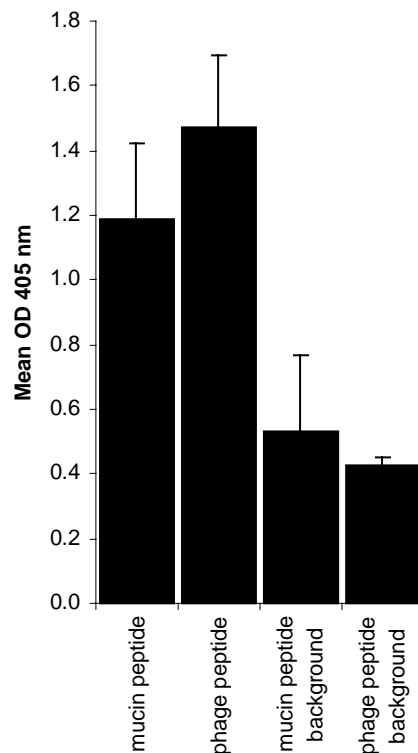


Figure 5.2: Sepharose bead assay comparing the mucin core peptide (**APDTRPAPG**) with the phage derived peptide (**RNREAPRGKICS**).

From the results presented in figure 5.2, it appears that the average level of binding of mAb C595 to the phage-derived peptide is greater than the level of binding observed for the mucin core peptide. These results indicate that the phage clones displaying the **RNREAPRGKICS** peptide may have been selected on the basis of affinity. However it is not possible to conclude whether phage displaying the **RNREAPRGKICS** clone emerged as a result of affinity selection, or selection as a result of growth advantage conferred to the phage clones by displaying this peptide. These results demonstrate that the phage derived peptide is able to bind mAb C595 in the absence of the phage.

5.4 Peptide Affinity Purification of antibody from solution

The use of immobilised ligands to analyse macromolecular interactions, particularly using analytical affinity chromatography techniques has been much documented (Chaiken, *et al.* 1992; Chaiken, *et al.* 1996). Here the technique will be used to compare the properties of peptide affinity matrices prepared using the phage derived peptide and the mucin core peptide. Peptide affinity matrices were also prepared using the **APDTRPAPGC** and **APDTREAPG** control peptides. The relative performance of the phage-derived and mucin core epitope peptide matrices will also be assessed by their abilities to purify antibody from hybridoma feedstock.

5.4.1 Peptide Affinity Purification using the phage derived peptide and the mucin core peptide.

The phage-derived peptide **RNREAPRGKICS** was linked to cyanogen-bromide activated sepharose 4B at a ratio of 1µmole of peptide per ml of swollen gel, as described in chapter 2. The mucin core peptide **APDTRPAPG** was also linked to sepharose 4B at an equivalent ratio, as were the two control peptides **APDTRPAPGC** and **APDTREAPG**. Antibody (mAb C595 at 15µg/ml) was loaded onto the respective columns under standard conditions of sample loading (0.3 ml/min), column size (2.0 ml swollen gel volume), ligand density (1 µmol/ml gel) and elution (3M NaSCN).

Figure 5.3 presents the results of the gradient elution of mAb C595 from the **RNREAPRGKICS** and **APDTRPAPG** peptide affinity matrices. Chromatograms demonstrating the elution of mAb C595 from the affinity matrices containing the peptides **APDTREAPG** and **APDTRPAPGC** are omitted for clarity. The elution profiles from the **APDTREAPG** and **APDTRPAPGC** were identical in shape and size to the elution profile of the **APDTRPAPG** matrix (figure 5.3). Note the sharp symmetrical peak for the antibody eluted from the **RNREAPRGKICS** peptide matrix. The maximum of this peak appears before the maximum of the peak for the elution of antibody from the **APDTRPAPG** peptide matrix. The elution of antibody bound to the **RNREAPRGKICS** matrix occurs lower down in the gradient elution than antibody eluted from the **APDTRPAPG** peptide matrix using 3M NaSCN.

Eluted fractions were collected and the total mass of protein was determined spectrophotometrically at 280nm by applying the Beer-Lambert Law (assuming an extinction coefficient of 14.3 for IgG), for each of the matrices. These results are presented in table 5.1.

5.4.2 Purification of C595 antibody from hybridoma supernatant.

To directly compare the mucin core epitope peptide and phage-derived peptide as peptide affinity ligands, mAb C595 was purified from 100 ml of clarified hybridoma supernatant (200 ml sample divided into two) using the **APDTRPAPG** and **RNREAPRGKICS** affinity matrices. Antibody was loaded onto the two columns under standard conditions (as described in chapter 3), and a step elution of the loaded antibody was conducted for each of the matrices. Eluted fractions were collected and the total mass of protein was determined spectrophotometrically at 280nm by applying the Beer-Lambert Law for each of the matrices. The results of this experiment are presented in figure 5.4 and table 5.1. There is very little difference between the two chromatograms for the step elution profile.

From the results of the protein determinations for the two sets of experiments presented in table 5.1, it can be seen that the amount of antibody recovered from both the phage-derived affinity matrix and the mucin-derived affinity matrix is almost identical, recovering 65% of protein. However, the results showing antibody recovery from the same sample of hybridoma supernatant are quite different. Less protein is recovered when the phage-peptide affinity matrix was used compared to the mucin-peptide affinity matrix (0.78 and 1.01 mg respectively).

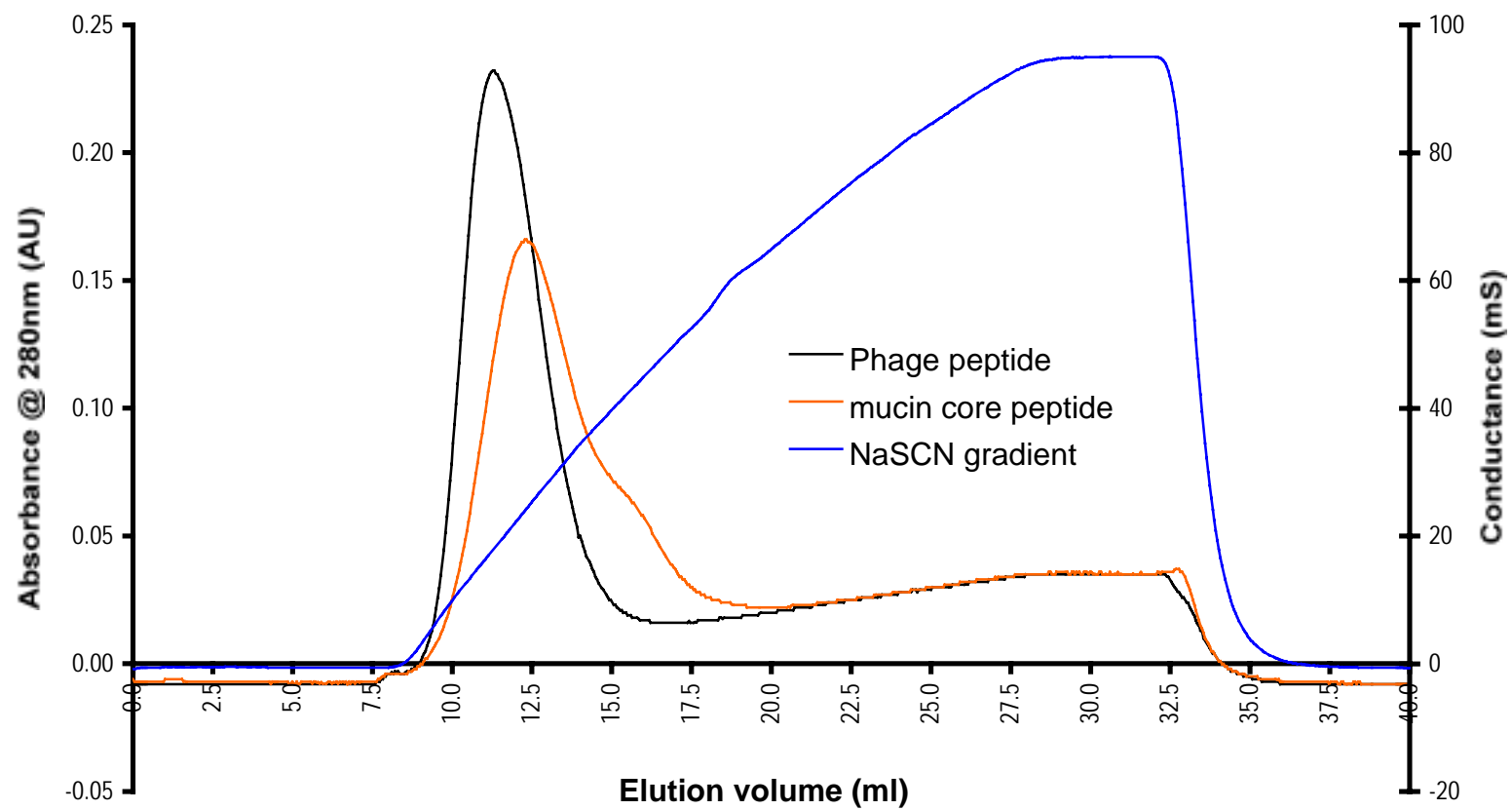


Figure 5.3: Gradient elution of the phage and mucin core peptide-Sepharose affinity matrices following column loading with 100 ml C595 antibody at 15 μ g/ml in PBS.

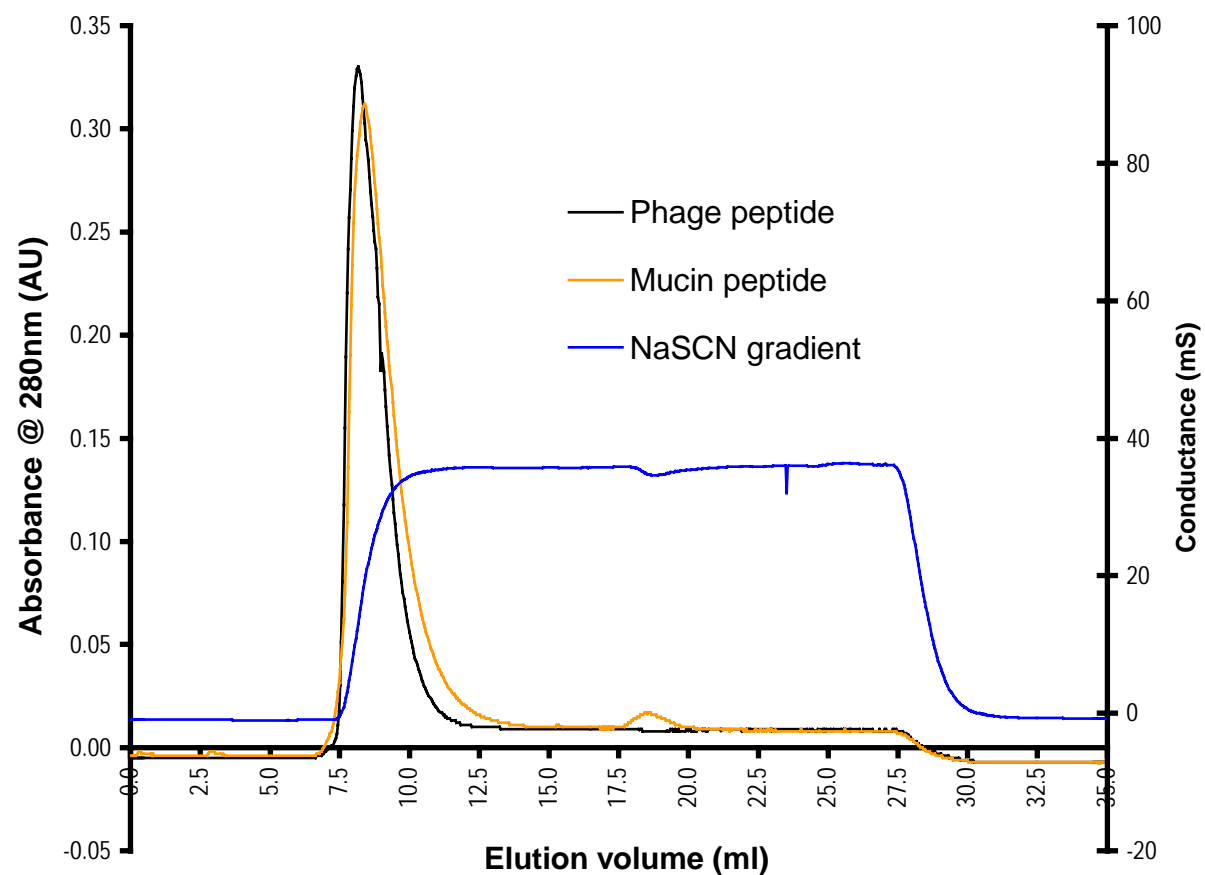


Figure 5.4: Step elution of the phage and mucin-core peptide-Sepharose affinity matrices following column loading with 100ml of clarified C595 hybridoma supernatant.

Expt	Matrix (Seph 4B)	Sample type	Sample volume (ml)	Elution method	Total Protein (mg) in each 2.5 ml fraction			Total (mg)	Mean Vmax (mOD/min) of F1
					F1	F2	F3		
1	Mucin peptide	Ab in PBSA (15µg ml ⁻¹)	100	0-3M Gradient over 20ml of NaSCN	0.35	0.47	0.16	0.98	-
2	Phage peptide	Ab in PBSA (15µg ml ⁻¹)	100	0-3 M Gradient over 20ml of NaSCN	0.70	0.25	0.04	0.99	-
3	Mucin peptide	*Hybridoma supernatant	100	Step to 1M NaSCN	0.85	0.16	-	1.01	15.47
4	Phage peptide	*Hybridoma supernatant	100	Step to 1M NaSCN	0.68	0.10	-	0.78	24.45

Table 5.1: Comparison of the performance of the mucin core peptide column (**APDTRPAPG**) and the phage derived peptide column (**RNREAPRGKICS**).

5.4.2.1 Immunoreactivity of purified antibody

A standard ELISA was conducted on the recovered protein fractions from the phage and mucin peptide affinity matrices (as described in chapter 3). BSA-peptide conjugate (using peptide **APDTRPAPG**) was adsorbed to the wells of a microtitre plate. The level of binding observed for the combined fractions from the elution of the Phage peptide affinity matrix was compared with the combined fractions from the elutions of the Mucin peptide affinity matrix. These were compared with a sample of the original hybridoma supernatant, prior to circulation around the columns. The pass-samples from the phage and mucin peptide columns were also compared in the assay. The results are presented in figure 5.5.

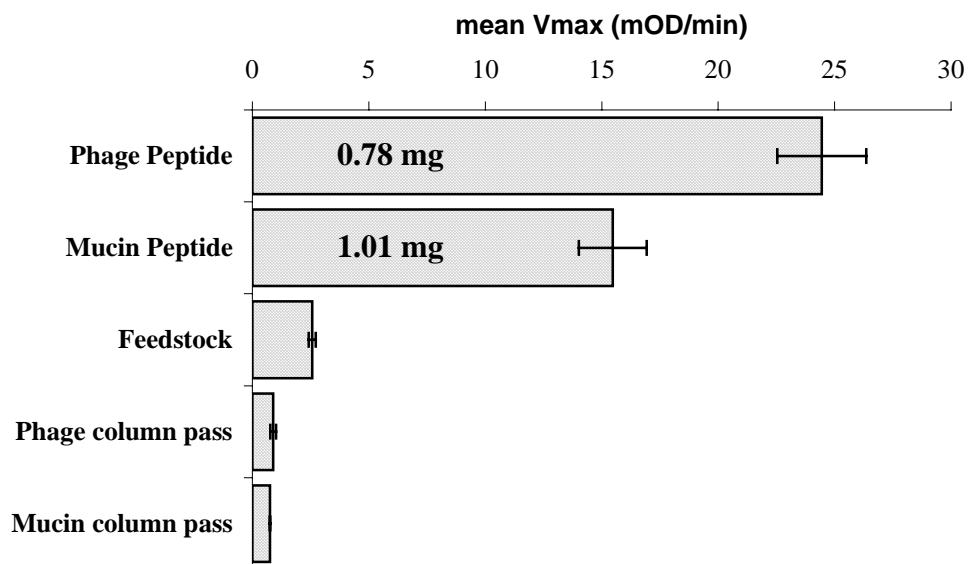


Figure 5.5: Mass in bars is the protein content of each fraction determined spectrophotometrically at 280nm by applying the Beer-Lambert Law and assuming an extinction coefficient for IgG of 14.3

From the results presented in figure 5.5, it appears that even though less total protein was recovered from the phage-derived peptide affinity matrix, it had a higher specific activity than the protein recovered from the mucin-core epitope peptide matrix.

The activity of the antibody eluted from the phage peptide affinity matrix was greater than that of the antibody eluted from the mucin peptide affinity matrix, as tested by ELISA (see figure 5.5).

The mucin derived peptide and the phage derived peptide affinity matrices demonstrated a 6-fold and 9.4-fold concentration of antibody from the clarified hybridoma supernatant respectively- with respect to the activity of the purified antibody in ELISA (see figure 5.5).

5.4.2.2 SDS-PAGE analysis of purified antibody.

The purity of the affinity purified antibodies recovered from the hybridoma supernatant using the phage-derived peptide affinity matrix and the mucin core peptide affinity matrix was analysed using SDS-PAGE as described in chapter 3. The results are presented in figure 5.6.

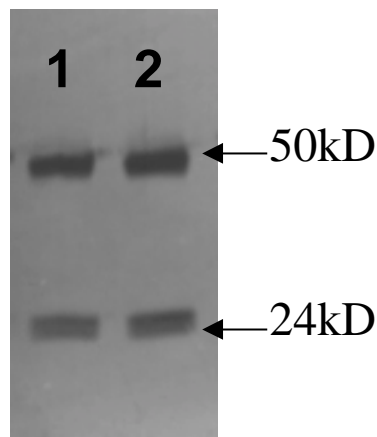


Figure 5.6: SDS-PAGE gel of purified antibody, conducted using 12.5% w/v homogeneous acrylamide as described in section 3.4.8. Samples were boiled in loading buffer containing β -mercaptoethanol for 5 min before gel loading. Lane 1 contains the antibody recovered from the purification of hybridoma supernatant using the phage-derived peptide (**RNREAPRGKICS**) affinity matrix. Lane 2 contains the antibody recovered from the purification of hybridoma supernatant using the mucin-core peptide (**APDTRPAPG**) affinity matrix. 50kD and 24 kD represent the approximate size of the bands corresponding to C595 heavy and light chains respectively.

As can be seen in the gel in figure 5.6 the purity of the antibody purified using the phage-derived peptide affinity matrix appears to be identical to the purity of the antibody purified using the mucin-core peptide affinity matrix.

5.5 Fluorescence Quenching (FQ) analysis of peptides.

The aromatic amino acid residues present in proteins exhibit a natural fluorescence. The aromatic amino acid tryptophan exhibits the greatest fluorescence, with excitation and emission maxima at approximately 295nm and 350nm respectively. The position of the emission maximum is highly dependent upon the local environment of the tryptophan residue (e.g. 320nm for internal residues c.f. 360nm for solvent exposed residues). This dependence on the local environment of the tryptophan residue can be used to monitor a specific binding event. Thus if a tryptophan residue is exposed in the binding pocket of an antibody, upon binding of a ligand, the intensity of the emitted radiation will be reduced. This technique is known as fluorescence quenching, and can be used to measure the equilibrium association constant for antibody-ligand interactions. FQ has been successfully used in the past to determine equilibrium association constants for interactions involving mAb C595 and MUC1 related peptides (Missailidis, *et al.* 1997; Spencer, *et al.* 1999).

The interaction of the synthetic peptides **APDTRPAPG**, **APDTRPAPGC**, **APDTREAPG**, and **RNREAPRGKICS** with antibody C595 were measured and expressed as an equilibrium association constant (K_A) using the technique of fluorescence quenching. Experimental binding curves were obtained by plotting the changes in fluorescence of the antibody emission versus the antigen concentration at each titration step (figure 5.7). The experimental data was then fitted to a mathematical equation describing the binding (Missailidis, *et al.* 1997; Spencer, *et al.* 1999) (see chapter 3), allowing the calculation of the equilibrium association constants for the above interactions. The equilibrium association constants for the peptides are presented in table 5.2.

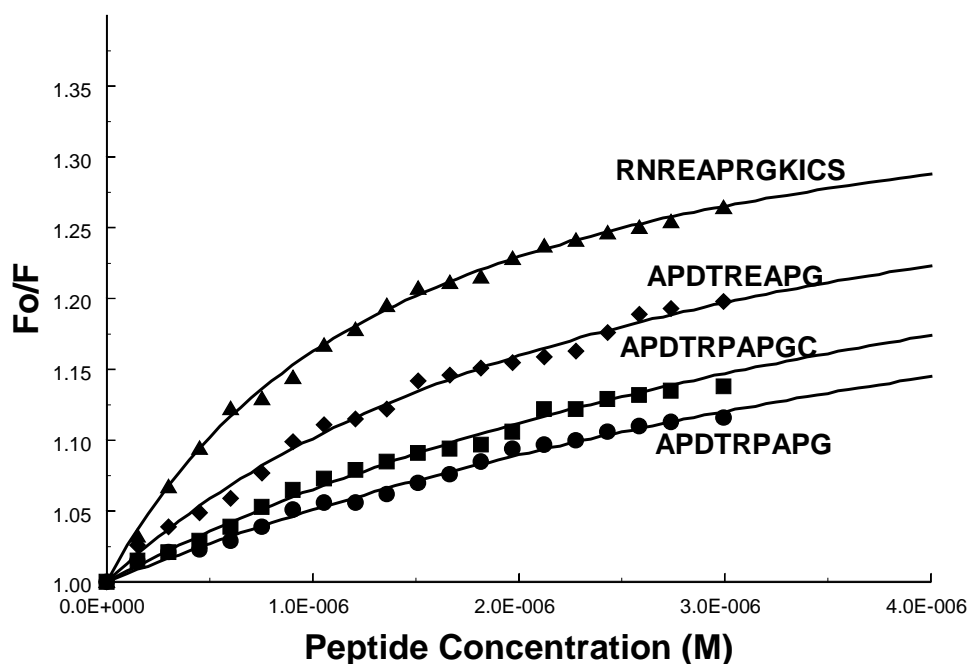


Figure 5.7: Binding of the APDTRPAPG, APDTRPAPGC, APDTREAPG and RNREAPRGKICS peptides to mAb C595. Changes in the natural fluorescence of the antibody were plotted versus peptide concentration to calculate the equilibrium association constants for formation of the antibody-antigen complexes.

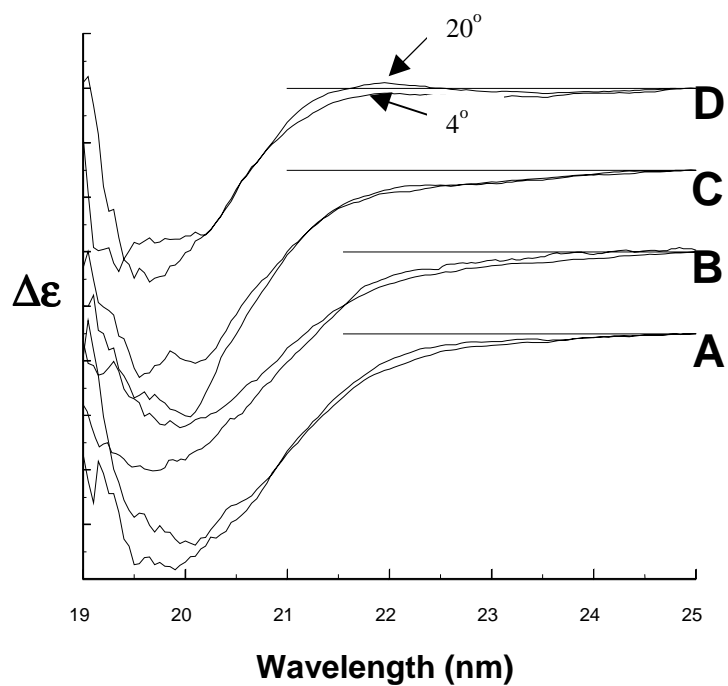
Peptide	Association constant (M^{-1})
APDTRPAPG	0.15×10^6
APDTRPAPGC	0.21×10^6
APDTREAPG	0.40×10^6
RNREAPRGKICS	0.75×10^6

Table 5.2: Affinity of C595 antibody for MUC1-related peptides and the phage derived peptide. The values shown in the table are calculated from the experimental data (in triplicate) using the method described in chapter 3. The precision of these values = $\pm 0.01 \times 10^6$ M.

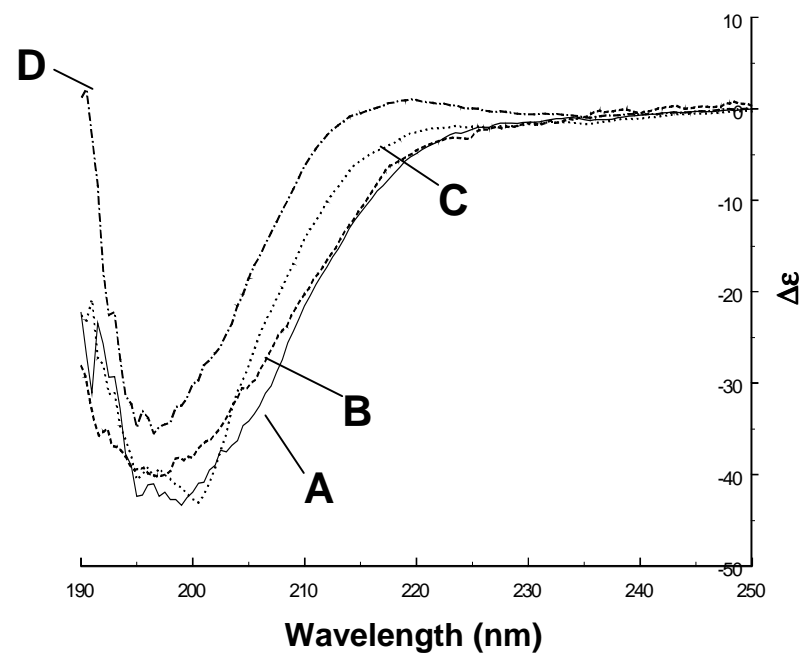
The peptides in the study all showed a significant affinity towards the C595 antibody, as expected from the results of the chromatographic and ELISA studies. The phage derived peptide **RNREAPRGKICS** was shown to have the highest affinity for the antibody ($K_A=0.75 \times 10^6 \text{ M}^{-1}$), followed by the substituted peptide **APDTREAPG** ($K_A=0.40 \times 10^6 \text{ M}^{-1}$), the natural antigenic peptide with the cysteine residue at the C-terminus **APDTRPAPGC** ($K_A=0.21 \times 10^6 \text{ M}^{-1}$) and the natural antigenic peptide **APDTRPAPG** ($K_A=0.16 \times 10^6 \text{ M}^{-1}$).

5.6 Circular Dichroism (CD) analysis of peptides.

Circular Dichroism is a spectroscopic technique for analysing the global secondary conformation of a protein or peptide. The CD of proteins or peptides is primarily the CD of the amide chromophore; secondary structure as measured by CD examines amide-amide interactions. The technique relies on the difference in the absorption of left and right circularly polarised light (which varies according to the secondary structure of the protein and the wavelength of the light). If a peptide has a secondary conformation then decreasing the temperature of its solvent will stabilise the conformation of the solute. Peptides **APDTRPAPG**, **APDTREAPG**, and **RNREAPRGKICS** were studied at temperatures of 4 °C and 20 °C. The results are shown in figure 5.9.



(i)



(ii)

Figure 5.9: (i) Structure / temperature relationship at 20 and 4 °C examined using CD on: the MUC1 core peptide **APDTRPAPG** (A), the MUC1 core related control peptides **APDTRPAPGC** (B), and **APDTREAPG** (C), and the phage derived peptide **RNREAPRGKICS** (D). Lines for $\Delta\epsilon = 0$ have been inserted at each case to assist assessment of the peptide signal. (ii) Comparison of the four peptides at 4°C.

The CD spectra of peptides **APDTRPAPG**, **APDTRPAPGC**, **APDTREAPG** and **RNREAPRGKICS** at room temperature (Figure 5.9) indicated that the peptides did not adopt an highly ordered structure, but there was a distinct trend of a preferred left-handed extended polyproline II helix (PII conformation) (Campbell and Sykes 1993). All the peptides in the study presented positive bands at 217-225 nm and negative bands at 195-200 nm. The presence and intensity of the positive band at 217-225 nm and the negative band at 195-200 nm confirms the population of a PII conformation (Dalcol, *et al.* 1996). The intensity of the positive band is directly proportional to the stability of the PII helix. It has previously been demonstrated that peptide **APDTRPAPG** exists in a PII helical conformation, which is stabilised in cryogenic studies and with increased glycosylation (Murray, *et al.* 1998), (Spencer, *et al.* 1999). All three peptides have demonstrated an increase in the intensity of the positive band at 217-225 nm with decrease in temperature.

There is a profound correlation between the structural content of the peptides, and their binding ability.

The C595 antibody has previously been studied by CD and its denaturation with temperature and pH variation has been reported (Spencer, *et al.* 1999). The melting profile of the C595 antibody was re-evaluated, and the possible stabilising effect of the binding of peptides containing the natural epitope (**APDTRPAPG** and **APDRPAPGC**) or the phage display derived sequences (**RNREAPRGKICS** and **APDTREAPG**) to the antibodies binding pocket was investigated. When the antibody was subjected to thermal denaturation the clear melting profile previously reported (Spencer, *et al.* 1999) emerged, with melting transitions at 61 and 68°C. Addition of the peptides **APDTRPAPG**, **APDRPAPGC**, **APDTREAPG** and **RNREAPRGKICS** did not have any stabilising effect on the antibody melting profile. This is not unexpected as these short peptides are occupying necessarily only one binding site. The binding of a single peptide per binding pocket would not seem to have any effect on the disulphide bonds stabilising the antibody's molecular structure. The antibody was shown to have two melting transitions as previously determined (Spencer, *et al.* 1999), in which case two T_m values were determined (T_{m1} , T_{m2}). Similar, two-melting transitions were obtained from the peptide bound antibody.

5.7 Kinetic analysis of the interaction between C595 antibody and the mucin core peptide APDTRPAPG using surface plasmon resonance.

Surface Plasmon Resonance (SPR) measurements were conducted using a BIAcore biosensor. Its configuration involves the interaction of soluble macromolecules in a flow cell with ligands (or receptors) immobilised on the dextran coating of a gold chip. The interaction is measured directly as an increase in refractive index, a change directly related to an increase of molecular mass on the chip.

Measurements conducted using an immobilised ligand are more likely to reflect the affinity constants observed in an affinity chromatography situation, than measurements taken in free solution in the FQ assay.

The purpose of these experiments was to determine the affinity constants for the interaction of the mucin core peptide **APDTRPAPG** and mAb C595, and compare the data obtained with the results obtained from the FQ experiments.

5.7.1 Optimisation of peptide APDTRPAPG immobilisation on the surface of a Pioneer CMD sensor chip.

The accurate measurement of the kinetics of biomolecular interactions using biosensor kinetic techniques requires data not limited by the effect of immobilisation of the ligand. High ligand immobilisation levels can lead to poor fitting of binding models to the data set. Factors that cause poor fitting include:

Mass transport limitation - the binding of ligate flowing over the sensor surface to the immobilised ligand requires the efficient delivery of ligate to all of the ligand sites. If delivery of ligate is slower than the specific binding, the measured kinetics (association rate constant - k_a) will be limited by this mass transport effect.

Rebinding of ligate - the dissociation rate constant k_d should be independent of ligate concentration. If a high concentration of ligand is present then the probability

of the ligate molecules rebinding to the surface on dissociation will be high, thus giving an incorrect representation of the value of k_d .

Steric hindrance within the CMD matrix – the binding of ligate to a particular site may prevent binding of other ligate molecules to an adjacent site. At low ligand loadings it has been demonstrated that the association rate constant is significantly higher than at higher loadings of the ligand (Edwards 1999).

Thus it is absolutely necessary to achieve a low concentration of peptide immobilised on the surface of the biosensor chip because of the above, and also because of crowding, avidity and aggregation effects (see section **3.4.14.1**).

Initial experiments were conducted using a BIAcore CM5 CMD chip. However it proved impossible to reduce binding levels of the peptide to the activated matrix to the required level using techniques described in section (**3.4.14.1**). A Pioneer Sensor chip F1 was used as this provided the same functionality as Sensor Chip CM5, but has a shorter dextran matrix. It was thought that the shorter dextran matrix would also limit mass transport and rebinding effects. Due to the shorter matrix the immobilization yield is typically around 30% of that obtained on Sensor Chip CM5 under comparable conditions (BIAcore 1997).

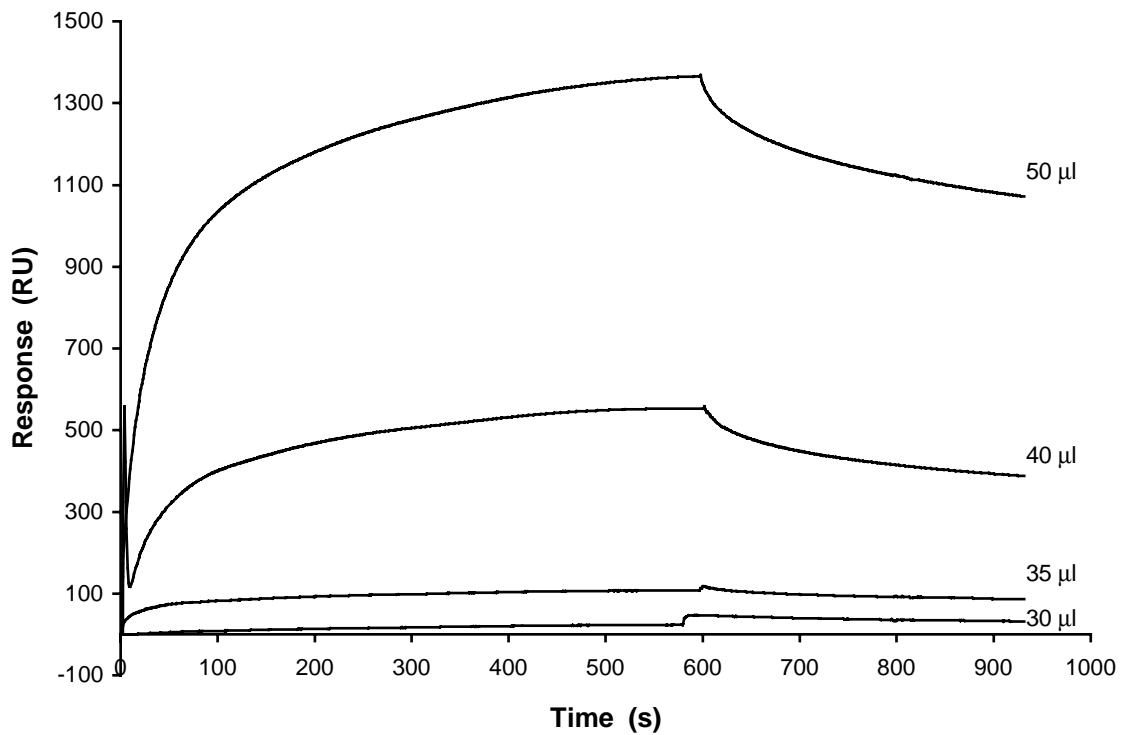


Figure 5.10: Optimization of peptide immobilisation on the surface of a pioneer L1 CMD sensor-chip. Repeat injections of peptide **APDTRAPAPG** (1mM) in HBS were injected into the four flowcells over the activated sensor-chip at volumes of 50, 40, 35 and 30 µL, at a flow rate of 5 µL/min. Remaining activated carboxyl groups were blocked with ethanolamine. Monoclonal antibody C595 was then passed over the four flowcells (3.0 µM) to visualize levels of binding.

5.7.2 Kinetic analysis of the interaction between immobilised mucin core peptide APDTRPAPG (ligand) and C595 mAb (ligate)

Model	k_a ($M^{-1}s^{-1}$)	k_d (s^{-1})	K_A (M^{-1})	χ^2
Langmuir	8.24×10^3	2.18×10^{-3}	3.78×10^6	5.38
Langmuir*	8.27×10^3	2.42×10^{-3}	3.41×10^6	4.15
Langmuir* + mass-transfer	8.29×10^3	2.41×10^{-3}	3.43×10^6	4.15

Table 5.3: Kinetic rate constants derived from Global Analysis of the monoclonal antibody C595 – mucin core peptide **APDTRPAPG** Biosensor data, using the Langmuir model and the Langmuir model with mass transfer model. * 2.0 μM concentration of C595 monoclonal antibody was omitted from the global analysis (see below).

Analysis of the individual values of k_a and k_d for each of the concentrations of the antibody used, indicated that the dissociation rate constant (which is independent of concentration of analyte) for the 2.0 μM concentration of C595 monoclonal antibody did not correlate with the other observed values.

[C595 mAb] (μM)	k_a	k_d	χ^2
3.0	9.10×10^3	2.76×10^{-3}	10.800
2.5	9.48×10^3	2.27×10^{-3}	2.600
2.0	1.01×10^4	1.36×10^{-3}	1.950
1.5	8.60×10^3	2.79×10^{-3}	2.130
1.0	1.15×10^4	2.36×10^{-3}	1.380
0.5	1.58×10^4	2.45×10^{-3}	0.898

Table 5.4: Results of local fitting of the Langmuir model individually to each antibody concentration.

In further analysis of the data the experimental results derived from the 2.0 μM concentration of monoclonal antibody C595 were excluded.

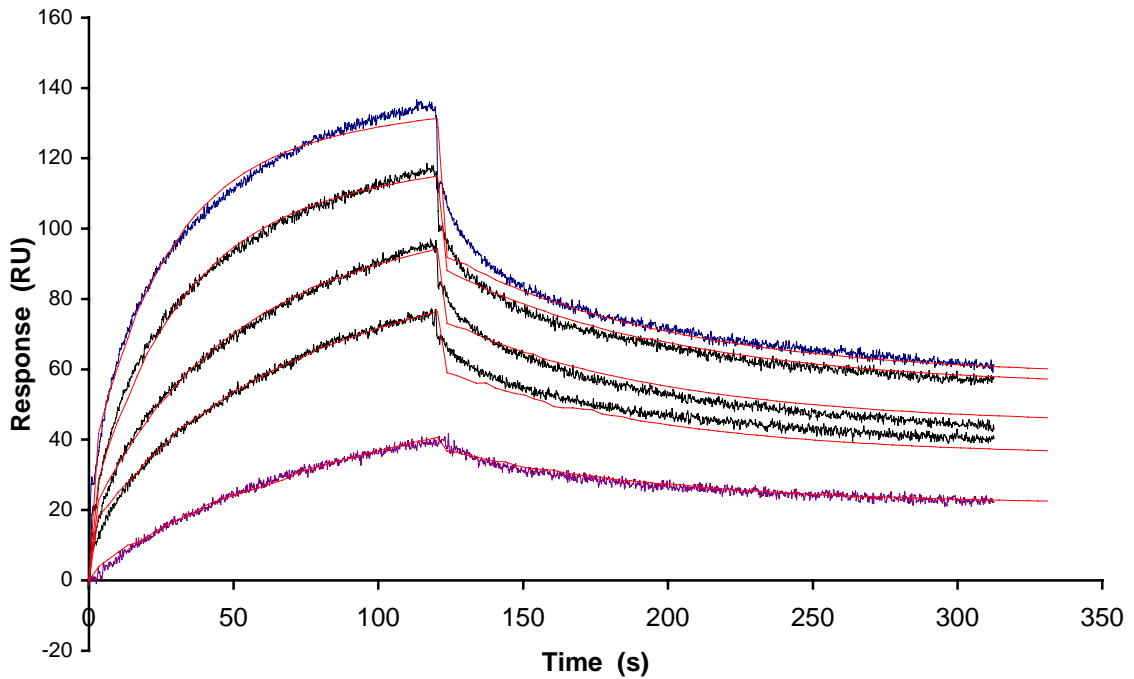


Figure 5.11: Corrected sensorgram overlays for the C595 monoclonal antibody-mucin peptide interaction. Repeat injections of C595 monoclonal antibody at 3.0, 2.5, 1.5, 1.0 and 0.5 μM . The data collection rate was set to high. The extended red lines represent the best global fits to the Langmuir model using BIAevaluation software version 3.0.2.

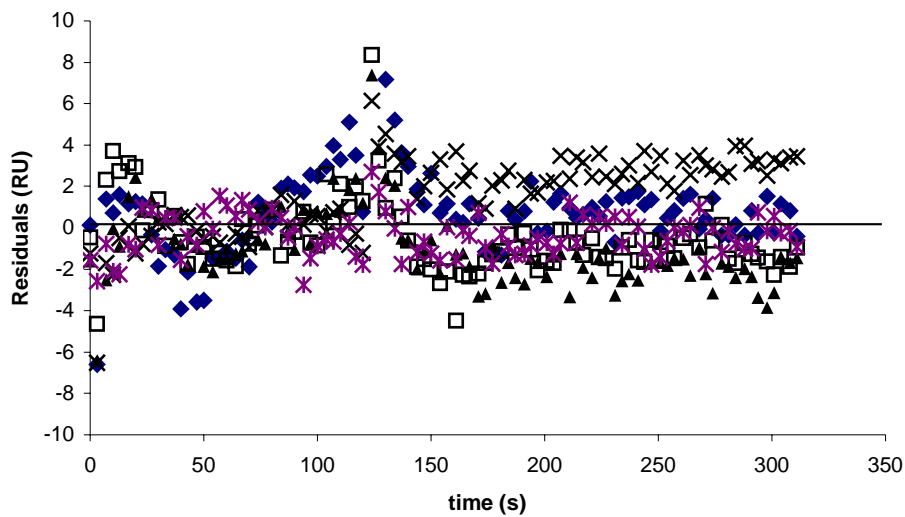


Figure 5.12: Residual plot for the global fit of the experimental versus modeled sensor data. Showing random scatter of points about the median line.

Model	k_{a1} (1/Ms)	k_{a2} (1/s)	k_{d1} (1/s)	k_{d2} (1/s)	K_A (M^{-1})	χ^2
2-state	1.01×10^4	5.12×10^{-3}	7.68×10^{-3}	3.21×10^{-6}	2.1×10^9	2.83
Parallel	1.15×10^4	114	3.08×10^{-3}	2.24×10^{-6}	(1) 3.73×10^6 (2) 5.10×10^7	3.43
Bivalent	3.8×10^3	2.86×10^{-5}	2.96×10^{-3}	4.94×10^{-6}	-	4.01

Table 5.5: Kinetic rate constants derived from Global Analysis of the monoclonal antibody C595 – mucin core peptide **APDTRPAPG** Biosensor data using more complex models.

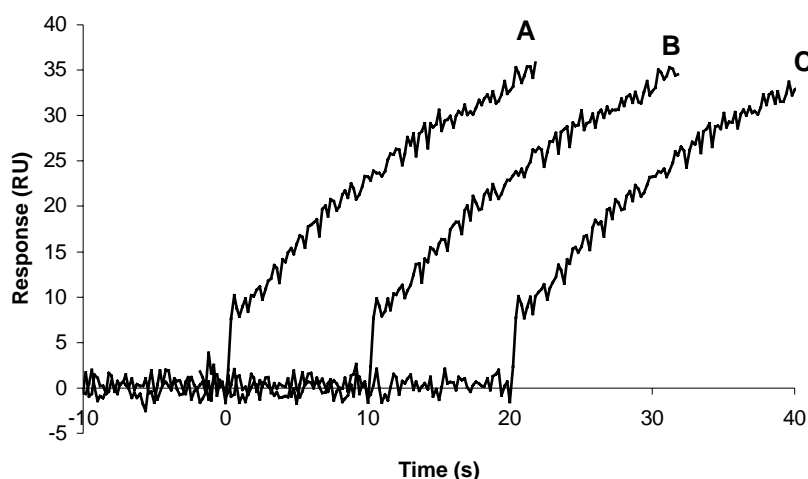


Figure 5.13: Initial binding responses for monoclonal antibody C595 injected at different flow rates over the peptide surface. A $1.0 \mu M$ concentration of antibody was injected over the peptide surface as a flow rate of 10 (A), 30 (B) and 90 (C) $\mu L/min$.

The initial binding responses indicate that mass-transport is not a limiting factor in the measurement of the kinetics of the interaction between the peptide and antibody at the surface of the sensor chip. This supported the global fitting data for the Langmuir model (1:1) interaction and the Langmuir model with mass transport, which did not indicate that mass transport of antibody to the peptide was a significant factor.

Global analysis of the data obtained indicated that the model which most accurately described the data set was the two-state (conformational change) model. It should be noted that conformational changes in ligand or complex do not normally give a response because the detection systems of optical biosensors is mass based and a conformational change does not produce any change in mass in and of itself. The affect is indirect, as formation of the second species will alter the equilibrium between the bound and free forms and so change the mass on the sensor surface.



However the significance of this result should not be overestimated, since all of the models fitted had very small values of χ^2 and so all are equally as applicable. From these result a value for $K_A \sim 3 \times 10^6 \text{ M}^{-1}$ appears likely.

5.8 Summary and Discussion

The phage-derived peptide **RNREAPRGKICS** and the mucin core peptide **APDTRPAPG** were conjugated to BSA, and the level of binding of C595 after equilibrium was reached compared. A significantly lower level of binding was observed for the phage-derived peptide conjugate compared with the mucin-core peptide conjugate. When the same peptides were linked to beaded agarose, the average level of binding of mAb C595 was greater for the phage-derived peptide than the mucin-core peptide. A possible explanation for this difference was the precipitation of the phage-derived peptide on conjugation to BSA. It was demonstrated that the phage-derived peptide could still bind mAb C595 in the absence of phage.

Affinity chromatography was performed using the phage-derived peptide **RNREAPRGKICS** linked to beaded agarose and compared with affinity matrices using: (i) the mucin-core peptide **APDTRPAPG**; (ii) the mucin-core peptide with a terminal cysteine residue (to control for dimerisation) **APDTRPAPGC**, and (iii) the mucin-core peptide with a glutamic substitution (to control for binding being enhanced by the **REAP** mimotope alone) **APDTREAPG**. NaSCN gradient elution

profiles of columns loaded with mAb C595 were compared. The elution profiles from the **APDTREAPG** and **APDTRPAPGC** matrices were identical in shape and size to the elution profile of the **APDTRPAPG** matrix. The maximum of the peaks in the elution of mAb C595 from the **APDTREAPG** and **APDTRPAPG** were directly in line in the gradient elution profile. The maximum of the peak from the elution of mAb C595 from the **APDTRPAPGC** matrix was further up the NaSCN gradient than any of the other maxima, this has previously been attributed to dimerisation of the peptide leading to an increased affinity (A. Murray, University of Nottingham – personal communication). The elution profile for the phage-derived peptide affinity matrix exhibited a sharp symmetrical peak, compared to the more broad, unsymmetrical peaks observed for the other peptide affinity matrices.

Antibody purified from hybridoma supernatant using the phage-derived peptide affinity matrix, exhibited a higher specific reactivity than antibody purified from hybridoma supernatant using the mucin-core peptide affinity matrix. SDS-PAGE analysis of the purified antibody from both matrices demonstrated that the antibodies were effectively purified from hybridoma supernatant, and contained no impurities.

Affinity determination using fluorescence quenching analysis and structural analysis using circular dichroism, of the phage-derived peptide **RNREAPRGKICS**, the mucin-core peptide **APDTRPAPG**, and the related control peptides **APDTRPAPGC** and **APDTREAPG** revealed a profound correlation between structural content of the peptides and their relative equilibrium association constants. The peptides showed a structural content and equilibrium association constant in the following order:

RNREAPRGKICS > APDTREAPG > APDTRPAPGC > APDTRPAPG

These results were in agreement with the relative performances of the phage-derived peptide affinity matrix and the mucin-core peptide affinity matrix (i.e. Antibody recovered from the phage-derived peptide affinity matrix exhibited higher specific reactivity than antibody recovered from the mucin-core peptide affinity matrix).

Analysis of the interaction of mAb C595 with immobilised mucin-core peptide **APDTRPAPG** using a BIAcore biosensor gave an equilibrium association constant

approximately 20x the value observed in the solution phase FQ assay. This can be attributed to the reduction in entropy of the immobilised peptide compared to the solution-phase peptide. This increased equilibrium association constant is likely to be reflected in the real value observed on the peptide affinity matrix. Thus the FQ assay can be used to give relative affinities of the repetitive ligands, but the actual equilibrium constants on the column are likely to be higher as a result of the reduction in entropy of the immobilised peptide compared to the solution-phase peptide.

The results of the gradient elution of antibody from the **RNREAPRGKICS** peptide affinity matrix are in contrast to several authors who have suggested that tolerance to thiocyanate elution is proportional to the strength of the antigen-antibody interaction. Examples of the disruption of antigen-antibody interactions using thiocyanate elution in ELISA based techniques to determine relative affinities of interaction have previously been published (Pullen, *et al.* 1986; Macdonald, *et al.* 1988; Ferreira and Katzin 1995). This relationship has also previously been used as an empirical measure of the affinity of the interaction between an immobilised antigen or ligand and the antibody by eluted a loaded chromatography column with thiocyanate (Murray, *et al.* 1997; Murray, *et al.* 1998; Murray, *et al.* 2000). Other chaotropic solvents have been employed to fractionate polyclonal antibodies (Narhi, *et al.* 1997). Here too, the authors note that “...tighter binding pAbs would require increasingly more denaturing solvents to elute them”. However Murray, *et al.* (2000) comment on the relatively low concentration of NaSCN required to elute antibody from an affinity column, even though the yield of antibody recovered was high.

These results suggest affinity selection played a part in the selection of the phage-derived peptide **RNREAPRGKICS** in the four rounds of biopanning. The fact that all of the nucleotides were identical for all of the phage clones displaying the **RNREAPRGKICS** peptide, does not prove that these clones were selected as a result of a particular growth advantage conferred to the phage as a result of the mutation of the 5' terminal cysteine residue. Measurements of the initial phage titer indicated that 311 copies of each clone would be displayed per ml of phage lysate. A 2.5 ml aliquot of phage lysate was used in the biopanning process, which equates to 777 copies of each phage clone. It is conceivable that a single clone that had acquired a point

mutation could be propagated in the amplification stages of the propagation process and be selected for enhanced affinity.

The equilibrium association constant for the interaction of mAb C595 with the MUC1 related peptide **CPAHGVTSAPDTRPAPGSTAP** has been determined using a BIAcore biosensor (Karanikas, *et al.* 1998). The value ($K_A = 5.6 \times 10^6 \text{ M}^{-1}$) is of the same order of magnitude as the value obtained in the interaction of the mucin core peptide **APDTRPAPG** ($3.41 \times 10^6 \text{ M}^{-1}$) using the Langmuir model of binding. The author does not describe any optimisation process for immobilising the ligand onto the sensor chip. The only information given regarding the immobilisation process is the chemistry used (NHS/EDC). The larger value is likely to be the result of immobilising too great a quantity of peptide onto the sensor chip, the result being that re-binding of antibody can occur, reducing the value measured for k_d , resulting in a higher value for K_A . Only one antibody concentration was used to determine the affinity constant in the published data.

6 Chapter 6 - Results. Mimotope peptides cross- reactive with an anti-steroid hormone antibody.

6.1 Introduction

Chapter two of this thesis described the approaches available for the discovery of novel peptide mimotopes using synthetic and biological libraries. Chapters four and five described the use of a phage display library to discover novel peptide mimotopes cross- reactive with antibodies to protein antigens, characterisation of the synthetic peptides derived from the phage display library, and their application in the affinity purification of monoclonal antibodies from supernatant. A number of examples exist in the literature, of synthetic phage-derived peptide mimotopes which (i) only bind very weakly to the target antibody (Murray, *et al.* 2000), or (ii) the synthetic versions of the phage peptide does not bind at all to the target antibody (Meloan *et al.*, 2000). Both of these examples have used small synthetic libraries to systematically optimise the phage-derived peptide in order to create a peptide that can be used for the paratope-specific affinity purification of the target antibody.

This chapter outlines the systematic optimisation process used in the first example (Murray, *et al.* 2000), and describes an approach to improve the signal to noise ratio in peptide arrays in order to reduce the number of candidate peptides for optimisation. An empirical analysis of the equilibrium constants of the interaction between the phage-derived peptide, the optimised peptide and the target antibody was conducted in an attempt to rationalise the optimisation process. An inhibition ELISA was conducted to obtain proof that the optimised and phage-derived peptides were binding specifically to the paratope of the antibody. A competition ELISA was created to determine if the optimised mimotope could be used in an assay to measure free E-3-G concentration in solution. Surface Plasmon Resonance was used to measure the kinetics of the interaction between the optimised peptide and the antibody, and the effect of temperature on the interaction was also investigated. Part of the work within this chapter contributed to a publication (Murray, *et al.* 2001) and served as an example in a patent application (Badley, *et al* 2001).

The second example above (Meloan *et al.*, 2000) describes the optimisation, using small peptide arrays, of a phage-derived, low affinity lead sequence (which only bound antibody when part of the phage) reactive with an antibody directed against a discontinuous epitope of glucoseoxidase. The systematic optimisation protocols were not described. Publications described as forthcoming in the article, which were to describe the optimisation process, have yet to be published since they form part of a patent application (R.H. Meloan – personal communication). The K_d of the original phage sequence **ASLQGMDT** was improved by a factor of 10^5 in the optimised synthetic sequence **GCAPDPFKQGVDTCG** that bound anti-glucoseoxidase antibody in the absence of phage. As can be seen the optimised sequence contains only two pairs of residues which were adjacent in the phage sequence (**QG** and **DT**). The optimised sequence is elongated compared to the phage sequence, which presumably gives rise to a better mimic of the discontinuous epitope.

The approach outlined in this chapter differs from the process outlined by Meloan *et al.* (2000), in the way the peptide libraries were constructed, and that the antibody is raised against a non-proteinaceous target. Thus the target ligand can neither be described as a continuous or discontinuous epitope. Scott (Scott, 1992) stated that phage-based epitope libraries can be used to select peptide mimics for non-peptide binding ligates (i.e. a non-proteinaceous target). As outlined in chapter 1, a number of peptide mimics have been discovered for non-proteinaceous targets, including DNA, biotin and carbohydrate moieties, but none had previously been reported for steroid hormones.

As described in chapter 1, monoclonal antibody 4155 is an anti-steroid antibody, which was raised against E-3-G, a metabolite of the steroid hormone estradiol. Section 1.5.3.4 described how mAb 4155 is purified using a competitive elution approach - after the antibody binds to estrone immobilised on an affinity column, the higher affinity analogue – estradiol 3-(beta-D-glucuronide) is then used to desorb the bound antibody from the affinity matrix. The antibody in the estradiol 3-(beta-D-glucouronide) – antibody complex can then go on to react with the higher affinity parent ligand E-3-G (to which the antibody was raised). This paratope-specific method of purification, whilst ensuring that purified antibody is fully immunoreactive

is far from ideal since it requires the use of equivalent quantities of E-3-G for each quantity of antibody purified. If a more facile paratope-specific interaction could be employed in the purification process, bound antibody could be eluted by employing an elution buffer which perturbs the antibody-ligand interaction, and the need to use a competing ligand to elute bound antibody would be eliminated. The elimination of the need to use a competing ligand in the purification process would provide a substantial saving in the cost of manufacture of purified mAb 4155.

Peptide mimotope affinity purification offers a solution, necessitating the discovery of a peptide mimotope ligand that is cross-reactive with an antibody raised against a non-peptide ligand. Peptide mimotopes of an analyte are also a valuable tool for the development of biosensors utilising mimotope-recombinant antibody constructs such as those described in the biosensor in section 1.1.3.

6.2 Optimisation of peptide mimotope ligands from lead sequences obtained from a phage display library

The overall strategy for the refinement of peptide mimotope ligands from lead sequences obtained from a phage display library as outlined in (Murray, *et al.* 2001) is illustrated in figure 6.1. The following describes each of these stages in the application of this process in the refinement of peptide mimotopes cross-reactive with the anti-E-3-G 4155 mAb.

6.2.1 Lead sequence identification

(Conducted by S. Williams, Unilever Research, Sharnbrook, UK)

A cysteine constrained, multivalent peptide library displaying random nonapeptides flanked at each end by cysteine residues fused to the major coat protein pVIII of f1 bacteriophage (Felici 1991) was used to screen for binders to mAb 4155 by affinity selection. The random insert was synthesised using an equimolar mixture of all four nucleotides at each codon. (This has the disadvantage that all three-stop codons are coded for compared to only two in the NNK strategy – see chapter 4). Screening was conducted using Nunc Immuntubes, and bound phage were eluted using 0.1M HCl, pH 2.2 adjusted with glycine containing 1 mg/ml ovalbumin. Three rounds of

Chapter 6 - Results. Mimotope peptides cross- reactive with an anti-steroid hormone antibody.

biopanning were conducted. ELISA and DNA sequencing were used to identify the sequences of peptides displayed on phage which bound above background level on ELISA. The following three peptides were identified:

AAERGLFED

TAWTYVLGP

TSWAYVLGP

antibody.

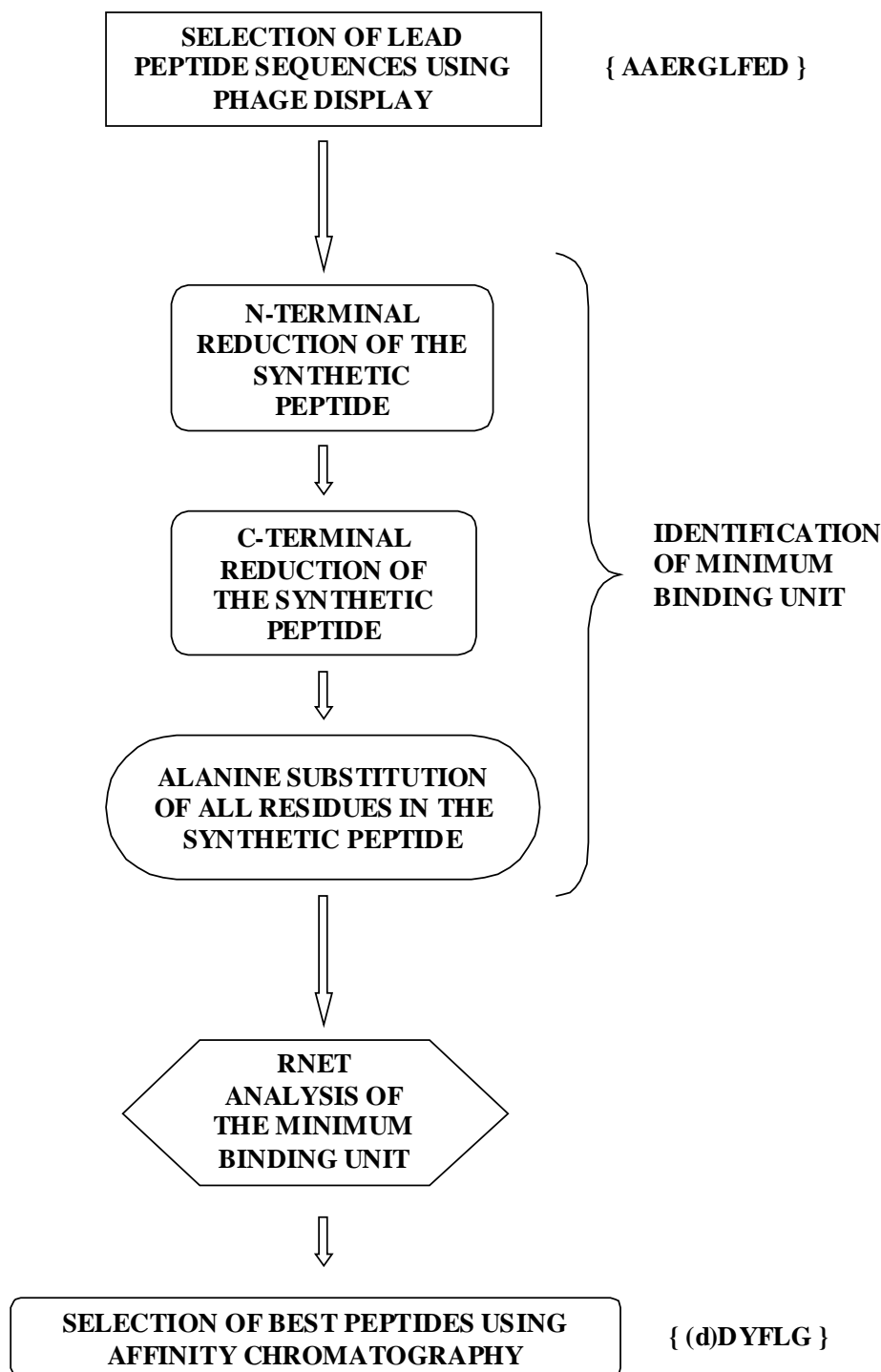


Figure 6.1: Strategy for the selection of peptide mimotopes from a phage display library, and the affinity maturation of these peptide mimotopes for application as a peptide mimotope affinity ligand.

6.2.2 Identification of the minimum binding unit

(Conducted by Dr A. Murray, University of Nottingham, UK)

The three lead sequences were then produced by solid phase peptide synthesis. Sequences TAWTYVLGP and TSWAYVLGP were found to be insoluble in aqueous solvent, and so investigation of these sequences ceased. Immobilisation of the synthetic peptide AAERGLFED onto cyanogen bromide activated Sepharose 4B, when used as an affinity matrix, failed to purify mAb from supernatant spiked with mAb 4155.

Three sets of peptides (based on the AAERGLFED lead sequence) were then synthesized on the heads of polypropylene pins (Geysen, *et al.* 1987). The array of pins were arranged in a plastic holder in the format of a 96-well microtitre plate, enabling ELISA to be conducted on the heads of the pins by inserting the array into a microtitre plate containing the ELISA reagents. The three sets consisted of: -

(i) The phage derived mimotope sequence AAERGLFED truncated from the N terminus, producing the peptides

AAERGLFED
AERGLFED
ERGLFED
RGLFED
GLFED
LFED
FED
ED

(ii) The phage derived mimotope sequence AAERGLFED truncated from the C terminus, producing the peptides

AAERGLFED
AAERGLFE
AAERGLF
AAERGL
AAERG
AAER
AAE
AA

The aim of these two libraries was to identify the core binding regions of the sequence.

(iii) In the third library, each of the residues in the phage derived peptide mimotope sequence AAERGLFED were replaced with alanine (or glycine if alanine already existed at that position)

GAERGLFED
AGERGLFED
AAERGLFED
AAEAGLFED
AAERALFED
AAEAGAFED
AAERALAED
AAERGAFAD
AAERGLFEA

The aim of this library was to assess the contribution of each residue in the sequence to the binding event.

ELISA conducted on these peptide arrays demonstrated that a minimum binding unit from the first two truncated libraries was identified as FED (Badley, *et al.* 2001). Since the alanine substitution library showed a gradual decrease in binding levels when each of the residues from the glycine onwards were replaced, the minimum binding unit was identified as the sequence GLFED (Murray, *et al.* 2001). Replacement of the phenylalanine residue was found to lead in a 75% reduction in antibody binding.

6.2.3 Affinity maturation of the minimum binding unit

A Replacement Net (RNET) analysis (as described in section 3.2.2) of the tetra peptide LFED was conducted, producing a set of 80 peptides with sequences GXFED, GLXED, GLFXD and GLFEX where X is each of the 20 naturally occurring amino acids, and two unrelated control peptides RPAPG and MPAPG. The results are presented in figure 6.2. Note that in this experiment the range of binding ability of peptides across each of the arrays is not particularly well defined, with little difference between the majority of the peptides in a particular array. i.e. These results demonstrate a low signal to noise ratio across the array. All of the peptide arrays

antibody.

demonstrated levels of antibody binding above the level observed for the two unrelated control peptides, apart from the GLXED array – where phenylalanine was replaced. In the GLXED array, the majority of peptides demonstrate binding levels equal to or below that of the control peptides.

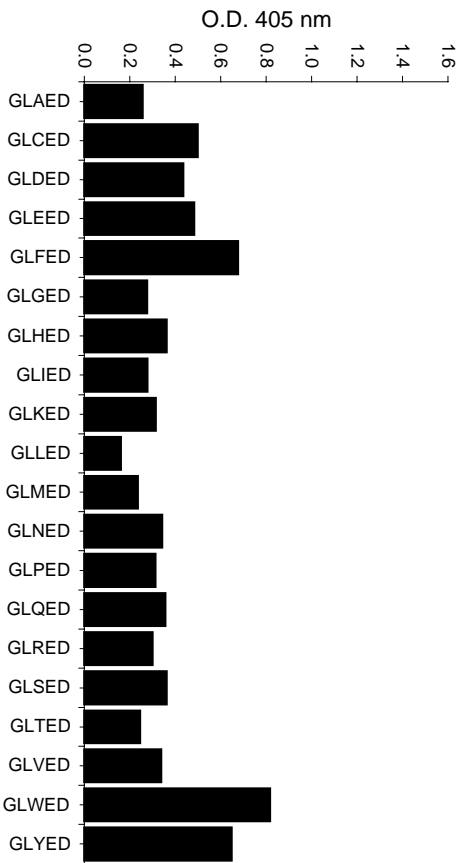
In order to improve the signal to noise ratio, a variation on the RNET assay was conducted. In this variation each of the duplicate peptides (synthesized in duplicate in the pin array) were incubated with a different mixture. The first pin was incubated with a pre-equilibrated mixture consisting of mAb 4155 and 10,000 x concentration of E-3-G, and the second pin was incubated with an equivalent amount of mAb 4155 only. (Several experiments were conducted to determine this concentration of E3G at which the optimum signal to noise ratio was achieved). -

Pin 1	75 μ l mAb 4155 @ 10 μ g/ml + 75 μ l E-3-G @ 3.33 μ M
Pin 2	150 μ l mAb 4155 @ 5 μ g/ml

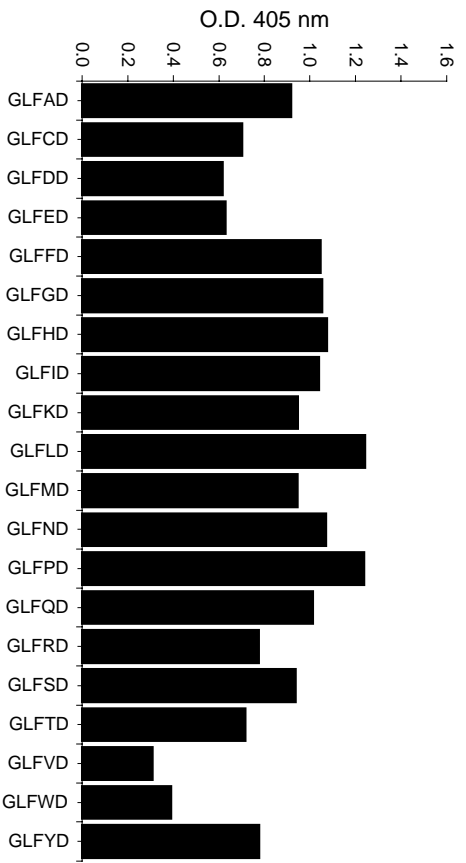
antibody.



A



B



C

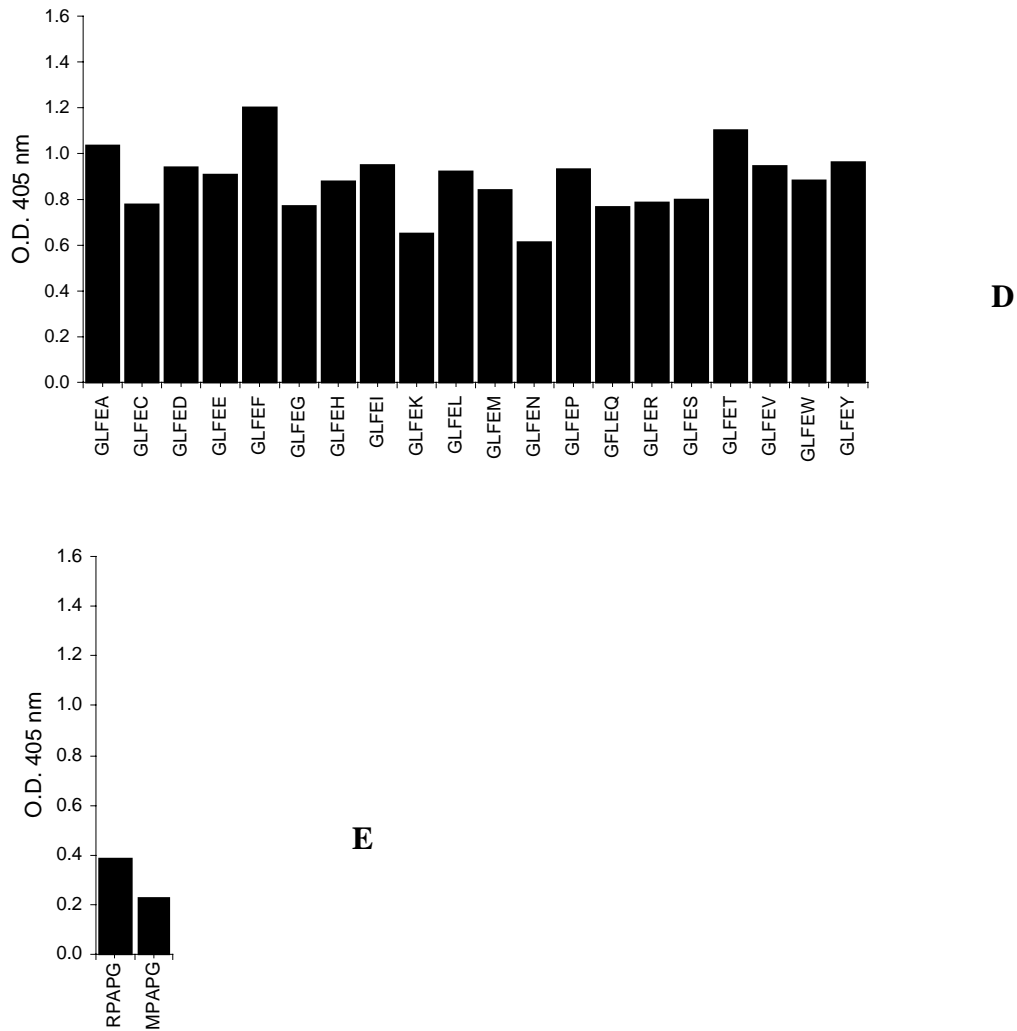
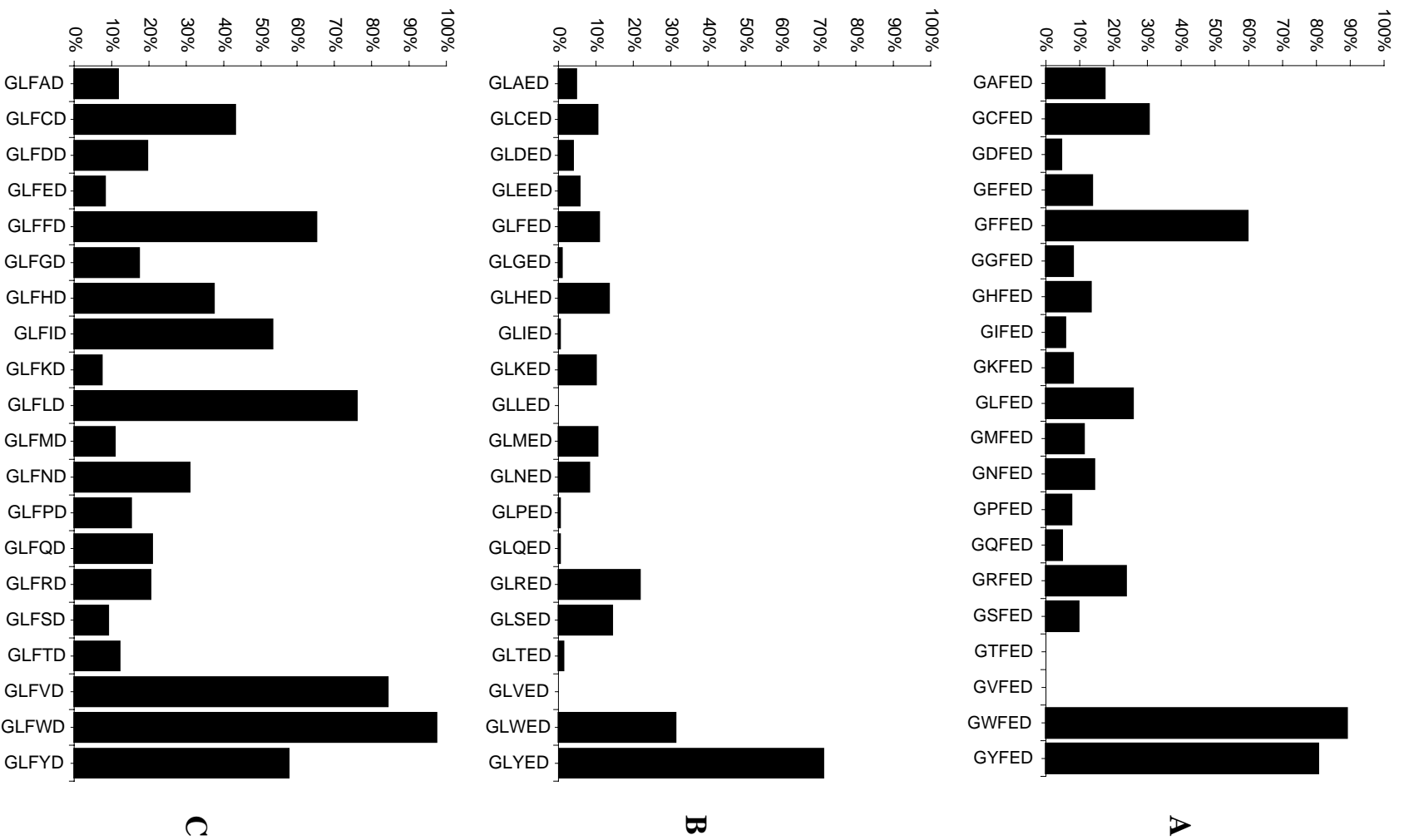


Figure 6.2: Results of an experiment demonstrating differential binding of mAb 4155 to an RNET array of peptides derived based on the **GLFED** minimum binding unit. (A) **GXFED** RNET; (B) **GLXED** RNET; (C) **GLFXD** RNET; (D) **GLFEX** RNET; (E) unrelated control peptides. X represents the 20 naturally occurring (L) amino acids. Peptides tethered to pins via their C-terminus.

antibody.



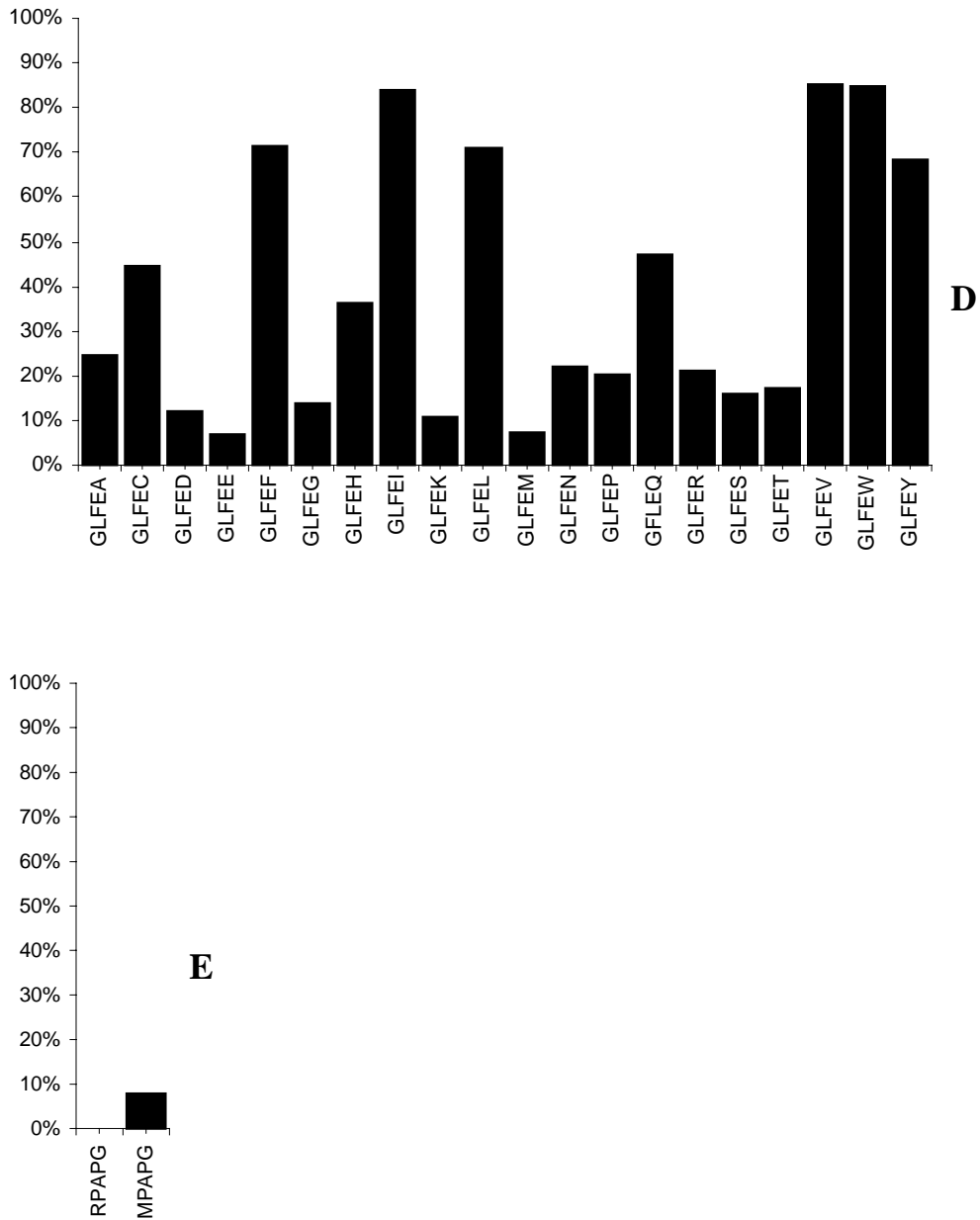


Figure 6.3: Results of an experiment demonstrating differential blocking of binding of mAb 4155 to an array of RNET peptides based on the phage derived **GLFED** minimum binding unit, using E3G. Percentages correspond to the fraction of antibodies binding to the peptide in the presence of E3G divided by the antibodies

Chapter 6 - Results. *Mimotope peptides cross-reactive with an anti-steroid hormone antibody.*

binding to the peptide in the absence of E3G. (A) **GXFED** RNET; (B) **GLXED** RNET; (C) **GLFXD** RNET; (D) **GLFEX** RNET and (E) unrelated control peptides. X represents the 20 naturally occurring (L) amino acids.

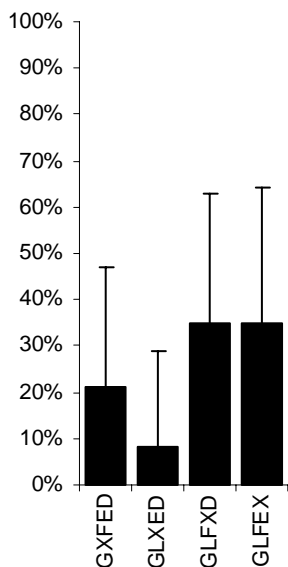


Figure 6.4: Average values for blocking of binding across the RNET for each of the **GXXXX** substituted peptides of the phage derived **GLFED** minimum binding unit. Error bars indicate the standard deviation of values across each substitution sequence. Note that the average level of binding is lowest in the array in which the phenylalanine residue was replaced.

Chapter 6 - Results. Mimotope peptides cross-reactive with an anti-steroid hormone antibody.

Using this approach the signal to noise was much improved compared to measuring the binding of antibodies to the array (see figures 6.2 and 6.3). A background measurement of secondary antibody binding to the pins was conducted prior to the experiment and subtracted from the values obtained in these experiments to correct for non-specific binding of the secondary antibody to the pins.

Results were expressed as a percentage of the OD₄₀₅ nm of pin 1 divided by OD₄₀₅ nm of pin 2. Low percentage values indicate a large difference of OD₄₀₅ nm between pin 1 and pin 2 exists (i.e. OD₄₀₅ nm (pin 1) \ll OD₄₀₅ nm (pin 2)). This would suggest that the peptide mimotope immobilised on the pin is a poor mimic of E-3-G, and so the peptide on the pin is unable to compete mAb 4155 from the mAb 4155-E-3-G complex. High values indicate only a small difference of OD₄₀₅ nm between pin 1 and pin 2 exists (i.e. OD₄₀₅ nm (pin 1) \simeq OD₄₀₅ nm (pin 2)). This would suggest that the peptide mimotope immobilised on the pin is a good mimic of E-3-G, and so the peptide on the pin is able to compete mAb 4155 from the mAb 4155-E-3-G complex.

Comparing the results of the RNET assay in fig 6.2 with the results of this RNET assay incorporating a displacement component (fig 6.3) a significant reduction in the background level of binding is observed. The non-specific binding of antibody to the pins is in effect cancelled out, and only the ability of each mimotope to compete mAb 4155 from the E-3-G – mAb 4155 complex is reported. The use of the E-3-G-mAb 4155 complex significantly reduces the level of background binding observed.

A control experiment was conducted using another array of peptides based on the sequence **RXXX** using mAb C595 (recognises **RXXP** epitope). The experiment was conducted in the same format as with the **GLFED** based RNET, to establish if E-3-G reduces the binding of an irrelevant antibody to other peptide ligands. Little variation across the array was observed, with the majority of peptides totally unperturbed by the presence of E-3-G. This provides evidence that the blocking of binding of mAb 4155 to the **GLFED** based RNET is a specific reaction for the paratope of the mAb 4155, and is not the result of non-specific interactions between the antibody and E-3-G.

The results of the analysis suggested that in the **GLFED** lead sequence phenylalanine was a critical contact or anchor residue; leucine could only be replaced by other large hydrophobic residues (indicative of the side chain of this amino acid contributing to the binding event); and the glutamate and aspartate residues tolerated a larger number of substitutions, suggesting less of a contribution to the binding event from these residues. See figures 6.3 and 6.4.

All of the previous observations lead to the focussing on the residues at positions 4 and 5 for affinity maturation. Substitution of amino acid residues at positions 4 and 5 of the lead sequence **GLFED** with aromatic or hydrophobic residues increased binding of the antibody to the peptide. Cysteine, tryptophan, and tyrosine were observed to give the highest levels of binding. Cysteine substituted mimotopes **GLFEC** and **GLFCD** were discounted for further study because of the potential for dimerisation. This left peptides **GLFWD**, **GLFEW**, **GLFEY** and **GLFYD**, which were synthesised and tested as affinity ligands. Significant peaks of eluted material were observed for the peptides **GLFWD** and **GLFEW**, but were found to be contaminated with non-antibody species (Dr A. Murray, University of Nottingham, personal communication). Elution from the affinity matrices containing peptides **GLFYD** and **GLFEY** respectively yielded small peaks corresponding to ~5% recovery of antibody from the spiked feedstock.

This was not in agreement with the binding studies conducted on the surface of the pins and the results of the ELISA where the mimotopes were able to compete with estrone in binding the antibody. Peptides were tethered to the pins via their C-termini, whereas peptides were bound to the CNBr activated Sepharose via their N-termini. Both N- and C- termini of the peptides were free in the ELISA competition assay. Thus presentation of the peptide mimotope to the antibody is an important factor in governing the peptide mimotopes success as an affinity matrix.

6.2.4 Establishing the correct presentation in the desired application

Synthesis of the peptide **GLFYD** in reverse using (D) amino acids (**DYFLG**) instead of the naturally occurring (L) amino acids, upon immobilisation to CNBr activated Sepharose 4B, enabled the side chains of the amino acids to be presented to the

Chapter 6 - Results. Mimotope peptides cross- reactive with an anti-steroid hormone antibody.

antibody in the same orientation as the (L) amino acid residues in the mimotope tethered to the pins via the C- terminus. A similar example is given by (Guichard, *et al.* 1994) “Antigenic mimicry of natural L-peptides with retro-inverso-peptidomimetics”. Recovery of 98% of the spiked mAb 4155 from tissue culture supernatant was achieved using the retro-inverso mimotope peptide (Murray, *et al.* 2001) – see figure 6.5.

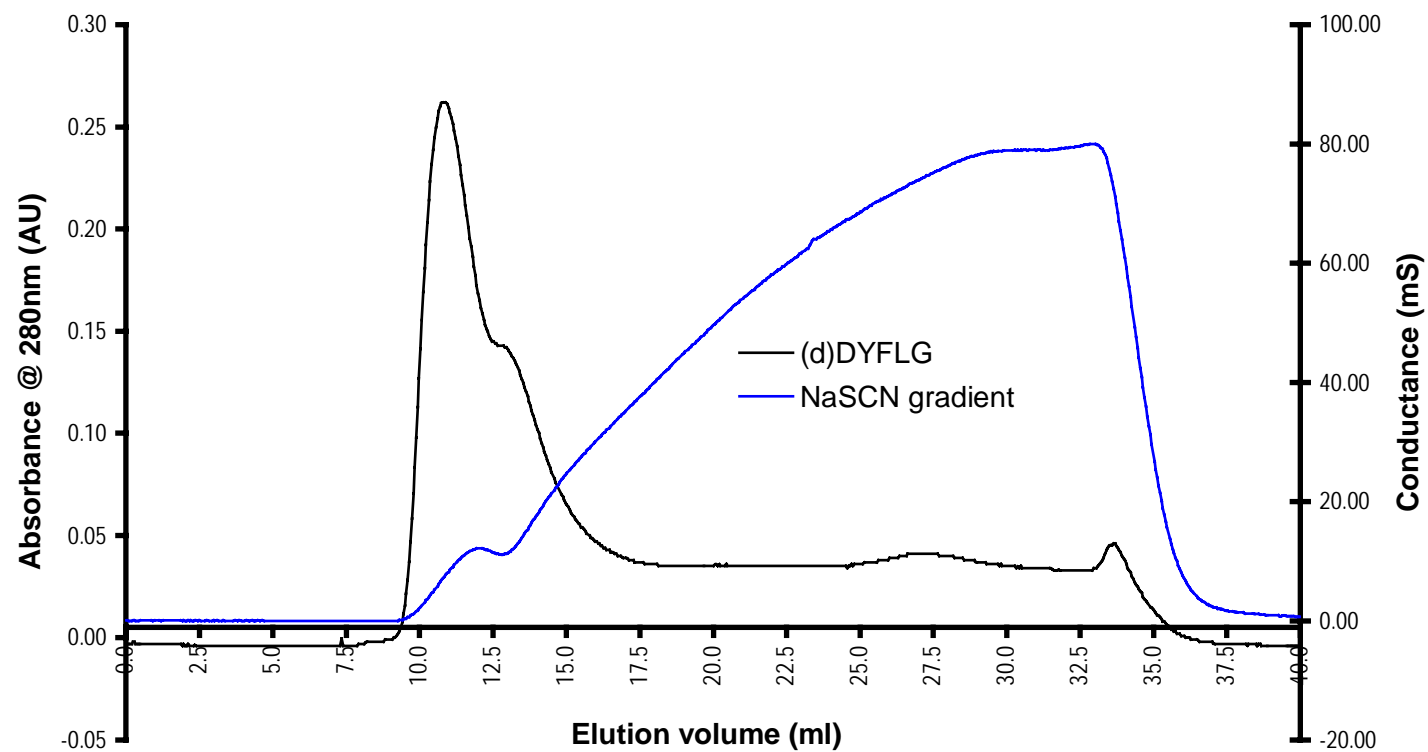


Figure 6.5: Gradient elution of the anti- E-3-G antibody (4155) from a peptide-Sepharose affinity matrices following column loading with 100 ml mAb 4155. The affinity matured mimotope (d) **DYFLG** was linked to the CNBr activated affinity matrix via the amino-terminus. Antibody at 15 μ g/ml in PBS.

6.3 Rationalisation of the process involved in the optimisation of peptide mimotope ligands from lead sequences obtained from a phage display library

The optimisation of peptide mimotope ligands from mimotope sequences derived from a phage display library has proved to be a successful strategy for the isolation of paratope-specific binding ligands capable of functioning as affinity ligands for the purification of monoclonal antibodies from feedstocks (Meloan *et al.*, 2000) (Murray, *et al.* 2001). A number of experiments were conducted to investigate the differences observed between the binding properties of the phage-derived peptide and the optimised peptide isolated using the process described in section 6.2.

6.3.1 An ELISA to estimate relative values of the equilibrium association constant (K_A)

As described in chapter 1, the current purification process for mAb 4155 involves the competitive elution of the antibody bound to an affinity matrix using estrone as the immobilised affinity ligand. This is a high affinity interaction, since 4155 mAb is not easily eluted from the matrix, and can only be removed using the higher affinity estradiol 3-(beta-D-glucuronide). An ELISA was conducted to establish the time taken for the reaction of mAb 4155 with a number of different ligands to reach equilibrium, and thus enable a qualitative assessment of the relative values of K_A for the interaction of each ligand with the antibody. BSA- conjugates of estrone, the phage derived lead peptide **AAERGLFED** and the optimised peptide (d)**DYFLG** were immobilised onto the wells of an ELISA plate. The mAb4155 was added to the wells of the plates for a range of incubation periods. Standard ELISA procedure were then conducted as described in chapter 3 to determine the level of antibody binding for each incubation period.

First an ELISA was conducted to examine the reaction between mAb 4155 and estrone. Estrone was conjugated to BSA as described in Chapter 3, and the resulting conjugate dried down onto the wells of an ELISA plate. mAb 4155 was incubated at

10µg/ml for varying incubation periods, in triplicate in the wells of the ELISA plate. The results are presented in figure 6.6.

The results presented in figure 6.6 demonstrate that the reaction between mAb 4155 and the BSA-estrone conjugate reaches equilibrium in a time period of approximately 10 minutes. i.e. the amount of antibody accumulating on the conjugate reaches a steady state, such that the amount of antibody binding equals the amount of antibody un-binding. Thus the curve reaches a plateau.

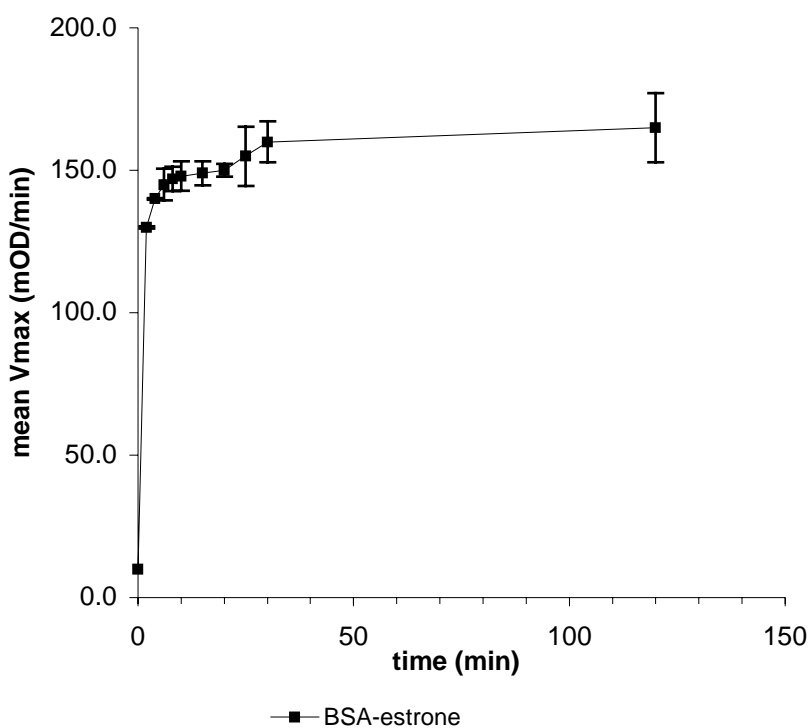


Figure 6.6: Results of an experiment to measure the empirical reaction rate of mAb 4155 to BSA- estrone conjugate. mAb 4155 @ 10 µg/ml; conjugate dried onto ELISA plate @ 10 µg/ml of BSA.

An identical experiment was conducted with the same concentrations of reagents, using the phage derived peptide **AAERGLFED**, and the optimised mimotope (d)**DYFLG** conjugated to BSA. The results are presented in figure 6.7. It can be seen that amount of antibody binding is greater than in figure 6.6. This probably

results from the two different chemistries used to create the estrone and the peptide conjugates. From this experiment it is clear that the rate at which the reactions reach equilibrium is slower than for the estrone conjugate. The reactions involving the peptide conjugates do not plateau, as was the case in figure 6.6 with the reaction of mAb 4155 and the estrone conjugate.

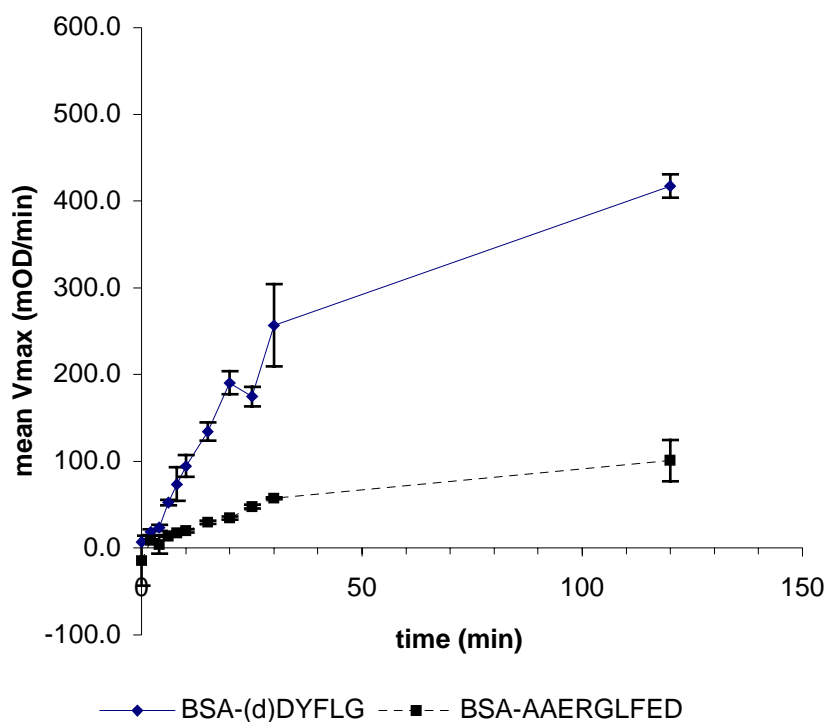


Figure 6.7: Results of an experiment to measure the empirical reaction rate of mAb 4155 to BSA- phage derived peptide mimotope conjugate, and BSA-affinity matured mimotope peptide adsorbed onto a single ELISA plate. mAb 4155 @ 10 µg/ml; conjugates dried onto ELISA plate @ 10 µg/ml of peptide.

From these experiments a simple deduction can be made about the relative values of the equilibrium association rate constant for each of the reactions. The equilibrium association rate constant (K_A) for the reaction $A + B = AB$ is defined as: -

$$K_A = \frac{[AB]}{[A][B]}$$

$$= k_a / k_d$$

antibody.

K_A thus has units of M^{-1} .

From the results presented in figure 6.7, assuming equivalent levels of peptide conjugation, and equivalent levels of conjugate immobilisation on the ELISA plates, it can be asserted that the equilibrium association constant (K_A) for the reaction between the optimised peptide (d)**DYFLG** is greater than the equilibrium association constant (K_A) for the reaction between the phage-derived lead sequence **AAERGLFED**.

When considering the two types of structure: the flexible peptide, and the rigid steroid structure, it is logical to assume that the on-rate (k_{on}) will be the dominant factor influencing the values observed for K_A . The peptides are able to adopt a much more flexible structure than the more rigid steroid molecule, and so the on-rate for the peptides is likely to be slower than the steroid molecule since the peptide is able to exist in many conformations.

Using this assumption that the on-rate is the dominant factor in these antibody – ligand interactions, then the results presented in figure 6.6 suggest that the equilibrium association constant (K_A) for the interaction of mAb 4155 with the BSA-estrone conjugate is larger than the values of K_A observed for the BSA-peptide conjugates, since the signal reaches a plateau in a short time period (compared with the time taken for the signal to reach a plateau in the experiments involving the peptide conjugates). The concentration of antibody is in excess of the concentration of binding sites in all of the experiments, and so can be assumed to be constant, for all of the experiments.

Thus the value of K_A decreases in the following order: -

Estrone > optimised mimotope (d)DYFLG > phage derived mimotope AAERGLFED

The equilibrium association constant for the interaction between mAb 4155 and the target antigen E-3-G has been determined to be $1 \times 10^{10} M^{-1}$ (Dr A. Badley, Unilever Research – personal communication). The cross-reactivity of the related steroids

estrone was also measured, and determined to be 0.1 % with respect to E-3-G. An approximate estimate of the affinity of mAb 4155 to estrone can be made (0.1 % of $1 \times 10^{10} = 1 \times 10^7 \text{ M}^{-1}$).

6.3.2 Inhibition ELISA's

The properties of the phage-derived peptide mimotope **AAERGLFED** and the optimised peptide mimotope **GLFYD** free in solution were investigated in an inhibition ELISA. The BSA-estrone conjugate used in section 6.3.1 was dried down onto the surface of a microtitre plate and an inhibition assay conducted as described in Chapter 3. The ability of the peptides to inhibit the binding of mAb 4155 to the BSA-estrone conjugate was tested. An unrelated peptide (**KSKAGVC**) was used as a negative control. The results are presented in figure 6.8. From the results it can be seen that the control peptide did not inhibit binding of mAb 4155 to the BSA-estrone at any of the concentrations used. Two completely different inhibition profiles resulted from the inhibition of antibody binding using the phage-derived peptide mimotope and the optimised mimotope. The phage-derived peptide only inhibited binding over a relatively small concentration range (3.0 mM to 1.0 mM) compared to the optimised mimotope peptide, which inhibited antibody binding over a much larger concentration range (3.0 mM to 0.03 nM).

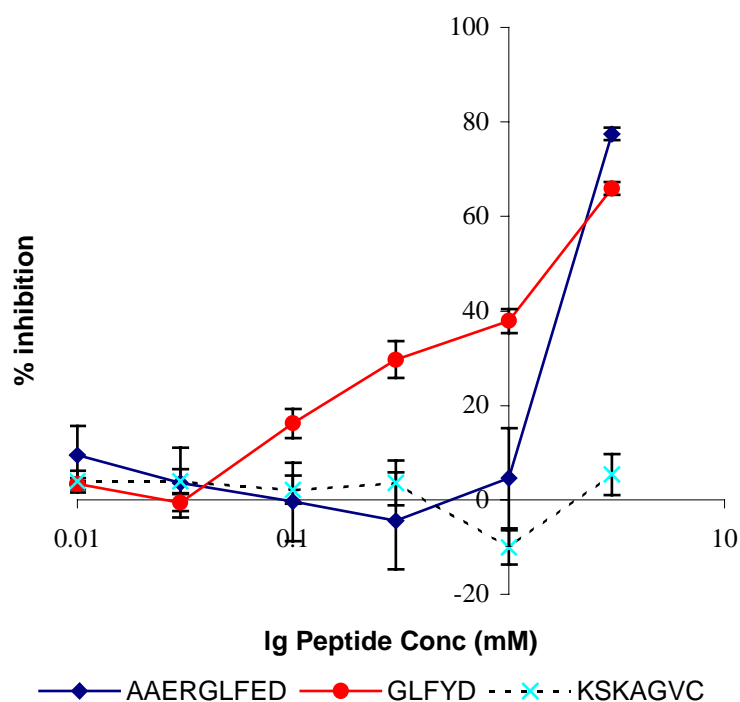
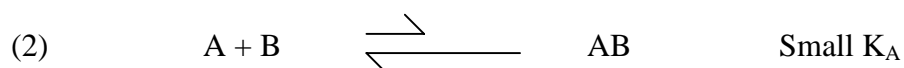
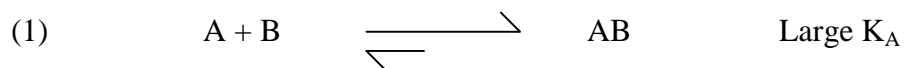


Figure 6.8: Results of an experiment to demonstrate inhibition of binding of mAb 4155 to a BSA-estrone conjugate using the phage-derived peptide **AAERGLFED** and the affinity-matured mimotope peptide **GLFYD** in solution. An irrelevant peptide **KSKAGVC** was employed as a negative control.

This is in agreement with the difference observed in the equilibrium association constants observed in section 6.3.1. This can be explained as follows: consider case (1) and (2) below: -



B represents the antibody and A represents the peptide. The concentration of B can be considered constant in both cases, with only the concentration of peptide varying in

each case. Equation (1) applies to the interaction of the optimised peptide **GLFYD** with mAb 4155. The reaction is less dependent upon the concentration of the peptide (A) than (2) where the reaction is more dependent upon the concentration of peptide **AAERGLFED**. This difference of concentration dependence (i.e. the difference in the K_A values) is reflected in the inhibition assay. Peptide (d)**DYFLG** showed a similar profile to peptide **GLFYD**. The fact that these mimotope peptides are able to inhibit the binding of the antibody to estrone, is strong evidence that these peptides are binding specifically to the paratope of the antibodies.

6.3.2.1 The use of a peptide mimotope in an inhibition ELISA to measure E-3-G.

As well as being useful as paratope-specific binding ligands for the purification of monoclonal antibodies, peptide mimotopes can be used as diagnostic reagents. An example of the use of synthetic peptides in an assay is the use of a synthetic peptide in a preclinical test for prion diseases (Scrapie) (Schreuder *et al*, 1996). Synthetic peptides are employed in such assays since they offer a number of advantages compared to the native protein with respect to production, storage and safety. A review of the use of synthetic peptides for diagnostic use is given by (Meloan, *et al*, 1997). There is very little published data on the use of peptide mimotopes reactive with antibodies raised against non-proteinaceous analytes such as E-3-G as is described here.

Using the optimised mimotope reactive with mAb 4155, a competitive ELISA assay was developed to measure the concentration of E-3-G in solution. The results of this assay for a range of concentrations of E-3-G are shown in figure 6.9, alongside an equivalent assay using the target antigen. Inhibition of binding of mAb 4155 to a BSA conjugate of the affinity-matured, phage derived peptide (d) **DYLFG** using E-3-G in solution was compared to the inhibition of binding of mAb 4155 to an E-3-G ovalbumin conjugate. The results have been normalised over the mean V_{max} to directly compare the two inhibition curves.

antibody.

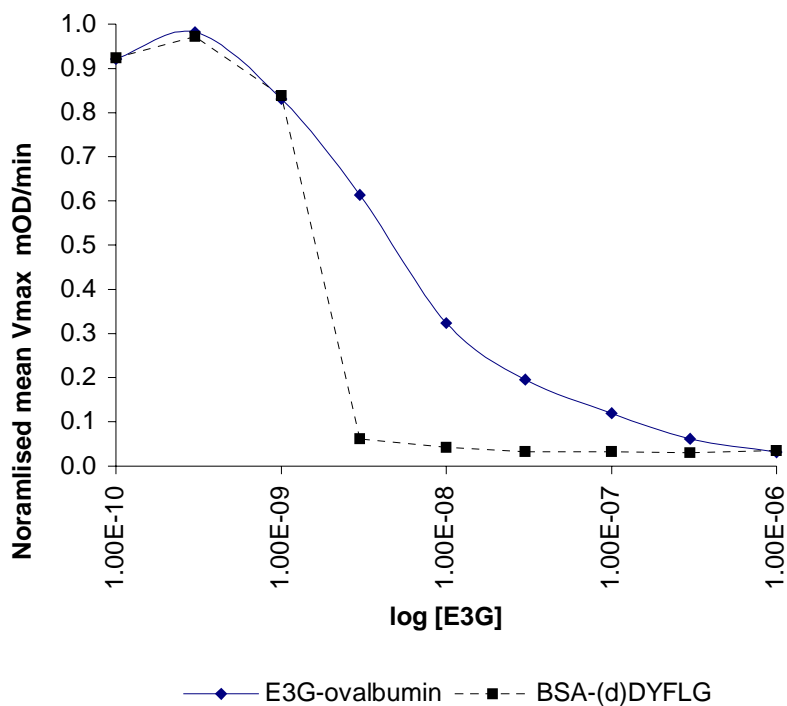


Figure 6.9: A comparison of results from competition ELISA's to measure free concentration of E-3-G in solution, using an ovalbumin-E3G conjugate, and a BSA-affinity matured peptide mimotope conjugate. Note Vmax values were normalised to aid comparison.

The results presented in figure 6.9 demonstrates that the optimised mimotope peptide (d) **DYFLG** can be used to create an assay for the determination of the concentration of E-3-G in solution. From these results, it is clear that the range of concentrations of E-3-G that could be quantified using the optimised peptide conjugate is much smaller (1×10^{-9} M to 3×10^{-9} M) - compared to the range quantifiable when using the E3G-ovalbumin conjugate (3×10^{-10} M to 3×10^{-7} M). However the switch from maximum inhibition to minimum inhibition as the concentration of E-3-G is increased, occurs over a much smaller range for the optimised mimotope peptide, compared to the gradual decrease in inhibition observed using the E-3-G-ovalbumin conjugate. This could be advantageous in a situation requiring the rapid detection of a particular analyte (e.g. a toxin), where a fast, definite “yes/no” answer is required. Detection of such a change would be much easier to detect and would be more sensitive than if the

E-3-G-ovalbumin conjugate had been used. The improved response exhibited by the optimised mimotope peptide would be useful in systems reliant on an electrical transducer to detect the signal, such as the biosensor utilising mimotope peptides outlined in Chapter 1, figure 1.1. This switch from maximum inhibition to minimum inhibition would circumvent problems of extracting a change in signal over the background noise which would be present when monitoring only small changes of inhibition using curves with a profile similar to that observed when using the E-3-G-ovalbumin conjugate. This work was used as an example in patent application (Badley *et al*, 2002).

The assay was repeated using a BSA conjugate of the phage-derived lead sequence **AAERGLFED** in place of the E-3-G ovalbumin conjugate. The results of this experiment are presented in figure 6.10. These results show that the range of the assay for the determination of E-3-G using the phage-derived lead sequence is at lower concentrations than when the optimised mimotope peptide is used.

All of these properties can be attributed by the differences in the equilibrium association constant (K_A) observed in section 6.3.1. The equilibrium association constant (K_A) is the reciprocal of the equilibrium dissociation constant (K_D). Thus from the experiments conducted in section 6.3.1, it would be expected that the equilibrium dissociation constants for the species used in the competition assays would decrease in the following order: -

BSA-AAERGLFED > BSA-(d)**DYFLG** > Ovalbumin-E-3-G

In the competition assay, mAb 4155 was pre-incubated on the ELISA plates on which the conjugates were immobilised, before washing and then adding the solutions containing the various concentrations of E-3-G. The E-3-G in solution most easily competed antibody from the BSA-**AAERGLFED** conjugate. The interaction between the antibody and the conjugate exhibits the highest K_D out of the three conjugates, and so the antibody-antigen complex can be expected to be the most dissociated and thus antibody is most easily competed from this conjugate. The same reasoning can be applied to explain why the range concentrations of E-3-G detectable using the BSA-

(d)**DYFLG** conjugate in the assay was higher. The reason for the much larger range of concentrations determinable in the assay using the ovalbumin-E-3-G conjugate results from the similarity of the K_D values for the interaction of mAb 4155 with E-3-G free in solution and E-3-G conjugated to ovalbumin. The difference in the K_D for these two interactions would not be expected to be significantly different (the interaction of mAb 4155 with immobilised E-3-G might be expected to exhibit a slightly higher on-rate and thus lower K_D than the interaction between antibody E-3-G in free solution).

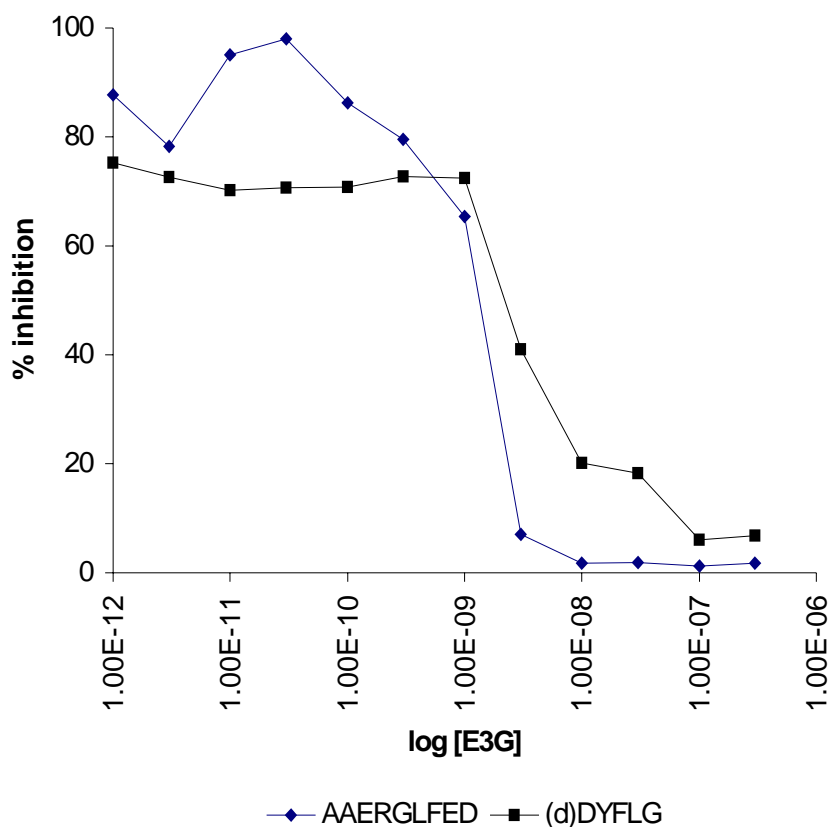


Figure 6.10: A comparison of the results from a competition ELISA to measure the free concentration of E-3-G in solution, using the phage-derived mimotope peptide **AAERGLFED** and the optimised peptide (d) **DYFLG**.

By utilising the differences in the equilibrium constants in such competition assays it would be possible to tailor an assay for a particular situation.

antibody.

e.g. (1) High sensitivity, but small dynamic range

or (2) Low sensitivity, but large dynamic range.

(1) and (2) can be considered to be the two extremes. Case (1) would be poor for the quantitative measurement of a particular analyte, but good for rapid qualitative measurements. Conversely, case (2) would be good for quantitative measurements, but poor for rapid qualitative measurements. It may be possible to use a combination of such mimotopes in a single assay to broaden the range of an assay utilising peptide mimotopes.

6.3.3 Determination of rate constants in the interaction of the affinity-matured, phage derived peptide (d) DYFLG and mAb 4155

It was observed in section 6.3.1 using an empirical ELISA approach, that the time taken for the reaction between the refined mimotope peptide sequence (d)DYFLG and mAb 4155 to approach equilibrium was much longer than the time taken for the interaction between mAb 4155 and estrone to reach a state of equilibrium. Several different methods were explored to quantify the kinetic parameters in the reaction between mAb 4155 and the peptide mimotope (d)DYFLG and these are described below.

6.3.3.1 Fluorescence quenching

Fluorescence quenching was attempted using the mimotope peptides, but a quenching of fluorescence could not be observed. This is probably a result of the aromatic amino acid residues present in the mimotope peptides, masking any quenching effect.

6.3.3.2 Surface Plasmon Resonance (SPR)

Initial experiments focussed on the direct immobilisation of the optimised mimotope peptide onto a BIAcore sensor chip, however the binding of antibody to these chips was unable to be detected. A BSA conjugate of the optimised mimotope peptide was immobilised on the BIAcore sensor chip, and antibody binding to the conjugates was detected. As described in chapter 5, the accurate measurement of the kinetics of antibody-antigen interactions requires data not limited by the method of ligand

immobilisation. Although BSA-conjugates are not ideal for the determination of the kinetics of antibody-ligand interactions (since it is difficult to control the ligand density in the BSA-conjugates), they can be used to gain information about the kinetics of the interaction. As in chapter 5, the response observed on antibody binding of the conjugate was limited to less than 100 RU at saturation to reduce crowding, avidity and aggregation effects.

SPR was conducted using the BSA-mimotope peptide conjugate, and mAb 4155. Two different configurations were employed to test the validity of the results obtained. The kinetics of the interaction of antibody with immobilised BSA-peptide conjugate were measured. The configuration was then reversed with antibody immobilised onto the sensor chip and the kinetics of the interaction of the BSA-peptide conjugate in solution binding to the antibody were measured. The results of these experiments are presented in figure 6.11 and 6.12. A simple Langmuir model of binding was used to fit curves to the experimental data using global analysis. The rate constants derived from these fitted curves are presented in table 6.12.

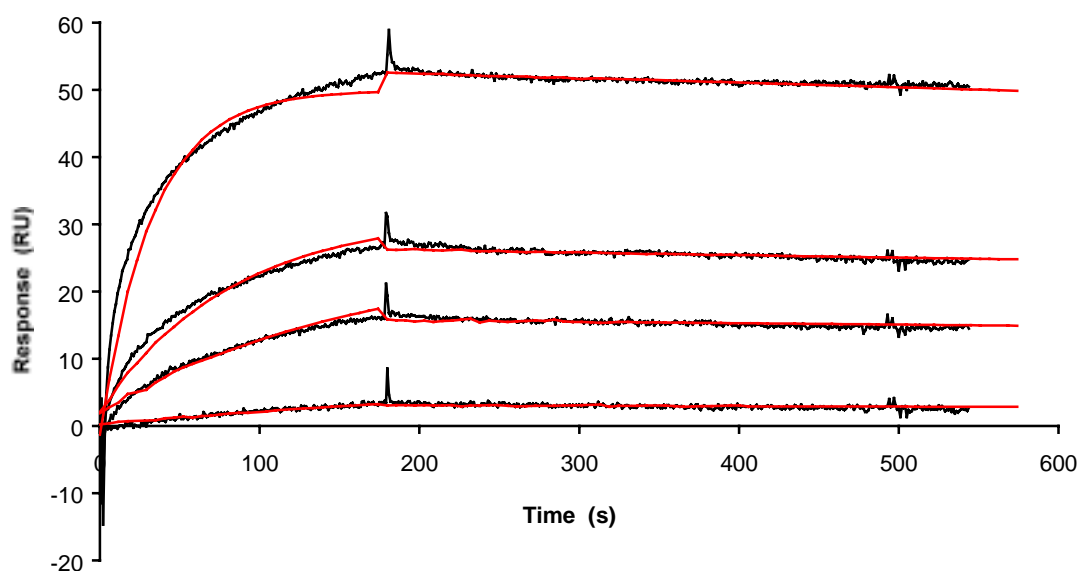


Figure 6.11: SPR analysis of the interaction between immobilised peptide conjugate BSA- (D) **DYFLG** and antibody 4155 at 25 °C. Antibody 4155 at 500 nM, 200 nM, 100nM and 50 nM from top down. A background signal consisting of the interaction of antibody with a flowcell derivatised with ethanolamine was subtracted from each

antibody.

of the curves. BSA-peptide conjugate immobilised using NHS/EDC coupling chemistry. HEPES buffer, flow rate of 1.0 ml/min. Red lines are model data, black lines are experimental data.

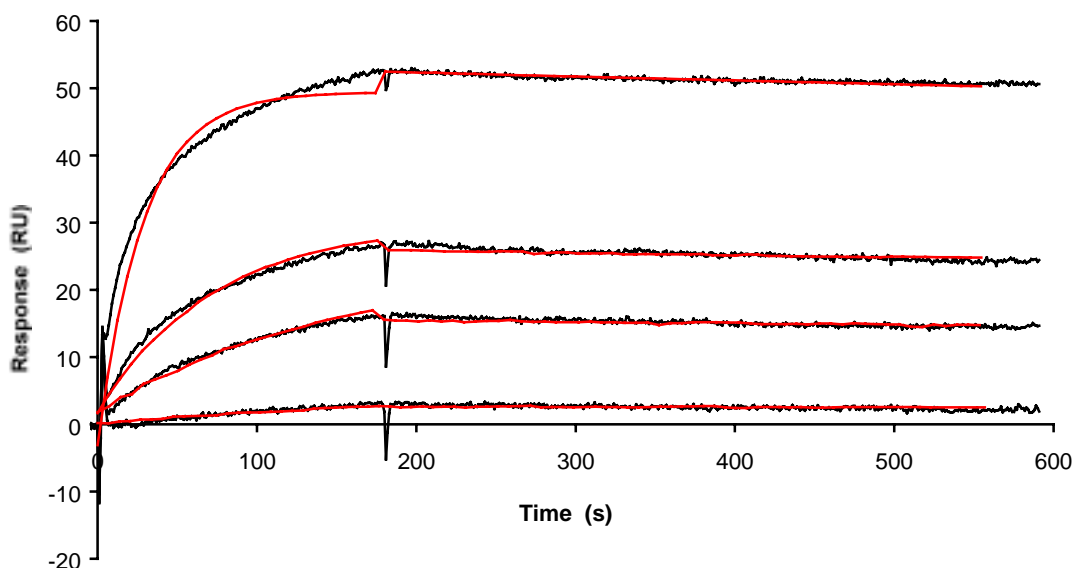


Figure 6.12: SPR analysis of the interaction between immobilised antibody 4155 and peptide conjugate BSA-(D)DYFLG at 4 °C. BSA-(D)DYFLG peptide conjugate at 500 nM, 200 nM, 100 nM and 50 nM peptide (assuming [peptide in conjugate] = 2.5 mg peptide per ml of undiluted conjugate solution). A background signal consisting of the interaction of antibody with a flowcell derivatised with ethanolamine was subtracted from each of the curves. HEPES buffer, flow rate of 1.0 ml/min. Red lines are model data, black lines are experimental data.

Species Immobilised	k_a (1/Ms)	k_d (1/s)	K_A (1/M)	χ^2
BSA – (D) DYFLG	6.06×10^4	1.40×10^{-4}	4.34×10^8	0.235
Antibody 4155	6.95×10^4	1.12×10^{-4}	6.19×10^8	0.329

Table 6.1: Comparing kinetic constants derived from the SPR analysis of the interaction between peptide conjugate BSA- (D)DYFLG and antibody 4155. The interaction of antibody in solution (ligate) with peptide conjugate immobilised

(ligand) is compared to the interaction of peptide conjugate in solution (ligate) and antibody immobilised (ligand).

The results presented in table 6.1 demonstrate a close agreement between the kinetic constants obtained from both orientations studied (immobilised BSA-peptide conjugate and immobilised antibody). The χ^2 values for the global fitting of the Langmuir association model indicate that a good fit has been achieved. However, from the data presented in figures 6.11 and 6.12 it can be seen that at higher levels of antibody concentration (for the interaction with immobilised BSA-peptide conjugate), and higher levels of BSA-peptide conjugate (for the interaction with immobilised antibody), differences start to occur between the model data and experimental data. This deviation at higher concentrations of solution-phase reagent is probably the result of mass-transport limiting effects as outlined in chapter 5. The dissociation phase of the modal data appears to be in good agreement with the experimental data, indicating that rebinding of antibody (immobilised BSA-peptide conjugate) or rebinding of BSA-peptide conjugate (immobilised antibody) is not a significant factor.

6.3.3.3 Analysis of the effect of temperature on the reaction rate using SPR

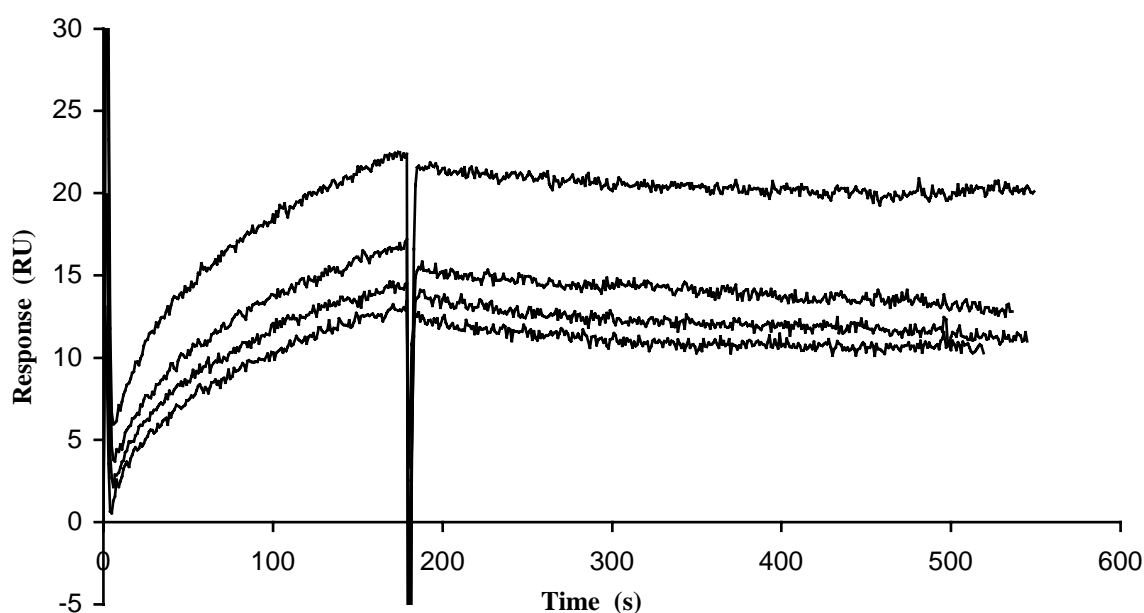


Figure 6.13: Analysis of the temperature dependence of the interaction between

antibody.

immobilised 4155 antibody and BSA-(D)DYFLG peptide conjugate in solution. Temperatures from top down are 30° C, 20° C, 15° C and 10° C. Example of sensorgrams used to investigate the variation in association rate constant and dissociation rate constant to peptide conjugate solution at the various temperatures. Here 500 mM peptide conjugate solution is being used. The dispersion spikes around the 180-s timepoint indicate the start of the dissociation phase.

Temp	k_a	k_d	K_A	χ^2
10° C	2.40×10^4	5.50×10^{-4}	4.36×10^7	0.0836
15° C	3.07×10^4	5.07×10^{-4}	6.06×10^7	0.0812
20° C	3.27×10^4	4.29×10^{-4}	7.61×10^7	0.0750
30° C	4.23×10^4	2.08×10^{-4}	2.07×10^8	0.1710

Table 6.2: Rate constants determined from SPR experiment, looking at the effect of temperature on the interaction between BSA-(D)DYFLG in solution and antibody 4155 immobilised on the surface of CMD BIACORE sensor chip.

From the results presented in table 6.2, it can be seen that in the temperature range investigated, increasing the temperature leads to a gradual increase in the association rate constant (k_a), and a gradual decrease in the dissociation rate constant (k_d); resulting in an overall increase in the equilibrium association rate constant with increase in temperature. The increase in the association rate constant with increase in temperature could be explained by the peptide adopting a high-energy preferential binding structure with greater frequency with increased temperature. The decrease in the dissociation rate constant with increase in temperature may suggest that the antibody can bind to a number of conformations of the peptide, but the higher energy conformation has a reduced off-rate, and as the temperature is increased the population of peptides adopting this more favourable structure increases. It was found that the hydrophobic phenylalanine and leucine residues are critical in the mAb 4155 – peptide interaction, another reason for the changes observed in the rate constants could be the result of water molecules being eliminated more effectively from hydrophilic regions around the binding pocket.

6.4 Summary and Discussion

In the example given by Meloen, *et al.* (2000), the affinity of a weak-binding phage-displayed mimotope peptide for a monoclonal antibody (anti-glucoseoxidase) was enhanced through a process of optimisation using small synthetic peptide libraries to produce a higher affinity ligand capable of functioning as an affinity ligand for use in the paratope-specific purification of monoclonal antibodies. In this chapter it has been demonstrated that a similar process applied to a weak-binding mimotope peptide reactive with a monoclonal antibody raised against a non-proteinaceous target molecule, can be used to produce a small peptide exhibiting enhanced affinity, which can be used as a paratope-specific affinity ligand for the purification of monoclonal antibodies.

The results presented in this chapter have demonstrated an improved method for screening small synthetic libraries for paratope specific binding ligands, using a competitive approach to measure the binding abilities of peptides across an RNET array. This approach succeeded in reducing the level of noise in the assay, as a result of non-specific binding interactions.

An empirical analysis of the equilibrium association constants for the interactions of the phage-derived mimotope peptide, the optimised peptide and estrone, demonstrated that the optimisation process had resulted in a peptide displaying an increased equilibrium association constant over the phage-derived mimotope peptide. The results from an inhibition ELISA were in agreement with the results from the previous assay to determine the relative K_A values for the peptides. The results of the inhibition ELISA also demonstrated that the phage-derived mimotope peptide and the optimised peptide bound specifically to the paratope of mAb 4155 – the anti-E-3-G antibody.

It was demonstrated that the optimised peptide mimotope could be used in an assay to determine the concentration of free E-3-G in solution. Furthermore it was demonstrated that such an assay employing the optimised peptide mimotope was more sensitive to changes in E-3-G concentration than an assay employing an E-3-G

ovalbumin conjugate. This increased sensitivity was explained by the different equilibrium constants observed for the interaction of the peptide mimotope and E-3-G.

Fluorescence quenching could not be conducted using mAb 4155, since the peptide mimotopes contained aromatic amino acid residues essential for binding, masking any observable quenching effects.

The interaction of mAb 4155 with a BSA-conjugate of the optimised peptide mimotope ((d) **DYFLG**) was conducted using Surface Plasmon Resonance. An equilibrium association rate constant (K_A) of order of magnitude 10^8 M^{-1} . Was obtained for the interaction. The effect of temperature on the interaction was also investigated. Increasing the temperature in the range 10°C to 30°C was found to lead to an increase in the on-rate (k_{on}), and a decrease in the off-rate (k_{off}), resulting in an increase in the equilibrium association rate constant (K_A) with increase in temperature. This could be the result of the peptide adopting a more favourable high-energy conformation at the higher temperatures, or the more effective elimination of water from hydrophilic regions around the binding pocket.

The ability to produce a peptide ligand that is capable of purifying monoclonal antibodies raised against a non-proteinaceous analyte is a significant achievement. No other examples of using a peptide ligand to purify monoclonal antibodies using peptide mimotope affinity chromatography have been found in the research literature at the time of writing. The advantages of using paratope-specific peptide mimotope affinity chromatography for the purification of antibodies from biological feedstocks were outlined in chapter 1. The use of the peptide ligand in place of estrone (which has previously been used as an affinity ligand for the purification of mAb 4155), means that use of a competitive elution procedure in the purification protocol (see section **1.5.3.4**) can be eliminated. The use of a peptide ligand in place of estrone also has advantages in terms of the cost of matrix production, and simplification of the ligand immobilisation chemistry. The use of (d) amino acid residues in place of the naturally occurring (l) amino acid residues should also improve the stability of the peptide to proteolysis in biological feedstocks.

Chapter 6 - Results. Mimotope peptides cross-reactive with an anti-steroid hormone antibody.

Peptide mimotopes could also provide valuable reagents for use in biosensors which measure non-protein analytes, offering advantages in terms of stability, reproducibility, and the ability to fine-tune the antibody recognition process for a particular assay requirement (e.g. qualitative or quantitative assays).

7 Chapter 7 - Results. Towards the production of a scFv-GFP fusion protein.

7.1 Introduction

Chapter 2 of this thesis outlined the different technologies that are currently available for the selection or screening of protein libraries. It was noted that the interrogation of such libraries using selection methodologies proved more powerful than screening methodologies. The amount of sequence space that can be surveyed using selection methodologies is greatest; and the cumulative combinatorial effects observed after successive rounds of selection leads to a faster evolution of protein structure than could ever be achieved in a screen-based approach.

The aim of the work presented in this chapter was to construct a library of randomly mutated C595scFv clones fused to GFP and displayed on the surface of bacteriophage. This would then allow the use of a more effective selection method - fluorescent activated cell sorting (FACS) (see section 7.1.5). Selection of scFv clones which demonstrate a higher specific affinity to MUC1 antigens expressed in their natural environment on tumour cell lines could prove more effective than selection based on synthetic peptides or on the isolated antigen. This would potentially enable the development of a scFv demonstrating a higher specific *in vivo* reactivity to tumour cells over normal cells. The scFv-GFP fusion could also be useful in its own right as a tumour marker.

7.1.1 Affinity maturation of antibodies

In vivo, antibodies are derived by selection from large repertoires of antigen-binding sites displayed on the surface population of B-cells. Active antibody genes are initially formed from unmodified germline gene segments. The limited number of these segments in the genome places a ceiling on the number of different antibody structures in the naïve repertoire. Each B-cell assembles and expresses on the surface a single antibody species and encounter with antigen leads to the selection of those B-cells of the repertoire with binding activities (the B-cell is effectively a package which

links the genotype and phenotype of the antibody). The rearranged V-genes, encoding the heavy and light chain variable domains responsible for binding to antigen are created by a combinatorial assembly of V-gene elements (heavy chain VH, D and JH; light chain V λ and J λ , or V κ and J κ) during lymphocyte development. Binding of antigen and help from T-cells triggers differentiation of the B-cell to plasma cells and production of soluble antibody. All of this occurs in the primary immune response, when the B-cell population is first exposed to the antigen. Antibodies produced in the primary response are likely to bind to the antigen with low affinity as a result of imperfect chemical complementarity to the immunising antigen. Enhancement of the combining-site geometries in the progeny of the originally activated B cell occurs by the combined action of somatic mutation and selection (Foote and Eisen 1995).

In the mouse, there are approximately 2.5×10^8 B-cells displaying a large repertoire of approximately 10^7 antigen binding sites. Each antigen binding site is selected from this large repertoire of structures and, typically, the antigen binding affinities are in the range 10^5 to 10^7 M⁻¹ (Hawkins, *et al.* 1993). These affinities can be improved by random mutation, by which variants are created with an estimated mutation rate of 10^{-3} to 10^{-4} point mutations per base pair per generation. Those with higher affinity of binding are selected on further immunisation with antigen – the secondary immune response. This *in vivo* “affinity maturation” process often leads to improvements in affinity of five- to tenfold (Hawkins, *et al.* 1993).

It is possible that a rare antibody gene with germ-line sequences could generate an antibody with optimum chemical complementarity to the antigen, thus demonstrating optimal antigen-binding properties without enhancement by somatic mutation and selection. The affinity of such an antibody has been termed *static* since the occurrence of somatic mutations would probably be neutral or deleterious, causing the elimination of cells making the sequence, or the cells may not be selectively simulated to produce the sequence (Foote and Eisen 1995).

The use of scFv molecules for tumour targeting offers potential advantages compared to using whole antibodies. IgG are large molecules (150 kDa) which diffuse slowly into tumours and are slowly cleared from the circulation, resulting in poor tumour:normal organ ratios. Smaller single-chain antibody fragments (scFv, 25 kDa), which are potentially less immunogenic than whole antibodies, penetrate tumours better than IgG and are cleared more rapidly from the circulation. The use of such engineered molecules also facilitates protein-engineering techniques. The scFv molecule is monovalent and is thus unable to exhibit higher apparent affinity due to avidity as is observed with the bivalent IgG molecule. Significant tumour retention beyond 24 h will require a dissociation rate constant (k_d) less than 10^{-4} s^{-1} ($t_{1/2} = 1.8 \text{ h}$).

Antibodies typically have rapid association rate constants ($k_{on} > 10^5 \text{ M}^{-1} \text{ s}^{-1}$), requiring $K_d < 10^{-9} \text{ M}$. An “affinity ceiling” exists for antibodies produced during normal immune responses (Foote and Eisen 1995). This is as a result of limits on the maximum on and off rates occurring in antibody-antigen interactions produced in the immune response. The on-rate constant has a maximum of 10^5 - $10^6 \text{ M}^{-1} \text{ s}^{-1}$ controlled by the diffusion coefficients of the reactant molecules, and has been verified experimentally (Raman, *et al.* 1992). The off-rate constant has been suggested to be fixed at $10^{-3} - 10^{-4} \text{ s}^{-1}$, since antibodies with slower off rates would not be selected *in vivo* (Foote and Eisen 1995). Thus $K_d < 10^{-9} \text{ M}$ is rarely observed in antibodies derived from a murine immune response (Schier, *et al.* 1996).

The sensitivity of an assay using monoclonal antibodies and their derivatives is ultimately linked to the affinity of the antibody for the analyte.

7.1.2 Selection of high affinity antibodies *in vitro*

The arrival of phage display and other display technologies as outlined in Chapter 2 allows the manipulation of selection conditions *in vitro*. This can enable the isolation of higher affinity antibody species such as scFv, which may not be obtained by *in vivo* antibody production methods. An example of this was published by Hawkins, *et al.* (1992). Here the use of excess biotinylated antigen was used to select for higher affinity scFv molecules from a library of mutants created by error-prone PCR. A four-fold increase in affinity over the parent molecule was obtained. The

disadvantage with this method is that the antigen is not in the natural environment, which may lead to the antigen exhibiting a different structure to that seen *in vivo*. FACS can potentially overcome this by using whole cells instead of the biotinylated antigen.

7.1.3 Anti-MUC1 scFv construction

The construction and characterisation of the anti-MUC1 scFv as used in this work is described in detail by (Denton, *et al.* 1997). Briefly the procedure consisted of first isolating mRNA from hybridoma cells expressing whole monoclonal C595 antibody. Hybridoma mRNA was then used as the template to construct C595 scFv using the Recombinant Phage Antibody System (RPAS; Pharmacia, Uppsala, Sweden). First a cDNA library was produced from mRNA through reverse transcription with random (N₆) primers. V_H and V_L specific oligonucleotide primers were used to amplify separate V_H and V_L chain encoding regions from the cDNA library. Purified V_H and V_L encoding DNA were spliced together by PCR using primers to introduce a linking sequence between the two segments and unique Sfi I/Not I restriction sites at 5' and 3' ends respectively, enabling directional cloning into the digested pCANTAB 5E vector. The system was then used to express C595 scFv in bacterial supernatant. A single immunoreactive clone was selected which bound to the synthetic peptide **APDTRPAPG** containing the **RPAP** epitope recognised by C595 mAb. Sequence analysis of the scFv demonstrated that the majority of the scFv representing the variable regions were homologous with those of the parent antibody, except for five conservative changes outside the CDR regions of the antibody.

7.1.4 Green fluorescent protein (GFP)

Antibodies conjugated to the fluorochromes such as fluorescein isothiocyanate (FITC) have been used extensively for immunofluorescence techniques (REFS). The use of such chemically conjugated fluorochromes can lead to partial or complete loss of antigen binding ability as a result of conjugation with residues (e.g. lysine) in the antigen-binding site. FITC is also very sensitive to photobleaching by illumination. GFP isolated from the jellyfish *Aequorea victoria* emits intrinsic intense and stable green fluorescence without any cofactors and exhibits less photobleaching than fluorescein (Arai, *et al.* 1998). Genetic fusions between antibodies and GFP encoding

genes circumvent the problems associated with chemical conjugation, giving a 1:1 ratio between antibody and fluorochrome. The intensity of fluorescence and stability of GFP has thus resulted in its use in fluoroimmunoassays *in vitro* (Aoki, *et al.* 1996; Arai, *et al.* 1998) (see section 7.1.4 also). GFP mutants exhibiting enhanced fluorescence and/or altered excitation/emission wavelengths have been developed. These have been extensively reviewed (Kendal and Badminton 1998). Briefly these include red-shifted variants (enhanced green fluorescent protein - EGFP), blue-shifted variants (enhanced blue fluorescent protein – EBFP), an enhanced cyan variant and an enhanced yellow variant.

7.1.5 Published examples of scFv-GFP fusion proteins

There are several examples of scFv-GFP fusion proteins, details of which were published during the period of research undertaken in this thesis. Interestingly not all of the authors are aware of previous publications.

The first to describe a fusion between a scFv and GFP was by (Wang 1999), this is a conference abstract describing fusion proteins between a single-chain antibody and several photoproteins (aequorin, obelin and GFP). These were used for assay development in the detection of Salmonella antigen, with a detection limit for Salmonella antigen of 2 ppm. All retained luminescent activity of the native photoproteins, as well as the binding affinity of the scFv to the antigen. A decrease in luminescence was observed and it was postulated that this could be due to a conformational change of the fusion proteins upon binding to the antigen.

The next publication describing a scFv-GFP fusion invented the term “Fluobody” to describe such fusion proteins (Griep, *et al.* 1999). No reference is made to the previous publication and the paper states that “genetic fusion between antibody and GFP encoding genes would be ideal”, suggesting the authors were unaware of the earlier example. The paper describes the expression of two N-terminal fusions of different scFv fragments (both directed against the lipopolysaccharide of the bacterium *Ralstonia solanacearum*) to a red-shifted GFP. A vector utilising a tetracycline promoter (inducible with anhydrotetracycline) and a CAT-signal peptide was used to direct expression of the fusion protein to the periplasm. A His-tag was

added to the C-terminus of the GFP protein to facilitate purification of fluorescent and active expressed protein, at a yield of ~101 µg per liter of bacterial culture.

A different approach was taken in the next paper published. Instead of labeling the whole scFv molecule, antibody variable domains were fused with green fluorescent protein variants, enabling the phenomena of fluorescence resonance energy transfer (FRET) to be utilised in an homogeneous immunoassay (Arai, *et al.* 2000). The work was based on previous work creating an “open sandwich ELISA”. Conventional sandwich ELISA techniques require the presence of at least two epitopes, and usually have a long measurement time as a result of the consecutive binding and washing steps. The open sandwich ELISA exploits the reassociation of the generally weak V_H-V_L complex by a bridging antigen. Using immobilised V_L and enzyme tagged V_H fragments, antigen was measured at concentrations <10ng/ml in a shorter time period than the conventional sandwich immunoassay (Suzuki, *et al.* 1999).

The FRET variation of this technique utilised fusions of GFP derivatives with V_H and V_L fragments of anti-hen egg lysozyme (HEL) antibody. Gene fusions were constructed and expression in the periplasm attempted. This proved unsuccessful, and a cytoplasmic expression system utilising a thioredoxin (Trx)-fusion expression vector was attempted. This approach proved successful and functional Trx-V_H-EBFP and Trx-V_L-EGFP fusion proteins were purified from the cytoplasm at 3mg per liter of culture. The addition of antigen (HEL) to a mixture of Trx-V_H-EBFP and Trx-V_L-EGFP induced heterodimerization of the two, accompanied by FRET from the EBFP to the EGFP domains tethered with V_H and V_L domains respectively. The authors state that to their knowledge this was the first report of antibody fragment-GFP variant fusion expressed in *E. coli*.

Schwallbach *et al* (Schwalbach, *et al.* 2000) describe the production of large amounts of Fluorescent Single-Chain Antibody Fragments in the cytoplasm of *E.coli*. scFv-GFP fusion protein production was monitored by analysing the GFP fluorescence of transformed cells under UV illumination. Several different combinations of promoters (lac and arabinose) and leader sequences (pel B) were tested. The highest levels of fluorescence were observed with expression under the control of an arabinose promoter and no pel B leader sequence. The GFP chromophore was found

not to form in the cytoplasm. Fusion protein was directed to the cytoplasm of the cell (no disulphide bridges in the scFv), and only about 1% of the molecules were able to bind antigen and exhibit fluorescence. It was reported that yields of scFv-GFP fusion proteins were highly dependent on the scFv sequence. When a different scFv molecule which had been adapted to cytoplasmic expression was used in place of the previous scFv in the same vector, large amounts of functional fluorescent antibody fragments were produced (~15mg/litre). The authors state that to their knowledge this was the first report of producing metabolically GFP-tagged scFvs and their application to direct immunoassays.

(Casey, *et al.* 2000) describe the production of Green Fluorescent Antibodies and their use as novel *in vitro* tools. The scFvGFP fusion protein was expressed in the periplasm of *E.coli*. The authors claim this as being the first report to describe a EGFP fusion protein that can be expressed in the periplasm of bacterial cells, to form a functional chimera that can be used *in vitro*. The scFv was specific for hepatitis B surface antigen. Both N and C terminal fusions of EGFP with the scFv were constructed. A pel B leader sequence was used to direct expression of the fusion proteins to the periplasm, and constructs in which the pel B leader was absent were also used to direct protein expression to the cytoplasm. N-terminal fusions (i.e EGFP-scFv) were demonstrated to be active and to demonstrate fluorescence. Only a small amount of the C-terminal scFv-EGFP periplasmic fusion protein was reported to have been detected, indicating that this fusion was not as stable as the N-terminal EGFP-scFv fusion. In addition there was no evidence of full-length fusion proteins for the cytoplasmic constructs. The remainder of experiments in the study were carried out using the full-length N-terminal EGFP-scFv. A yield of ~200 µg per litre of bacterial supernatant was reported for the N-terminal EGFP-scFv fusion protein.

7.1.6 Fluorescence activated cell sorting and affinity maturation

Fluorescence activated cell sorting (FACS) offers an effective alternative to screening by solid support capture and elution (see chapter 4). FACS instrumentation is commonly used for the detection and isolation of rare cells in clinical medicine. The following are examples where FACS has been used to screen libraries.

- The screening of a library of short synthetic peptides immobilised on beads for high-affinity peptide ligands (Needels, *et al.* 1993).
- The quantitative isolation of high affinity proteins from libraries displayed on the surface of microorganisms (Francisco and Georgiou 1994).
- The isolation of red-shifted excitation mutants of GFP with a 20- to 35- fold increase in fluorescence intensity has also been demonstrated (Cormack, *et al.* 1996).
- Affinity maturation of scFv molecules displayed on *E.coli.* has been demonstrated using FACS (Daugherty, *et al.* 1998).

Like phage display, FACS offers the potential for the isolation of rare clones from a very large excess of non or weakly binding background proteins, but offers the advantage of using soluble hapten, eliminating artefacts due to binding to solid surfaces. The whole selection system using FACS can be considered as a totally soluble selection system where neither the ligand nor ligand binding protein are immobilised onto a solid support. Both ligand and ligand binding protein are more likely to retain structures associated with their natural chemical environment. The work presented in this chapter sought to use the advantage of a totally “solubilised” selection system to screen tumour cells expressing tumour-related mucin which bound with high affinity to a C595 scFv mutant protein.

This work can be divided into five stages:-

Stage 1: Production of C595 scFv-GFP gene fusion containing the required restriction sites.

Stage 2: Ligation of scFv-GFP fusion into pCANTAB 5E.

Stage 3: Expression and purification of scFv-GFP fusion protein.

Stage 4: Creation of a library of C595 scFv mutants – optimisation of mutagenesis conditions.

Stage 5: Selection of mutant – GFP fusions using FACS.

7.2 Strategy for the production of a scFv-GFP gene fusion

Figure 7.1 outlines the strategy which was finally used for the production of the scFv-GFP gene fusion for ligation into the digested pCANTAB 5E vector.

Initially it was planned to amplify the C595 scFv and GFP genes from the respective plasmids by PCR using the primers described in section 7.3, and after purification of the PCR products, carry out a ligation reaction with the scFv and GFP fragments. The success of this ligation reaction was confirmed by PCR of the ligation reaction using C595 SfiI FOR and GFP NotI REV primers (see figure 7.2).

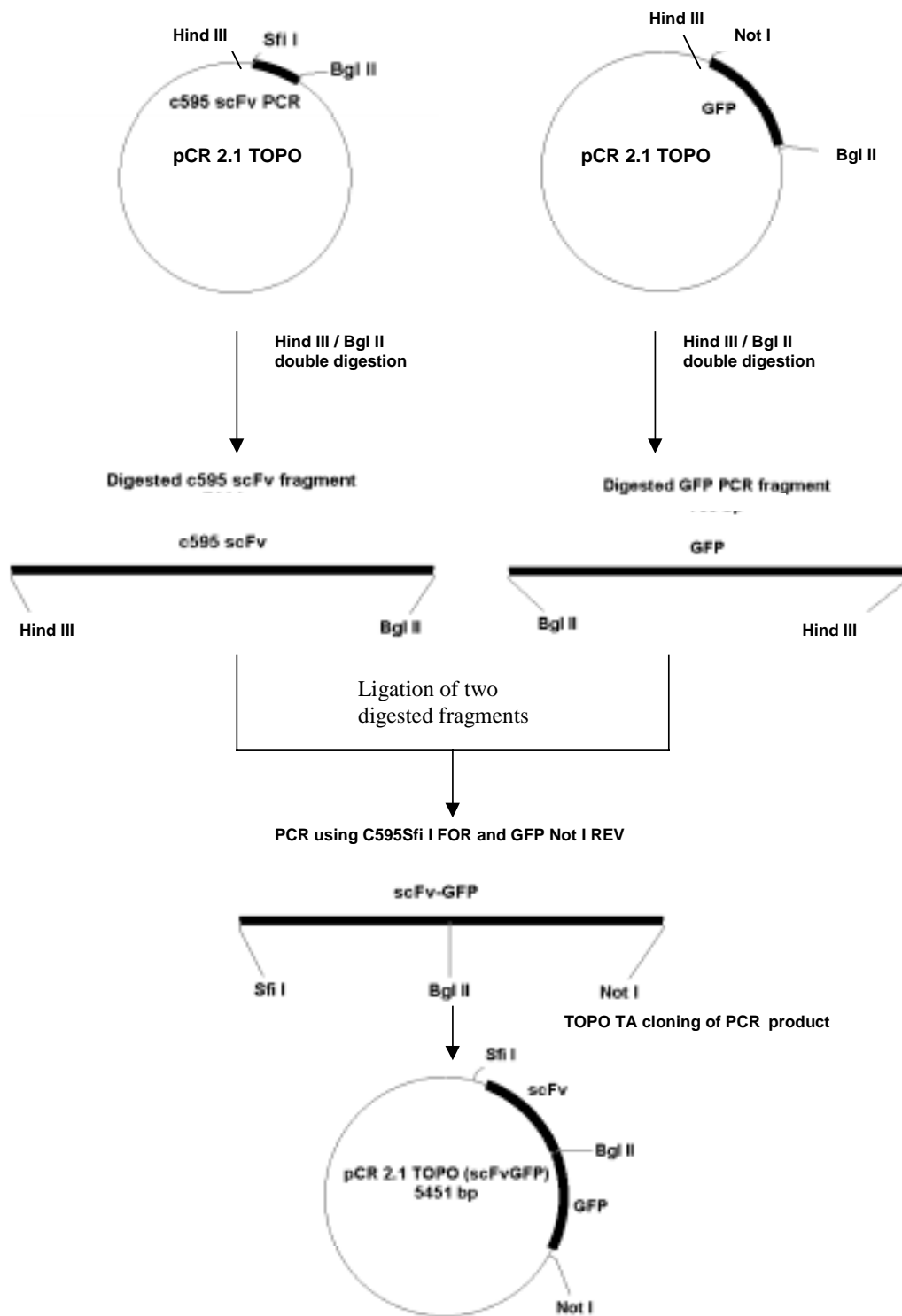


Figure 7.1: Strategy for the production of the scFv-GFP gene fusion. A Sfi I/Not I double digest was conducted on the resulting vector and the gene fusion was ligated into Sfi I/Not I digested pCANTAB 5E vector.

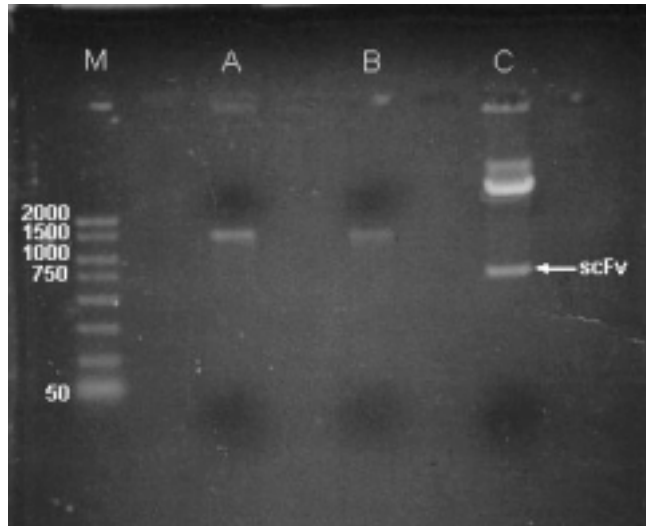


Figure 7.2: Ligation of C595 scFv to GFP confirmed by PCR, showing bands ~1500bp for two different ligation reactions – (A) ligation using 1/10 dilution of scFv PCR product + neat GFP PCR product; (B) ligation using 1/30 dilution of scFv and neat GFP PCR product. (C) Sfi I / Not I digestion of pCANTAB 5E containing C595 scFv, showing the size of scFv gene in relation to the PCR product of the ligation reaction.

Experiments to ligate the purified (ethanol/chloroform extraction and gel purification methods both tried) and SfiI/NotI digested PCR product of the scFv-GFP ligation reaction into SfiI/NotI digested pCANTAB 5E were unsuccessful. Very few colonies grew after transformation with the ligation reaction, and analysis of the plasmids of the colonies that did grow always only contained the C595 scFv gene (Situating between the Sfi I and Not I restriction sites of the pCANTAB 5E vector).

It was decided to clone the PCR products into a TOPO-TA cloning vector so that the PCR products could be sequenced to confirm only the required mutations had occurred in the amplified sequences before proceeding to the next stage. Cloning of the amplified genes into the cloning vectors also enabled (by agarose gel electrophoresis) the verification that a successful restriction digest had occurred, when the scFv-GFP fragment was cut out of the vector.

A restriction digest was then conducted on the TOPO vectors containing the scFv and GFP genes with the required mutations introduced. The digested scFv and GFP fragments were purified by agarose gel electrophoresis, and an "in-gel" ligation conducted (as described in chapter 3). The ligated fragment was amplified by PCR and cloned into a TOPO cloning vector to confirm the sequence and to enable the confirmation of the integrity of the restriction sites by agarose gel electrophoresis of the products of a Sfi I / Not I restriction digest.

A sample of the original vector from which the C595 scFv gene was amplified was used as the source of pCANTAB 5E vector. Use of this vector containing the scFv gene enabled the verification that the scFv gene had been "cut out" of the vector in the restriction digest.

7.3 Mutagenic Primer design

A novel Bgl II restriction site was introduced at the 3' end of the scFv gene, and at the 5' end of the GFP gene. The scFv and GFP genes were designed to be linked by the unique Bgl II site at the centre of the scFv-GFP gene fusion, to enable later manipulations when the mutated scFv library was constructed. The Bgl II restriction site is a unique restriction site (i.e. not present anywhere in the pCANTAB 5E plasmid, or anywhere else in the scFv and GFP genes) enabling the insertion of mutated scFv genes into Sfi I / Bgl II digested pCANTAB 5E plasmid containing the scFvGFP gene fusion. A novel Not I restriction site was also introduced at the 3' end of the GFP gene to enable ligation of the final gene fusion into pCANTAB 5E.

To facilitate the introduction of these novel restriction sites, primers were designed using Amplify 1.2. The program contains an algorithm which determines a theoretical figure for the stability of match, which is expressed as a percentage. It is desirable to have a Stability of match that is not too low or non-specific annealing of the primer could occur at sites other than those intended, leading to unexpected PCR products.

1	5' CCTTTCTATGCGGCCAGCCGGCCATGGCCCAGG ³	87%
2	5' CCGGCGCACCTGCAGATCTCCGTTTCAGCTCCAGC ^{3'}	68%
3	5' CGACAAGGTGAGGAGATCTACCATGGCTAGCAAAGGAGAAGAAC ³	63%
4	5' GCGCGCGGTGAGCACCGGAACGGCACTGGTTCGCGGCCGCATCCATGCCATGTGTAATC ^{3'}	60%

Table 7.1: Stability of match for primers used to create scFv-GFP gene fusion. C595 SfiI For, (2) C595 Bgl II Rev; (3) GFP Bgl II For and (4) GFP Not I Rev.

7.4 Amplification of C595 scFv and GFP genes with concurrent introduction of unique restriction sites

The polymerase chain reaction (PCR) was used to introduce unique Bgl II restriction sites at the 3' end of the scFv gene and the 5' end of the GFP gene; and a unique Not I site at the 3' end of the GFP gene.

7.4.1 Initial plasmid preparation

Before the scFv and GFP genes could be amplified from the pCANTAB 5E and the pTRACER plasmids, a pure sample of plasmid had to be prepared. This was done as described in Chapter 3 of this thesis.

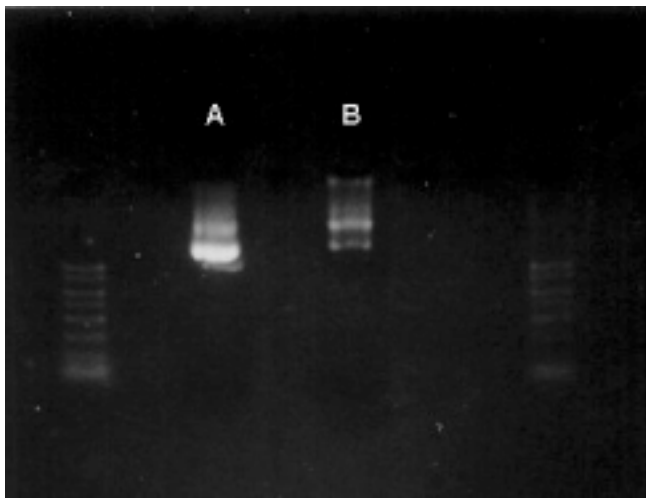


Figure 7.4: Gel of plasmid preparation of C595 scFv in pCANTAB 5E and GFP in pTRACER.

The two bands indicate the presence of circular and supercoiled plasmid.

7.4.2 Polymerase Chain reaction to amplify C595 scFv and GFP

To isolate the C595 scFv and GFP genes and introduce the mutations outlined in section 7.3, a Polymerase Chain Reaction (PCR) was performed using the primers outlined in section 7.3. The amplified fragments should be approximately 750 bp in size. The DNA from the PCR was run on an agarose gel to confirm the correct portion of DNA had been amplified from the plasmids.

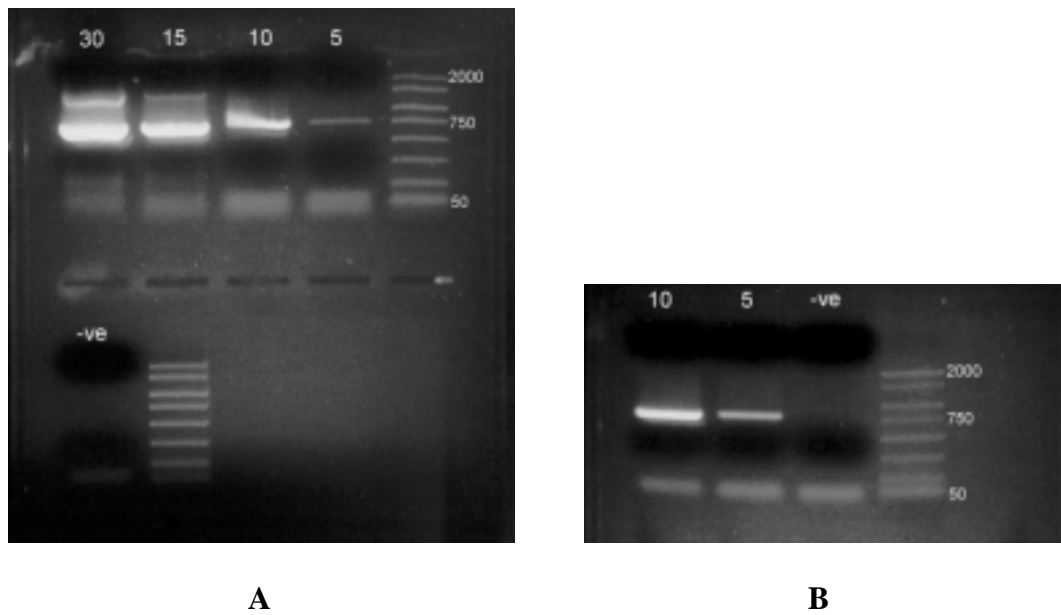


Figure 7.5: Agarose gel of PCR products confirming the amplification of C595 scFv and GFP genes from plasmids pCANTAB 5E and pTRACER respectively. (A) demonstrates optimisation of the number of PCR cycles for the amplification of the C595 scFv gene and (B) demonstrates the optimisation of the number of PCR cycles for the amplification of the GFP gene. Negative control PCR reactions (run in lanes marked -ve) consisted of reactions excluding the target DNA (i.e. the respective plasmids).

From these results it can be seen that 5 cycles of PCR amplification gives the most distinctly defined PCR products for the scFv and GFP genes. Also from this gel, it is clear that the PCR reaction produced reaction products of the expected size. The bands in the lanes where the PCR product for the 5-cycle amplification was run were excised and used in the TOPO-TA cloning reaction.

7.4.3 TOPO-TA cloning of PCR products

In order to confirm that the required mutations outlined in section 7.3 were introduced in the PCR reaction, and to ensure the integrity of the introduced restriction sites, PCR product from both reactions was cloned into respective TOPO-TA cloning vectors (pCR 2.1), as described in chapter 3. The plasmids were used to transform *E.coli* TOP10F cells (UltraComp Competant Cells, Invitrogen). After overnight incubation with the transformation mix, white colonies were picked from the

LB/Ampicillin agar plates and suspended in 10µl of LB media. 1µl of the suspended cells was used in a PCR as in the previous section. The remainder of each suspended colony mix was used to inoculate 5ml samples of LB/Ampicillin, which were incubated overnight at 37°C with shaking at 200rpm.

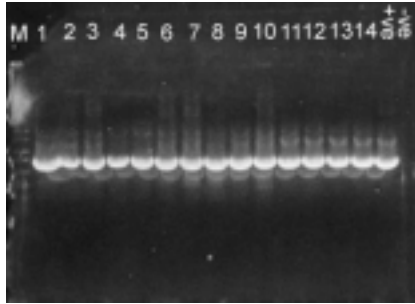


Figure 7.6: Agarose gel of PCR products obtained from PCR of the TOPO-TA cloning reactions. PCR was conducted as described in Chapter 3 using the primers C595 Sfi I For and C595 Bgl II Rev (lanes 1-10 for TOPO clones expected to contain the scFv PCR product) and GFP Bgl II For and GFP Not I Rev; (lanes 11,12,13 and 14 for TOPO clones expected to contain the GFP PCR product); in the lane marked +ve the results of a PCR conducted using C595 Sfi I For and C595 Bgl II Rev using pCANTAB 5E (C595 scFv) as the template DNA were used; in the lane marked -ve a PCR was conducted using all primers but no DNA template, a pick from an area of the plate containing no colonies was used.

Sequence analysis of the clones showed that the required mutations were successful and the unique restriction sites were introduced. Sfi I/Bgl II and Bgl II/Not I restriction digests also confirmed the integrity of the restriction sites.

7.5 Production of scFv-GFP gene fusion

After the sequence and integrity of the restriction sites in the scFv and GFP PCR products had been demonstrated, the next step was to ligate the two genes at the Bgl II restriction site.

7.5.1 Restriction digests of pCR 2.1 vectors containing the C595 scFv and GFP mutated PCR products

A Hind III / Bgl II restriction digest was conducted on the clones isolated in section 7.4 to create scFv and GFP fragments with a Bgl II site at the 3' and 5' ends respectively.

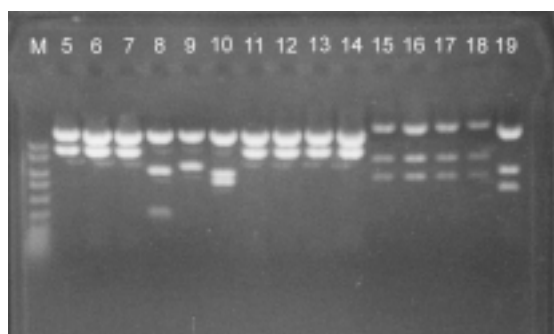


Figure 7.7: Hind III / Bgl II double restriction digests on TOPO clones isolated in section 7.4. The lane marked M contains molecular weight markers (2000,1500,1000, 750, 500, 300, 150 and 50 base pairs respectively from top to bottom of the gel). Lanes marked 5-14 contain digested TOPO vector thought to contain scFv genes. Lanes marked 15-19 contain digested TOPO vector thought to contain GFP genes.

The pCR 2.1 vector itself contains one unique Bgl II restriction site, when the PCR products containing a Bgl II restriction site are introduced, the vector contains two Bgl II restriction sites. The PCR product can be cloned into the pCR 2.1 vector in two different directions. Digestion of the plasmids with Hind III and Bgl II should yield three bands of the following size:

Orientation	TOPO (scFv)	TOPO (GFP)
Forward	2874	2874
	984	1717
	792	74
Reverse	2874	2874
	1698	980
	78	811

Restriction digests in lanes labelled 5, 6, 7, 11, 12,13 and 14 contain two very clear bands, one >2000 bp, the second between 2000 and 1500 bp, and a third very faint band (not clearly visible on the scanned gel) between 50 and 150 bp. This is

consistent with a reverse orientation of the scFv PCR product. The very faint band at 78 bp could be explained by the reduced amount of DNA available for the ethidium bromide to intercalate compared to the much larger fragments. The bands in the lanes marked 8 and 9 are not consistent with either of the orientations. The bands in the lane marked 10 (>2000 bp, ~1000 bp and ~750 bp) are consistent with the forward orientation of the PCR product. For the GFP TOPO clones, the bands in the lanes marked 15,16, 17 and 18 are not consistent with either of the orientations; the bands in the lane marked 19 (>2000 bp, ~1000 bp and ~750 bp) are consistent with the forward orientation of the PCR product.

7.5.2 Ligation of C595 scFv fragment to GFP fragment

The scFv and GFP fragments isolated in section 7.5.1 were ligated in gel as described in Chapter 2. (R141)

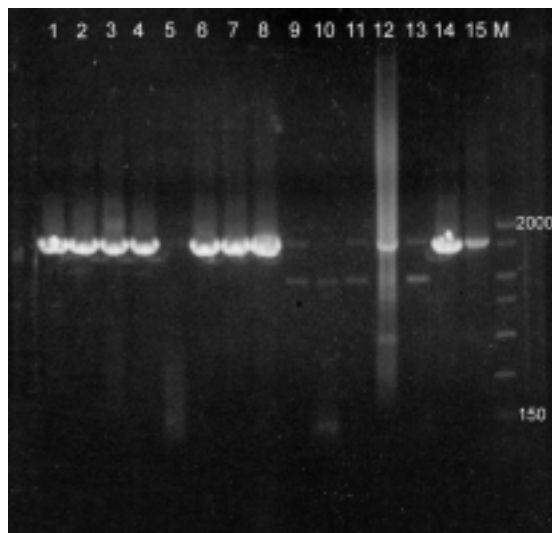


Figure 7.8: PCR on a sample of the ligation reaction showing the presence of the band ~1500 bp, indicating a successful ligation reaction.

7.5.3 TOPO TA cloning of the PCR product of the ligation reaction

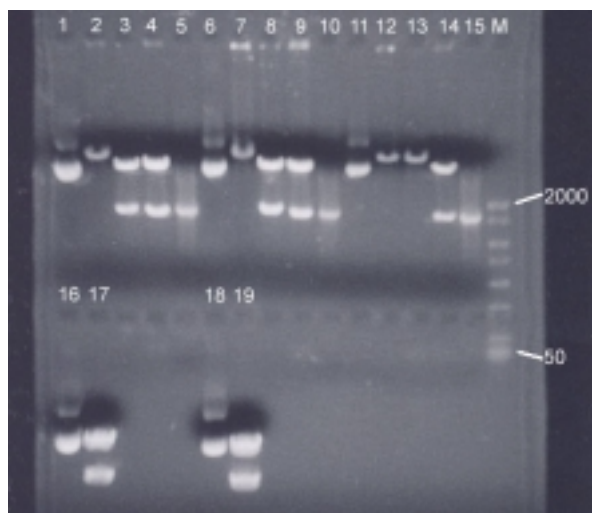


Figure 7.9: Restriction digests of a number of pCR 2.1 (scFv-GFP) clones (R145 lanes 1-5 and 16-17; R146 lanes 6-10 and 18-19; and R147 lanes 11-15). A sample of the PCR product for the ligation reaction was used as a marker (~1500 bp) in lanes 5, 10 and 15. Lanes marked 1,6 and 11 contain uncut plasmid. Lanes marked 2,7 and 12 contain plasmid digested with Sfi I restriction enzyme only. Lanes marked 3, 8 and 13 contain plasmid digested with Not I restriction enzyme only. Lanes marked 4, 9 and 14 contain plasmid digested simultaneously in a double digest with Sfi I and Not I restriction enzymes. Lanes marked 16 and 18 contain undigested plasmid; and lanes marked 17 and 19 contain plasmid digested with the restriction enzyme Bgl II.

The pCR 2.1 TOPO vector contains one unique Not I restriction site. When the scFv-GFP fusion is cloned into the vector two Not I restriction sites are present. Depending on the orientation of the cloned scFv-GFP fragment in the vector, Not I restriction digests yield the following sized fragments:

Orientation	Fragment sizes (bp)		
	Sfi I	Not I	Sfi I / Not I
Forward	~3900	~3700 ~170	~2300 ~1300 ~173
Reverse	~3900	~2400 ~1500	~2400 ~1442 ~73

(Figures in italics represent the band which contains the scFv-GFP gene fusion).

From this analysis it can be seen that TOPO clones R145 and R146 contain the scFv-GFP gene in the reverse orientation, and the scFv-GFP gene fusion is located in the band ~1400 bp in the Sfi I / Not I double digest. TOPO clone R147 contains the scFv-GFP gene in the forward orientation and the scFv-GFP gene is located in the band ~ 1300 bp. It was decided not to use the TOPO clone containing the scFv-GFP fusion in the forward orientation since the Not I restriction sites were relatively close (~100 bp between), and it was not easy to determine whether both Not I sites were cleaved (band ~ 173 not clearly visible). The presence of only a two bands when a restriction digest using Bgl II was conducted on TOPO clones R145 and R146 is indicative of both the Bgl II site in the cloned gene and the Bgl II site in the pCR 2.1 vector being active (The pCR 2.1 vector contains a unique Bgl II restriction site). Hence it can be said that the Bgl II restriction site joining the scFv and GFP genes is fully functional. Sequence analysis of the clone R145 using M13 forward and reverse primers confirmed the presence of the engineered restriction sites and the integrity of the scFv and GFP genes (see appendix 1).

7.6 Ligation of scFv-GFP gene fusion into pCANTAB-5E

7.6.1 The pCANTAB 5E vector

The pCANTAB vector is part of the Recombinant Phage Antibody System (RPAS, Amersham Pharmacia Biotech). The RPAS kit is designed to provide a tool for the synthesis of phage-displayed and soluble recombinant antibodies. A detailed description and critical appraisal of this system is given by (Krammer 1998). Antibody fragments can be expressed as a fusion with fd gene 3 protein and displayed on the tips of M13 phage. Once antigen positive clones are isolated, the phage can then be used to infect a nonsuppressor strain of *E.coli* to produce soluble antibody fragments. The crucial components of the vector are summarised below: -

An antibiotic resistance gene, Amp R enables selection of bacteria which contain the pCANTAB 5E plasmid. Amp R encodes for the protein β -lactamase, which degrades the antibiotic ampicillin.

A cloning region, scFv genes are cloned in-between the Sfi I / Not I restriction sites.

An inducible LacZ promoter (pLac) regulates transcription of the scFv gene. The binding of the transcription inhibition protein, Lac I, to a sequence immediately downstream of the promoter prevents transcription of the scFv gene, preventing inhibition of the growth of cells transformed with pCANTAB 5E containing a scFv gene insert. When a sufficient cell density is obtained, the addition of IPTG to the cells inhibits binding of Lac I, enabling gene transcription to proceed.

A signal peptide is encoded prior to the Sfi I restriction site. This signal peptide allows the expressed protein to be transported from the cytoplasm to the periplasmic space of the bacteria cells, allowing leaching of expressed protein into the supernatant for simplified purification. The signal peptide is cleaved off in this process.

An E-tag peptide (see chapter 2) is coded for in the sequence immediately downstream of the Not I restriction site, enabling detection of the expressed protein using anti-E-tag antibody, or purification using anti-E-tag antibody.

An amber stop codon is placed between the cloned gene, and the fd gene 3 protein. This enables the vector to be used in conjunction with different strains of *E.coli* to produce both phage-displayed recombinant antibody fragments and soluble antibodies. For example *E.coli* TG1 cells produce a suppressor tRNA which allows read-through (suppression) of the amber stop codon. In *E.coli* TG1 cells, suppression of the amber stop codon is only about 20% efficient and so soluble antibodies will be produced as well as phage-displayed antibodies. However, when *E.coli* HB2151 cells, (which is a nonsuppressor strain) are transformed with pCANTAB 5E, the amber stop codon halts protein translation and only soluble antibody fragments are produced (no scFv-gene 3 fusions are produced).

7.6.2 Preparation of pCANTAB 5E vector for ligation

As described in section 7.6.1, in pCANTAB 5E, the scFv gene is directionally inserted between the Sfi I and Not I restriction sites. In order to ligate the scFv-GFP gene fusion into the pCANTAB 5E vector, a restriction digest was conducted on the Sfi I and Not I restriction sites to enable cloning of the Sfi I / Not I digested scFv-GFP

fragment into this region. pCANTAB 5E vector is provided by the manufacturer already in Sfi I / Not I digested form. It was felt that Sfi I / Not I digestion of an existing sample of pCANTAB 5E vector containing the C595 scFv gene alone would yield a fresher sample of plasmid digest, leading to a lower vector background (i.e. Cells transformed with self-ligated vector). The success of the digest would also be evident from the appearance of the scFv gene in the digested product when analysed using agarose gel electrophoresis.

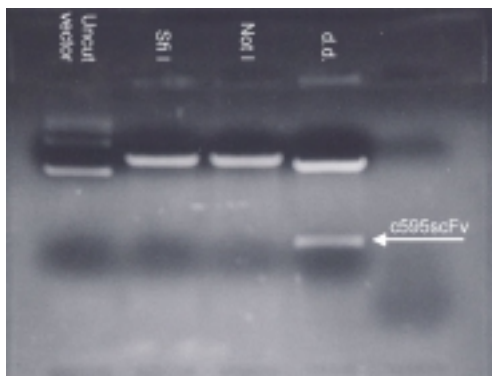


Figure 7.10: Agarose gel of restriction enzyme digest pCANTAB 5E vector containing C595 scFv gene. Note the clear presence of the scFv gene (marked with arrow) after the “double-digestion” with both Sfi I and Not I restriction enzymes. Note the presence of the three forms of DNA (supercoiled, linearised and negatively supercoiled) in the lane containing the circular uncut plasmid, compared to only the linearised form of plasmid in the remaining lanes.

7.6.3 Preparation of scFv-GFP gene fusion for ligation

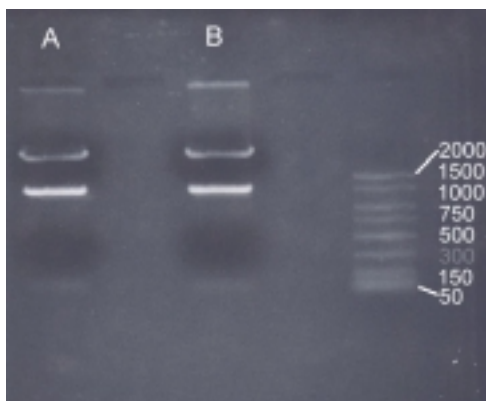


Figure 7.11: Agarose gel of the gel purification of the scFv-GFP gene fusion from two separate TOPO clones in lanes marked A (Clone R145) and B (Clone R146). A double restriction digest using Sfi I and Not I restriction enzymes was used to cleave the scFv-GFP gene from the TOPO vector.

From the agarose gel it is clear that a single band ~ 1500 bp was isolated, the size expected for the scFv-GFP gene fusion.

7.6.4 Ligation of scFv-GFP gene fusion into pCANTAB-5E

The ligation mix was used to transform chemically competent *E.coli* TOP10 cells (Invitrogen). 0.5 µl of the ligation mixture was added to 50µl of the chemically competent cells, and transformed as per the manufacturers instructions. The transformation mix was then spread onto LB-agar plates containing 100 µg/ml ampicillin and incubated overnight at 37°C. Approximately 50 colonies were observed to have grown. Colony picks were taken from ten colonies and suspended in 10 µl of LB media. PCR was used to verify whether the ligation reaction had been successful for each colony (1 µl of the suspended cell mixture was used in the PCR reaction). C595 Sfi I For and GFP Not I Rev primers were used in the PCR reaction. The remainder of the cell suspension was used to inoculate 5 ml of LB media containing ampicillin at 100 µg/ml, and grown overnight at 37°C with agitation at 200rpm.

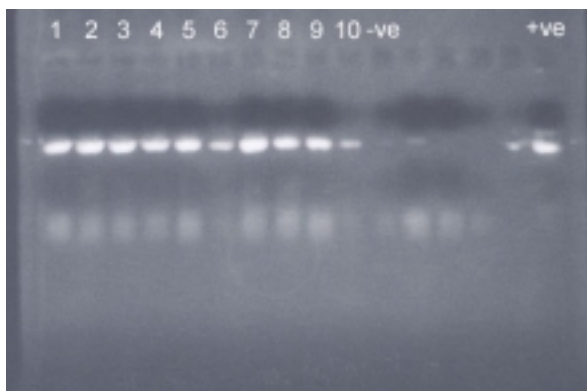


Figure 7.12: Agarose gel of PCR reaction products of colony picks from colonies transformed with pCANTAB 5E – scFv-GFP ligation reaction, using PCR primers

Chapter 7 - Results. Towards the production of a scFv-GFP fusion protein.

C595 Sfi I For and GFP Not I Rev. The negative control consisted of a PCR reaction conducted on a pick from the plate, but where no colonies were present. The positive control consisted of a PCR conducted on a diluted sample of the ligation reaction.

The very faint band in the negative control could be the result of carry-over from lane 10. However the results of three other picks from the plate where no colonies could be seen (lanes 12-14) suggest that this is not an ideal negative control, since a very faint band is observed in lane 12, suggesting colonies were present even though they were no clearly visible.

From this gel it appears that the scFv-GFP gene fusion is present in the ten colonies tested.

Plasmid was isolated from four of the overnight samples inoculated with the colony picks. Restriction digests were conducted to demonstrate the presence of the scFv-GFP gene sized fragment on digestion with Sfi I and Not I restriction enzymes.

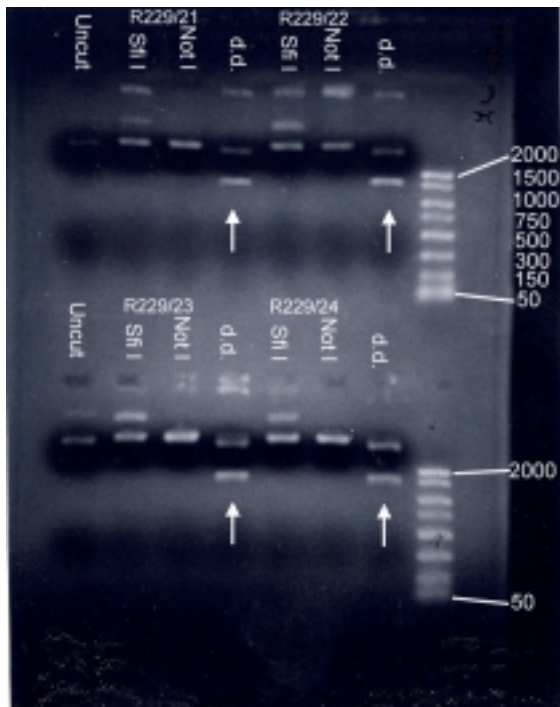


Figure 7.13: Agarose gel electrophoresis of restriction digests of pCANTAB-5E clones R229/21, R229/22, R229/23 and R229/24 containing the scFv-GFP gene

fusion. Arrows indicate scFv-GFP gene fragment (~1500 b.p.) which has been cut out of the plasmid using a double digest.

The PCR and the restriction digest analysis demonstrate that the ligation reaction was successful and the scFv-GFP gene fusion was ligated into the digested pCANTAB 5E vector.

7.7 Expression of scFv-GFP fusion protein using pCANTAB-5E

Details of the important components of the pCANTAB-5E vector were described in section 7.6.1. The presence of the amber stop codon between the cloned scFv gene and the fd gene 3 enable the expression of the cloned gene. If expression is conducted in *E.coli* HB2151 cells (a nonsuppressor strain of *E.coli*), transformed with pCANTAB 5E containing the cloned gene, the amber stop codon halts protein translation and soluble cloned gene product is expressed.

It was decided to experiment with the production of soluble scFv-GFP fusion protein from the newly synthesised plasmid before attempting phage display of the construct. The rationale being that if scFv-GFP fusion proteins could not be expressed in their own right, display on the surface of phage was probably unlikely to be successful.

7.7.1 Small scale expression experiment

Electrocompetent *E.coli* HB2151 cells were produced as outlined in chapter 3. 50 µl of cells were electroporated with 5 µl of the plasmid clone R229/21 (see figure 7.13), pCANTAB 5E containing the C595scFv-GFP gene fusion.

Electroporation details pCANTAB 5E (scFv-GFP)

High Voltage: 2500 v

Capacitance: 25 µF

Shunt: 201 Ω

Pulse: 5 ms

50 ml size , induction conditions.

After electroporation, 1ml of SOC medium was added, and the mixture was agitated at 37°C for one hour. 10 µl, and 50 µl of the cells were then spread onto LB-agar

plates containing ampicillin (100 µg/ml). After overnight incubation a dense carpet of cream-coloured colonies was observed, individual colonies just visible on the plate with 10 µl of media spread. Six colonies were picked (consisting of three large colonies ~3mm diameter (1, 5 and 6) and three smaller colonies (2,3 and 4)), and suspended in 10 µl of LB media. 1 µl was used in PCR reactions using primers C595 Sfi I For and GFP Not I Rev to determine if the scFv-GFP gene was present in the transformed colonies, and the remainder was grown up overnight in LB media containing ampicillin (100 µg/ml) at 37°C with agitation at 400 rpm. A pick from the plate in an area where no colony was present was also used in the PCR, and a second negative control consisting of a PCR with no source of template DNA. A positive control was used which consisted of a sample of the TOPO vector containing the scFv-GFP gene fusion.

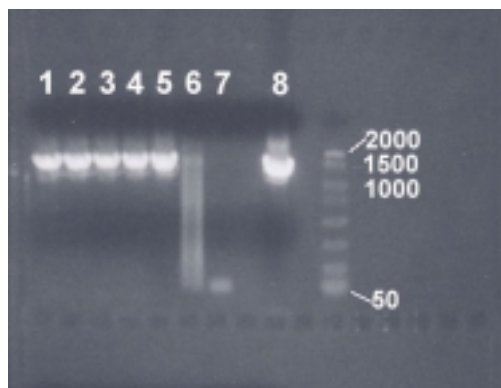


Figure 7.14: Agarose gel of the six colony picks from the plate containing *E.coli* HB2151 cells transformed with pCANTAB 5E containing the scFv-GFP gene fusion. Lanes 1, 2, 3, 4 and 5 all show bands equal in size to the positive control ~ 1500 bp. Lane 6 contains a smear all down the lane. Lane 7 has no bands around ~1500 bp. Lane 8 contains a band ~1500 consistent with the scFv-GFP gene present in the TOPO clone.

Clearly from the agarose gel in figure 7.14, it appears that the transformation reaction was successful, and that five of the six colonies picked contain the pCANTAB 5E (scFv-GFP) plasmid. Glycerol stocks of the five positive colonies were made as outlined in chapter 3.

Soluble antibody production was then tested using the procedure outlined in chapter 3. The supernatant from the induction process was used in section 7.7.2, after ELISA using immobilised BSA-**APDTRPAPG**, anti-E-tag antibody- HRP conjugate failed to give any signal above background.

A periplasmic extraction was conducted on the clones as outlined in chapter 3. ELISA failed to show any signal above background for any of the clones using immobilised BSA-**APDTRAPG** and anti-E-tag antibody failed to give any signal above background.

A whole cell extraction was also conducted on the clones as outlined in chapter 3. Here too ELISA failed to show any signal above background for any of the clones using immobilised BSA-**APDTRAPG** and anti-E-tag antibody-HRP conjugate failed to give any signal above background. This was expected, the fusion protein was unlikely to be stable in the reducing environment of the cytoplasm.

7.7.2 Affinity purification of protein from the supernatant of a small-scale expression experiment

Affinity purification has shown to be the method of choice for the purification and concentration of antibodies and their derivatives. It was decided to employ affinity chromatography of the supernatant from the soluble protein expression experiments to see if any functional expressed protein could be concentrated and purified using affinity chromatography. 50 ml supernatant from clone 1 was loaded onto an affinity column consisting of 2 ml of sepharose 4B with peptide **APDTRAPAPG** covalently linked (see chapter 5), and an elution consisting of a 0-100% gradient of 3M NaSCN over 20 ml was conducted. The eluted fractions were collected in 2.5 ml aliquots and de-salted using PD10 columns (Amersham Pharmacia Biotech). The resulting fractions were assayed by ELISA. The ELISA consisted of BSA-**APDTRAPG** conjugate adsorbed to the wells of a microtitre plate. A normal ELISA protocol was conducted as described in chapter 3. The same procedure was conducted for *E.coli* cells transformed with pCANTAB 5E containing the C595 scFv gene alone. Anti-E-

tag antibody was used to detect and bound species. The results of the ELISA are presented in figure 7.15.

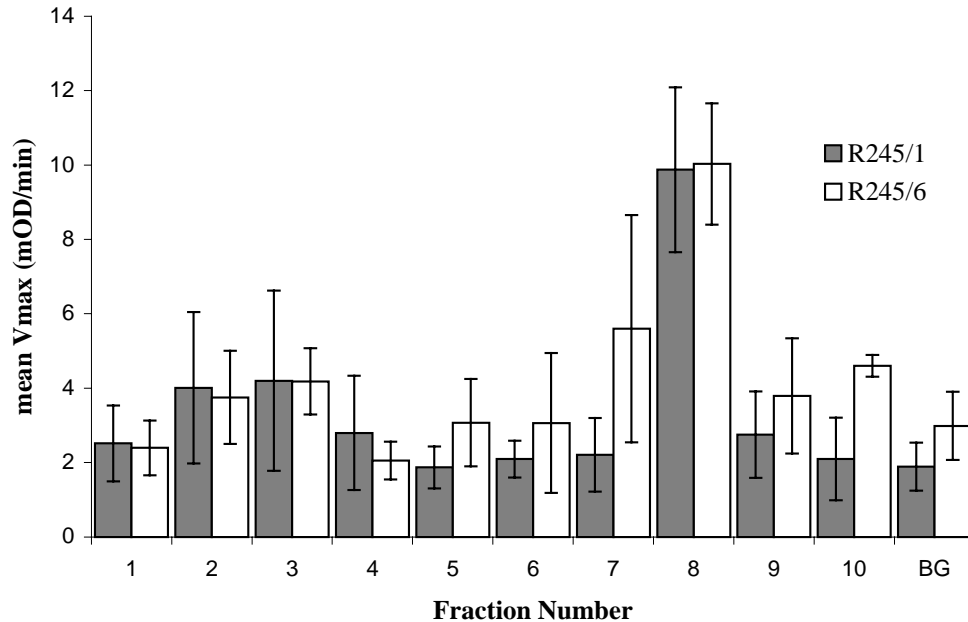


Figure 7.15: Results from ELISA conducted on the de-salted fractions from the affinity purification of small scale protein expression experiments (50ml) of *E.coli* HB2151 cells transformed with pCANTAB 5E containing the C595 scFv-GFP gene fusion (R245/1); and pCANTAB 5E containing only the C595 scFv gene (R245/6). Numbers 1-10 represent the 2.5 ml de-salted fractions which were collected from the affinity column during the elution with the 3M NaSCN gradient. BG represents the background signal with PBS in place of the purified fraction. Detection of bound species was conducted using anti - E-tag HRP conjugate (Amersham Pharmacia biotech), using ABTS as the revealing substrate (using the method described in chapter 3 of this thesis).

It can be seen from figure 7.15 that signal observed for fraction eight of the affinity purification is above the background signal for both cells transformed with pCANTAB 5E containing the scFv-GFP gene fusion, and cells transformed with pCANTAB 5E containing the C595 scFv gene alone. This suggests that functional scFv protein was produced from both of the clones (this is in the region where whole antibody would also be eluted from the column).

No green fluorescence was observable from colonies transformed with the pCANTAB 5E containing the scFv-GFP gene fusion. TCA precipitation of protein from the purified fractions did not reveal the presence of protein by ELISA or western blot analysis.

7.8 Production of a library of mutated C595 scFv genes

It was stated in the introduction to this chapter that when an organism is exposed to a foreign antigen, a process of *in vivo* affinity maturation and selection occurs producing antibodies with an improved affinity for the antigen, enabling the organism to recognise non-self from self. It has been postulated that this *in vivo* affinity maturation process has a natural "affinity ceiling" (Foote and Eisen 1995) limiting the typical maximum affinity observed for such antibodies. Also, as was outlined in the introduction, there are a number of publications which have used *in vitro* methodologies to produce antibody species with affinities above this "affinity ceiling". The aim of the next stage of work was to use *in vitro* methods to produce more stringent selection criteria so that the natural limit of this "affinity ceiling" could be exceeded.

7.8.1 Mutagenesis of C595 scFv

The first step involved in the production of a library of C595 scFv mutants was the optimisation of the mutagenesis protocol. It was desired to achieve a mutation rate that produced a library containing multiple mutations in the scFv gene, since such multiple mutations are more likely to lead to complex combinatorial changes in the structure of the expressed protein. As described in chapter 2 of this thesis, the power of selection techniques lies in the enrichment of rare clones exhibiting enhanced activities as a result of these combinatorial effects. The PCR-based mutagenesis was conducted as described in chapter 3 of this thesis.

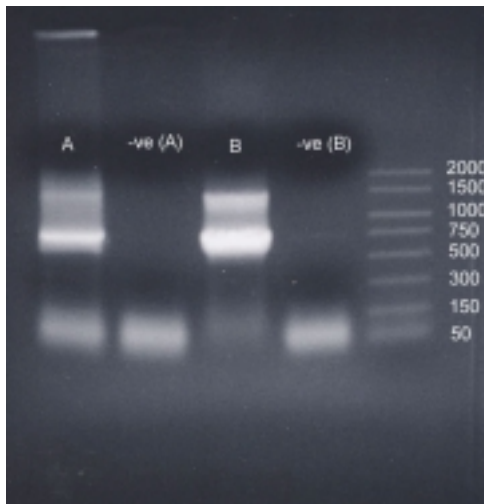


Figure 7.16: An agarose gel comparing the reaction products of a PCR amplification of the C595 scFv gene conducted using normal non-mutagenic conditions (Lane A), with a PCR reaction using mutagenic buffer conditions (Lane B). Negative controls were also run alongside the PCR reactions, in which the template DNA (pCANTAB 5E plasmid containing C595 scFv gene) was omitted. Reaction conditions were as described in chapter 3, 30 PCR cycles were used.

From the agarose gel in figure 7.x it can be seen that both of the PCR reactions produce bands ~750 bp, and a second fainter band ~1500 bp (see section 7.4.2). The main band at ~750 appears more diffuse for the mutagenic PCR than for the non-mutagenic PCR.

The PCR was repeated for the mutagenic PCR reaction using only 5 amplification cycles (as in section 7.4.2).

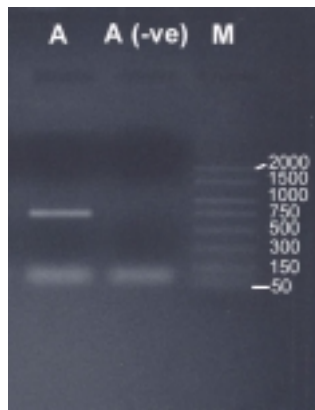


Figure 7.17: Agarose gel of PCR product under mutagenic conditions, employing only 5 amplification cycles. The lane marked A contains the product of the PCR reaction, and the lane marked B contains the products of the negative control reaction, consisting of a PCR in which the template DNA (pCANTAB 5E containing scFv) was omitted.

From the agarose gel it appears that 5 cycles of PCR under mutagenic reaction conditions produce a DNA fragment of the expected size.

The PCR product was excised from the agarose gel and cloned into the pCR 2.1 vector in the TOPO-TA cloning system. This enables individual clones to be isolated – i.e. only one piece of mutated DNA will be present in the plasmid of a transformed cell, enabling sequencing of the particular PCR fragment. *E.coli*. TOP10 cells were transformed with the pCR 2.1 plasmid containing the library of mutated scFv genes. The transformed cells were plated out onto LB plates containing ampicillin. 29 colony picks were taken from the plate and suspended in 10 µl of LB media. 1 µl of the sample was used in a PCR using M13 For and M13 Rev primers. A negative control consisted of a PCR on a pick from an area of the plate in which no colonies were present.

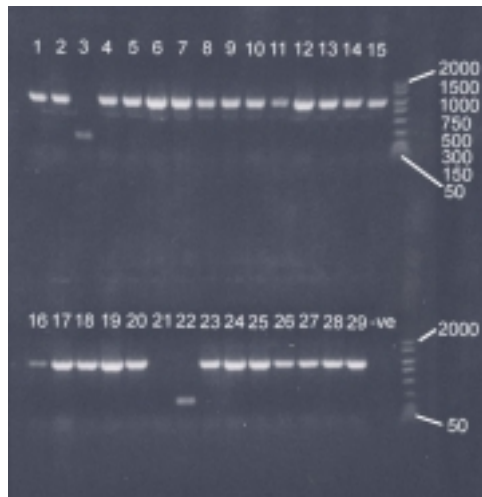


Figure 7.18: PCR analysis of a number of error-prone PCR clones showing the majority have inserts corresponding to the size of the scFv amplification product.

Colony numbers 1, 2, 4, 5, 6 and 7 were grown up overnight in 5 ml of LB media containing 100 µg/ml at 37°C with agitation at 250 rpm. Plasmid preps for each of the clones were prepared as described in chapter 3.

7.8.2 Sequence analysis of C595 scFv mutants

Figure 7.19 illustrates where the mutations occurred in the error-prone PCR clones. It can be seen that the mutations consist of a mixture of transversions (C-G) and transitions (T-C or T-G).

An average mutation rate of 16.5 mutations per scFv gene was obtained.

Figure 7.19: Over page, illustrating the position and frequency of mutations in six selected scFv genes.

scFv CTT TTC TAT GCG GCC CAG CCG GCC ATG GCC CAG GTC CAA CTG CAG CAG TCA GGG GGA GGC TTA GTG CAG CCT GGA GGG TCC CTG AAA CTC TCC TGT GCA GCC
 MUT1 C A A C A
 MUT2 G A C
 MUT4 G C A
 MUT5 G A C T A
 MUT6
 MUT7
 TCT GGA TTC ACT TTC AGT AGC TAT GGC ATG TCT TGG GTT GCG CAG ACT CCA GAC AAG AGG CTG GAG TTG GTC GCA ACC ATT AAT AGT AAT GGT GGT AGC ACC TAT TAT
 A G G C T G C A
 T T T A C G C G
 CCA GAC AGT GTG AAG GGC CGA TTC ACC ATC TCC AGA GAC AAT GCC AAC ACC CTG TAC CTG CAA ATG AGC AGT CTG AAG TCT GAG GAC ACA GCC ATG TAT TAC TGT GCA
 G T T T T A T G T T
 A T T T T C C G T
 AGA GAT CGG GAT GGT TAC GAC GAG GGA TTT GAC TAC TGG GGC CCA GGC ACC ACG GTC ACC GTC TCC TCA **GGT GGA GGC GGT TCA CGC GGA GGT GGC TCT GGC GGT**
 T T A A A A A
 G A A A T C A
GGC GGA TCG GAC ATC GAG CTC ACT CAG TCT TCA ATC ATG TCT GCA TCT CCA GGG GAG AAG GTC ACC ATG ACC TGC AGT GCC AGC TCA AGT GTA AGT TAC ATG CAC TGG
 - A C G T A T
 TAC CAG CAG AAG TCA GGC ACC TCC CCC AAA AGA TGG ATT TAT GAC ACA TCC AAA CTG GCT TCT GGA GTC CCT GCT CGC TTC AGT GGC AGT GGG TCT GGC ACC TCT TAC
 C N N T T A G G
 T T T C A G A
 TCT CTC ACA ATC AGC AGC ATG GAG GCT GAA GAT GCT GCC ACT TAT TAC TGC CAG CAG TGG AGT AGT AAC CCA CCC ACG TTC GGA GGG AGG ACC AAG CTG GAG CTG AAA
 T G A G T

7.9 Summary and Discussion

The advantages associated with the use of genetically engineered antibody fragments (scFv) for use in cancer therapy were outlined. These advantages included better tumour penetration, rapid clearance from the circulation resulting in enhanced tumour: normal organ ratios, and the fact that such species are potentially less immunogenic than whole antibodies. However the key disadvantage described, was the decrease in retention time compared to whole antibodies as a result of the loss of the avidity effect which is present in the whole antibody.

The existence of an “affinity ceiling” was described for antibodies produced during a normal immune response. It was stated that the use of scFv fragments for cancer therapy, which were derived from such an immune response, would require significant improvements in their affinity for the target antigen to be of clinical use. An example was given of the use of an *in vitro* method to enhance the affinity of a scFv for an antigen outside its natural environment.

This chapter described a novel method of isolating high affinity scFv clones reactive with tumour cells, by creating a scFv-GFP gene fusion which could be used in a phage display system. Selection of high-affinity binding clones from this library using FACS could enable the selection of scFv clones exhibiting a higher specific *in vivo* reactivity to tumour cells over normal cells. A scFv-GFP gene fusion was created and inserted into the pCANTAB-5E phagemid vector. A method was developed utilising error-prone PCR to introduce mutations into the scFv gene at an average rate of 16.5 mutations per gene (n=6). Small-scale expression experiments were conducted to determine whether it was possible to express soluble fusion protein. Significant levels of protein expression could not be detected using conventional ELISA techniques. Peptide epitope affinity chromatography was then used in an attempt to concentrate any expressed proteins which may have been present. Analysis of eluted fractions by ELISA, demonstrated a small peak above background, in identical fractions, for pCANTAB-5E clones containing (i) the C595 scFv gene alone and (ii) the scFv-GFP gene fusion. Protein could not be observed using agarose gel electrophoresis, after TCA precipitation of the fractions giving a signal above background.

The very low level of protein detected for both the scFv and the scFv-GFP gene fusion suggest that the low expression levels observed may not be the result of fusing scFv to the GFP. Levels of scFv expression have been detected in the past using this system at a rather low concentration of ~80 µg/ml (Denton, *et al.* 1997). However the production of soluble scFv using this system has proven to be highly problematic and unreliable (G Denton – Personal communication). Current strategies for the expression of soluble C595 scFv include the use of a pET expression vector utilising a more tightly controlled T7 RNA polymerase promoter in place of the rather “leaky” *lac* promoter. Protein expression in the pCANTAB-5E vector, under the regulation of the *lac* promoter, can occur (especially at higher temperatures) prior to induction with IPTG (see section 7.6.1). Such protein expression may be deleterious to cell growth and will thus result in a much-reduced yield of protein when the culture is induced, as a result of cell death. This is one possible explanation for the low yields of protein observed for both the scFv and the scFv-GFP gene fusion. The absence of expressed protein in the periplasmic and whole-cell extracts for clones containing the scFv and the scFv-GFP gene fusion add further support to this hypothesis. The use of other expression systems should be considered to find the optimum conditions for expression. R. Griep (Griep, *et al.* 1999) describe the use of a tetracycline promoter which can be induced at much lower temperatures (16°C) to produce scFv-GFP fusion proteins. Other expression systems could be considered for the production of the C595 scFv-GFP fusion protein such as insect cells or in other eukaryotic expression systems in which the folding and secretion of proteins is guided by more adequate chaperone proteins.

It is of note that peptide epitope affinity chromatography can be used as a tool for the determination of cloned gene expression at very low levels - as was demonstrated in this chapter. As outlined in chapter 1, and the results presented in chapters 5 and 6, peptide affinity chromatography offers the advantage of concentrating antibodies from feedstocks. The results presented in this chapter further emphasise the great utility of peptide epitope affinity chromatography as an analytical tool as well as a method of purification.

8 Chapter 8 - General Discussion and Future Work.

8.1 Introduction

Peptide epitope / peptide mimotope affinity chromatography was described as the method of choice in chapter 1, for the purification of monoclonal antibodies exhibiting high purity, high specific activity, and homogeneity from biological feedstocks. The major obstacle in the application of this technique for the purification of monoclonal antibodies, and the reason why this technique has not found more widespread use, was thought to be the extra work involved in tailoring specific affinity ligands for each monoclonal antibody to be purified. The extra effort involved may be thought unnecessary when one considers all of the other antibody purification techniques which are available and are described in chapter 1. However, none of the other techniques offer the unique advantages of paratope specific purification, which have been described and demonstrated in this thesis.

Chapter 2 described the various techniques available for the regulation of peptide epitope – antibody interactions. Polyvalent phage display using a T7 phage display system was chosen as a display system because it was thought this system could most closely simulate the presentation of ligands to the antibody in an affinity matrix

The results from chapter 4 and 5 demonstrated that it is possible to discover a novel peptide mimotope affinity ligand using phage display that functions as a more effective paratope-specific affinity ligand than the parent linear epitope sequence. It was demonstrated that using relatively simple selection procedures, it is possible to isolate phage displaying peptides, which when chemically synthesized exhibit higher affinity for the target antibody than the synthetic natural epitope sequence. Chapter 7 demonstrated the application of peptide epitope chromatography for the concentration of a novel scFvGFP fusion protein which was expressed at low levels in bacterial superantant.

8.2 Phage display of peptides

Phage display was used to discover novel peptide sequences that bound to the therapeutic monoclonal antibody C595. A number of biopanning experiments were

conducted using a T7 phage library (displaying ~415 copies of each peptide), with the anti-MUC1 mAb C595 and the anti-steroid hormone mAb 4155 as the target receptor. No enrichment of titer of eluted phage was observed when mAb 4155 was used as the target receptor. A 500-fold level of enrichment was observed when mAb C595 was used as the target receptor. Although no enrichment of phage titre was observed using the T7 library to screen for novel peptides reactive with mAb 4155, using a filamentous phage library (each phage also displaying hundreds of copies of each peptide), peptide sequences that bound to the antibody have been identified (see chapter 6). Clearly since both libraries were polyvalent- displaying a large number of peptides fused to the phage coat proteins, it appears that the number of peptides displayed using a particular system is not the only factor influencing the successful isolation of binding peptides. The two libraries are structurally distinct – in the T7 library 9-mer constrained peptides were displayed on the icosahedral capsid head (Rosenberg, *et al.* 1996); whereas filamentous bacteriophage such as f1 consist of a long cylindrical structure comprising of the pVIII coat protein (Kay, 1996). This difference in the supporting structure has a significant bearing on the arrangement of displayed peptides on the surface of the bacteriophage, and thus has a significant effect on how the peptides are presented to the target molecule.

These results illustrate how the choice of a particular phage type to display a peptide library has an important bearing on whether peptide sequences are isolated, and demonstrates the advantage of using several different types of library in the selection process.

Further experiments were then conducted to determine if the observed overall enrichment was the result of a specific growth advantage conferred to the phage (as a result of a displayed peptide sequence being beneficial to phage growth), or the selective enrichment of specific phage clones based on affinity. Analysis of phage populations from each of the four rounds of biopanning revealed that affinity-based enrichment was occurring, with eluted phage recovered from each round producing a much larger signal in a phage capture ELISA compared with naïve library and bacteriophage with no degenerate oligonucleotide insert. Using Surface Plasmon Resonance (SPR), the real-time binding of a phage clone displaying the **RXXP** motif, to immobilised mAb C595 was demonstrated.

Sequence analysis of the enriched phage clones revealed the emergence of two novel consensus motifs: **RXXP** and **RXP**. A possible third consensus motif of **RP** also emerged, but the two clones displaying peptides containing this motif were from separate experiments. A predominant peptide sequence of **RNREAPRGKICS** emerged in one experiment, with highest frequency in the third round of biopanning, reducing in the fourth round of biopanning. Sequence analysis of the phage clones from all rounds of biopanning, also revealed the extent of mutation occurring in the constant regions flanking the degenerate oligonucleotide insert. The majority of mutations were found to have occurred in the third round of biopanning, at the 5' flanking cysteine residue. This residue is closest to the capsid head of the phage particle. Only two mutations were detected at the 3' terminal cysteine residue.

The peak of mutation frequency at the 5' terminal cysteine residue was coincidental with the emergence of the **RNREAPRGKICS** peptide sequence displayed on the selected phage in round 3. The phage capture ELISA also demonstrated a peak at the third round of biopanning. This mutation could have potentially conferred a specific growth advantage to a particular phage clone displaying this sequence, enabling this clone to overtake the rest of the population. The use of ELISA experiments, could not alone determine whether the **RNREAPRGKICS** peptide was isolated as a result of affinity selection.

These results demonstrate that a T7 phage library can be used to discover novel peptide mimotopes and motifs not observed when using solid phase peptide libraries or filamentous phage libraries.

8.3 Analysis of peptides derived from phage display

Experiments conducted in chapter 5 were able to demonstrate that the phage-derived synthetic **RNREAPRGKICS** peptide was able to effectively bind mAb C595. When the mucin core peptide **APDTRPAPG** and the phage derived peptide **RNREAPRGKICS** were linked to beaded agarose a higher level of binding was observed for the phage derived peptide compared to the mucin core peptide.

Affinity chromatography was performed using the phage-derived peptide **RNREAPRGKICS** linked to beaded agarose and compared with affinity matrices using: (i) the mucin-core peptide **APDTRPAPG**; (ii) the mucin-core peptide with a terminal cysteine residue (to control for dimerisation) **APDTRPAPGC**, and (iii) the mucin-core peptide with a glutamic substitution (to control for binding being enhanced by the **REAP** mimotope alone) **APDTREAPG**. NaSCN gradient elution profiles of columns loaded with mAb C595 were compared. The elution profiles from the **APDTREAPG** and **APDTRPAPGC** matrices were identical in shape and size to the elution profile of the **APDTRPAPG** matrix. The maximum of the peaks in the elution of mAb C595 from the **APDTREAPG** and **APDTRPAPG** were directly in line in the gradient elution profile. The maximum of the peak from the elution of mAb C595 from the **APDTRPAPGC** matrix was further up the NaSCN gradient than any of the other maxima, this has previously been attributed to dimerisation of the peptide leading to an increased affinity (A. Murray, University of Nottingham – personal communication). The elution profile for the phage-derived peptide affinity matrix exhibited a sharp symmetrical peak, compared to the more broad, unsymmetrical peaks observed for the other peptide affinity matrices.

Antibody purified from hybridoma supernatant using the phage-derived peptide affinity matrix, exhibited a higher specific reactivity than antibody purified from hybridoma supernatant using the mucin-core peptide affinity matrix. SDS-PAGE analysis of the purified antibody from both matrices demonstrated that the antibodies were effectively purified from hybridoma supernatant, and contained no impurities. This result illustrates the huge potential of using phage display to discover novel paratope-specific peptide affinity ligands.

Affinity determination using fluorescence quenching analysis and structural analysis using circular dichroism, of the phage-derived peptide **RNREAPRGKICS**, the mucin-core peptide **APDTRPAPG**, and the related control peptides **APDTRPAPGC** and **APDTREAPG** revealed a profound correlation between structural content of the peptides and their relative equilibrium association constants. The peptides showed a structural content and equilibrium association constant in the following order:

RNREAPRGKICS > APDTREAPG > APDTRPAPGC > APDTRPAPG

These results were in agreement with the relative performances of the phage-derived peptide affinity matrix and the mucin-core peptide affinity matrix (i.e. Antibody recovered from the phage-derived peptide affinity matrix exhibited higher specific reactivity than antibody recovered from the mucin-core peptide affinity matrix).

The use of gradient elution using thiocyanate was demonstrated not to fit the pattern suggested by several authors (Pullen, *et al.* 1986; Macdonald, *et al.* 1988; Ferreira and Katzin 1995), for the interaction of mAb C595 with the phage derived peptide **RNREAPRGKICS**, the mucin core peptide **APDTRPAPG**, and the two control peptides **APDTREAPG** and **APDTRPAPGC**. These authors suggest that the tolerance of an antibody-antigen interaction to thiocyanate elution is proportional to the strength of the antigen-antibody interaction. From these results it is not clear why this should be the case. Other authors have also demonstrated that only a relatively low concentration of sodium thiocyanate is required to elute antibody from an affinity matrix in high yield (Murray, *et al.* 2001). Analysis of the kinetics of the interaction between the antibody with the mimotope peptide presented in this publication yielded an association equilibrium constant (K_A) = $\sim 10^8 \text{ M}^{-1}$. Compare this value with that determined for the interaction of mAb C595 with the epitope peptide **APDTRPAPG**, where $K_A = \sim 10^6 \text{ M}^{-1}$. The kinetics of the interaction between the peptides described above and mAb C595 merit a more in-depth kinetic analysis using SPR to determine on and off rates, to gain more information regarding the interaction of these peptides with the antibody.

Analysis of the interaction of mAb C595 with immobilised mucin-core peptide **APDTRPAPG** using a BIAcore biosensor gave an equilibrium association constant approximately 20x the value observed in the solution phase FQ assay. This can be attributed to the reduction in entropy of the immobilised peptide compared to the solution-phase peptide. This increased equilibrium association constant is likely to be reflected in the real value observed on the peptide affinity matrix. Thus the FQ assay can be used to give relative affinities of the respective ligands, but the actual equilibrium constants on the column are likely to be higher as a result of the reduction in entropy of the immobilised peptide compared to the solution-phase peptide.

The equilibrium association constant for the interaction of mAb C595 with the MUC1 related peptide **CPAHGVTSAPDTRPAPGSTAP** has been determined using a BIAcore biosensor (Karanikas, *et al.* 1998). The value ($K_A = 5.6 \times 10^6 \text{ M}^{-1}$) is of the same order of magnitude as the value obtained in the interaction of the mucin core peptide **APDTRPAPG** ($3.41 \times 10^6 \text{ M}^{-1}$) using the Langmuir model of binding. The author does not describe any optimisation process for immobilising the ligand onto the sensor chip. The only information given regarding the immobilisation process is the chemistry used (NHS/EDC). The larger value is likely to be the result of immobilising too great a quantity of peptide onto the sensor chip, the result being that re-binding of antibody can occur, reducing the value measured for k_d , resulting in a higher value for K_A . Only one antibody concentration was used to determine the affinity constant in the published data.

These results suggest affinity selection played a part in the selection of the phage-derived peptide **RNREAPRGKICS** in the four rounds of biopanning. The fact that all of the nucleotides were identical for all of the phage clones displaying the **RNREAPRGKICS** peptide, does not prove that these clones were selected as a result of a particular growth advantage conferred to the phage as a result of the mutation of the 5' terminal cysteine residue. Measurements of the initial phage titer indicated that 311 copies of each clone would be displayed per ml of phage lysate. A 2.5 ml aliquot of phage lysate was used in the biopanning process, which equates to 777 copies of each phage clone. It is conceivable that a single clone that had acquired a point mutation could be propagated in the amplification stages of the propagation process and be selected for enhanced affinity.

In summary phage display was used to discover a novel peptide mimotope reactive with mAb C595, exhibiting an enhanced affinity and increased structural content compared to the mucin core peptide **APDTRPAPG**. The application of the novel mimotope peptide in peptide mimotope affinity chromatography demonstrated an improved chromatographic performance compared to peptide epitope chromatography using the mucin core peptide (i.e. antibody purified using the mimotope peptide exhibited a higher specific reactivity than antibody purified using the epitope peptide).

8.4 Mimotope peptides cross reactive with an anti-steroid hormone antibody

Chapter 6 illustrated how, using a combination of phage display and small peptide libraries, the equilibrium association constant (K_A) for a weakly binding synthetic peptide (the sequence selected from a phage library) could be enhanced by employing a systematic optimisation methodology, to yield a novel peptide mimotope exhibiting an increased equilibrium association constant (K_A). (An improved method for screening small synthetic peptide libraries using a competitive approach to measure binding was also demonstrated.) The optimised mimotope peptide was capable of purifying monoclonal antibodies from biological feedstocks. Furthermore the target antibody was an antibody raised against a non-proteinaceous molecule – estriol-3-glucouronide - a metabolite of the steroid hormone estrone.

In an example given by Meloen, *et al.* (2000), the affinity of a weak-binding phage-displayed mimotope peptide for a monoclonal antibody (anti-glucoseoxidase) was also enhanced through a process of optimisation using small synthetic peptide libraries to produce a higher affinity ligand capable of functioning as an affinity ligand for use in the paratope-specific purification of monoclonal antibodies. Note that the antibody was raised against a proteinaceous target. The results in chapter 6 demonstrated that a similar process applied to a weak-binding mimotope peptide reactive with a monoclonal antibody raised against a non-proteinaceous target molecule, can be used to produce a small peptide exhibiting enhanced affinity, which can be used as a paratope-specific affinity ligand for the purification of monoclonal antibodies.

This result is completely unique, no other publications describing the use of a synthetic peptide to purify a monoclonal antibody against a non-proteinaceous ligand were discovered at the time of writing.

An empirical analysis of the equilibrium association constants for the interactions of the phage-derived mimotope peptide, the optimised peptide and estrone, demonstrated that the optimisation process had resulted in a peptide displaying an increased equilibrium association constant over the phage-derived mimotope peptide. The

results from an inhibition ELISA were in agreement with the results from the previous assay to determine the relative K_A values for the peptides. The results of the inhibition ELISA also demonstrated that the phage-derived mimotope peptide and the optimised peptide bound specifically to the paratope of mAb 4155 – the anti-E-3-G antibody.

Chapter 6 also demonstrated the application of peptide mimotopes in an assay to determine the free concentration of E-3-G in solution. The use of a peptide mimotope possessing a lower equilibrium association constant (K_A) in the interaction with antibody than the target antigen, was demonstrated to be of utility by enabling the sensitivity of a competition assay to be increased.

Fluorescence quenching could not be conducted using mAb 4155, since the peptide mimotopes contained aromatic amino acid residues essential for binding, masking any observable quenching effects.

The interaction of mAb 4155 with a BSA-conjugate of the optimised peptide mimotope ((d) **DYFLG**) was conducted using Surface Plasmon Resonance. An equilibrium association rate constant (K_A) of order of magnitude 10^8 M^{-1} . Was obtained for the interaction. The effect of temperature on the interaction was also investigated. Increasing the temperature in the range 10°C to 30°C was found to lead to an increase in the on-rate (k_{on}), and a decrease in the off-rate (k_{off}), resulting in an increase in the equilibrium association rate constant (K_A) with increase in temperature. This could be the result of the peptide adopting a more favourable high-energy conformation at the higher temperatures, or the more effective elimination of water from hydrophilic regions around the binding pocket.

In summary, the ability to produce a peptide ligand that is capable of purifying monoclonal antibodies raised against a non-proteinaceous analyte is a significant achievement. No other examples of using a peptide ligand to purify monoclonal antibodies using peptide mimotope affinity chromatography have been found in the research literature at the time of writing. The advantages of using paratope-specific peptide mimotope affinity chromatography for the purification of antibodies from biological feedstocks were outlined in chapter 1. The use the peptide ligand in place

of estrone (which has previously been used as an affinity ligand for the purification of mAb 4155), means that use of a competitive elution procedure in the purification protocol (see section 1.5.3.4) can be eliminated. The use of a peptide ligand in place of estrone also has advantages in terms of the cost of matrix production, and simplification of the ligand immobilisation chemistry. The use of (d) amino acid residues in place of the naturally occurring (l) amino acid residues should also improve the stability of the peptide to proteolysis in biological feedstocks.

Peptide mimotopes could also provide valuable reagents for use in biosensors which measure non-protein analytes, offering advantages in terms of stability, reproducibility, and the ability to fine-tune the antibody recognition process for a particular assay requirement (e.g. qualitative or quantitative assays).

8.5 Towards the production of scFv-GFP fusion protein

The advantages associated with the use of genetically engineered antibody fragments (scFv) for use in cancer therapy were outlined. These advantages included potentially enhanced tumour penetration, rapid clearance from the circulation resulting in enhanced tumour: normal organ ratios, and the fact that such species are potentially less immunogenic than whole antibodies. However the key disadvantage described, was the decrease in retention time compared to whole antibodies as a result of the loss of the avidity effect which is present in the whole antibody. It was also noted that higher affinities may also lead to reduced penetration into the tumour as a result of strong binding to tumour markers expressed on the cell surface. The work in chapter 7 set out to produce a scFv-GFP fusion protein which could be used as a tumour marker and used to generate a higher affinity scFv molecule.

The existence of an “affinity ceiling” was described for antibodies produced during a normal immune response. It was stated that the use of scFv fragments for cancer therapy, which were derived from such an immune response, would require significant improvements in their affinity for the target antigen to be of potential clinical use. A novel method was described, using an *in vitro* method to enhance the affinity of a scFv for an antigen in its natural environment. By creating a scFv-GFP gene fusion that could be used in a phage display system, it was envisaged that

selection of high-affinity binding clones from this library using FACS could enable the selection of scFv clones exhibiting a higher specific *in vivo* reactivity to tumour cells over normal cells. A scFv-GFP gene fusion was created and inserted into the pCANTAB-5E phagemid vector. A method was developed utilising error-prone PCR to introduce mutations into the scFv gene at an average rate of 16.5 mutations per gene (n=6). Small-scale expression experiments were conducted to determine whether it was possible to express soluble fusion protein. Significant levels of protein expression could not be detected using conventional ELISA techniques.

Peptide epitope affinity chromatography was then used in an attempt to concentrate any expressed proteins which may have been present. Analysis of eluted fractions by ELISA, demonstrated a small peak above background, in identical fractions, for pCANTAB-5E clones containing (i) the C595 scFv gene alone and (ii) the scFv-GFP gene fusion. Protein could not be observed using agarose gel electrophoresis, after TCA precipitation of the fractions giving a signal above background.

The very low level of protein detected for both the scFv and the scFv-GFP gene fusion suggest that the low expression levels observed may not be the result of fusing scFv to the GFP. Levels of scFv expression have been detected in the past using this system at a rather low concentration of ~80 µg/ml (Denton, *et al.* 1997). However the production of soluble scFv using this system has proven to be highly problematic and unreliable (G Denton – Personal communication). Current strategies for the expression of soluble C595 scFv include the use of a pET expression vector utilising a more tightly controlled T7 RNA polymerase promoter in place of the rather “leaky” *lac* promoter. Protein expression in the pCANTAB-5E vector, under the regulation of the *lac* promoter, can occur (especially at higher temperatures) prior to induction with IPTG (see section 7.6.1). Such protein expression may be deleterious to cell growth and will thus result in a much-reduced yield of protein when the culture is induced, as a result of cell death. This is one possible explanation for the low yields of protein observed for both the scFv and the scFv-GFP gene fusion. The absence of expressed protein in the periplasmic and whole-cell extracts for clones containing the scFv and the scFv-GFP gene fusion add further support to this hypothesis. The use of other expression systems should be considered to find the optimum conditions for

expression. R. Griep (Griep, *et al.* 1999) describe the use of a tetracycline promoter which can be induced at much lower temperatures (16°C) to produce scFv-GFP fusion proteins. Other expression systems could be considered for the production of the C595 scFv-GFP fusion protein such as insect cells or in other eukaryotic expression systems in which the folding and secretion of proteins is guided by more adequate chaperone proteins.

It is of note that peptide epitope affinity chromatography can be used as a tool for the determination of cloned gene expression at very low levels - as was demonstrated in this chapter. As outlined in chapter 1, and the results presented in chapters 5 and 6, epitope affinity chromatography offers the advantage of concentrating antibodies from feedstocks. The results presented in this chapter further emphasise the great utility of peptide epitope affinity chromatography as an analytical tool as well as a method of purification.

8.6 Future work

The research undertaken in this thesis has met the majority of the aims and objectives originally described, but the research has highlighted areas for further investigation. The emergence of the phage-derived peptide **RNREAPRGKICS** reactive with mAb C595, and exhibiting a more highly-ordered structure and increased affinity compared to the mucin core peptide **APDTRPAPG** merits further study to investigate the structural effects of the other residues in the phage-derived sequence. A more rigorous investigation into the kinetics of the interactions of the peptides described in chapter 5 with mAb C595, using SPR to determine on- and off-rates could provide an insight into the validity of the technique of thiocyanate elution to gauge relative affinities for antibody-ligand interactions. SPR could also be used to provide a more detailed understanding of the kinetics involved in the optimisation process of lead peptide sequences derived from phage display, as described in chapter 6 of this thesis. Rate constants could be obtained for peptides isolated at each step of the optimisation process to assess the relative contribution of each optimisation step to the overall process. The results presented in this thesis highlighted a change in rate constants

observed with variation of temperature for the interaction of an antibody and a peptide mimotope. The implications of this variation with temperature for the performance of the affinity ligand would be of interest. The creation of a functional scFv-GFP fusion displayed on the surface of phage, as described in chapter 7, would be of great benefit – potentially enabling the selection of high-affinity binding scFv clones by selection *in vivo* (i.e. using whole cells as the target). Although the work described in chapter 7 focussed initially on the production of soluble scFv-GFP fusion protein, further experiments to assess whether such a fusion protein exhibiting both binding ability and fluorescence could be expressed on the surface of phage would be worthwhile. The assessment of other expression systems would also be a worthwhile endeavour, since the C595 scFv-GFP fusion protein could be a useful reagent in its own right, with potential for use in histopathology and tumour marker assays.

8.7 Summary

The work in this thesis has demonstrated some of the vast utility of peptide epitopes, peptide mimotopes, antibodies and antibody fragments. Peptide mimotopes / epitopes find application in areas such as biosensors, affinity ligands and vaccines. To gain a greater understanding of how to discover such mimotopes is of fundamental importance to these areas. This thesis has demonstrated that using phage display alone or in tandem with small synthetic peptide libraries, it is possible to discover new molecules, and sets of molecules exhibiting a range of affinities suitable for many applications. The importance of using a number of different phage types when screening phage libraries was illustrated. A greater insight into the processes occurring when a phage library is screened for binders has been presented, demonstrating that mutagenesis of the library upon successive rounds of propagation is not necessarily a bad thing. This thesis also presents part of the work which was undertaken by a team investigating the processes involved in the discovery of novel mimotopes cross reactive with an anti-steroid hormone antibody. This is the first case such a mimotope has been described. The work in this thesis also demonstrated how peptide epitope affinity chromatography can be used as a tool for the detection of low levels of protein in bacterial supernatant.

9 Chapter 9 - Bibliography.

Amersham Pharmacia Biotech. (2000). Multi-step purification strategies. Antibody Purification Handbook. Uppsala, Sweden: 63-67.

Agadjanyan, M., Luo, P., Westerink, M.A.J., Carey, L.A., Hutchins, W., Steplewski, Z., Weiner, D.B., Kieber-Emmons, T. (1997). Peptide mimicry of carbohydrate epitopes on human immunodeficiency virus. *Nat. Biotech.* 15: 547-551.

Aoki, T., Takahashi, Y., Koch, K., Leffert, H.L., Wantabe, H. (1996). Construction of a fusion protein between protein A and green fluorescent protein and its application to Western blotting. *FEBS LETT* 384: 193-197.

Arai, R., Ueda, H., Nagamune, T. (1998). Construction of chimeric proteins between protein G and Fluorescence enhanced green fluorescent protein and their application to immunoassays. *J. Ferment. Bioeng.* 86(5): 440-445.

Arai, R., Ueda, H., Tsumoto, K., Mahoney, W., C., Izumi, K., Nagamune, T. (2000). Fluorolabeling of antibody variable domains with green fluorescent protein variants: application to an energy transfer - based homogeneous immunoassay. *Protein Eng.* 13(5): 369-376.

Bacher, J., M. and Ellington, A., D. (1998). Nucleic acid selection as a tool for drug discovery. *Drug Discov. Today* 3(6): 265-273.

Badley, R.A., Berry, M.J., Howell, S. (1999). Improvements in or relating to displacement assays. International Patent WO 99/27368.

Badley, R.A., Berry, M.J., Porter, P., Wattam, T. (1999a). Recovery of and uses of specific binding agents. US Patent US005989926A.

Badley, R.A., Berry, M.J., Williams, S.C. (2000). Peptides capable of functioning as mimotopes for estradiol analytes. International Patent WO 02/12270 A1.

BIAcore (1997). BIAevaluation software handbook. Version 3.0, Biacore AB, Uppsala, Sweden.

Chapter 9 - Bibliography.

BIAcore (1997a). PIONEER Sensor Chip F1 - Instructions for use. Biacore AB, Uppsala, Sweden.

Boder, E., T. and Wittrup, K., D. (1997). Yeast surface display for screening combinatorial polypeptide libraries. *Nat. Biotech.* 15(6): 553-557.

Boldicke, T., Struck, F., Schaper, F., Tegge, W., Sobek, H., Villbrandt, B., Lankenau, P., Bocher, M. (2000). A new peptide-affinity tag for the detection and affinity purification of recombinant proteins with a monoclonal antibody. *J. Immunol. Methods* 240: 165-183.

Briggs, S., Price, M.R., Tendler, S.J.B. (1993). Fine Specificity of Antibody Recognition of Carcinoma-associated Epithelial Mucins: Antibody Binding to Synthetic Peptide Epitopes. *Eur. J. Cancer* 29A(2): 230-237.

Cadwell, R.C., Joyce, G.F. (1994). Mutagenic PCR. *PCR Meth. Appl.* 36: S136-S140.

Campbell, A.P., Sykes, B.D. (1993). The 2-dimensional transferred nuclear overhauser effect -theory and practice. *Annu. Rev. Bioph.. Biom.* 22: 99-122.

Casey, J.L., Coley, A.M., Tilley, L.M., Foley, M. (2000). Green Fluorescent Antibodies: novel in vitro tools. *Protein Eng.* 13(6): 445-452.

Chaiken, I., Rose, S., Karlsson, R. (1992). Analysis of macromolecular interactions using immobilized ligands. *Anal. Biochem.* 201: 197-210.

Chaiken, I., Myszka, D., Morton, T. (1996). New Opportunities for using ligands to characterize macromolecular recognition and design recognition molecules. *Adv. Mol. Cell Biol.* 15B: 553-568.

Chamow, S.M. and Ashkenazi, A. (1999). Antibody fusion proteins. Wiley-Liss Inc. New York 1-12.

Chapter 9 - Bibliography.

Chen, G., Hayhurst, A., Thomas, J.G., Harvey, B.R., Iverson, B.I., Georgiou, G. (2001). Isolation of high-affinity ligand-binding proteins by periplasmic 24 expression with cytometric screening (PECS). *Nat. Biotech.* 19(6): 537-542.

Chowdhury, P.S. and Pastan, I. (1999). Improving antibody affinity by mimicking somatic hypermutation in vitro. *Nat. Biotech.* 17(6): 568-572.

Christian, R.B., Zuckermann, R.N., Kerr, J.M., Wang, L., Malcolm, B.A. (1992). Simplified methods for construction, assessment, and rapid screening of peptide libraries in bacteriophage. *J. Mol. Biol.* 227: 711-718.

Clackson, T. and Wells, J.A. (1994). In vitro selection from protein and peptide libraries. *Trends Biotechnol.* 12(5): 173-188.

Coen, D. M. (1991). *The Polymerase Chain Reaction*, Wiley Interscience, New York.
Current Protocols in Molecular Biology. Wiley Interscience. New York.

Colas, P. and Brent, R. (1998). The impact of two hybrid and related methods on biotechnology. *Trends Biotechnol.* 16: 355-363.

Cormack, B.P., Valdivia, R.H., Falkow, S. (1996). FACS-optimized mutants of the green fluorescent protein (GFP). *Gene* 173: 33-38.

Cull, M.G., Miller, J.F., Schatz, P.J. (1992). Screening for receptor ligands using large libraries of peptides linked to the C terminus of the lac repressor. *Proc. Natl. Acad. Sci. USA* 89(3): 1865-1869.

Cunun, F., Schmedake, T.A., Link, J.R., Chin, V., Koh, J., Bhatia, S., Sailor, M.J. (2002) Optically encoded nanoporous silicon particles for biological screening applications. *Proceedings of 3rd International Conference, Porous Semiconductors – Science and Technology*. Puerto de la Cruz, Spain.

Chapter 9 - Bibliography.

Cwirla, S.E., Peters, E.A., Barret, R.W., Dower, W.J. (1990). Peptides on phage: a vast library of peptides for identifying ligands. *Proc. Natl. Acad. Sci. USA* 87: 6378-6382.

Dalcol, L., Pons, M., Ludevid, M.D., Giralt, E. (1996). Convergent synthesis of repeating peptides (Val-X-Leu-Pro-Pro-Pro)₈ adopting a polyproline II conformation *J. Org. Chem.* 61(20): 6775-6782.

Danielsson, A., Ljunglof, A., Lindblom, H. (1988). One-step purification of monoclonal IgG antibodies from mouse ascites - an evaluation of different adsorption techniques using high-performance liquid-chromatography *J. Immunol. Methods* 79: 115.

Daugherty, P.S., Chen, G., Olsen, M.J., Iverson, B.L., Gergiou, G. (1998). Antibody affinity maturation using bacterial surface display. *Protein Eng.* 9(11): 825-832.

Daugherty, P.S., Chen, G., Iverson, B.L., Gergiou, G. (1999). Quantitative analysis of the effect of the mutation frequency of the affinity maturation of single chain Fv antibodies. *Proc. Natl. Acad. Sci. USA* 97(5): 2029-2034

Dean, P.D.G., Johnson, W.S., Middle, F.A. (1985). *Affinity Chromatography - a practical approach.* IRL Press Washington DC.

Denton, G., Davies, G.M., Scanlon, M.J., Tendler, S.J.B., Price, M.R. (1995). Primary sequence determination and molecular modelling of the variable region of an anti-MUC1 mucin monoclonal antibody. *Eur. J. Cancer* 31A(2): 214-221.

Denton, G., Sekowski, M., Spencer, D.I.R., Murray, A., Hughes, O.D.M., Price, M.R. (1997). Production of a recombinant anti-MUC1 mucin scFv. Properties and comparison with the parental monoclonal antibody. *Brit. J. Cancer* 76 (5): 614-621.

Denton, G., Brady, K., Lo, B.K.C., Murray, A., Graves, R.L., Hughes, O.D.M., Tendler, S.J.B., Laughton, C.A., Price, M.R. (1999). Production and characterization

Chapter 9 - Bibliography.

of an anti-(MUC1 mucin) recombinant diabody. *Cancer Immunol. Immun.* 48(1): 29-38.

Denton, G., Murray, A., Simms, M., Smith, R.G., Perkins, A., Price, M.R. (1999a). Purification of immunoreactive antibody for clinical use by peptide epitope affinity chromatography. *Br. J. Cancer.* 80:p95 Suppl 2.

Denton, G., Murray, A., Price, M.R., Levison, P.R. (2001). Direct isolation of monoclonal antibodies from tissue culture supernatant using cation-exchange cellulose Express-Ion S. *J. Chrom. A.* 908: 223-234.

Devlin, J.J., Panganiban, L.C., Devlin, P.E. (1990). Random peptide libraries: a source of specific protein binding molecules. *Science* 249: 404-406.

Dixon, A.R., Price, M.R., Hand, C.W., Sibley, P.E.C., Selby, C., Bramey, R.W. (1993). Epithelial mucin core antigen (EMCA) in assessing therapeutic response in advanced breast-cancer - a comparison with CA15.3. *Brit. J. Cancer* 68(5): 947-949.

Dougan, D.A., Malby, R.L., Gruen, L.C., Kortt, A.A., Hudson, P.J. (1998). Effects of substitutions in the binding surface of an antibody on antigen affinity. *Protein Eng.* 11(1): 65-74.

Edwards, P. (1999). The Use of optical Biosensors for Kinetic Analysis: A Critical Appraisal. PhD Thesis. Department of Chemistry, Imperial College of Science, Technology and Medicine, London.

Efimov, V.P., Nepluev, I.V., Mesyanzhinov, V.V. (1995). Bacteriophage T4 as a surface display vector. *Virus Genes* 10: 173-177.

Farlie, D.P, West, M.L., Wong, A.K. (1998). Towards protein surface mimetics. *Curr. Med. Chem.* 5: 29-62.

Fassina, G., Verdoliva, A., Odierna., M.R., Ruvo, M., Cassini., G (1996). Protein A mimetic ligand for affinity purification of antibodies. *J. Mol. Recognit.* 9: 564-569.

Chapter 9 - Bibliography.

Felici, F. (1991). Selection of antibody ligands from a large library of oligopeptides expressed on a multivalent exposition vector. *J. Mol. Biol.* 222: 301-310.

Felici, F., Luzzago, A., Folgori, A., Cortese, R. (1993). Mimicking of discontinuous epitopes by phage-displayed peptides, II. Selection of clones recognized by a protective monolonal antibody against the *Bordetella pertussis* toxin from phage peptide libraries. *Gene* 128: 21-27.

Ferreira, M.U. and Katzin, A.M. (1995). The assessment of antibody affinity distribution by thiocyanate elution: a simple dose-response approach. *J. Immunol. Methods* 187: 297-305.

Fields, S. and Song, O. (1989). A novel genetic system to detect protein protein interactions. *Nature* 340: 245-246.

Fitzgerald, K. (2000). In vitro display technologies – new tools for drug discovery. *Drug Discov. Today* 5(6): 253-258.

Foote, J. and Eisen, H.N. (1995). Kinetic and affinity limits on antibodies produced during immune responses. *Proc. Natl. Acad. Sci. USA* 92(February): 1254-1256.

Forsgren, A. and Sjoquist, J.J (1966). Protein A from *S. aureus*. I. Pseudo-immune reaction with g-globulin. *Immunology* 97: 822-827.

Fox, S. (2000). Biovation's human-antibody display technology - Identification of antibody-antigen binding at the protein level. *Genet. Eng. News* 20(6): 22-.

Francisco, J.A. and Georgiou, G. (1994). The expression of recombinant proteins on the external surface of *Escherichia coli*. *Ann. NY Acad. Sci* 745: 372-382.

Gama, L. and Breitwiser, G.E. (1999). Generation of epitope tagged proteins by inverse PCR mutagenesis. *Biotechniques* 26(5): 814-816.

Chapter 9 - Bibliography.

Gendler, S., Taylor-Papadimitriou, J., Duhig, T., Rothbard, J., Burchell, J. (1988). A highly immunogenic region of human polymorphic epithelial mucin expressed by carcinomas is made up of tandem repeats. *J. Biol. Chem.* 263: 12820-12823.

Getzoff, E.D., Tainer, J.A., Lerner, R.A., Geysen, H.M. (1988). The chemistry and mechanism of antibody-binding to protein antigens. *Adv. Immunol*(43): 1-98.

Geysen, H.M., Rodda, S.J., Mason, T.J., Tribbick, G., Schoofs, P.G. (1987) Strategies for epitope analysis using peptide synthesis. *J. Immunol. Methods* 102: 259-274.

Giebel, L.B., Cass, R.T., Milligan, D.L., Young, D.C., Arze, R., Johnson, C.R. (1995). Screening of cyclic peptide phage libraries identifies ligands that bind streptavidin with high affinity. *Biochemistry* 34: 15430-35.

Gram, H., Marconi, L.A., Barbas III, C.F., Collet, T.A., Lerner, R.A., Kang, A.S. (1992). In vitro selection and affinity maturation of antibodies from a naive combinatorial immunoglobulin library. *Proc. Natl. Acad. Sci. USA* 89: 3576-3580.

Griep, R.A., vanTwisk, C., van der Wolf, J.M., Schots, A. (1999). Fluobodies: green fluorescent single-chain Fv fusion proteins. *J. Immunol. Methods* 230(1-2): 121-130.

Guichard, G., Benkirane, N., Zeder-Lutz, G., Van Regenmortel, M.H.V., Biand, J., Muller, S. (1994). Antigenic mimicry of natural L-peptides with retro-inverso-peptidomimetics *Proc. Natl. Acad. Sci. USA* 91: 9765-9769.

Hagihara, M., Anthony, N.J., Stout, T.J., Clardy, J., Schreiber, S. (1992). Vinylogous polypeptides - an alternative peptide backbone. *J. Am. Chem. Soc.* 114: 6568-6570.

Han, M., Gao, X., Su., J.Z., Nie, S. (2001) Quantum-dot-tagged microbeads for multiplexed optical coding of biomolecules. *Nature Biotech.* 19: 631-635.

Hanes, J., Jermutus, L., Weber-Bornhauser, S., Bosshard, H.R., Pluckthun, A. (1998). Ribosome display efficiently selects and evolves high-affinity antibodies in vitro from immune libraries. *Proc. Natl. Acad. Sci. USA* 85: 14130-14135.

Chapter 9 - Bibliography.

Hansson, M., Stahl, S., Hjorth, R., Uhlen, M., Moks, T. (1991). *Bio/Technology* 12: 285-288

Harris, B. (1999). Exploiting antibody-based technologies to manage environmental pollution. *Trends Biotechnol.* 17(July): 290-296.

Hawkins, R.E., Russell, S.J., Winter, G. (1992). Selection of phage antibodies by binding affinity. Mimicking affinity maturation. *J. Mol. Biol* 226: 889-886.

Hawkins, R.E., Russel, S.J., Baier, M., Winter, G. (1993). The Contribution of contact and non-contact residues of antibody in the affinity of binding to antigen. The interation of mutant D1.3 antibodies with lysozyme. *J. Mol. Biol* 234: 958-964.

Hink, M.A., Griep, R.A., Borst, J.W., van Hoek, A., Eppink, M.H.M., Schots, A., Visser, A.J.W.G. (2000). Structural dynamics of green fluorescent protein alone and fused with a single chain Fv protein. *J. Biol. Chem.* 275(23): 17556-17560.

Houghten, R.A., Pinilla, C., Blondelle, S.E., Appel, J.R., Dooley, C.T., Cuervo, J.H. (1991). *Nature* 354: 84-86.

Hudson, P., J (1999). Recombinant antibody constructs in cancer therapy. *Current Opinion In Immunology* 11(5): 548-557.

Hudson, P.J. and Kortt, A.A. (1999). High avidity scFv multimers; diabodies and triabodies. *J. Immunol. Methods* 231: 177-189.

Hughes, O.D.M., Perkins, A.C., Frier, M., Wastie, M.L., Denton, G., Price, M.R., Denly, H., Bishop, M.C. (2001). Imaging for staging bladder cancer: a clinical study of intravenous 111indium-labelled anti-MUC1mucin monoclonal antibody C595. *BJU Int.* 87: 39-46.

Jung, S., Honegger, A., Pluckthun, A. (1999). Selection for improved protein stability by phage display. *J. Mol. Biol.* 294: 163-180.

Chapter 9 - Bibliography.

Kay, B.K., Adey, N.B., He, Yun-Sheng., Manfredi, J.P., Mataragnon, A.H., Fowlkes, D.M. (1993). An M13 phage library displaying random 38-amino-acid peptides as a source of novel sequences with affinity to selected targets. *Gene*: 59-65.

Kay, B. (1996). Principles and Applications of Phage Display - Phage Display of Peptides and Proteins. A Laboratory Manual. Academic Press: 21-34.

Karanikas, V., Patton, K., Jamieson, G., Pietrsz, G., McKenzie, I. (1998). Affinity of antibodies to MUC1 antigens. *Tumor Biol.* 19(Suppl. 1): 71-78.

Katz, B., A (1997). Structural and mechanistic determinants of affinity and specificity of ligands discovered or engineered by phage display. *Annu. Rev. Bioph. Biom.* 27: 27-45.

Kendall, J.M. and Badminton, M.N. (1998) *Aequorea victoria* bioluminescence moves into an exciting new era. *Trends Biotechnol.* 16(5): 216-224.

Kerschbaumer, R.J., Hirschl, S., Schwager, C., Ibl, M., Himmler, G. (1996). pDAP2: a vector for construction of alkaline phosphatase fusion proteins. *Immunotechnology* 2: 145-150.

Kerschbaumer, R.J., Hirschl, S., Kaufmann, A., Ibl, M., Koenig, R., Himmler, G. (1997). Single-chain Fv fusion proteins suitable as coating and detecting reagents in a double antibody sandwich enzyme-linked immunosorbent assay. *Anal. Biochem.* 249: 219-227.

Kieber-Emmons, T. (1998). Peptide mimotopes of carbohydrate antigens. *Immunol. Res.* 17(1-2): 95-108.

Kohler, G. and Milstein, C. (1975). Continuous cultures of fused cells secreting antibody of predefined specificity. *Nature* 256: 495-497.

Chapter 9 - Bibliography.

Krammer, K. (1998). Synthesis of pesticide-specific single-chain F-V utilizing the recombinant phage antibody system (RPAS, pharmacia) - A detailed protocol. *Anal. Lett.* 31(1): 67-92

Laing, P., Tighe, P., Kwaitkowski, E., Milligan, J., Price, M.R., Sewell, H. (1995). Selection of peptide ligands for the antimucin core antibody C595 using phage display technology: definition of candidate epitopes for a cancer vaccine. *J. Clin. Pathol: Mol Pathol* 48: M136-M141.

Lam, K.S., Salmon, S.E., Hersh, E.M., Hruby, V.J., Kazmierski, W.M., Knapp, R.J. (1991) A new type of synthetic peptide library for identifying ligand-binding activity. *Nature* 354: 82-84.

Lewis, J.C., Feliciano, J., Daunert, S. (1999). Fluorescence binding assay for a small peptide based on a GFP fusion protein. *Anal. Chim. Acta.* 397: 279-286.

Li, R.X., Dowd, V., Stewart, D.J., Burton, S.J., Lowe, C.R. (1998). Design, synthesis and application of an artificial protein A. *Nature Biotech.* 16: 190-195.

Low, N.M., Holliger, P., Winter, G. (1996) Mimicking somatic hypermutation: affinity maturation of antibodies displayed on bacteriophage using a bacterial mutator strain. *J. Mol. Biol.* 260: 359-368.

Lu, Z., Murray, K.S., Van Cleave, V., LaVallie, E.R., Stahl, M.L., McCoy, J.M. (1995). Expression of thioredoxin random peptide libraries on the *Escherichia coli* cell surface as functional fusions to flagellin: a system designed for exploring protein-protein interactions. *Biotechnology* 13: 366-372.

Luzzago, A., Felici, F., Tramontano, A., Pessi, A., Cortese, R. (1993). Mimicking of discontinuous epitopes by phage-displayed peptides, I. Epitope mapping of human H ferritin using a phage library of constrained peptides. *Gene* 128: 51-57.

Chapter 9 - Bibliography.

Macdonald, R.A.C., Hosking, S., Jones, C.L. (1988). The measurement of relative antibody affinity by ELISA using thiocyanate elution. *J. Immunol. Methods* 106: 191-194.

Makeyev, E.V., Kolb, V.A., Spirin, A.S. (1999). Cell-free immunology: construction and in vitro expression of a PCR-based library encoding a single-chain antibody repertoire. *FEBS Lett.* 444: 177-180.

Maruyama, I.N., Maruyama, H.I., Brenner, S. (1994). Lambda foo: a lambda bacteriophage vector for the expression of foreign proteins. *Proc. Natl. Acad. Sci. USA* 91: 8273-8277.

May, K. (1994). The Unipath Personal Contraceptive System. Natural Contraception Through Personal Hormone Monitoring. Proceedings of a Symposium at the XIV FIGO World Congress of Gynecology and Obstetrics. Montreal, Canada. 35-44.

McConnell, S.J., Kendall, M.L., Reilly, T.M., Hoess, R.H. (1994). Constrained peptide libraries as a tool for finding mimotopes. *Gene* 151: 115-118.

Meloan, R.H., Puijk, W.C., Slootstra, J.W. (2000) Mimotopes: realization of an unlikely concept. *J. Mol. Recognit.* 13: (6) 352-359.

Missailidis, S., Cannon, W.V., Drake, A., Wang, X.Y., Buck, M. (1997). Analysis of the architecture of the transcription factor sigma (N) (sigma(54)) and its domains by circular dichroism. *Mol. Microbiol.* 24: 653.

Murray, A., Sekowski, M., Spencer, D., Denton, G., Price, M.R. (1997). Purification of monoclonal antibodies by epitope and mimotope affinity chromatography. *J. Chrom. A.* 782: 49-54.

Murray, A., Spencer, D.I.R, Missailidis, S., Denton, G., Price, M.R. (1998). Design of ligands for the purification of anti-MUC1 antibodies by peptide epitope affinity chromatography. *J. Peptide. Res.* 52: 375-383.

Chapter 9 - Bibliography.

Murray, A., Simms, M.S., Denton, G., Hughes, O.D.M., Price, M.R., Bishop, M.C., Perkins, A.C. (1999). Technicium-99m labelling of monoclonal antibody, C595 for bladder cancer immunoscintigraphy - Pre-clinical evaluation. *Eur. J. Canc.* 35(Suppl 4).

Murray, A., Perkins, A.C., Denton, G., Price, M.R. (2000). Delivery of radionuclides, toxins and drugs, in *Antibody Targeted Therapy* 105- 213. Kluwer Academic Publishers, Dordrecht, The Netherlands

Murray, A., O'Sullivan, D.A, Price, M.R. (2000). Synthetic peptides for the Analysis and Preparation of Antimucin Antibodies. *Glycoprotein Methods and Protocols: The Mucins*. Humana Press Inc., New Jersey. 125: 129-141.

Murray, A., Simms, M.S., Scholfield, D.P., Vincent, R.M., Denton, G., Bishop, M.C., Price, M.R., Perkins, A.C. (2001). Production and Characterisation of ¹⁸⁸Re-C595 Antibody for Radioimmunotherapy of Transitional Cell Bladder Cancer. *J. Nucl. Med.* 42: 726-732.

Murray, A., Smith, R.G., Brady, K., Willaims, S., Denton, G., Badley, R.A., Price, M.R. (2001a). Generation and refinement of peptide mimetic ligands for paratope-specific purification of monoclonal antibodies. *Anal. Biochemi* 296:(1) 9-17.

Myszka, D.G. (1999). Improving biosensor analysis. *J. Molec. Recog.* 12: 279-284.

Narhi, L.O., Caughey, D.J., Horan, T.P., Kita, Y., Chang, D., Arakawa, T. (1997). Fractionation and Characterization of Polyclonal Antibodies Using Three Progressively More Chaotropic Solvents. *Anal. Biochem.* 253: 246-252.

Needels, M.C., Jones, D.G., Tate, E.H., Heinkel, G.L., Kochersperger, L.M., Dower, W.J., Barrett, R.W., Gallop, M.A. (1993). Generation and screening of an onlignucleotide-encoded synthetic peptide library. *Proc. Natl. Acad. Sci. USA* 90: 10700-10704.

Chapter 9 - Bibliography.

Nygren, P., Stahl, S., Uhlen, M. (1994). Engineering proteins to facilitate bioprocessing. *Trends Biotechnol.* 12(May): 184-188.

Olsson, A. (1987). Structure and evolution of the repetitive gene encoding streptococcal protein G. *Eur. J. Biochem.* 168: 319-324.

Pearlson, A.S. and Oster, G.F. (1979). Theoretical studies of clonal selection: minimal antibody repertoire size and reliability of self-non-self discrimination. *J. Theor. Biol.* 81(645-670).

Perkins, A. (1993). Genetically-engineered immunoconjugates - a dosimetric dilemma. *Nucl. Med. Commun.* 14(12): 1047-1049.

Pinilla, C., Appel, J.R., Houghten, T.A. (1993) Functional importance of amino-acid residues making up peptide antigenic determinants. *Mol. Immunol.* 30: 577-585.

Pluckthun, A., Skerra, A. (1989) Expression of functional antibody Fv and Fab fragments in *E. coli*. *Methods Enzymol.* 178: 497-515.

Pollock, D.P., Kutzko, J.P., Birck-Wilson, E., Williams, J.L., Echelard, Y., Meade H. M. (1999). Transgenic milk as a method for the production of recombinant antibodies. *J. Immunol. Methods* 231: 147-157.

Price, M.R., Pugh, J.A., Hudecz, F., Griffiths, W., Jacobs, E., Symonds, I.M., Clarke, A.J., Chan, W.C., Baldwin, R.W. (1990). C595 - a monoclonal antibody against the protein core of human urinary epithelial mucin commonly expressed in breast carcinomas. *Brit. J. Cancer* 61: 681-686.

Price, M.R., Sekowski, M., Tandler, S.J.B. (1991). Purification of anti-epithelial mucin monoclonal antibodies by epitope affinity chromatography. *J. Immunol. Methods.* 139: 83-90.

Pullen, G.R., Fitzgerald, M.G., Hosking, C.S. (1986) Antibody avidity determination by ELISA using thiocyanate elution. *J. Immunol. Methods* 86: 83-87.

Chapter 9 - Bibliography.

Raman, C.S., Jemmerson, R., Nall, B.T., Allen, M.J. (1992) Diffusion-limited rates for monoclonal-antibody binding to Cytochrome-C. *Biochemistry* 31: 10370-10379.

Regenmortel, M.H.V., (1995) Transcending the structuralist paradigm in immunology - affinity and biological activity rather than purely structural considerations should guide the design of synthetic peptide epitopes. *Biomedical Peptides, proteins & Nucleic Acids* 1: 109-116.

Roberts, R.W and Szostak, J.W. (1997) RNA-peptide fusions for the in vitro selection of peptides and proteins. *Proc. Natl. Acad. Sci. USA* 94: 12297-12302.

Roberts, R.W. (1999) Totally in vitro protein selection using mRNA-protein fusions and ribosome display. *Curr. Opin. Chem. Biol.* 3: 268-273.

Rodi, D.J. and Makowski, L. (1999) Phage-display technology - finding a needle in a vast molecular haystack. *Curr. Opin. Biotech.* 10: 87-93.

Romig, T.S., Bell, C., Drolet, D.W. (1999). Aptamer affinity chromatography: combinatorial chemistry applied to protein purification. *J. Chrom. B.* 731: 275-284.

Rondot, S., Anthony, K.G., Dubel, S., Ida, N., Wiemann, S., Beyreuther, K., Frost, L.S., Little, M., Breitling, F. (1998) Epitopes fused to F-pilin are incorporated into functional recombinant pili. *J. Mol. Biol* 279: 589-603.

Rosenberg, A., Griffing, K., Studier, F.W., McCormick, M., Berg, J., Novy, R., Mierendorf, R. (1996). T7Select Phage Display System: A powerful new protein display system based on bacteriophage T7. *Innovations* 6(December): 1-6.

Rye, P.D. and Price, M.R. (1996) Tumor Biology From Basic Science to Clinical Application. Proceedings of ISOBM TD-4 international Workshop on Monoclonal Antibodies against MUC1, Sna Diego, Calif. S. Karger. 1-152

Chapter 9 - Bibliography.

Sambrook, J.E., Fritsch, F., Maniatis, T. (1989). *Molecular Cloning: a laboratory manual*, 2nd edn. Cold Spring Harbor, Newyork, Cold Spring Harbor Press.

Schaffitzel, C., Hanes, J., Jermutus, L., Pluckthun, A. (1999) Ribosome display: an in vitro method for selection and evolution of antibodies from libraries. *J. Immunol. Methods* 231: 119-135.

Schier, R., McCall, A., Adams, G.P., Marshall, K.W., Merritt, H., Yim, M., Crawford, R.S., Weiner, L.M., Marks, C., Marks, J.D. (1996) Isolation of picomolar Affinity Anti-c-erbB-2 Single-chain Fv by Molecular Evolution of the Complementarity Determining Regions in the Center of the Antibody Binding Site. *J. Mol. Biol* 263(4): 551-567.

Schuck, P. and Minton, A.P. (1996) Analysis of Mass Transport-Limited Binding Kinetics in Evanescent Wave Biosensors. *Anal. Biochem.* 240: 262-272.

Schwalbach, G., Sibler, A., Choulier, L., Derykere, F., Weiss, E. (2000) Production of Fluorescent Single-Chain Antibody Fragments in *Escherichia coli*. *Protein Express. Purif.* 18(2): 121-132.

Scopes, R.K. (1999) Longer is better - random elongation mutagenesis. *Nature Biotech.* 17:(1).

Scott, J.K. and G. Smith, P. (1990) Searching for peptide ligands with an epitope library. *Science* 249: 386-390.

Scott, J.K. (1992) Discovering peptide ligands using epitope libraries. *Trends Biochem Sci.* 17(7): 241-245.

Shimizu, M. and Yamauchi, K. (1982) Isolation and characterisation of mucin-like glucoprotein in human-milk fat globule-membrane. *J. Biochem.* 91(2): 515-524.

Chapter 9 - Bibliography.

Sibille, P., Ternynck, T., Nato, F., Buttin, G., Strosberg, D., Avrameas, A. (1997) Mimotopes of polyreactive anti-DNA antibodies identified using phage-display peptide libraries. *Eur. J. Immunol.* 27: 1221-1228.

Sieber, V., Pluckthun, A., Schmid, F.X. (1998) Selecting proteins with improved stability by a phage-based method. *Nature Biotech.* 16(10): 955.

Simms, M.S., Murray, A., Denton, G., Scholfield, D.P., Price, M.R., Perkins, A.C., Bishop, M.C. (2001) Production and characterisation of a C595 antibody- ^{99m}Tc conjugate for immunoscintigraphy of bladder cancer. *Urol. Res.* 29: 13-19.

Simon, R.J., Kania, R.S., Zuckermann, R.N., Huebner, V.D., Jewell, D.A., Banville, S., Ng S., Wang, L., Rosenberg S., Marlowe, C.K., Spellmeyer, D.C., Tan, R.Y., Frankel, A.D., Santi, D.V., Cohen, F.E., Bartlett, P.A. (1992) Peptoids - a modular approach to drug discovery. *Proc. Natl. Acad. Sci. USA* 89: 9367-9371.

Smith, G.P. and Petrenko, V.A. (1997) Phage Display. *Chem. Rev.* 97: 391-410.

Smith, R.G. and Price M.R. (2000). Discovery of novel mimotopes using polyvalent phage display technology - their use in peptide mimotope affinity chromatography. *Downstream GAb 2000 abstracts.* 36-38.

Smith, R.G, Missailidis, S., Price, M.R. (2001). Purification of anti-MUC1 antibodies by peptide mimotope affinity chromatography using peptides derived from a polyvalent phage display library. *J. Chrom. B* 766: (1) 13-26.

Sparks, A.B., Rider, J.E., Hoffman, N.G., Fowlkes, D.M., Quilliam, L.A., Kay, B.K. (1996) Distinct ligand preferences for SH3 domains for Src, Yes, Abl, Cortactin, p53bp2, PLCg, Crk and Grb2. *Proc. Natl. Acad. Sci. USA* 93: 1540-1544.

Spencer, D.I.R., Missailidis, S., Denton, G., Murray, A., De Matteis, C.I., Searle, M.S., Tendler, S.J.B., Price, M.R. (1999) Structure Activity Studies of The Anti-MUC1 Monoclonal antibody C595 and Synthetic MUC1 Mucin-Core-Related Peptides and Glycopeptides. *Biospectroscopy* 5(2): 79-91.

Chapter 9 - Bibliography.

Stephen, C.W. and Lane, D.P. (1992) Mutant conformation of p53: precise epitope mapping using a filamentous phage epitope library. *J. Mol. Biol.* 225: 577-583.

Suzuki, C., Ueda, H., Tsumoto, K., Mahoney, W.C., Kumagai, I., Nagamune, T. (1999) Open sandwich ELISA with V-H/V-L-alkaline phosphatase fusion proteins *J. Immunol. Methods* 224: 171-184.

Swallow, D.M., Gendler, S., Griffiths, B., Corney, G., Taylorpapadimitriou, J., Bramwell, M.E. (1987). The human tumor-associated epithelial mucins are coded by an expressed hypervariable gene locus PUM. *Nature* 328(6125): 82-84.

Tawfik, D.S. and Griffiths, A.D. (1998) Man-made cell-like compartments for molecular evolution. *Nature Biotech.* 16: 652-656.

Tighe, P.J., Powell-Richards, A., Sewell, H.F., Fischer, D., Donos, L., Sing Dua, H. (1999) Epitope Discovery Using Bacteriophage Display: The Minimum Epitope of an Anti-IRBP Antibody. *Exp. Eye. Res.* 68: 679-684.

Wang, J., Ensor, C.M., Dubuc, G.J., Narang, S., Daunert, S. (1999). Fusion proteins of a single-chain antibody and photoproteins for assay development in the detection of Salmonella antigen. *Abstr. Pap. Am. Chem. S.* 217: U111 part 1.

Wilchek, M. and Miron, T. (1999) Thirty Years of affinity chromatography. *React.Funct. Polym.* 41: 263-268

Yang, W., Green, K., Pinz-Sweeney, S., Briones, A.T., Burton, D.R., Barbas III, C.F. (1995). CDR walking Mutagenesis for the Affinity Maturation of a Potent Human Anti-HIV-1 Antibody into the Picomolar Range. *J. Mol. Biol.* 254: 392-403.

Zuckermann, R.N. (1993). The chemical synthesis of peptidomimetic libraries. *Curr. Opin. Struct. Biol.* 3: (4) 580-584.

10 Appendices.

10.1 Appendix 1 - Sequence Data

10.2 Appendix 2 - Publications

Some of the work presented in this thesis has been presented at the following conferences and published in the following articles. Articles marked * are included at the back of this thesis.

Price, M.R, Denton, G., Murray, A., Smith, R.G., Simms, M., Perkins, A. (1999) Purification of monoclonal antibodies and recombinant antibody fragments by mimotope affinity chromatography. *International Journal of Molecular Medicine*, **4**, S1, 188.

Denton, G., Murray A., Simms M., Smith R.G., Perkins A. & Price M.R., Purification of immunoreactive antibody for clinical use by peptide epitope affinity chromatography. *British Cancer Research Meeting abstract*. (1999)

Oral and Poster presentation given at GAb 2000, an international symposium on downstream processing of genetically engineered antibodies and related molecules. Sponsored by Amersham Pharmacia Biotech. Barcelona, Spain - October 2000.

*Smith, R.G. and Price M.R. (2000). Discovery of novel mimotopes using polyvalent phage display technology - their use in peptide mimotope affinity chromatography. Downstream Gab 2000 abstracts. 36-38.

*Murray A., Smith R.G., Brady K., Williams S., Badley R. A. & Price M. R., Generation and refinement of Peptide Mimetic Ligands for Paratope-Specific Purification of Monoclonal Antibodies. *Anal. Biochem.* **296**, 9-17 (2001)

*Smith R. G., Missailidis S., Price M., R., Purification of anti-MUC1 antibodies by peptide mimotope affinity chromatography using peptides derived from a polyvalent phage display library. *J. Chrom. B.* 766 (2001) 13-26.